INVESTIGATION AND IMPLEMENTATION OF THE 'PV-CHIMNEY' SYSTEM ON BUILDING ENVELOPES

Gratuation project
2018-2019
Program: Building Technology Track

Antri Lysandrou, 4748395

Mentors:
Pr.Dr. Andy van den Dobbelsteen
Dr. Regina.M.J. Bokel
Zoheir Haghighi

Exrenal examiner:
Dr.ir. MC (Martijn) Stellingwerff

ABSTRACT

This study refers to the PV/T-chimney system, an innovative system that combines two solar systems, a Trombe wall system and a PV/T system in order to gain more energy per square meter of application. The research analyzes the impact of the PV-chimney system on the energy performance of residential high-rise buildings and the architectural integration of the system as part of the facade. Different facade design alternatives, which investigate different facade patterns and their limitations in terms of functional and practical issues, provide a categorization of different ways of its use. Based on that, for each architectural category, by the help of energy simulations, a multicriteria analysis of the system is done. The aim is to understand the behavior of the proposed PV-chimney system under different geometrical characteristics in different climate conditions, in order to find the most optimal parameter combinations in terms of performance. In the second part, having as case study the Europoint Towers, in Rotterdam, a detailed facade design of PV/T-chimney is proposed based on the findings of the architectural and multicriteria analysis. This design, was developed in order for the system to adapt in the climate of the Netherlands, where the case study building is located as well as the climate of Hungary, where, it was constructed in 1:1 scale under the framework of Solar Decathlon 2019 competition, which took place in Hungary. In Hungary, an experiment of the system was conducted, in order to test the efficiency of the Photovoltaics under high temperatures and the potential use of this system for ventilation purposes. The results of the experiment indicate the viability of the simulations and underline the possible future improvements of the system for higher energy performance. According to the experiment measurements and the simulations, a comparison of the proposed system with conventional products proves that there is a reduction of the PV efficiency due to high temperatures. Thus, there are energy losses in the operation of the PVs. However, the electricity losses are depreciated by the thermal gains of the system, which give a final positive energy sign to the system.

Key words – 'Trombe walls', 'PV/T systems', 'high-rise', 'sustainable high-rise', 'passive ventilation', 'high-rise facade', 'passive design strategies'

MSc Thesis 2018/2019
TU Delft - Faculty of Architecture - MSc Building Technology

Acknowledgements

First of all, I would like to express my sincere gratitude to the people of the facade company De Groot en Visser for their immense help. Especially, I would like to thank Peter Zegwaard for his guidance and patience during the detailing of the system and Martin Vandeketterij for his enormous contribution to the completion of construction of the facade. Additionally, this work would not have been possible without the financial support of the sponsors which are mainly the De Groot en Visser, Steinfort for the detailing and the construction, Kameleon Solar for the BIPVs, VPT for the aluminum structure, Steinfort for the glazing and all the other companies which gave a financial support to the project. Moreover, I would like to thank my mentors, Prof.dr.ir. A.A.J.F. van den Dobbelsteen, Dr. Regina Bokel and Zoheir Haghighi for their guidance at every stage of this process. Special thanks also go to my family and especially my parents whose love and guidance are with me in whatever I pursue. Lastly, I wish to thank my supportive friend, Panayiota, for always keeping me motivated throughout my study years.

CONTENTS

1 INTRODUCTION

Over the last decades, high rise buildings have become increasingly popular as they became a more convenient solution to the modern living and the urbanization trends. In order to manage the population growth, the intensifying urbanization and the desire to shorten commute time inside the city centers, the multi-floor buildings have become more prevalent as a major factor in managing city infrastructure.

Similar to global population growth, the primary energy demands are increasing and will double by 2050, according to the World Energy Council *(Lee & Strand Richard, 2009).* Simultaneously, the lack of resources and the rise in energy costs will have a tremendous impact on the living standards of the next generations. Currently, as a large part of the energy production is based on fossil fuels, a lot of emissions and greenhouse gases are releasing to the environment causing global environmental warming. Consequently, energy consumption issues and environmental issues are some of the most critical global concerns. Moreover, the European Union target for 2020, and the future is very ambitious and requires every building to generate more energy than it will consume *(Garcia, 2018).*

As the building sectors consume 40% of the total of energy in the world *(figure 1)* and produce CO2 emissions, according to the European Commission (2017), the buildings and their relation with the energy consumption and thus, the environment are key issues that the building professions are facing worldwide *(Lam et al. 2006).* Considering the significant impact that buildings have on the ecosystem, regulations concerning the energy efficiency of the building and the development of energy strategies were introduced globally. In the UK, the government introduced the CIBSE guide in 2006 to reduce national greenhouse gas emissions and to push for further improvements in the energy efficiency of the buildings and, thus, to approach zero carbon building *(CIBSE, 2012).* Also, in 2004, the ASHRAE guidelines were introduced as Thermal guidelines with the goal of creating a common set of environmental guidelines in order to maintain high reliability in the most energy-efficient manner.

In these circumstances, the reduction of energy generation by fossil fuels and the enhancement of the use of renewable sources and passive techniques, to generate and reduce the energy consumption, would contribute to the accomplishment of more net-positive buildings. As can be seen in figure 2, ventilation, heating, and space conditioning are approximately more than half of the total energy consumption of the building. Moreover, in the effort to reduce the energy consumption of buildings, it is important to maintain the high-quality comfort levels and promote the approach which balances the energy use, the energy efficiency and the implementation of renewable energy systems. In this context, efficient utilization of renewable energy resources, such as the sun, which releases an enormous amount of radiation energy to the earth's land *(Smil, 1991),* is a promising solution. Designing passive solutions, integrated into buildings, to reduce the energy demands by external sources is a way to approach a more energy neutral and even energy-positive future in the building sector.

1.1. Problem statement

High-rise buildings are spreading throughout the world while strict national energy requirements are willing to cope with the effects of climate change. Consequently, high-rise buildings need to be designed in such a way that the design has an energy efficiency strategy based on environmental factors which might affect the building performance.

The orientation, the shape and envelope of the building are the main influential parameters that determine the energy performance of a high-rise. Hence, the orientation and shape of the building are usually base on the architectural intentions and the urban context. In this case, the development of an energy strategy for the design of the envelope is crucial, as it can significantly affect the future energy performance of the building.

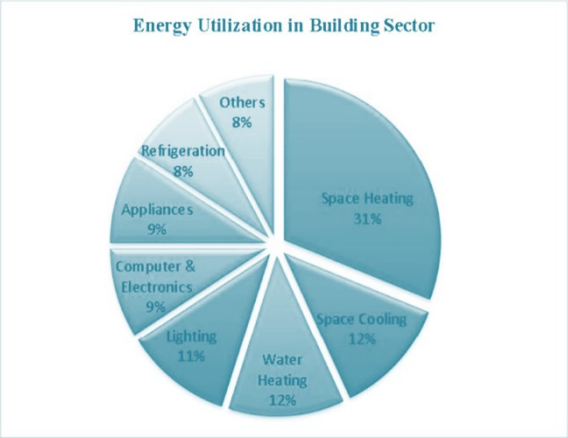

Figure 1: Energy consumption of building sectors in relation with the total energy consumption of the world *(Shiv et al., 2013).*

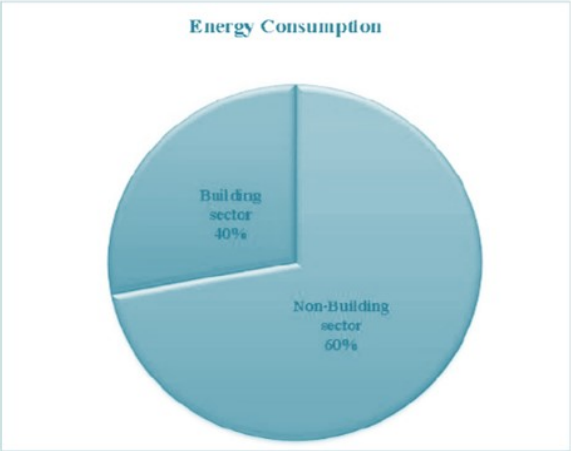

Figure 2: Energy utilization by various applications in building *(Shiv et al., 2013).*

As mentioned above, the envelope can play an important role to the energy performance of a building and especially in high-rise buildings where the facade is the main part of the envelopes. Moreover, as the facade is exposed to the sun and wind, can be used for the integration of passive solar systems, in order to reduce annual cooling and heating loads or to produce energy. An efficient passive technique with almost zero running cost, for passive ventilation, are the Trombe Walls, known also as solar heating walls or storage walls *(Hami et al., 2012; Fang & Yang, 2008).* Similarly, building integrated photovoltaic systems are an imperative in this context to generate electricity, although a very small percentage of 16% of solar energy is converted to electricity and the rest is absorbed and transformed into heat *(Bouzoukas, 2008).* For these reasons Photovoltaic thermal collectors have received considerable attention in recent years *(Agarwal & Garg, 1994).* PV/T collectors produce electrical energy and store the excited heat to use it for other domestic applications. Therefore, a design of facade system that reduces the energy demands of the building by utilizing renewable sources, as the

sun, can be fundamental to address future facade design for more sustainable buildings.

Although, both technologies are very promising and approachable, there is a literature gap in the field of vertical applications of BIPV/T systems, while the use of solar chimneys or Trombe walls in multi floor buildings are scarce. Key barriers for their adoption are cost, performance, aesthetics and technical complexity and thus, their implementation on the building facade is rare. Further research is needed to assess their potential and to identify the obstacles in façade design.

1.2. Research objectives

Taking into consideration the environmental and the energy requirements of the future high-rise, the development of energy strategies for facades, in order to comply to future energy efficiency targets, it will be a future challenge for Architects and Engineers.

This study aims to design and investigate how a Trombe wall and photovoltaic systems can be combined in one facade system for multi-floor building facade applications and if this new 'system' can represent a sustainable and a viable solution that can reduce the energy demands of the building and generate energy. This work is part of the full project "PV-Chimney", supported by TUDelft, which aims to develop a system which combines PV technology in a Trombe Wall. The general idea of the proposed system is to enhance heat production while, by use the air buoyancy, can cool down the PVs and probably cause cross ventilation. In this way, the efficiency of the PV modules will not drop and simultaneously, the produced heat, which is released from both systems could be used possibly for heating purposes.

The objective is to provide an understanding of the approbation of the PV-chimney in different climates and different "PV-chimney" system scales. Secondly, the research aims to provide a facade implementation of the "PV-chimney" system for high-rise buildings considering both architectural and performance parameters.

1.3. Research questions

The scope of this research paper is to answer the following question:

> *"How can the proposed PV-chimney technology be designed, optimized and integrated on a multi-floor building envelope by maintaining the basic functions of the facade, high aesthetic values and improving the energy performance of the building?"*

In order to answer this main research question, a series of sub-questions will help reach the goal of the project:

A) How the proposed PV-chimney system can be incorporated aesthetically with the building, maintaining high energy performance?

DESIGN QUESTION

a) What are the proper materials in terms of aesthetics and its efficiency.

b) What are the proper geometrical characteristics in terms of aesthetics and its efficiency.

B) How can architectural integration of PV-chimney technology be implemented in the HVAC system of the building and how will the new energy system of the building works to exploit the energy gains from the proposed design?

C) Is the proposed facade system more beneficial than common Trombe wall or PV/T systems in terms of energy gains?

1.4. Methodology

The following master thesis will start by a literature research to give an overview of the current Trombe walls systems and types as well as the parameters and factors that affects their performance. Similarly, an analysis will be done about BIPV systems. The literature study will serve the variables for the simulation of the system which is the next step. The understanding of the above topics of the literature lead to the next phase of the thesis, "multicriteria analysis" where hand calculations are done. In this phase, the proposed system is simulated with variable geometrical alternatives, in different weather conditions. For the implementation of the PV-chimney system on a facade, the case study building of Europoint Towers by SOM, which are located in Rotterdam is selected. The system is designed in detail, together with an upgraded facade, for the Towers. The system detailing is based on the literature findings and the previews multicriteria analysis results. In this case, for the detailing of the facade and the system itself, the AutoCAD software is used while the facade is reconstructed in 3D using the Revit software. The specific "PV-chimney", is designed by real products that are available on market as it is the first application of the system in real prototype. In order to complete the prototype, a collaboration with the facade company "Groot en Visser" takes place. The proposed PV-chimney is designed and built within the framework of the competition Solar Decathlon 2019, in Hungary. After the construction of the prototype, real measurements are done in order to test the proposed design under real conditions. Lastly, an evaluation of the system is done by the comparison of the energy efficiency of the proposed design with conventional system.

The following methodological scheme *(figure 3)* provides an overview of the whole research. The different steps that will be carried out for completing this research and answering the research questions.

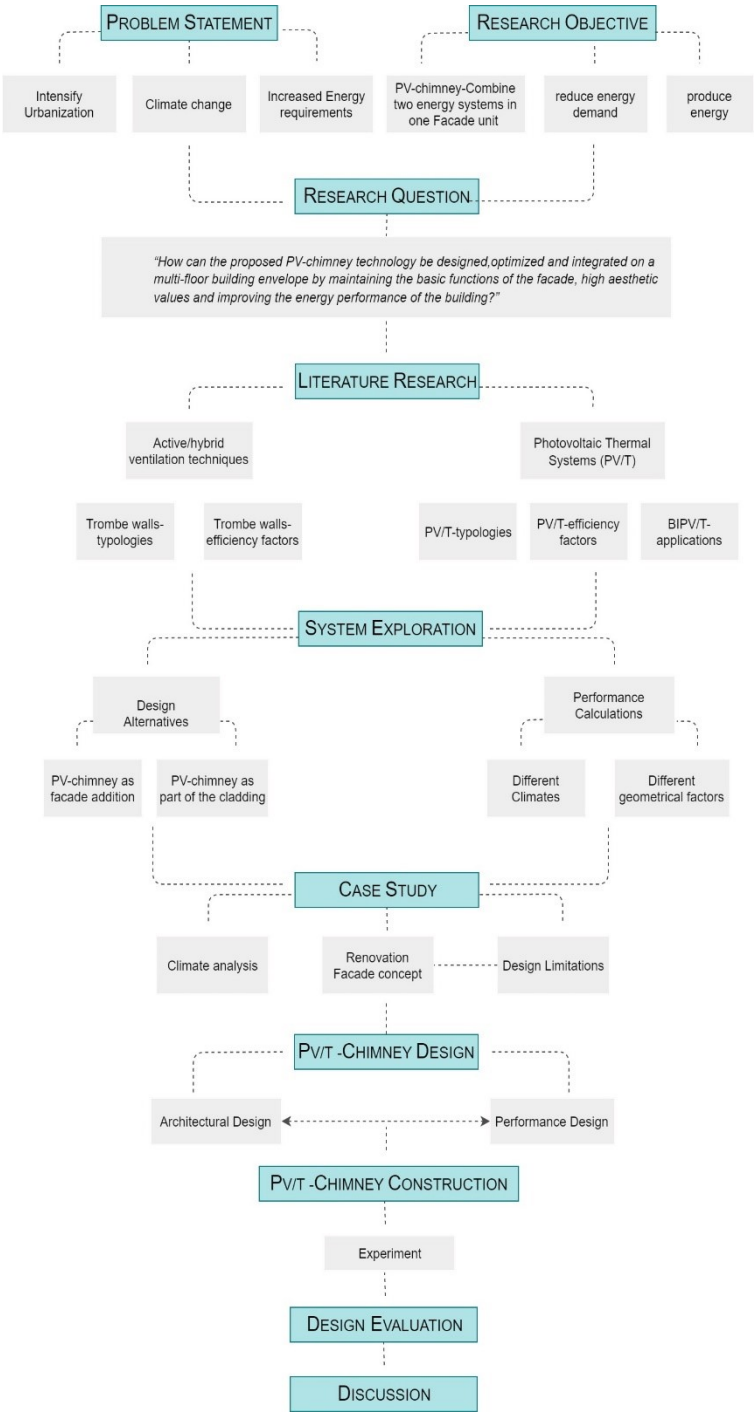

Figure 3: Framework diagram of the thesis.

LITERATURE REVIEW 2

2.1. Active/hybrid ventilation techniques

The general purpose of the ventilation of a building is to provide fresh air. Passive or active techniques are used to provide ventilation in order to offer a comfortable indoor environment. The difference between passive and active ventilation is that passive ventilation directly uses natural energy from wind and thermal buoyancy to drive outdoor air through the building. Therefore, the ventilation is done with almost zero cost. On the other hand, active ventilation systems refer to systems where mainly electricity, or another kind of energy is consumed for its operation. Those systems consist of mechanical components or other energy-consuming components *(Atkinson et al. 2009).* The hybrid ventilation systems are the systems that combine active and passive ventilation in order to use the mechanical system only when it is needed and, therefore, to reduce energy consumption *(Steven, 2011).* Usually, in hybrid systems, heat recovery is used in order to reduce the heating demands and to exploit natural ventilation during warm periods. Thus, to reduce electricity demands *(Antvorskov, 2008).*

As mentioned above, one of the most promising passive ventilation systems for facades, are the Trombe Walls, which are a subcategory of Solar Chimneys *(Shiv et al., 2013)*. Trombe walls are vertical solar chimneys and specifically thermo-syphoning air channels. Through thermal buoyancy, as their principal driving mechanism of airflow, solar walls provide natural ventilation for both heating and cooling the building. Trombe Walls can be combined with a mechanical or electrical system of the building, creating a new hybrid system. Also, their advantages, such as simple configuration, high efficiency, zero running cost, and the fact that they are environmentally friendly, are raising the attention of many researchers. Research shows that, by implementing a Trombe wall in a building, the building's energy consumption is reduced up to 30% *(Hordeski 2004).* Similar research indicates that a façade Trombe Wall achieved 16.36% energy heating savings *(Briga-Sá, 2014).* The design of a Trombe Wall, and especially in combination with other building systems, requires extensive and multidisciplinary research of different physical parameters that can affect its operation. Additionally, the climate conditions and the purpose of its implementation play a crucial role in the design decisions. Different typologies, research examples, and parameters that affect the performance of wall Solar chimneys will be analyzed further below.

2.1.1. Trombe Walls

As mentioned above, Trombe Walls, utilize solar radiation to enhance the natural stack effect ventilation *(Lee & Strand Richard, 2009).* the North hemisphere, Trombe walls are located usually on South, South West, South East sides of the building. *(Guohui, 1997).*

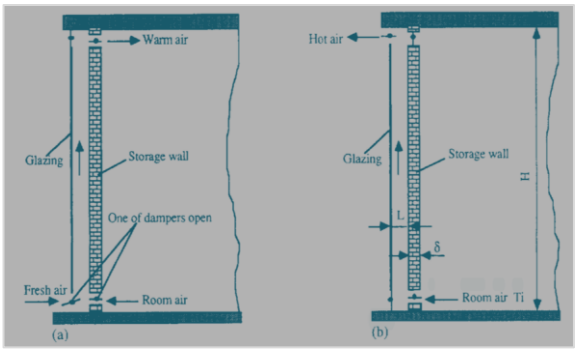

Figure 4: Schematic diagram of Trombe wall for a) winter heating and b) summer cooling (Gan & Riffat, 1998).

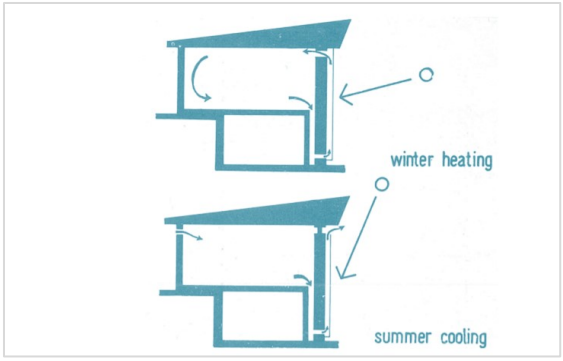

Figure 5: Trombe Wall, Winter heating and summer cooling. Section of the detached house with Trombe Wall, built in 1967 in Odeillo, France. (Hogan, 1975)

Trombe wall generally consists of a blackened concrete or masonry wall, which on the outside is covered by glazing, in order to create a channel between the glass and the wall for the air to flow *(Ong, 2003).* The solar walls are designed to enhance airflow by buoyancy effect; therefore, high solar transmissivity glazing is used to increase solar gains. The thermal mass of the wall serves to collect and store solar energy, which is transferred to the inside of the building during the winter and facilitates air movement through the inside space during summer *(Shiv et al., 2013).* In figure 4, the operation of a Trombe wall in winter and summer scenarios are illustrated. During heating periods, the bottom vent of the glazing is open, and the top close to keep the heated air while both vents of the massive wall are open. Cold air enters the shaft from the bottom vent and heated up by the solar energy, which is stored in the wall *(Guohui, 1997).* Consequently, the air density drops, and the heated air flows upward due to the buoyancy effect. Then, warm air enters the living space through the upper vent of the wall. For summer cooling, the top vent of the wall is close to prevent hot air from entering the building while the upper vent of the glazing is open to enhance natural cross ventilation. The air from the inside space is drawn into the solar shaft through natural convection, and is then heated, and then is exhausted into the atmosphere by the buoyancy effect.

By this effect, the shaft draws air from the room by the bottom vent while fresh air rushes into the room through open windows or vents in other exterior walls *(figure 4).*

The Trombe wall owned its name to Félix Trombe and Jacques Michel, who developed and popularized the concept of solar walls in 1957 at C.N.R.S laboratory in France, which was used for space heating only. Although the initial concept was patterned by E.S.Morse during the 19th century (Shen et al., 2007; Shiv et al., 2013). Some years later, in 1967, the first house with the Trombe wall was built in France to collect the solar heat and provide the interior space heating and is known as classic or standard Trombe wall (Shen et al., 2007) *(figure 5).* Over time, Trombe wall modifications have been done in order to achieve also solar cooling and to improve its efficiency. In 1993, Bansal did the first mathematical model of the Trombe wall in order to increase airflow by the increase of solar irradiations *(Shiv et al., 2013).* Many simulations have been done later to investigate different parameters and new configurations in order to improve the efficiency of the Trombe wall. Recent researches have proposed the Hybrid System Trombe Wall system trying to reduce the mechanical system's use.

2.1.1.1. Typologies

Based on the main functions of Trombe walls, they can be classified in heating based Trombe walls, cooling based Trombe walls, and Trombe walls for both functions. An overview of the

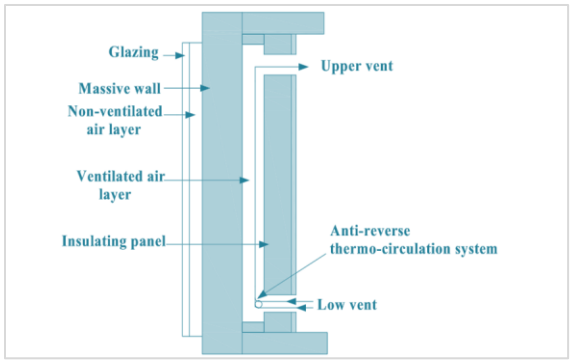

Figure 6: A composite Trombe wall configuration (Shen et al., 2007).

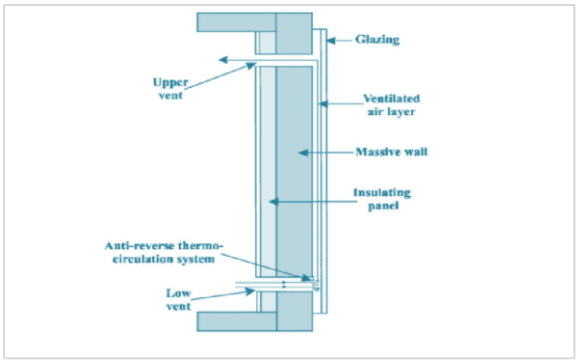

Figure 7: An Insulated Trombe wall configuration (Zalewski et al., 2002).

different typologies of the Trombe wall will be elaborated further below.

Heating based Trombe-Walls

Different configurations of Trombe walls for heating have been developed as the simple Trombe wall *(figure 4)* has some significant disadvantages in terms of its operation while the heat exchange is done by transmission through the massive wall and by ventilation through the vents. The classic Trombe wall suffers from low thermal resistance, which could cause excessive heat loss from the inside to outside when the weather is cloudy or during the winter *(Shen et al., 2007).* Moreover, when the massive wall is colder than the air in the shaft, the air is cooled and re-injected into the room, causing the opposite results (drop in temperature) *(Zalewski et al., 2002).* Finally, its low aesthetic value leads to the need for more advanced design investigation *(Ji et al. 2007).* Accordingly, in order to increase thermal resistance, reduce heat losses, enhance heat generation, or to improve aesthetical issues, different configurations need to be investigated to improve the heating function of the system.

Composite Trombe wall or Trombe-Michel type of wall, as it is known, was developed to increase the thermal resistance of the classic Trombe wall by adding more layers to the system and managing supplies (Shen et al., 2007). This type of Trombe wall is not using outside air, but it's recycling and warming the inside air of the room to heat up more efficiently the air of the inside, which is already moderate in temperature. Moreover, the added thermal resistance minimizes thermal fluxes from indoor to outdoor. As can be seen in figure 6, a composite Trombe wall consists of more layers than the classic design. The enclosed air in the front is warmed by sun radiation, which passes through the transparent layer. The hot enclosed air inside heats up the massive wall. The massive wall in this type works as the medium for thermal energy transfer from outside to the interior air layer (Zhongting et al., 2017). Composite Trombe wall eliminates the heat losses and allows the control of air circulation by the users. Furthermore, the fact that composite Trombe walls do not allow the outside air to enter the building, disclaims their use as cooling systems.

Moreover, a simpler configuration that increases the thermal resistance of the Trombe wall and control supplies is the Insulated Trombe wall. The insulated Trombe walls have an insulation layer that is added on its back *(figure 7)* while a transparent, fully airtight cover is on the front *(Omidreza et al., 2013).* The additional thermal resistance (insulation layer) results in control of the flow rate with the addition of air circulation. Furthermore, the fact that there is a 'strong' barrier of insulation on the back prevents heated air from entering the building during summer by closing the vents; thus, no solar shield is needed. The main disadvantage of this kind of walls is that they cannot operate during the summer periods

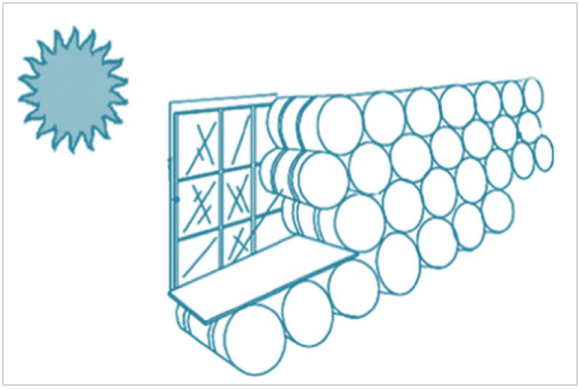

Figure 8: A water Trombe wall configuration (Saadatian et al., 2012).

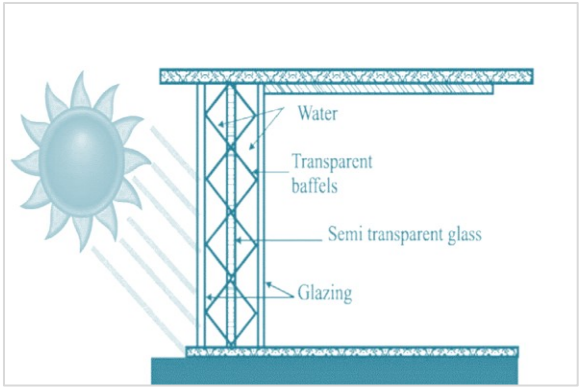

Figure 9: A Transwall Trombe wall configuration (Saadatian et al., 2012).

and that all the collected energy is released into the building by the air layer *(Omidreza et al., 2013).*

An alternative configuration to reduce heat losses is to use storage materials which their specific heat is higher. The water Trombe wall, follows this approach and works on an operation principle similar to that of classic solar wall using water for heat storage instead of masonry, which fills the air gap behind the glass *(figure 8) (Omidreza et al., 2013; Tyagi and Buddhi, 2007; Yang et al., 2011)*. The glass panel is placed on the front of the water storage medium accommodating the flow of the radiated heat which is absorbed by the water. Then, by convection, the heat that water absorbed is distributed to the inside room *(Agrawal and Tiwari, 2011).* The water barrels should have dark color to increase heat absorption. Although the water walls are gently more efficient than masonry walls, they require more design consideration such as containing of liquid (water) instead of solid material, the cost and maintenance, as well as the aesthetical issues *(John, 2006).*

An alternative configuration to reduce heat losses is to use storage materials in which their specific heat is higher. The water Trombe wall, follows this approach and works on an operation principle similar to that of classic solar wall using water for heat storage instead of masonry, which fills the air gap behind the glass *(figure 8) (Omidreza et al., 2013; Tyagi and Buddhi, 2007; Yang et al., 2011)*. The glass panel is placed on the front of the water storage medium, accommodating the flow of the radiated heat, which is absorbed by the water. Then, by convection, the heat that water absorbed is distributed to the inside room *(Agrawal and Tiwari, 2011).* The water barrels should have a dark color to increase heat absorption. Although the water walls are gently more efficient than masonry walls, they require more design considerations such as containing liquid (water) instead of solid material, the cost, and maintenance, as well as the aesthetical issues *(John, 2006).*

Another heat-based Trombe wall which uses water as a heat transfer medium is the Transwall *(figure 9).* Transwall is a transparent modular wall that has an aesthetic role, as it provides visual access and allows light penetration to the interior of the building *(Prakash and Garg, 2000).* The system stands on a metal frame that holds a water container which is enclosed between two parallel glass panes. A semi-transparent absorbing plate is placed in the middle. The incident solar radiation is mainly absorbed by the semi-transparent glass plate, part of it by water, and the rest is transmitted inside. Therefore, the Transwall uses the direct and indirect gain systems but requires high daytime temperatures to operate well *(Al-Karaghouli & Kazmerski, 2010)*, while convective heat transfer in a Transwall reduces its efficiency. In this type of Trombe wall, the operation of the system is based on heat transfer to the existing inside air preventing renewed air from entering the room. Therefore,

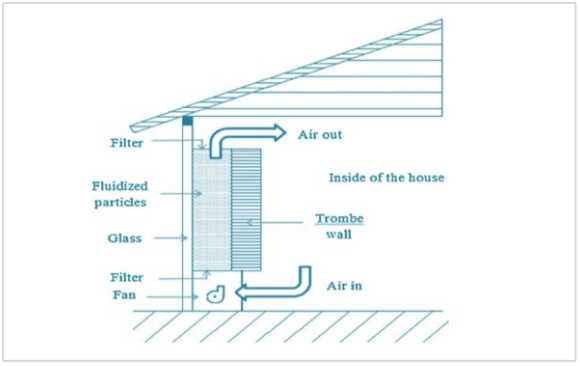

Figure 10: A fluidized Trombe wall configuration (Haleh & Saeed Reza, 2013; Tunç & Uysal, 1991).

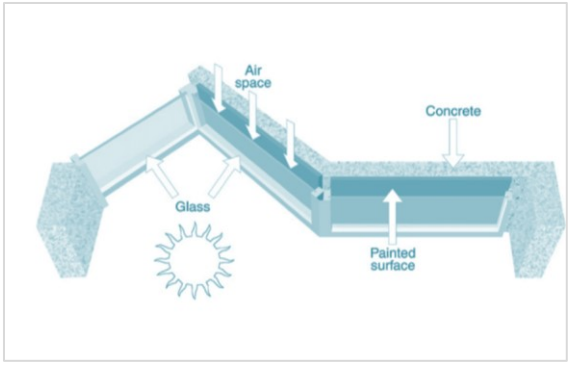

Figure 11: A zig-zag Trombe wall configuration (Hordeski, 2011).

they do not allow natural ventilation, and the air change should be control from a separate system.

As described above, the material and its thermal properties have a crucial role in the final efficiency of the Trombe Wall. The previous types of solar walls used construction materials or water as a medium. The fluidized Trombe wall system is a novel system based on the operational principle of the classic Trombe wall but is using the air, which heated directly from solar radiation, like heat transfer material. In this kind of wall, the heat absorption is enhanced by filling the air gap with highly absorbing, low-density particles *(figure 10) (Haleh & Saeed Reza, 2013; Tunç & Uysal, 1991)*. The direct contact of the fluid with the particles warm up the air achieving higher temperatures; therefore, its efficiency increases *(Zhongting et al., 2017)*. To prevent the fluidized particles from entering the inside of the room, special filters are used at the bottom and top of the air compartment *(Sadineni et al., 2011)*. Research comparisons of the fluidized and classic Trombe walls show that the fluidized Trombe wall system performs far more efficient than the classic ones *(Tunc and Uysal, 1991)*. However, there is no air circulation with the outside air and the quality of the air that re-enters the room depends also on the quality of the filter system..

Another design approach is the zig-zag Trombe wall, which aims to reduce the excessive heating gain, the glare phenomena and to provide the required heating on different periods of the day *(Saadatian et al., 2012)*. The zig-zag Trombe wall consists of three parts that have different orientations. As can be seen in figure 11, the east part of the system is a window while the other parts which are facing southwest, and south are classic Trombe walls. The window is used to provide immediate solar heat and light in the morning when it is needed while the two faces Trombe walls store heat even during the afternoon *(Hordeski, 2011)*. The zig-zag concept implemented recently with five V-shaped sections at the visitors' center of NREL *(Nelson, 2011; NREL, 2005)* and for a residential building near Asheville in North Carolina. This kind of Trombe wall requires space and should be incorporated in the design from the early design stages as it creates a very specific aesthetic view of the building.

Cooling based Trombe-Walls

The solar wall is famous for its heating effects during winter and is designed for cold climates. Recently, many researches investigate the use of Trombe wall as cooling passive system. The novel concepts for cooling are based on the reduction of solar and convective heat input, the reduction of heat transmission and the increase of heat losses. For cooling concepts air circulation from outside is required for to cool the Trombe wall. Also, water or cross ventilation can be used to achieve lower temperatures *(Alejandro, 2018)*.

The solar wall is famous for its heating effects during winter and is designed for cold climates. Recently, many researches investigate the use of Trombe wall as a passive cooling system.

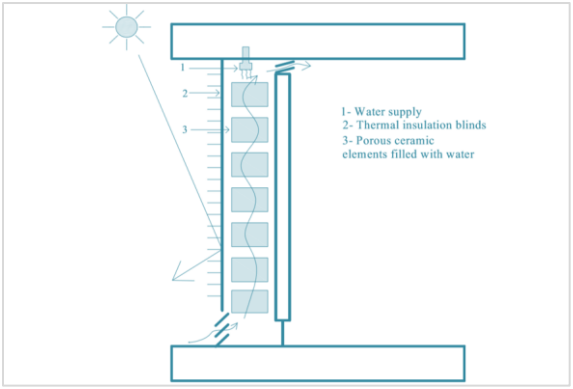

Figure 12: A ceramic evaporative cooling Trombe wall configuration (Melero et al., 2011).

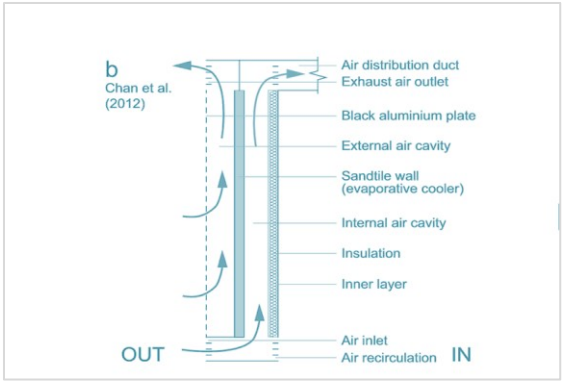

Figure 13: Experimental evaporative cooling Trombe wall configuration (Chan et al., 2010).

The novel concepts for cooling are based on the reduction of solar and convective heat input, the reduction of heat transmission, and the increase of heat losses. For cooling concepts, air circulation from outside is required to cool the Trombe wall. Also, water or cross ventilation can be used to achieve lower temperatures *(Alejandro, 2018)*.

As mentioned above, cooling systems use water and cross ventilation for cooling. Research shows that the efficiency of the cooling system could be improved by approximately 30% by the use of the water spraying system *(Rabani et al., 2015)*. The ceramic evaporative cooling wall *(figure 12)* is the first cooling-based configuration that uses both water and cross ventilation. The evaporative ceramic Trombe wall is presented by Spanish scholars and aims to reduce solar and convective heat input and increase heat loss by evaporation *(Melero et al., 2011)*. As the figure 12 shows, thermal insulation blinds are placed on the outside side of the wall to prevent direct solar gains and the air gap a special ceramic porous material, which can absorb water, is placed. As the air enters and passes from the bottom vent to the upper one is cooled by the wet ceramic flanges and enters the room from the top. The evaporative Trombe wall works well for cooling in summer, but it cannot be used during winter in very cold and humid days as the water, which will be absorbed from the ceramic material, will cause opposite results.

Another experimental Trombe wall that combines both evaporation and cross-ventilation techniques is proposed by Chan et al., 2010. The system *(figure 13)* consists of two air cavities. The outer cavity cools down the evaporative cooler plate (sand tile wall), which is in the middle, and it's moist by pumps while the inner air cavity cools the air that enters from the bottom vent and finally reaches the inner living space. The outer layer is a black aluminum transpired plate and the inner one, an insulated wall. According to Chan's research, the cooling effect was approximately the same as the simpler version. Therefore, more research is required for the integration of the system. Generally, Trombe walls that are used evaporation techniques have a risk that the air that enters the living space could be very humid. In order to dehumidify the air which enters living spaces, desiccant cooling façade concepts are investigated. Fernandez-Hernandez et al. (2015), proposed a desiccant Trombe wall system for façades. The cavity of desiccant of Trombe wall is divided into two parts, and it is an opaque ventilated wall system. This system can be work for two operations using the different parts of the wall. The upper part carries the desiccant material, which is a layer of silica gel allowing for intermittent operations while on the bottom part, a solar collector is placed for regeneration mode. As can be seen in figure 14, the bottom part is sealed by a damper to prevent hot air from flowing upward to the upper part. Ambient air enters the upper shaft, is dried, and then threaded air passes through ducts to the interior space. During

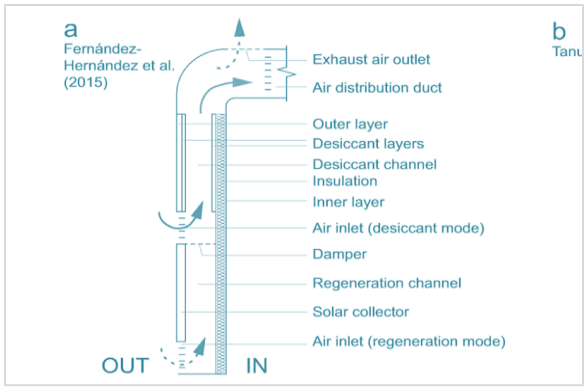

Figure 14: Desiccant Trombe wall configuration (Fernandez-Hernandez et al., 2015).

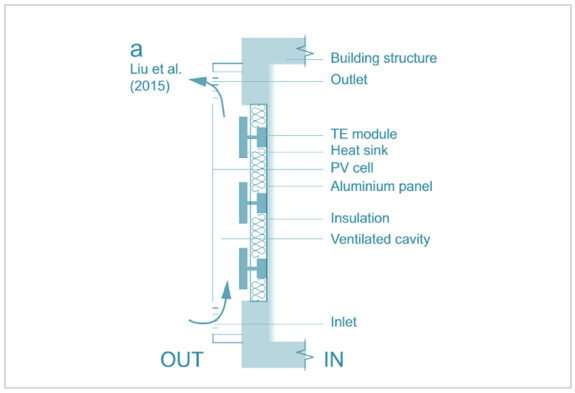

Figure 15: Thermoelectric Trombe wall configuration (Liu et al., 2015; Ibáñez-Puy et al., 2015).

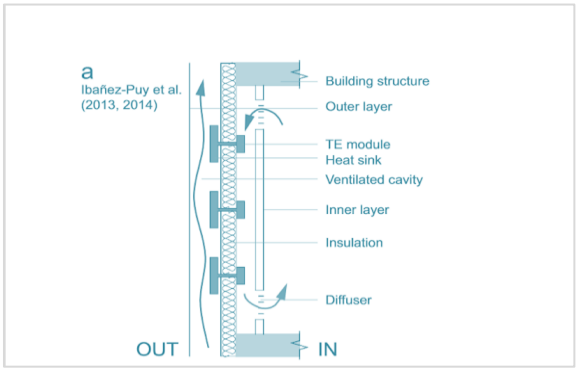

Figure 16: Thermoelectric Trombe wall configuration (Ibáñez-Puy et al., 2015).

regeneration mode, both parts are operated. Air is heated while it flows through the solar collector and flows upward, passing through the desiccant channel to evaporate the moisture previously absorbed by the silica gel layer *(Alejandro, 2018).* Then, the hot and humid air is discharged externally through an air outlet located at the top end of the façade. Summarizing, this system dehumidifies the air before entering the building, but an additional cooling element should be added to be able to cope with very hot climates. Also, an automatic system is required to control both operations.

In 2015, Liu and Ibáñez-Puy et al. (2015) developed a concept where the thermoelectric principle used to attach a solid conductive aluminum radiant panel to the cold end of the thermoelectric module *(figure 15).* The thermoelectric module or thermoelectric cooler or Peltier cooler is working as a small heat pump that transfers heat from one side to the other by conduction. In both designs, the thermoelectric modules are attached directly to the inner layer to transfer the cold and are connected to heat sinks placed in the air cavity, with insulation in between. The idea developed further transforming the system from a solid-based system on an air-based distribution system, including an air cavity in the inner side of the wall which is cooled by conduction with the thermoelectric modules and deliver it to the room through diffusers *(figure 16).* In this scenario, both cavities are openable, and therefore, buoyancy ventilation could be used when needed *(Alejandro, 2018).*

Hybrid systems

In recent approaches, solar walls are presented as a supportive part of the active system or other renewable energy systems of the building integrated into a hybrid building system. This is since the solar wall, as its operation is mainly depending on climate conditions, they cannot be autonomous systems. Therefore, they cannot replace the mechanical air conditioning system, but they can crucially reduce their use. Khedari et al. (2003), reported that a reduction of 10-20% of the energy that air conditioning system is needed to cool a house in a hot climate could be achieved with the utilization of solar chimneys. Moreover, integration of natural cooling systems, such as ground cooling, with solar chimneys (vertical or inclined), can achieve pre-cooling of the external air before entering the building *(Macias et al., 2009).* Both vertical and inclined solar chimneys can be used for heat recovery to

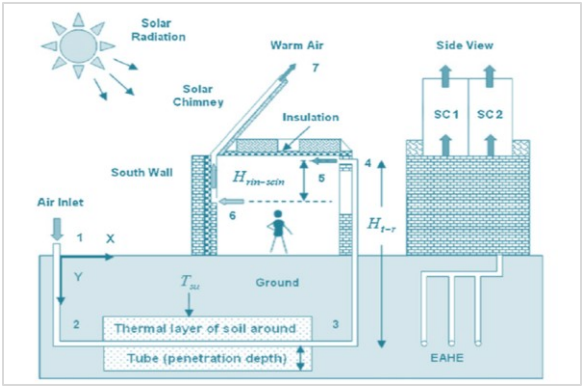

Figure 17: Hybrid system with solar chimney and earth to air heat exchanger (Maerefat & Haghighi, 2010).

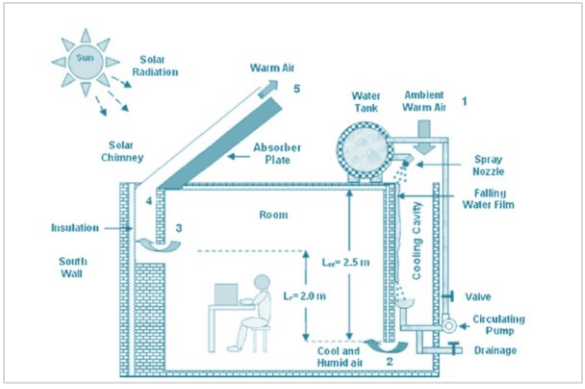

Figure 18: Hybrid system with solar chimney and water tank system (Maerefat & Haghighi, 2010).

support systems as hot water systems, to increase the efficiency of the heat pump system, decreasing the temperature difference, or the efficiency of other mechanical systems in which heat can affect their efficiency. Furthermore, Solar chimneys can be combined with photovoltaic thermal systems to utilize the heat generated by them, to enhance natural ventilation by stack effect or to cover energy demands of their operation (operation of their automation system, fans, evaporation system, etc.). Experimental real application and researches are trying to investigate the attitude and energy gains by the combination of the passive function of Solar chimneys (vertical or inclined) with other passive systems or mechanical supported systems. Different system combinations and their results will be analyzed below.

A passive solar system of Solar Chimney inclined which proposed for natural day ventilation and is amalgamated with earth to air heat exchangers presented by Maerefat and Haghighi (2010). The system achieves both cooling with the help of the earth to the air heat exchanger and ventilation utilized solar energy to challenge the stack effect and, thus, to suck cold air through the ground pipe. As can be seen in figure 17, the system consists of the solar chimney on the roof and the earth to air heat exchanger system. The earth to air system cools the air that enters the room, and the solar chimney works as a driving force, which causes cross ventilation inside the room. It was shown, according to Maerefat and Haghighi (2010), that the collaboration of the two systems could provide sufficient cooling during the daytime without any mechanical support and that with proper configurations could succeed good indoor cooling even in climate condition with low solar intensity of 100W/m^2 and high outside air temperature of 50 ◦C. The same authors published an article with the title "Natural cooling of stand-alone houses using a solar chimney and evaporative cooling cavity", proposing the same system of a solar chimney, but in collaboration with an evaporative cooling system *(figure 18)*. In this system, ambient air penetrates the cavity where is cooled by evaporation (water tank close system provides sprayed water in the cavity). Then, the cooler and humid air enters the room while the solar chimney is sucked new fresh air continuously. According to their investigation, the ventilation rate was influenced by climate conditions (ambient temperature and solar radiation) and by geometrical configurations of the solar chimney (e.g. inlet dimensions) and the cooling cavity. Moreover, numerical experiments define that this system could provide thermal comfort during the day even at a low solar intensity of 200W/m2 and high ambient air temperature of 40 ◦C in a moderate and arid climate and that its collaboration with air conditioning system could be energy efficient and environmentally friendly *(Song et al., 2011)*.

The systems described are passive systems that work together to improve the efficiency of solar walls. Other configurations propose a combination of solar walls with a heat

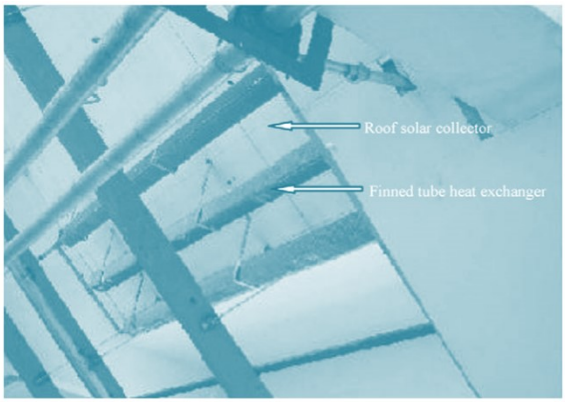

Figure 19: Finned tube heat exchanger inside the air channel (Dai et al., 2007).

recovery system or with a photovoltaic system to utilize the heat for other household applications and produce electricity, respectively. A heat recovery system with heat pipes in a glazed solar chimney is investigated by Gan and Riffat (1998). CFD simulations show that heat recovery by heat pipes decreases the buoyancy effect, and thus, wind forces or other mechanical support should be used to achieve the required airflow rates. A different configuration for heat recovery is presented by Dai et al. (2007), where a solar hot water system enhances natural ventilation. Real testing has been done by the installation of tubular solar collectors in an area of 150m^2 of the roof of the Shanghai Institute of Architecture. In this configuration, the solar chimney is created under the roof of the green building and covered by opaque solar collectors in order to exhaust indoor air through natural ventilation. The solar collectors were used to supply heating and cooling in winter and summer, respectively, while in transition seasons, they were utilized to enhance natural ventilation by stack pressure in collaboration with heat exchange elements which are placed inside the air channel *(figure 19)* and to supply hot water. The experiment presents that in transition seasons with solar insolation of 17 MJ/m2 and the average ambient temperature of 10◦C, the airflow by stack pressure was double in relation to the standard natural ventilation rate. Therefore, in addition to providing hot water for the office building, the system was able to cause an air change rate of 3 air changes per hour *(Dai et al., 2007).*

Finally, recent approaches, which focus on heat storage and recovery, are proposing to use phase-change material instead of massive walls for solar walls. Phase-change materials are materials that can store more energy in a smaller volume and, therefore, could replace construction materials with less volume and thus less weight *(Cabeza et al., 2007; Zalewski et al., 2012).* A numerical study for different phase change materials was done by Bourdeau (1980) shows that a 15-cm concrete wall can be replaced by a 3.5-cm wall of phase-change material, maintaining similar performance. Another research investigates the melting process of PCM and arrives at potential solutions. The study shows that segmenting the block of PCM using PCMs with different melting temperature along its height was is the most promising results for minimizing this overheating effect *(Tenpierik et al., 2019)*. A computational fluid dynamics (CFD) simulation by a group of Japanese scientists tests solar walls with three different kinds of phase change materials and their influence on the thermal behavior of a room *(Onishi et al., 2001).* The group established that the use of phase-change materials in Trombe walls is beneficial for the reduction of the energy consumption of buildings. Moreover, a similar study has been done by Khalifa and Abbas in Baghdad, Iraq, where again different phase change materials on solar walls where simulated and compared. The simulations present that each phase change material has a different reaction and that the volume of the storage wall can eliminate at more than half with the use of phase change material *(Khalifa and Abbas, 2009).*

Except for heat storage, an invention is the photovoltaic (PV) solar walls where photovoltaic panels are covered the front side of the glazing and simultaneously generate electricity and convert solar radiation into heat *(Sun et al., 2011).* The new configuration with photovoltaic panels based on the operational principle of conventional Trombe walls. However, in this case, the air that is drawn in the cavity from the lower vent is heated up by the absorption of the heat generated by PVs and then moved upward to enter the room for heating or to be stored or to be exited through the upper

vent ventilation. The absorption of the heat created by PV operation from the air, cool down the PVs, and consequently increases their efficiency *(Chow et al., 2003; De Pascale et al., 2012).* Although that there is simultaneous use of the heat to heat up air and electricity production, the fact that PVs are replaced by the glazing, they reduce the efficiency of The Trombe wall in terms of heat gain significantly. Accordingly, various researches are done to assess the influence of PV panels, which cover the glazing on the efficiency of solar chimney. A numerical model simulation with a PV panel installed on a solar wall on a building is done by Sun et al. (2011) in order to measure the indoor temperature of the building. The simulation results show that the replacement of the glazing by PVs reduces the performance of the Trombe Wall by 17% while PV opaque surface obstructs solar rays' penetration into the mass wall. Furthermore, the roof solar chimney system with PV panels investigated by Khedari et al. (2002). The proposed system shows to provide a more comfortable indoor temperature in contrast with the conventional system of the solar chimney for the reduction of cooling loads through the roof.

2.1.1.2 Factors to be considered when designing Trombe wall/wall solar chimney

Solar walls or Trombe walls are mentioned as a sustainable architectural technology as the utilization of solar energy is done to cover the heating and cooling demands of buildings in different climate conditions. The Design of the chimney and of each separate element of it can influence the efficiency of the system. Some important parts of the Trombe wall that influence a lot its efficiency, and must be considered when designing or improving a Trombe wall, are Design and geometrical parameters (glazing properties, surface wall area ratio, channel depth and height, massive wall properties, vents and fans and parts as insulation and shading devices), and Building parameters (solar radiation, orientation, wind speed). Therefore, various studies and researches are done to investigate the effect of these parameters on Trombe wall efficiency as the idea of Solar walls is very promising in terms of energy reduction, environmentally friendly and sustainable solutions, and spurs the interest of engineers and architects.

2.1.1.2.1 Design Parameters

Glazing properties

The glazing is an essential part of the Trombe wall, and its properties such as the material or the thickness of glazing the number of layers and coatings influence significantly the amount of solar gain that is either absorbed, transmitted or reflected. Also, the glazing can affect the heat losses between the indoor and outdoor space *(Stazi et al., 2012).* Accordingly, the glazing choice is crucial for Trombe wall efficiency. Generally, the layers of glazing depend on climate conditions *(Zhongting et al., 2017),* and the use of double glazing enhances passive cooling and reduces heat losses in winter *(Lee & Strand Richard, 2009).* However, according to Kundakci Koyunbaba et al. (2012) research, in Turkey, single glass during the cooling season is preferable and improving Trombe wall efficiency during the day because of the higher solar radiation transmissivity, while in Italy, during the heating season a double glazing is preferred due to lower heat losses and therefore the reduction of heating energy *(Stazi et al. 2012).* In contrary to Yilmaz & Irshad et al. (2014), found that in Malaysia, the application of double-glazing during the cooling period saved cooling energy and reduced CO2 emission in comparison with mechanical air-conditioning systems.

A study about the material of glazing conducted by Zalewski et al. (2002) in Trappes (longitude: 201#, latitude: 4846#) and Carpentras (longitude: 503#, latitude: 4408#) shows that the glazing influenced the performance of Trombe Wall significantly *(Zalewski et al., 2002).* Their study shows that the absorbed energy was increased using low-emittance double glazing by 242% in non-ventilated solar walls and 193% on ventilated solar walls, 188% in solar walls, which includes insulation and 217% for composite solar walls. Moreover, the investigation of two different areas revealed that the glazing materials are also depended on the location of solar walls application, the longitude, and latitude. Furthermore, higher

solar transmittance of the glass cover could increase the ventilation rate by approximately 38% *(Lee & Strand Richard, 2009),* since more solar radiation is absorbed. Finally, for heating periods, Low-E coating is more beneficial as the solar gains increase *(Richman & Pressnail, 2009).*

Massive Wall properties

The massive wall is the most crucial part of the solar wall *(Hami et al., 2012),* as it is the key heat storage medium *(Zalewski et al., 2012).* Therefore, the material properties of the storage wall influence the heat storage capacity significantly, and the heat transfer by convection and conduction. The massive wall parameters which influence its behavior are its thickness, material, and the insulation level. Concerning the wall material, Knowles conducted an experimental study comparing the paraffin-metal texture wall and a concrete wall as store walls. The results show that concrete performs better than the paraffin wall increasing the system efficiency by 20%. A relevant study where concrete, brick, and massive aerated wall during the pre-use phase and the use stage of the solar wall are compared was carried out by Stazi et al. (2012). The material investigation obtained with the aerated concrete blocks with lower environmental impacts and high energy performance. Similarly, Boji´c et al. (2014), testing two Trombe walls in Lyon in France, one with a massive concrete wall and the other with clay bricks conclude that the concrete wall energy performance is higher than clay brick wall. Moreover, an investigation study by Hassanain et al. (2011) of Egypt's Suez-Canal University examined the behavior of different adobe material massive walls, and he found that different compositions of adobe can influence the solar wall performance greatly.

Except from the wall material itself, coatings that coat the mass wall are also significant as they can change the heat absorption amount. Research at the University of Nigeria investigates the effect of different coating of the performance of a Trombe wall *(Nwachukwu & Okonkwo, 2008).* Although the study presents that high-absorptive coatings could improve the solar wall storage capacity, there is a risk of overheating if there is no analysis of the project individually. Additionally, an investigation study by Nwosu (2010) and Ji et al. (2007), revealed that highly absorptive materials could improve the storage capacity and meliorate system efficiency. In addition, a numerical study of a composite Trombe wall with an insulation layer on the inside side of the massive wall revealed that insulated massive walls improve the efficiency of a composite Trombe wall *(Ji et al. 2009).* Especially in hot climates, where solar walls could cause overheating due to reverse heat transfer, Trombe walls should be properly insulated *(Stazi et al., 2011).* An experimental study by Guohui (1997) revealed that suitable insulation is needed to increase natural ventilation by solar walls during the summer period, while according to Ji et al. (2007), thermal insulation leads to better operational results for both winter and summer. Relevant simulation for both winter and summer scenarios was conducted by Stazi et al. (2011) for a residential building in Alcona. A comparison between and normal Trombe wall and super-insulated Trombe wall showed that during heating periods, the super-insulated wall works more efficient as the energy demands were only 28% of the energy that the building needed using the normal Trombe wall. Contrary, during summer, using the super-insulated wall, the energy demands for cooling are more than 50% of the demands by the use of a classic Trombe wall. However, the insulated Trombe wall provides more energy savings on an annual base *(Stazi et al., 2011).*

The thickness of the massive storage wall is also a vital issue of the heat storage capacity that the wall could achieve. A study for different thicknesses investigation based on ISO 13790:2008(E) was done by Briga-Sá et al. (2014) for thicknesses 15cm-40cm increasing each time by 5 cm. The study represents that the heat gains increase with the increase of the thickness in the case of a ventilated wall, while in the case of a non-ventilated wall is the opposite *(Figure 20)* as the heat takes more time to reach the interior. Similar studies show that the optimal thickness for a concrete Trombe

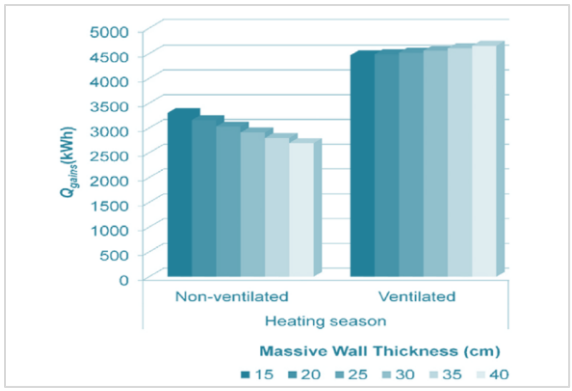

Figure 20: Trombe wall global heat gains depending on the thickness of the concrete massive wall (Briga-Sá et al., 2014).

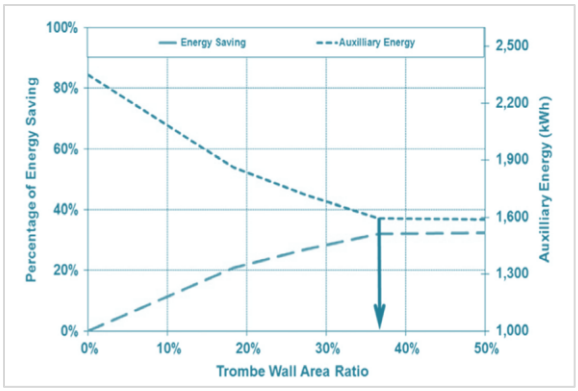

Figure 21: Annual auxiliary energy savings for variable Trombe wall area ratio (Jaber et al., 2011).

wall is 30–40 cm *(Agrawal & Tiwar, 2011),* approximately 35 cm for clay brick Trombe wall *(Stazi et al., 2012),* 37 cm for brick Trombe wall and around 35–40 cm for low-concrete walls and 40–45 cm for high concrete walls *(Fang et al., 2000).*

As it turned out from the literature, the volume of the massive wall can increase the thermal capacity of the wall and, thus, the thermal gains. However, with the increase of its volume, the dead loads increase significantly, which is a problem both for architects and aesthetic reasons and for structural engineers for practical reasons. The phase change materials, after a lot of researches seem to be a possible solution *(Pielichowska & Pielichowski, 2014; Tian & Zhao, 2013; Tyagi et al., 2012,2007; Cabeza et al., 2007)* as they can store a big amount of energy in smaller volumes *(Fiorito, 2012).* Despite the fact that PCM materials can reduce the volume more than half compared with construction materials, they transfer the heat very fast, and this could be an important drawback especially during winter, where heating is needed during the night *(Zalewski, 2012).* Various studies, experimenting with different types of PCM materials and the combination of them, are investigating the PCMs as the future basic heat storage materials. A more detailed analysis of PCM materials is done in the next chapter.

Surface wall Area

The ratio between the Trombe wall area to the total area of the facade has been considered as a parameter that affects the performance of the Solar Chimney by Gomez et.al. (2011). Generally, taking into consideration that the south wall is used, the larger ratio(a), the higher efficiency *(Zhongting et al., 2017).* A study by Tunisia & Abbassi et al. (2014) evaluates the impact of ratio (a) on the energy savings of ta Trombe wall in an annual base and concludes that the increase in the Trombe wall area reduces the heating energy demand. Moreover, a simulation study of a typical Jordanian house with the Trombe wall system on its South side was done by Jaber et al. (2011). In this study, the investigation of ratio(a) is done in terms of thermal and economic points of view by using the Life Cycle Cost (LCC) criterion. As can be seen in figure 21, the annual energy savings are increased by the increase of the Trombe wall to total surface area ratio until the ratio of 0.37, which corresponded to 32.1% of heating auxiliary annual energy savings.

Channel Depth and Height

The depth of solar Wall shaft it consists another crucial element of the Trombe Wall *(Dragic Evic & Lambi 2011)* as it can affect the friction pressure losses and thus the flow resistance and the mass flow rate *(Chen et al., 2003)* and the air temperature *(Zhongting, 2017).* Similarly, the height of the channel can affect the airflow rate inside the chimney and that as the height increases, the airflow increases regardless of

location *(Lee & Strand Richard 2009).* Investigation studies about the depth of the channel and its influence on airflow shows contrasting results while some conclude that the increase of the depth cause friction pressure losses reduction and therefore, the mass flow increases *(Chen et al., 2003)* while other study concluded that the airflow decreases with the increase of the depth *(Lee & Strand Richard 2009).* As an answer if that, Song et al. (2011) mentioned that the effect of the depth on mass flow rate is more complicated and also depends on other parameters like the height and the dimensions of the vent. As it is observed for the size of the vent of 0.1 m in width, the influence of the channel depth is almost neglectable. In terms of depth to height ratio, 1/10 ratio seems to be optimal for the airflow *(Liping & Angui, 2006; Shakeel et al., 2017).* Specifically, an air gap of 0.3m with channel height at 3m revealed as the optimum to increase airflow *(Shakeel et al., 2017).* Additionally, a dynamic simulation of the annual thermal performance of a PV Trombe wall in Hong Kong found that the optimal ratio of depth and height, in this case, is not 1/10 while 0.06, depth, and 3.6m height found as optimal dimensions *(Peng et al., 2013).* Finally, in terms of heat transfer, relevant researches show that the heat transfer drops dramatically if the depth of the channel is at the same order of magnitude as the boundary layer thickness *(Sparrow & Azevedo, 1985; Anderson & Kreith 1987).*

Vents

Generally, Trombe Walls can be categorized in ventilated and non-ventilated *(Yezioro, 2009).* In vented Trombe walls, vents are placed at the bottom and top part of the air channel for air circulation and consist of an important control mechanism of the system for the different operation phase of the solar wall (heating and cooling of the building) *(Hami et al., 2012).* Vented or unvented Trombe wall efficiency has preoccupied many scientists in passive energy research. An essential investigation of ventilated and not ventilated solar walls have to be done by Balcomb and McFarland (1978) who were studied the performance of the two kinds of Trombe walls in nine different climates within United State. The research shows that the vents cause reverse flow, under certain conditions, during the night reducing the performance of the system while the utilization of controlled dampers had been proposed to prevent the reverse flow effect and to prevent overheating. The study in different climate conditions presents that the use of controlled vents in mild climates affects the performance of the Trombe walls slightly, while in severe climates, such as Boston climate, the use of vented solar walls increases the efficiency of the system by 10-20% *(Balcomb $ McFarland, 1978).*

Plenty of studies are conducted in order to define the importance of vents on the efficiency of solar walls and to find the proper dimensions of them. The role of vents is to control the heat loss, which occurs between the outer cover and the massive wall by conduction, convection, and radiation back to the ambient. Consequently, the vents (open or close) change the heat transfer coefficients between the transparent cover, massive wall, and the enclosed air *(Jaber & Ajib,2011).* Furthermore, a simulation study in Energy plus software occurred in three climatic regions of Portugal by Ferreira and Pinheiro (2011) to define the effect of the vent size on the performance of Trombe walls. The study found that the size of the vents is vital and depends on the solar saving fraction. A subcategory in the research of vents is the use of fans to enhance the circulation of heat through the vents. The feasibility of using fans is questionable *(Balcomb, 1992),* as the influence of fans on the performance of the solar wall depends on other parameters such as wall's thickness and climate zone *(Sebald et al., 1979)* and most of the research conducted relies only on computer simulations. A computer simulation for fans which are controlled by thermostats in three different regions, was conducted by Sebald et al. (1979) and shows that the use of fans can improve the performance of solar wall for room area of 37m2 by 22%, 20% and 7% in Albuquerque, Santa Barbara and in Madison respectively. Furthermore, a simulation about the effect of fans on PV solar wall conducted at the University of Science and Technology of China determined that the fan can cause internal temperature to

drop of 0.5C and can cool down the PV cells by 1.28C (between 7:00 a.m. and 05:00 p.m), increasing their efficiency *(Jie et al., 2007).*

2.1.1.2.2 Building Location Parameters

Solar radiation and orientation

The Solar wall technology bases its operation on solar radiation as well as the orientation, and they both play a crucial role in the operational efficiency of Solar Walls. In general, the efficiency of Trombe Wall increases with higher solar radiation as the stuck effect become more intense. Several studies study the effect of different levels of solar radiation on the airflow inside the chimney. An experimental investigation which studies this was conducted by Burek and Habeb (2007) and shows that the mass flow inside the chimney depends mainly on heat inputs and confirmed by a similar study from Yongcai Li and Shuli Liu (2014). As previously mentioned, also the orientation is important as it directly affects the heat fluxes. Speaking about the northern hemisphere, the preferred orientation for Trombe walls is due south, southeast, and southwest *(Krüger et al., 2013).*

Wind speed and direction

The wind speed and direction are also a vital key for the thermal behavior of Trombe Walls. According to relevant research, the performance of the Trombe wall increases with the increase of wind speed between 0-5 m/s and remains roughly the same for air velocities above 5m/s *(Bhandari & Bansal 1994; Dragic Evic et al., 2011).* Similar studies recommend that the effect of the solar chimney was relatively much higher with lower wind speeds *(Moshtegh & Sandberg, 1996),* while in other studies, the solar wall was suggested to be working under zero ambient airspeed *(Tan & Wong, 2014).*

2.2. Building Integrated Photovoltaic Thermal Systems (BIPV/T)

BIPV/T systems is a promising technology for sustainable construction, which makes use of the building envelope to produce electricity by photovoltaic cells and to utilize the thermal energy generated by them for other domestic applications, reducing the total building energy consumption. In other words, it is a hybrid system that combines the function of PV and solar collectors. The BIPV/T systems not only provide a multiplicity of functions but also increase the electrical efficiency of PV modules as a cooling fluid is used to remove thermal energy from BIPV systems and store this thermal energy *(Ricardo, 2015).*

BIPV/T systems are a recent concept, although the idea of PV/T technology began in the 70s *(Wolf, 1976; Florschuetz, 1979).* During the 90s they started emerging while in 2000 they swept interest due to its great potential to be an important solar application promoting net-zero energy buildings *(Yangn & Athienitis, 2016).* The first implementations of BIPV/T systems have been done in North Carolina, in the United States on a roof of a restaurant *(Hayter & Martin, 1998)* for electricity and hot water and in the Aerni Fenster factory in Switzerland which consists the first facade BIPV/T system in Europe *(Eiffert, 2000).* Moreover, although the technology of BIPV/T systems has been discussed a lot as a category of PV/T systems, there is a lack of literature about the particular case of BIPV/T systems and especially for facade BIPV/T systems, considering their building integration configuration, difficulties etc. *(Yangn & Athienitis, 2016).*

2.2.1. Typologies

BIPV/T systems can be categorized according to the fluid or material is used for heat recovery. Hence, the BIPV/T systems could be categorized in air-based systems, water-based systems, and phase change systems, which recently attracted interest. Additionally, the collaboration of these systems with

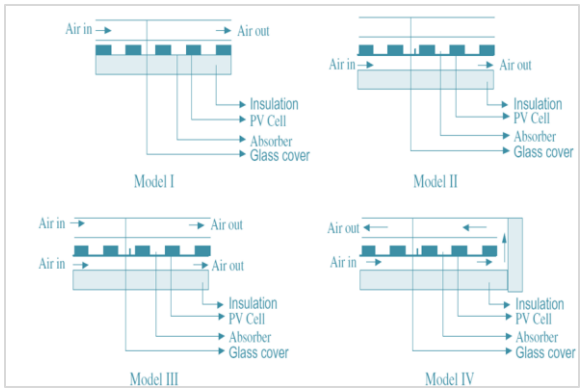

Figure 22: Various PV/T configurations (Hegazy, 2000).

other energy systems of the building generates an extra subcategory of the above categories of hybrid BIPV/T systems.

Air based BIV/T systems

The air-based BIPV/T systems have as a heat removal medium air, which is lightweight, easy to transfer, and it does not need specific maintenance, providing flexibility on their application on various building elements. As it can be seen in figure 22, a typical PV/T air system is constructed by attaching an air cavity below the PV while another common configuration locates the air gap above or on both sides of the absorber *(Hegazy, 2000).* The air-based PV/T and consequently, and the BIPV/T systems can be categorized in active and passive systems (which are based on buoyancy force) *(Yangn & Athienitis, 2016).* The active systems are usually implemented in an open-loop system in which ambient air, using a fan, is sucked and passes through the air channel in order to remove air from PVs for better PV performance. The passive air-based PV/T systems, a natural air force is used for air movement; therefore, extra ducting or fans are not usually required since the heated air is either exhausted into the atmosphere or fed into the building. Trombe walls with PV fall into this category. In this system type of installations, thermals issues must take into consideration during the design process as the system have an interaction with the indoor climate conditions.

Water based BIPV/T systems

The water-based PV/T systems use water as a heat absorber medium because the water has a high heat capacity and good optical properties *(Tian & Zhao, 2013).* Conventional designs of PV/T water collectors have the thermal absorber attached to the back side of PVs. Their connection is made by high conductivity thermal paste *(Zondag, 2003; Ji et al., 2007)* or welding *(Kalogirou & Tripanagnostopoulos, 2006)* or mechanical force *(Fraisse et al., 2007).* Moreover, the water has natural compatibility with Pv modules *(Palmer & Williams, 1974; Robles-Ocampo et al., 2007).* Water absorbs solar light mainly on infrared region, and due to its absolute transparency at the short-wavelength area, long-wavelength irradiation is absorbed warming up the water while short-wavelength irradiation can be utilized by Photovoltaics to produce electricity *(Robles-Ocampo et al., 2007).* However, water-based PV/T systems are difficult to respond to in extremely cold climates where the collectors can easily break up *(Gang, 2012).* Usually, water-based PV/T systems are combined with domestic hot water systems or heat pump systems.

2.2.2. Applications of BIPV/T systems

The concept of BIPV/T systems is to have a double role in buildings. First, an architectural role is replacing the conventional building components totally or partially, and a mechanical-functional role is participating in the energy system of the building. The integration of PV/T systems on the building is not a simple addition and requires proper analysis and design. BIPV/T technology applied on the envelope of the building and typically, either on the roof of its facade. Facade applications are implemented usually as additional elements such as vertical curtain wall, inclined curtain wall, or stepped curtain wall, while roof applications are normally inclined roofs or skylight monitors *(Ricardo, 2015).* The integration of this kind of system on a building works as an energy provider, and consequently, it depends on the building demands and the function that they want to enhance (heating, cooling, ventilation). Also, the selection of the heat removal material is an important issue that affects the design of the system and

depends on the location and the application purpose. However, most of BIPV/T applications are air-based because if difficulties on liquids in maintenance.

Additionally, by the application of BIPV/T technology covering part of the building envelope, the building performance of the building is influenced. Due to the addition of material layers, the U-value of the building envelope changes, especially if the coverage is a lot. Therefore, the heat transfer between the interior space and the ambient changes influencing the thermal behavior of the building. Moreover, the use of conventional opaque PV modules obstructs the solar radiation to reach the envelope as it works as shading layers of the structure. With semitransparent PV modules, the phenomena are less obvious, but they affect the transmittance of light and, therefore, passive lighting performance of the building. All these parameters have to be considered in BIPV or BIPV/T technology. However, recent studies and application analysis focus only on the efficiency of the system, excluding the effects that the system causes to the building performance itself. Below, real and experimental application examples are listed and are categorized on facade and roof applications.

Facade

Facades applications of photovoltaic thermal are mostly an additional intervention in the building and work as cladding front of thermally insulated envelopes. Although that facade application is more challenging to be connected with other systems of the building, different applications based either on the water, air, or phase change materials have been done. An important theoretical study for the application in relation to water as a working fluid of PV modules is done by Chow et al. (2003,2007-2010). Moreover, a wall-mounted water PV/T system was performed by Ji et al. (2003,2006). In this study, the performance of PV/T evaporator system in collaboration with heat pump was experimented in real conditions and concluded that this system improved the coefficient of performance (COP) of the heat pump significantly *(Ji et al., 2008,2009; Liu et al. 2009).* A design of facade BIPV/T system

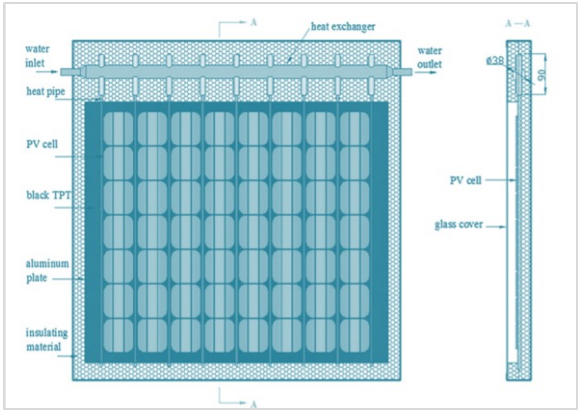

Figure 23: Scheme of a typical tube heat pipe PV/T system (Ibrahim et al. 2014)

for both electricity and hot water design by Ibrahim et al. (2014). In figure 23, an example of the system is presented. A spiral flow absorber adhered to the back of the PV is absorbed the heat and warm up the water.

Air-based PV/T systems installed either themselves as cladding systems or in combination with Trombe Walls. A BIPV/T collector for cooling was designed by Chemisana et al. (2013) to reduce cooling loads during the summer of a three-story building in Barcelona. The proposal design uses Fresnel reflectors both to prevent direct solar rays and for illumination control of the building. The project covers 540m2 and shows to cover 39% of the cooling loads that the buildings require *(Chemisana et al., 2013).* An innovative and complicated air-based window system was developed by Davidsson et. al. (2010) in which different functions are incorporated. The window is functioned as glazing, as electricity and hot water generator, and as a shading system for the window. In figure 24, the proposed BIPV/T window system is illustrated. The horizontal reflectors are movable and work as shading on its vertical position and as solar heat reflectors, to heat up the room, on its horizontal position. The results of the research show that 40% of the electrical energy generation was the account from diffuse radiation and that the system reduces annually the auxiliary energy by 600kW *(Davidsson et al., 2012).* Moreover, heat pipes pass through the front part of the reflectors to warm up water *(figure 24).*

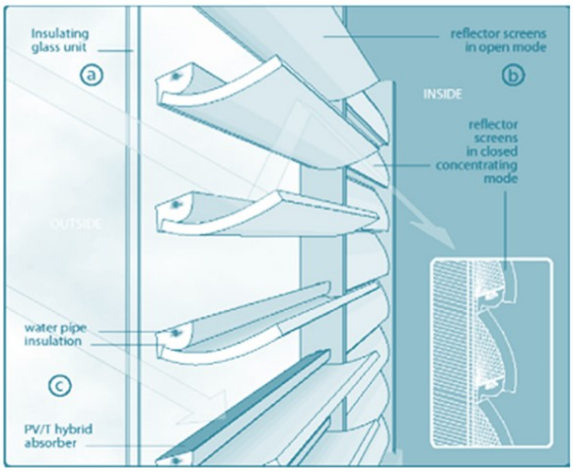

Figure 24: Schematic of the window-integrated concentrating BIPV/T system (Davidsson et. al., 2010).

As previously mentioned, installations of air-based BIPV/T technology are combines with Solar walls. A full-scale prototype is proposing an open-loop and highly efficient Unglazed Transpired Collector (UTC) for an office building, investigated by Athienitis et al. (2011). As can be seen in figure 25, the system consists of dark porous cladding, through which ambient air is sucked and heated by absorbed solar radiation and dark aluminum frame to maximize heat absorption and to create a nice aesthetic view of the system. Also, the PV coverage of UTC was based on the needs of ventilation and electricity of the building, in this case, the proposal is not an additional element to the facade but constitute itself the building wall and creates a ventilation system to provide preheated air to the building *(figure 25).* Although a comparison between this innovative system with common BIPV/T system shows that is slightly less efficient *(Athienitis et al., 2011),* this concept was further applied an addition at the John Molson School of Business (JMSB) at Concordia University in Montreal, Canada (see figure) and provided 24.5kW and 75kW, electrical and thermal energy respectively. Furthermore, another study by Ji et.al (2007) proposed BIPV/T Trombe Wall system and concluded that BIPV/T Trombe Walls

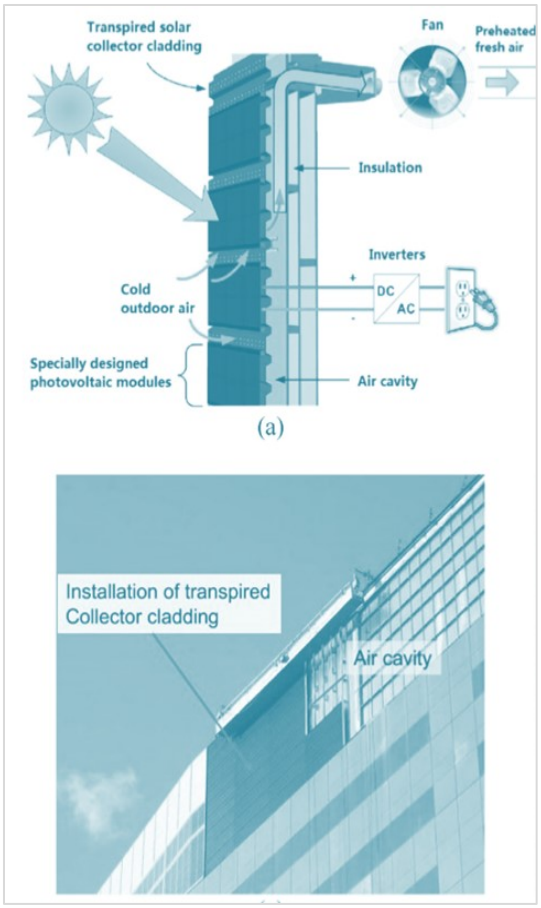

Figure 25: Schematic illustration and a photo of a BIPV/T system integrated with UTC (Athienitis et al., 2011).

could increase the inside temperature more than classic Trombe Wall systems. The same observation, revealed by Jiang et al. (2008), Koyunbaba and Yilmaz (2012) and Sun et al. (2011).

Finally, other innovative experimental facade applications were presented by Aelenei et al. (2013, 2014), who studied various configurations and materials. An interesting research for PCM materials in order to regulate the temperature peaks of PV module during the day and release the stored heat during the night. An example of air-based BIPV/T configuration is illustrated in figure 26. Although PCM materials attracted important attention recently, the application of them is lacking.

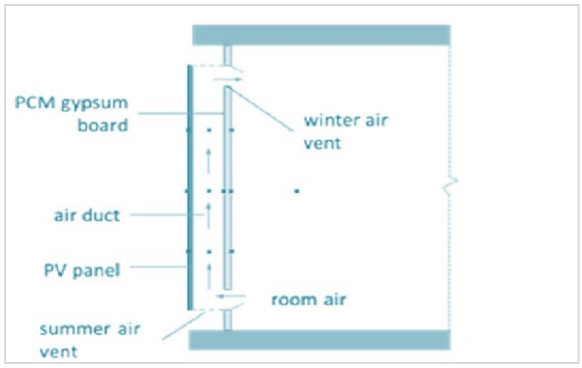

Figure 27: Schematic of the composition of the BIPV/T air system installed in Eco-Terra low-energy solar demonstration house (not in scale) (Chen et al., 2010).

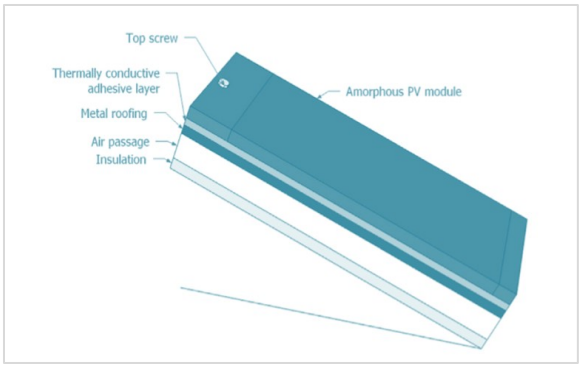

Figure 26: Example of a scheme of an air based BIPV/T with PCM, applied on a facade (Aelenei et al., 2013,2014).

Roof

Roofs consist of the top part of the building, and most of them are horizontally flat or inclined. Therefore, the application of BIPV/t systems is occurred mostly incline due to an increase of PV/ efficiency and absorption of energy by the system. The system is similar to facade systems and is categorized in the same way in air and water-based systems. A BIPV/T system for both hot air and water developed by Assoa et al. (2007), where PV/T system with bi-fluid thermal collectors installed on a rib structure and riched 80% thermal efficiency. Another design for both hot air and water proposed by Jarimi et al. (2013). The unglazed BIPV/T system observed to develop high output temperatures under stable low water flow rate and proper airflow rate, and that it can potentially be used for other applications such as agricultural drying, fresh air warming and domestic hot water heating. Experimental work for roof mounted BIPV/T water collector, investigate the effect of heat recovery on PV efficiency, and asses the PV/T as a solar water collector. Corbin and Zhai (2010) and Yin et al. (2013) studied a complicated water-based roof system with interior room storage. With this idea, the substance of the system was integrated with a building roof providing additional protection of the roof from water penetration and was served also as a structural element.

Equally widespread are the air-based BIPV/T roof systems and they have been applied to various real and experimental cases. A roof passively integrated air BIPV/T system with the use of a ridded sheet steel as an absorbing medium implemented to a manufacturing company building for two years, and it showed that with natural ventilation, the thermal production was less than with forced ventilation. Additionally, Wang et al. (2006), assessed the impact of BIPV/T systems in heating and cooling loads experimenting with parameters such ventilated, or no air gap, close-roof mounted, and conventional roof, while a study by Agrawal and Tiwari (2010) assessed different configurations of BIPV/T air systems, based on life cycle cost assessment. Moreover, an innovational design was the Ecco-Terra design, which challenged with the issue of thermal expansions of the PV and a metal roof *(Chen et al., 2010).* A schematic composition can be seen in figure 27, where the PV glued into the metal roof and affixed using only a screw on the top side of the module. This fixed system results in the delamination of the two parts (PV and the roof), and therefore thermal expansion problems are prevented. The Eco-Terra was constructed in Quebec, Canada, and installed on the roof EcoTerra low energy solar demonstration house in Canada *(figure 27).* The installation measurements of the system show that a difference of 20°C between the PVs and metal was achieved (50-60°C the PVs and 70°C the roof). That proved the effective air cooling of the PV panels. Finally, a research project at the

University of Delaware by Boer and Tamm (2003), examine and compare BIPV/T air and water systems. The results indicated that air collectors are more expensive than water collectors, because of more expensive equipment such as ducting, fins, pumping power, but they can operate in higher temperatures than water systems.

Phase change materials have already been an interesting material and are investigating for many researchers as heat storage materials. An application that PDM combined with a roof air BIPV/T system studied by Lin et al. (2014). The PCM material gave many benefits to the system as solar heating during the day in winter, radiative cooling during the night in summer, extra thermal energy storage, and additional insulation layer of the roof. The results of the study show that the system could maintain a constant room temperature of 18.9 °C during winter in Australia.

2.2.3. Investigation of PV/T and factors that affect their efficiency

Researchers strive to improve the energy efficiency of BIPV/T system, focusing either on the enhancement of heat production or for the PV performance improvement. Also, experimentation studies evaluate the combination of BIPV/T system with another system of the building. Therefore, more complex systems are created, and sometimes additional components make the system less efficient than simple systems *(Ricardo, 2015).* Improving the performance of systems that include energy conversions, as BIPV/T systems, can serve the concept of neutral-energy buildings reducing their impact on the environment simultaneously. Design parameters such as PV module material properties, absorber properties as well as building parameters like solar radiation, the orientation of the system and wind inputs can affect the performance of BIPV/T systems.

Glazing

Depending on the local climate and temperature conditions, glazing can be added on top of the PV to form an additional stationary air layer and to increase thermal gains. However, the addition of glazed cover can reduce energy absorptance due to the reflection of solar rays by the glass. Glazed or unglazed PV/T collectors and the properties of the optional glazing employ various scientific researches which try to increase solar gains of the system. A PV/T water collector, constructed with polymer absorber, has been assessed with and without glass cover and was aimed to achieve PV temperature below 45 °C for efficiency issues. The study indicates that the water temperature should maintain below 40 °C for an unglazed system and 30 °C for a single glazed system in order to keep the PV temperature lower than 45 °C Sandnes and Rekstad (2002). Also, the result shows that PV/T unglazed system performs better than a standard PV module or a glazed system. The electrical energy output per day for the plane PV module was 306.9 W h, for the unglazed PV/T was 339.3 W h and for the PV/T with a glass cover was 296.2 Wh. In a numerical investigation of air PV/T collector it was discovered that the glass transmissivity is the parameter that affects the electrical efficiency of the system the most, while high transmissivity/low emissivity glass above the photovoltaic cells are proposed as the optimum choice *(Cox & Raghuraman, 1985).* Moreover, a comparison of common PV, PV/T system with glazing, and an unglazed PV/T system in terms of electric and thermal performance of the systems was done by Fujisawa and Tani (1997). The evaluation of the systems shows that the electrical exergy of a coverless PV/T collector is higher than the other systems, while the thermal performance of the coverless system is significantly lower than the other systems due to heat losses from the top to surroundings. Another numerical study by Zondag et al. (2003) revealed that unglazedPV/T systems have poor thermal efficiency and define that double-glazing covers reduce the electrical efficiency of the system dramatically because of low transmission value and the reflection from both glazings. Also, Fraisseet al. (2007) studied water-based PV/T collectors and found that the

electricity output decreases by 28% in the glazed system in comparison with a convention PV module while the electrical output increases by 6% with the unglazed system in ration with PV standard module electrical output. Additional study on glazed and unglazed system indicates that the energetic efficiency of glazed collectors is better than unglazed ones and that site solar radiation, the ambient temperature, are important parameters for the selection of glazing *(Chow et al., 2009).*

Solar cells

Solar cells absorptivity is another important factor mainly for the electrical efficiency of the system, while the thermal performance can be improved by adding coatings on PV surface area. Santbergen et al. (2010), conducted research for coatings and determined that anti-reflective coatings improve both thermal and electrical efficiencies of the system. Contrary, low-emissivity coatings on the PV cells reduce electrical efficiency and increase the thermal performance of the system. Also, he proposed that the white PVF back-sheet of the PV, which is highly reflective to reduce PV temperature (the surface area which is not covered by solar cells), can also be utilized for heat absorption. Furthermore, computational analysis to investigate the system performance with different kinds of solar cells has been done by Kalogirou and Tripanagnostopoulos (2006). For the research, poly c-Si (polycrystalline solar cells) and a-Si (amorphous solar cells) modules are compared. The results present that poly c-Si modules marked greater generation of electricity per unit collector are than the a-Si modules and that their solar thermal contribution is slightly lower. The same authors tested PV/T collector systems with and without glazing on the top for both water and air as the working fluids *(Tripanagnostopoulos et al., 2002).* The prototype measurement indicated that the basic polycrystalline silicon (pc-Si) PV/T model had 3.2% higher electrical efficiency than the simple pc-Si PV module.

Absorption medium

The absorption medium of PV/T systems has a vital role in their performance; the medium absorption affects the thermal gains directly and simultaneously the electrical efficiency of PVs as they work as heat removers. Consequently, thermal conductivity between the PV and thermal absorber can be encouraged further by choosing the material with proper thermal properties and consists of the subject of various scientific studies. Literally, the conductivity can be improved by laminating the PV surface with absorber coatings *(Dupeyrat et al., 2011),* using square instead of round ducts *(Sobhnamayan et al. 2014),* or by replacing Tedlar/PET/Tedlar back surface of the PV by aluminum alloy *(Shan et al. 2013).* A study for lamination of PV/T panels conducted by Bakker et al. (2005). Both solar cells and the sheet-and-tube copper absorber are laminated, and the system coupled with ground-source heat pump and the results shows that the system can cope space heating, hot water and electricity demands of a typical Dutch single-family dwelling. Buker et al. (2014) used polyethylene pipes as absorbers and attached them directly on the back side of PV. The prototype measurements show that the energy performance of the system was improved and conclude that polyethylene tubes are a good solution as they have low maintenance costs, and they can be manufactured and installed. A water based BIPV/T system designed by Yin et al. (2013), where a layer of aluminum and insulation of polyethylene incorporated with the water tubes. The system evaluation shows that the extra layer worked successfully as an absorber and that the system can be used to provide also thermal insulation to building skin. Ghani et al. (2012) investigated the flow distribution and pipe ratio issues; His study concluded that manifold to riser pipe ratio of 4:1 and that 0.44 and higher array aspect ratios lead to more uniform flow distribution. Another study for piping ratios conducted by Bergene and Lovvik (1995) - specifically, tube spacing to tube diameter ratio was investigated. Their study determines that the thermal efficiency reduced to half when the fin width to tube diameter increases, causing a temperature drop of the working fluid. Garg and Adhikari (1999) revealed that both

thermal and electrical efficiency of the system increases with the increase of collector length, air mass flow rate and packing factor while an increase of duct length caused opposite results. In addition, a study by Zakharchenko et al. (2004) indicates that greater performance was observed when the collector's area is more than the PV area.

Packing factor

The packing factor is the fraction of the absorber plate area covered by the solar cells and can affect the performance of BIPV/T systems. Research work for the effect of packing factor on the performance of PV/T hot water system in Malaysia indicates that a rise in packing factor increases the auxiliary heating rate and a decrease of the solar fraction. Also, the results show that by the increment in the packing factor, the electricity production increases for both glazed and unglazed collectors *(Daghigh et al., 2011).* Another study by Santbergen et al. (2010) for PV/T water system with Low-E coating shows that the packing factor of PVs affects the electrical output significantly. The study recommended packing factors of 0.8-1 for higher system performance. Furthermore, computer simulations of PV/T air and water systems found a 13% increase in packing factor results in both thermal and electrical efficiencies *(Cox & Raghuraman, 1985).*

Solar radiation, air temperature and orientation of the system

Basically, the efficiency of PV/T systems depends on solar radiation, and system orientation as the whole concept of PV/T operation is based on solar radiation. The electrical energy production can transform into work irrespective of the environment condition while the thermal energy is fully dependent on ambient conditions *90*This is due to the fact that thermal energy cannot produce work if a temperature difference between the high-temperature source and a low-temperature source does not exist. Additionally, a study by Fraisse et al. (2007), which examines a hybrid system of PV/T and floor heating in low and high temperatures, shows that low temperatures enhance PV performance and prevent overheating of the floor heating system. Also, in high temperatures (100 °C and above), the degradation and yellowing of EVA film were observed.

3 SYSTEM EXPLORARION

The research of the PV-chimney system aims to investigate the architectural integration of the system on building facades and how it can be combined aesthetically and conceptually with the designer's intentions. Thus, different design alternatives are developed, and they evaluated according to functional and geometrical factors. In parallel, the study aims to explore the technical implementation of the innovative system in different climate zones and the different parameters that can affect its efficiency. Therefore, multicriteria Analysis in different scales and hand calculations of different system scenarios will be done to cover both research objectives.

3.1. Design Exploration and Multicriteria Analysis

3.1.1. Design Exploration

For the design exploration of facade and the PV-chimney system, a categorization of the facade itself and of the PV-chimney as an element on it, that creates different facade patterns, is done. This leads to different conceptual design alternatives which are analyzed according to architectural-functional and performance evaluation criteria.

The skins of the buildings are the media between the building environment and the ambient environment, and they have an important functional and aesthetical role. The Building Scale Exploration involves the study of skins of high-rise which are categorized into two main categories according to the "flatness" of the facade. The first category is called "Mask" as it includes the facades where the proposed system covers some parts of the building creating a non-flat skin surface. The second category is called "Full closed mask" and it is referring to the facades where the proposed system is merged with the rest facade components creating a flat final surface *(figure 28).* Then, the conceptual proposals of each category can be incorporated into pattern typologies according to the lines-shapes they create on the facade *(figure 29).* Similar analysis of the grammar pattern of the facades of several high-rise buildings according to different facade items (such as skin patterns, windows, renewable solar energy panels etc) is done by Sharon Sung and Yingjui Tseng (2016). In this research, the

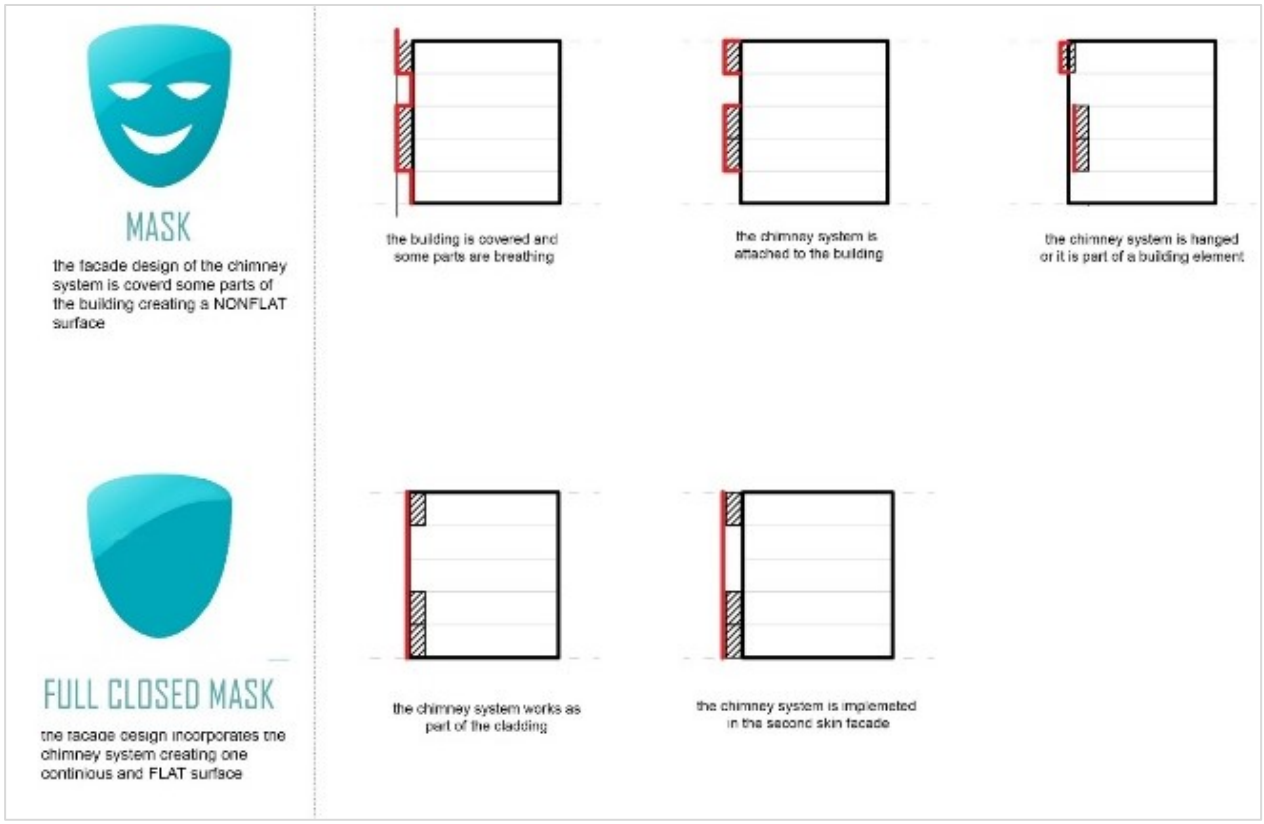

Figure 28: The two main categories of facades according to how they are implementing the PV-chimney system and their "flatness" with their subcategories.

Figure 29: Possible facade patterns.

Figure 30: Classification of the PV-chimney shaft according to its size. First the "Building scale chimneys", in the middle the symbol of "floor scale buildings" and on the right the "column chimneys".

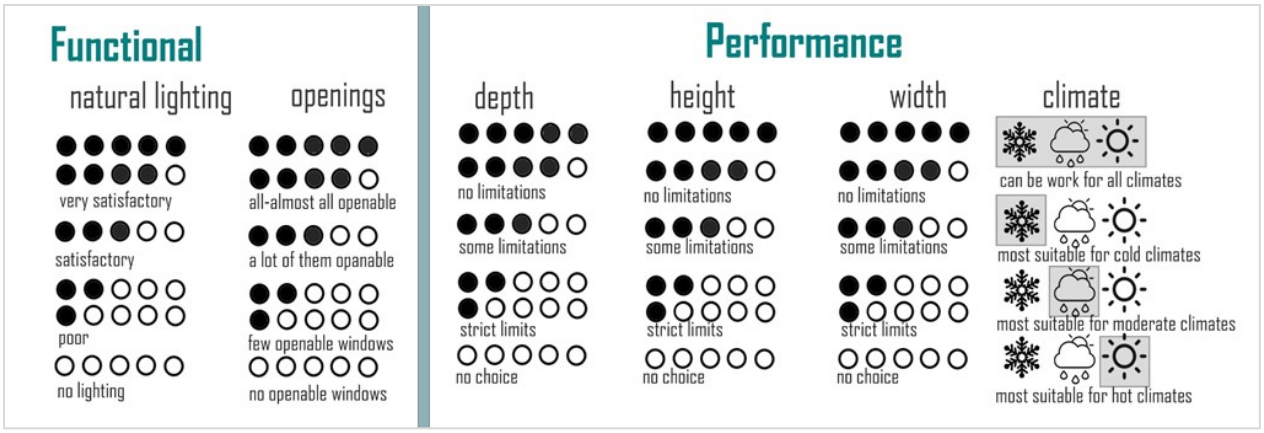

Figure 31: Description of the evaluation criteria.

pattern typologies are based on the shapes that the PV-chimney create on the facade and the relation between transparency and opaqueness.

Evaluation Criteria

The evaluation criteria are based on the functional requirements and the design limitations, in terms of geometrical factors. Firstly, the conceptual facade proposals are evaluated for how much they allow the natural light penetration inside the building for passive lighting and secondly, they are rated based on how much the design allows the window to be openable. Also, they are evaluated for their design limitations in terms of their height, depth and width which could affect their performance (as it is determined in the literature research). The evaluation criteria rates are shown in figure 31.

3.1.2. Shaft Geometry Exploration Typologies and evaluation criteria

The classification of the shaft geometrical characteristics is based on the scale of the shaft in comparison with the whole surface of the facade. Accordingly, there are three categories *(figure 30)*: 1) "floor scale chimneys" which refers to shafts that are applied per floor, 2) "column chimneys" which refers to shafts that cover the whole height of the building or a big part of it and are applied mainly only in front of the structure of the building (not necessarily) and 3) "building scale chimneys" which are applied to the whole facade as a second skin.

As the operation of the system and its efficiency it depends on the geometrical characteristics of the shaft, as it is discussed in chapter 2, the shaft evaluation criteria and aspects are based clearly on their geometrical and climate limitations. These criteria are called "Performance" limitations, as they refer to parameters which can affect the performance of the system and includes depth, height, width expansion possibilities and the climate evaluation criterion, which shows the facade potentials to be adapted in certain climate zone.

3.1.3. Design Alternatives_Analysis and evaluation

As it is described in chapter 3.1.1., the conceptual design alternatives are categorized into "Mask" and "Full closed mask". For each category and its subcategories, conceptual facades are proposed, and they are analyzed according to the typologies and the evaluation criteria which are described above (chapter 3.1.1., 3.1.2.). The facade proposals and their analysis are described below.

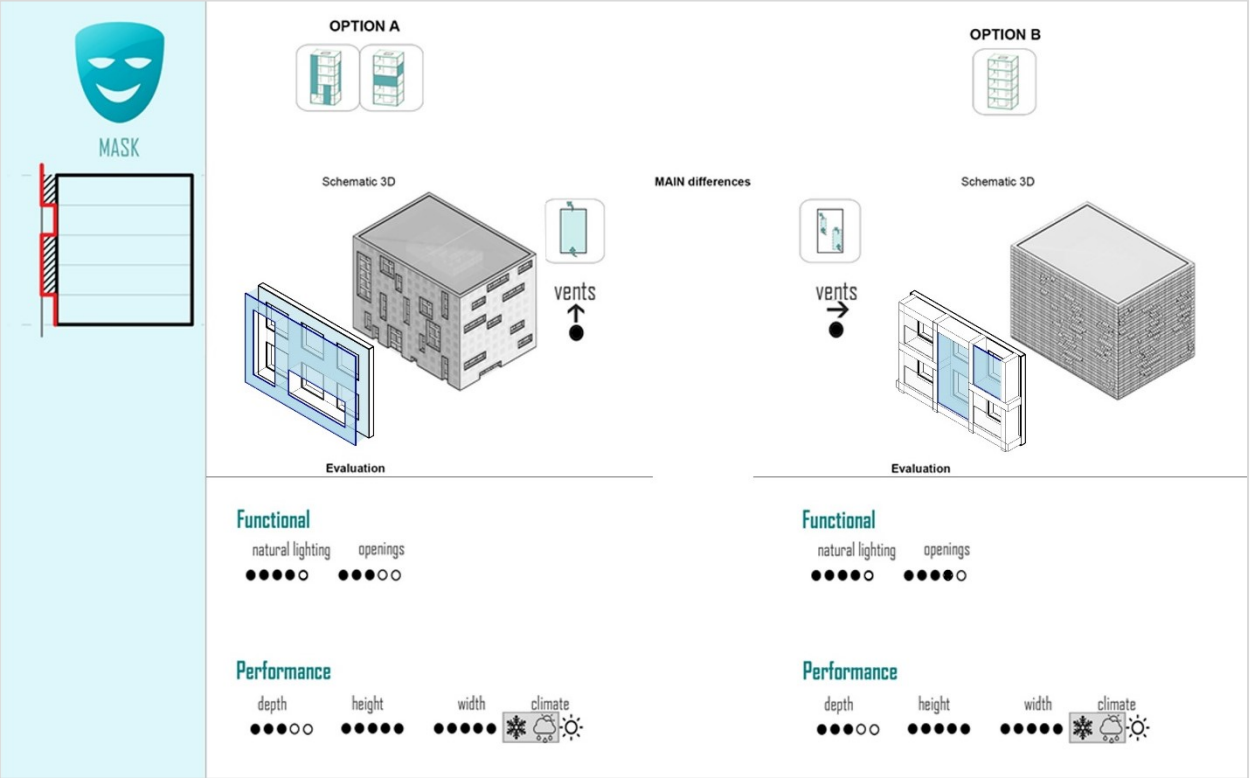

Figure 32: "Mask facades": Subcategory I analysis of the facades that covers the building leaving some parts to breath.

"Mask facades"

This category is split into three subcategories: 1) the facade that covers the building leaving some parts to breath, 2) the facades where the PV-chimney system is attached to the building and 3) the facades where the PV-chimney system is part of a curtain wall facade or it is part of the building elements.

In figure 32, two options of the subcategory I can be seen. The first proposal represents the idea of a building with second skin facade (which it is works as the shaft of the system) with holes, which follow the grid of the structure and leave some parts of the building to be openable for fresh air. With this concept, the designer is free to create vertical and horizontal patterns or a combination of them. Moreover, in terms of natural lighting, this concept offers the possibility of natural lighting through the non-openable windows which are located inside the shaft and the openable windows of the holes. On the other hand, there are overhangs around the openable windows and there is an attenuation of light rays when they pass through the first layer of glass and then through the non-openable glazing. Therefore, is rated medium to good in natural lighting. In terms of openings that can open, is rated bad to medium since the facade it works as one shaft. That means that a lot of "holes" can disturb the air flow inside the shaft and reduce the whole efficiency. The geometrical evaluation of the system is good as the width and height can be controlled by the designer with the use of "holes". However, the depth is limited because of the extra weight which can add, and this concept is not suitable for warm climates as the transparent double skin would warm up the building structure.

The second option is also representing a split unit that can create a second layer in front of the extensions of building. The main difference between the two proposals is that the second layer of option B is covered the whole building and the pieces in front of the openable windows use the second skin

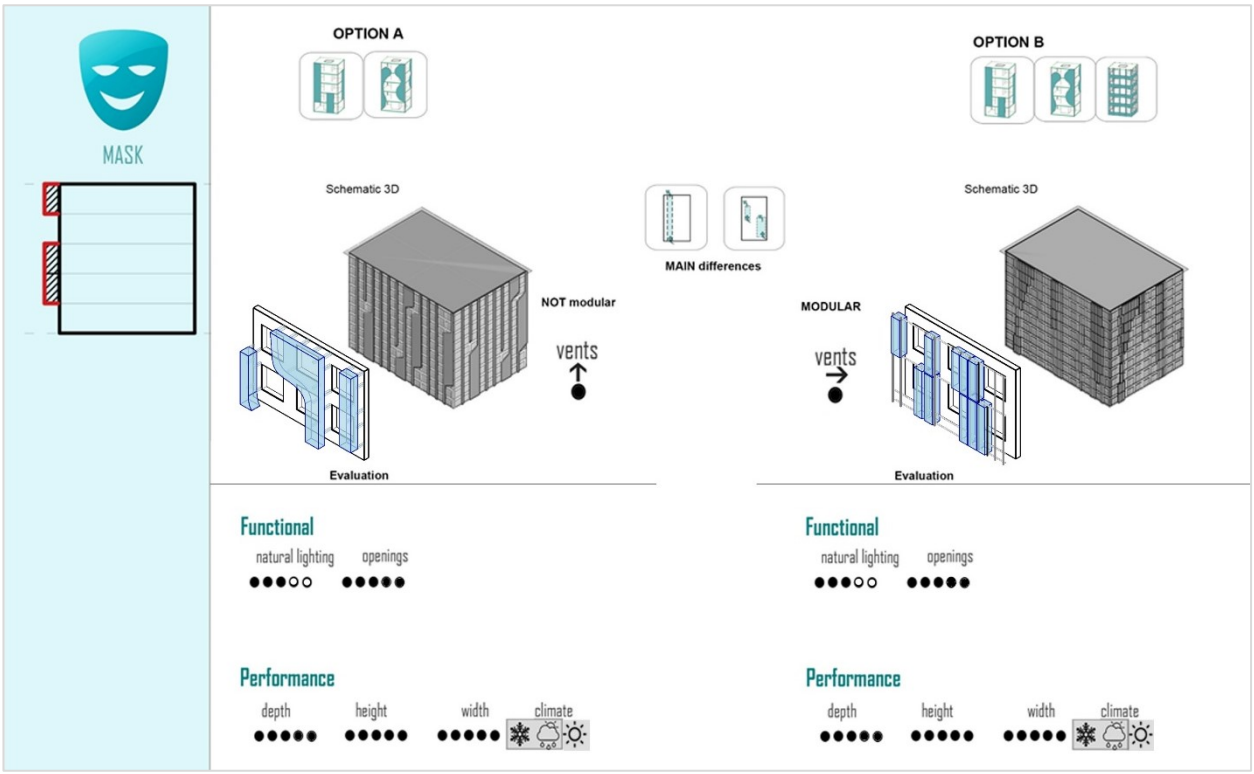

Figure 33: "Mask facades": Subcategory 2 analysis of the facades where the PV-chimney system is attached to the building.

as an extension of the space. Furthermore, the PV-chimney system in this case is split into pieces and covers the favorable areas. Consequently, the number of openable windows and the size or shape of the system's shaft could be more efficient for the building function. Accordingly, in the category of openings is rated as good while in natural lighting is rated medium to good because of the overhangs. Moreover, the geometrical characteristics of the PV-chimney is fully controlled by the designer. However, it can also be risky for hot climates.

The second subcategory refers to the design where the PV-chimney is attached as an extra element with its own structure in the front of the building. Two proposals of this subcategory are shown in figure 33. At the first option the PV-chimney system, in a free from shape, is attached in front of the facade covering the favorable areas while in the second option, the PV-chimney is added according to the building grid, maintaining the initial main lines of the facade. Although the additional skeleton follows the facade lines, the ability of addition of PV-chimneys in any skeleton unit can also provide free form solutions. Moreover, the second option offers the development of the structural and the PV-chimney itself in modules for mass and faster production and assembly. In both cases the openings of the facade have some distance from the additional skeleton. That means that all the windows can be openable (it depends on the distance of the additional skeleton to the facade) but some of them are partly shaded due to the additions of the front. Accordingly, both options are rated good in the category of openings and medium in natural lighting. Moreover, in terms of geometrical characteristics, both proposals can provide plenty of design ideas.

In figure 34, two options of the third subcategory are revealed. In this category the PV-chimney is a separate independent product that can be fixed on any kind of facade. The first option shows a product that comes prefabricated and is hung from the existing building structure where is needed. In this case, the system is modular and every product works

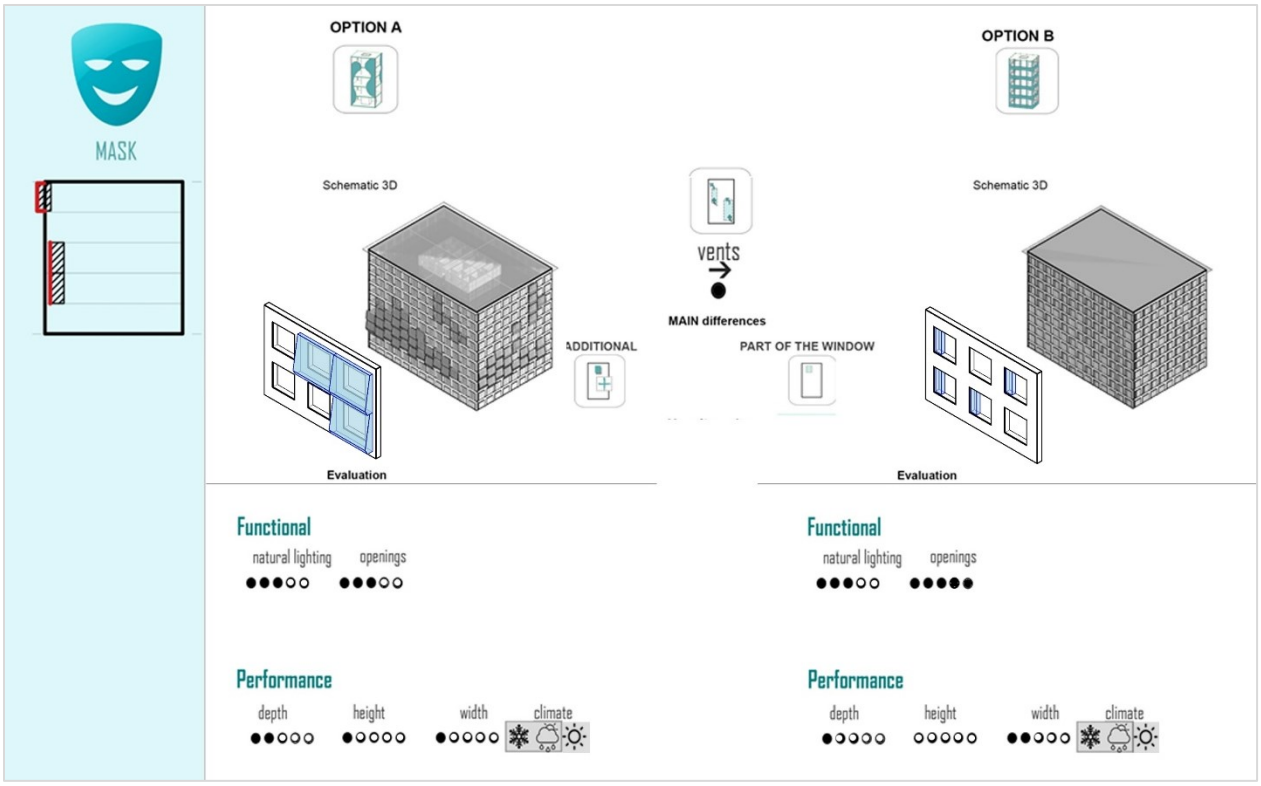

Figure 34: "Mask facades": Subcategory 3 analysis of the facades where the PV-chimney system is hung, or it is part of the building element.

independently. This addition presupposes that a big part of the mechanical installations will be part of the product and that the connection with the building should be easy and be designed smartly. Regarding this, it will be a beneficial solution for renovation products where the system should be additional element. In this case, the sizing of the product will depend on the designer but also on the required mechanical space. Additionally, in terms of natural lighting, the consequences cannot be determined as they depend on the dimensions and the placement of the products. However, because of the freedom of their position are ranged medium in both in the categories of openings and lighting while in geometrical characteristics are bad to well due to the need of installation of the mechanical support within the product. The main difference between the first and second option is that the product in the second case is part of the glazing module. It is an additional module that can be connected with the mullions of the glazing units. The product could be implemented from the initial design or later by the change of glazing units (probably renovation of facade for higher energy performance). Moreover, option B, is marked high in opening and medium on natural lighting because of the reduction of the glazing surface area. In terms of geometrical characteristics, it is limited to glazing sizes while its placement in favorable areas can create a strict of a free form pattern of the facade.

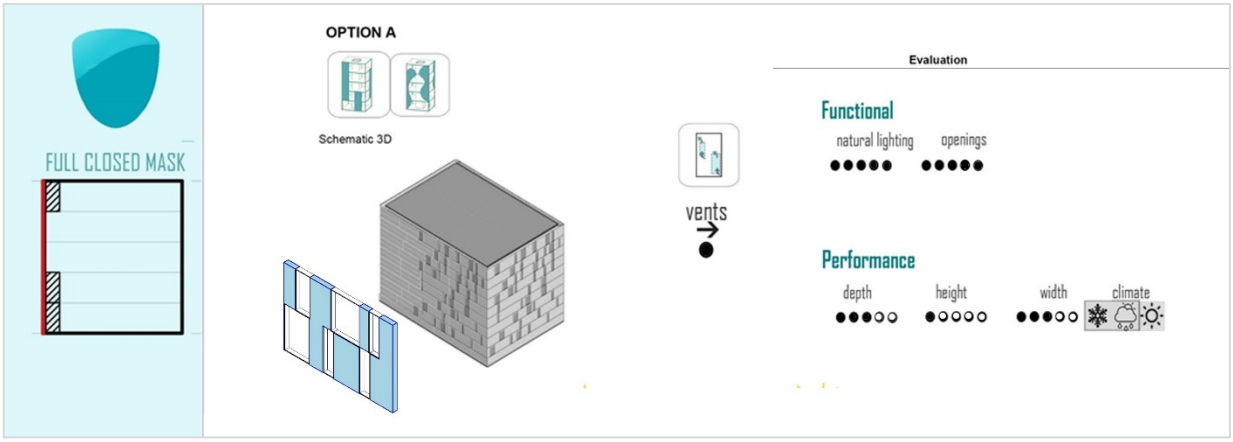

Figure 35: "Full Mask facades": Subcategory I analysis of the facades where the PV-chimney system part of cladding.

"Full closed mask"

In this category there are the facades where the proposed system is added as part of cladding and the facades where the system acts as a second skin creating a flat facade surface.

A conceptual visualization of the PV-chimney as cladding can be seen in figure 35. The proposed system in this design scenario it is implemented on the facade from the stage of the initial design and it is appeared as part of the cladding. By the addition of the system as the opaque part of the building, while the rest are transparent, a lot of different kinds of patterns can be achieved by a clear design view of contrasts. Moreover, regarding the mechanical support of the system, the fact that the system has a direct access to inside, provide an advantage in mechanical installation and maintenance. Furthermore, the system it follows the height of the facade module while in width it is free to expand. Therefore, in geometrical characteristics is marked medium and high for the openings as it does not prevent any window configuration. In terms of natural lighting, it will be a design choice according to the favorable pattern. Accordingly, this category is rated high in natural lighting.

The second subcategory represents a facade design where the system is part of a second skin. The system is fully implemented on the additional skin using the space between the building line and the second skin for the placement of the system. In figure 36, a design where the proposed system is implemented, as a vertical element in series. is presented. In this scenario, the shaft can easily be high covering the the whole building. This idea matches mostly with vertical patterns and provides also the feeling of taller buildings. Furthermore, the fact that the system is implemented within the package of the second skin facade has the risk to be shaded. Second skin facades are usually used as an extension of the spaces containing either shading systems. Consequently, the system, which has to be exposed to the sun, may be temporarily shaded during the day, decreasing the energy generation. Therefore, the idea is mostly for high interventions. The idea is rated with a high score in the category of openings as the amount and large transparent surfaces for openings is determined by the designer. In the category of natural lighting is scores medium

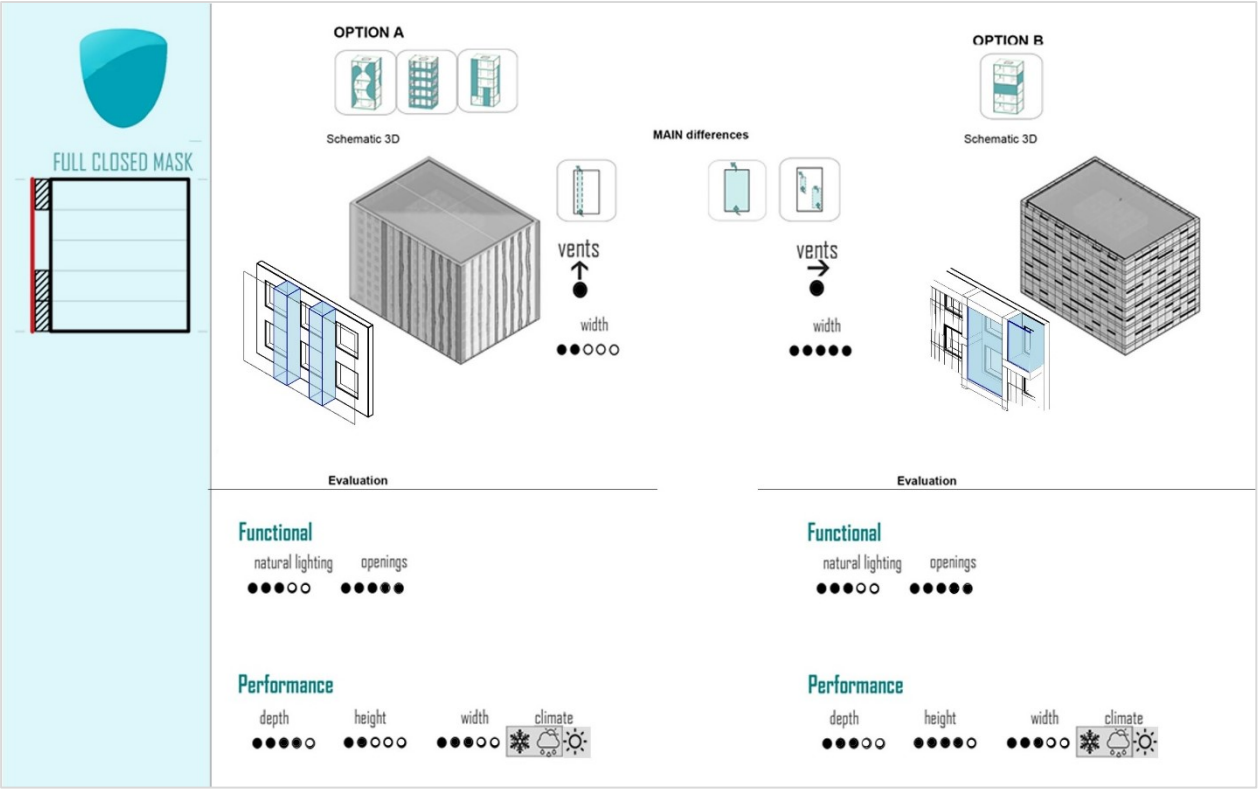

Figure 36: "Full Mask facades": Subcategory 2 analysis of the facades where the system it acts as a second skin creating a flat facade surface.

as the system will be extruded from the real facade and may shadow some parts. The category of Geometrical characteristics is scored low to medium because the design freedom of the system is limited by the height of the floor. The option B represents also a second skin facade where its segments are modular, and the PV-chimney occupies some modules *(figure 36).* That provide the design freedom of different facade patterns as well as the opportunity to combine adjacent modules to create larger systems. For this reason, it is scored high on geometrical characteristics category. In the category of openings is scored high as it does not prevent the openings functionality while in natural lighting is rated similarly with option A.

3.1.3.1. System operation and restrictions

In general, all the design alternatives are included in the three main categories which mentioned above. These main categories can be chosen from before as they can work differently with the active system of the building. The "floor chimneys" are working per floor. During summer can be used for cross ventilation extracting the warm air from inside towards outside passively. For the cold periods can be also used to warm up the indoor air by air circulation. In this case the cold air enters the shaft from the bottom of the room is warmed up and returns to the room. Usually, these systems are combined to the HVAC systems of the building in order to control the air temperature and air flow. Under this scenario, there is a circulation of the same air which is needed an additional filtering before re-enter the room and the HVAC system it has to be work per floor. A common HVAC system for the whole building is not practical and quite complicated for the proper control of "per floor chimneys".

In the case of "column chimneys" and "building scale buildings" the operation of the system is totally different as they have the height of the building. During summer it can be used to cause air movement from inside to outside where the warm air will enter the shaft and it will release out from the outlet of the channel. During winter, the system cannot work per room, the outside air has to enter the chimney and warm up while it goes upwards. Then, the warm air can be used as an inlet to the HVAC system reducing the operation energy demands of the system. Therefore, the HVAC system cannot be independent per floor. An HVAC system for the whole building is needed to unitize the thermal gains.

3.2. Performance investigation

In this chapter, calculations of different scenarios of the PV-chimney system, in different climates and geometrical characteristics are described. As it is explained, the PV-chimney system proposes the placement of PVs in a chimney, in order to utilize the thermal energy from both the chimney effect and the PV operation. In parallel, the air flow within the shaft, is used to cool down the PVs, which, according to the circumstances, may prove to be essential, because of the fact that the increase of the PV temperature, due to their placement on the glass shaft, has a negative impact on the PV efficiency. Therefore, for the enhancement of the cooling of the PVs, a PV/T system is simulated instead of PVs, in order to absorb heat from the rear surface of the PV panels.

A 2D representation of the model is shown in figure 37. The model describes a PV/T system which is enclosed by glass creating a shaft around it. As it can be seen, the PV/t system is simplified in a thin black surface of glass and the water flow as a sheet of water over the entire surface instead of single pipes. Behind the system there is a surface of insulation. For the simulation of the glass enclosure, a surface of transparent glass is placed at a distance from the PV/T system which simultaneously, creates an air cavity between them. For the calculations, climate data for the three different regions (the Netherlands, Hungary and Cyprus) are obtained from a typical mean year weather file by the Climate Consultant 6.0 Software. Moreover, material properties are used as input data which will be presented below.

The investigation of the system in different scenarios is conducted, in order to acquire better understanding of the system reactions in different cases. Therefore, thermal comfort standards are presented below as they will be used for the evaluation of the results. Then, follows a display of the scenarios, the used data, as well as the methodology that is implemented. After that, a section of the results is developed, where the results are discussed and compared. Finally, the last section consists of the main conclusions.

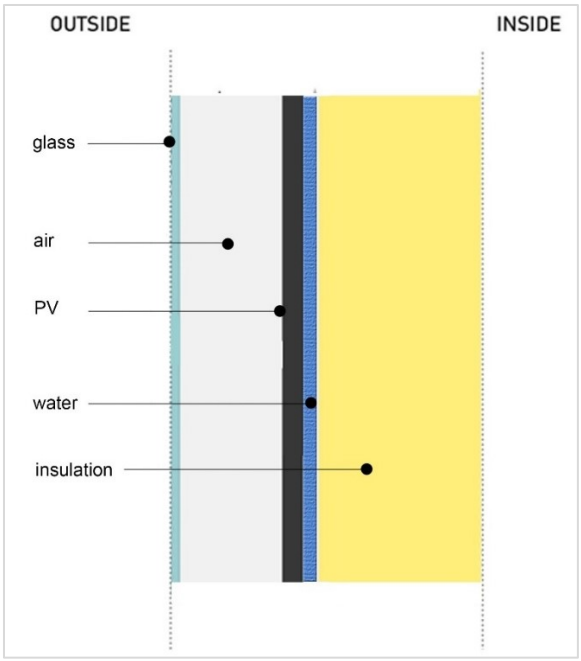

Figure 37: Hand calculations scenario scheme.

3.2.1. Thermal comfort standards

The investigation aims to evaluate the different scenarios based on thermal comfort values which will show if the air or the produced heat can be used. For that, thermal comfort values are used. Thermal comfort is the sense of satisfaction in respects to the environment. Although that each person has different preferences, statistical data are used to define comfortable conditions. In principle, in order to define the conditions of thermal comfort, a lot of factors such as the metabolic rate, clothing insulation of the occupants, air temperature, radiant temperature, air speed and humidity have to be taken into account. For the technical investigation of the PV-chimney, the temperature and the air velocity are the most important factors.

Currently, there are the ISO 7730 *(ISO 7730, 2005)* and the ASHRAE 55 *(ASHRAE, 2010)* where the general comfort conditions are indicated. According to the current standards,

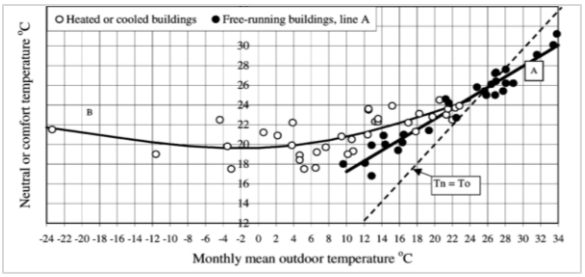

Figure 38: Comfort temperatures from different surveys for heated od cooled buildings and for free running buildings.

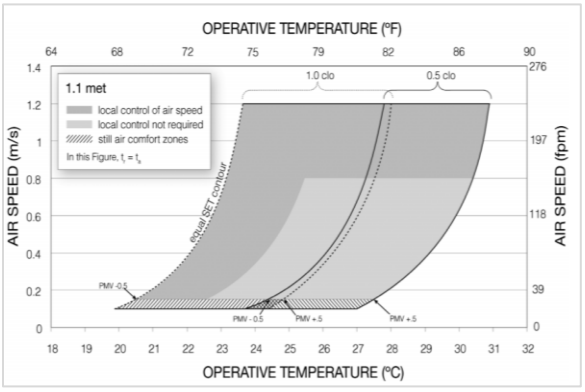

Figure 39: Comfort temperatures from different surveys for heated or cooled buildings and for free-running buildings.

comfortable temperatures are 23 to 25.5 °C (73 to 78 °F) during the summer and 20 to 23.5 °C (68 to 74 °F) during the winter. Generally, the room temperature should be around 22-23 °C and below 24 °C (75 °F). Figure 38 shows the change in comfort temperature for mechanically ventilated and free running buildings with different outdoor temperatures where each point represents the mean value for one survey. As it can be seen, the comfortable values are fluctuated mainly from 20-25°C *(Fengus & Humphreus, 2002).*

Regarding ventilation, the Dutch regulations *(Dr. Van Overveld et al., 2012),* advise a minimum air flow of 25 m^3/h per person(~ 7 dm^3/s) while the desired values during a permanent use of a room is 35 m^3/h per person during winter and 50 m^3/h per person during summer. The air speed limits for thermal comfort, depend on the operating temperature. As it can be seen in figure 39, for room temperatures above 25.5°C (77.9°F), the max value of air speed shall be 0.8 m/s (160 fpm) while in lower temperatures (22.5°C (72.5°F)) the air speed should be below 0.15 m/s (30 ft/min) in order to avoid local cold discomfort due to draft.

3.2.2. Scenarios

For the technical investigation of the system, different scenarios of different kinds of PV-chimney, different geometrical characteristics in different climate regions are analyzed. In figure 40, the different cases are shown. According to the Design exploration of the system and the design alternatives (chapter 3.1.3) there are three main kinds of PV-chimney that can roughly describe any kind of design. These three kinds are based on the size of the system in comparison with the building and are: 1) "floor chimneys": which are described as the systems that expeand and operate within one floor of the building, 2) "column chimneys": that represent PV-chimneys that cover the whole height of the building covering mostly the vertical structural elements of the building and 3): the "building scale chimneys" that represent the system as a second skin. Consequently, the calculation scenarios are divided into three main scenarios. For each kind of system, calculations are done for 3 different climates, in order to understand the reaction of the system and if it can be implemented in different environments. For Moderate climates, the Netherlands is chosen while for Temperate and Mediterranean climates, Hungary and Cyprus are chosen respectively.

Lastly, for each of the aforementioned scenarios, the PV-chimneys are analyzed on different geometrical variations that primarily affect their efficiency. These were considered to be the size of the vents and the depth of the shaft. In order to examine the possibility of natural ventilation by the air within the cavity, the temperature of the air, the air velocity, the pressure difference within the shaft and the produced air flow are calculated. Moreover, the temperature of the glass is found, in order to ensure the safety of the people who may come in touch with it. Lastly, the temperature of the PVs and of the water is calculated, in order to determine the level of the PV temperature (overheating has negative impact on their

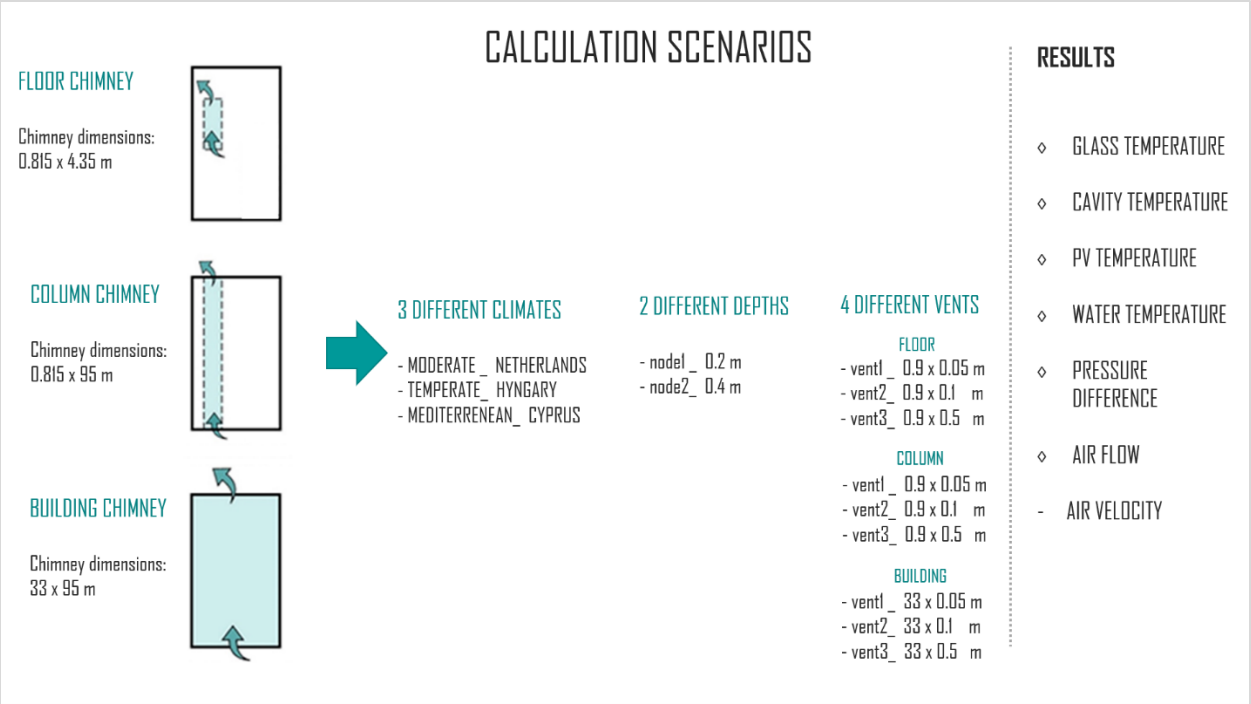

Figure 40: Calculation scenarios.

efficiency) and whether the water flowing in the system can be used as domestic hot water or a heating source as well as to what extent can it benefit the system by coupling other heating sources.

3.2.3. Hand calculations

The objective of this chapter is the calculation of the Temperatures inside the system based on stationary heat transfer and the fundamental "energy conservation law" where the temperatures and heat fluxes are constant in time. Also, for the calculation of the ventilation within the shaft, stack effect equations were used.

3.2.3.1. Climate and General Data

As mentioned above, the weather data are extracted from Climate Consultant 6.0 Software. The information required are the hourly average direct irradiance on a vertical plane and the daily average of sunshine. Moreover, the average temperature during summer and winter were used.

Solar Irradiance

The power per unit area that is received from the sun, when sunlight is falling on any surface, can be described as solar irradiance and it is expressed in W/m^2 *(Landsberg & Sands, 2011)*. The solar radiation can be described in four categories. The total Solar irradiance (TSI) which measures the power of the sun incident on the Earth's upper atmosphere over all wavelengths *(Stickler, 2016).* Second, the direct Normal Irradiance (DNI), is part of the solar irradiance that excludes the radiation that is scattered of reflected along its path and is measured on a surface at a given location. The radiation that is scattered by the atmosphere is called Diffuse Horizontal Irradiance (DHI) and it includes radiation that comes from all points in the sky. Finally, there is the Global Horizontal Irradiance (GHI), that includes both direct and diffuse radiation *(NREK, 2017).*

For the calculations, the direct radiation on a vertical surface (90°C from horizontal) on an hourly average is considered and it is derived from the weather data file of Szombathely in Hungary (with latitude/longitude of 47.27°

North and 16.63° East), of Amsterdam in the Netherlands (with latitude/longitude of 52.3° North and 4.77° East) and of Larnaca city in Cyprus (with latitude/longitude of 34.86° North and 33.630° East). In figure 40,41,42 the solar irradiation for each of the aforementioned regions can be seen per month, based on hourly average. Additionally, in table 1, the average hourly sun load for winter period (as an average of the winter months) and summer period (as an average of the summer months) for the different regions is presented. The rough estimation of the sunshine time per day is calculated by the division of the average daily radiation with the average hourly radiation by the same weather files.

Table 1: Average solar irradiance for winter and summer for Netherlands, Hungary and Cyprus.

SOLAR IRRADIANCE	$[W/m^2]$		
		winter	summer
CLIMATE	COUNTRY		
moderate	Netherlands	120	420
temperate	Hungary	180	450
mediteranean	Cyprus	450	760

Ambient temperature

The temperature of the surrounding air is also necessary for the simulation of the behavior of the system. In the following figures (figure 44,45,46), the average monthly temperature of the Netherlands, Hungary and Cyprus are presented respectively. Also, in table 2, the average winter and summer temperature which are used for the calculations are shown.

Table 2: Average solar irradiance for winter and summer for Netherlands, Hungary and Cyprus.

TEMPERATURE	$[^\circ C]$		
		winter	summer
CLIMATE	COUNTRY		
moderate	Netherlands	4	17
temperate	Hungary	1	20
mediteranean	Cyprus	14	29

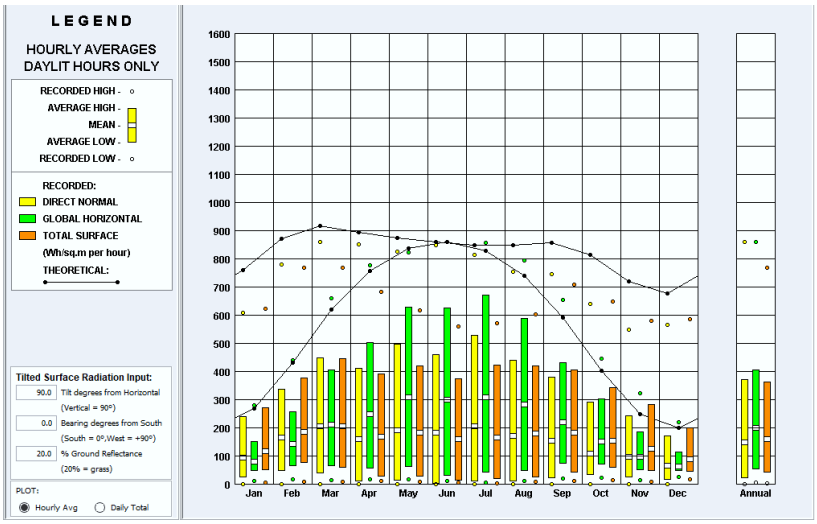

Figure 41: Hourly irradiance range in vertical surface for the Netherlands.

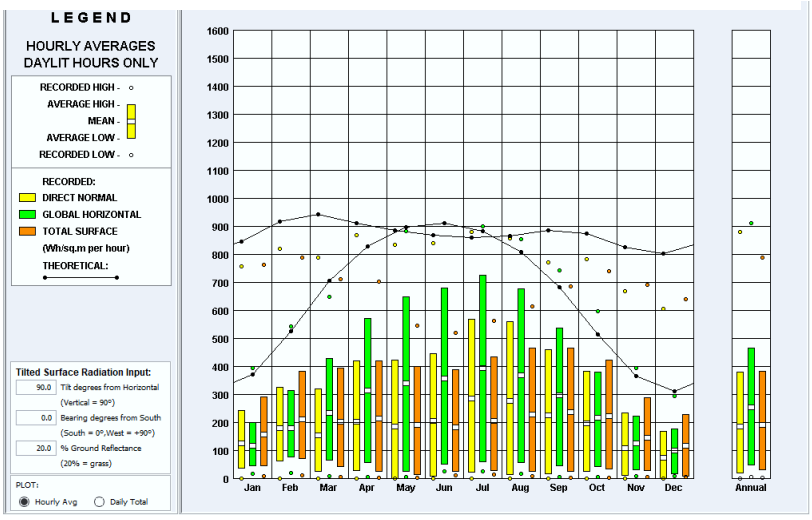

Figure 42: Hourly irradiance range in vertical surface for Hungary.

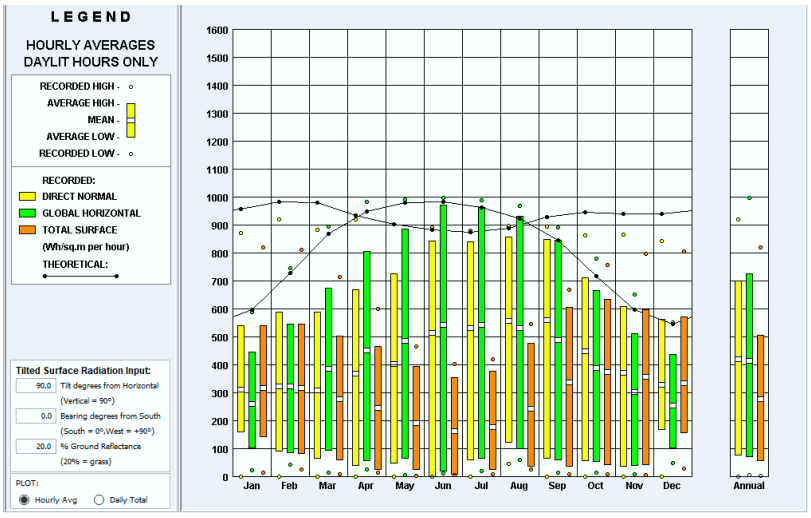

Figure 43: Hourly irradiance range in vertical surface for Cyprus.

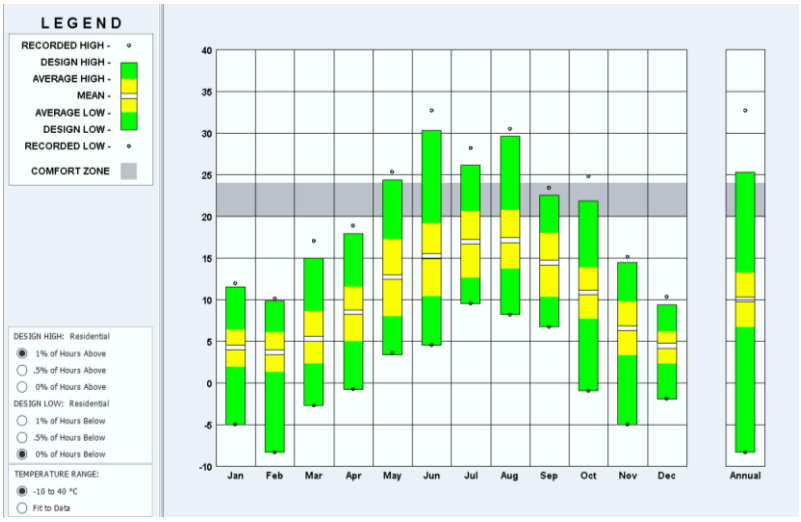

Figure 44: Monthly temperature values in the Netherlands.

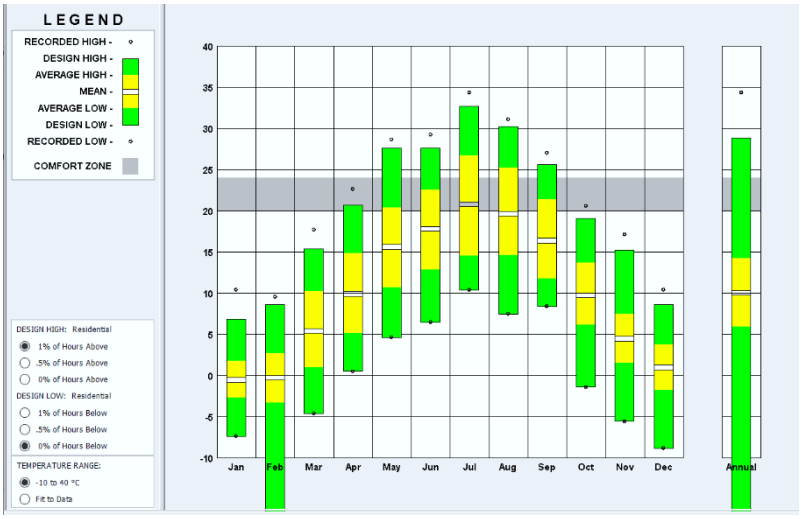

Figure 45: Monthly temperature values in Hungary.

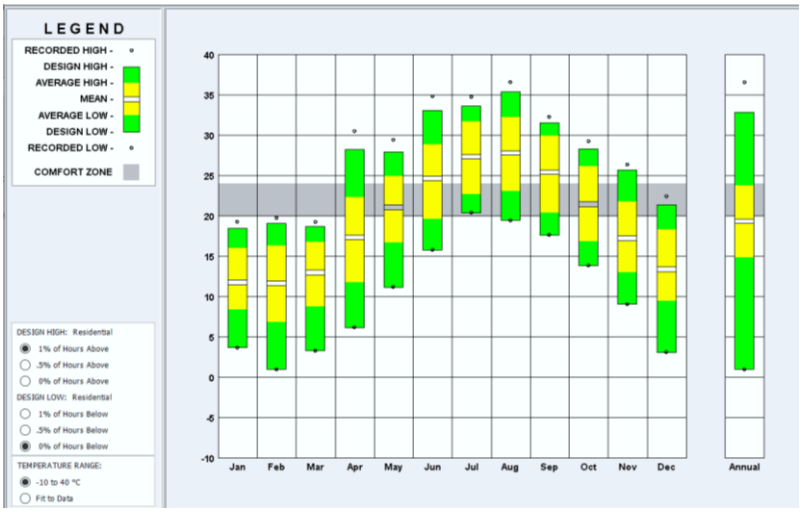

Figure 46: Monthly temperature values in Cyprus.

Table 3: Known values that are used for hand calculation.

	SYMBOL	UNITS (S.I.)		NOTES
air density	(ρ_a)	[kg/m^3]	1.2	it is assumed stable but it is changing accorging to its T
water density	(ρ_w)	[kg/m^3]	1000	
heat transfer coefficient (ambient- glass)	(a_e)	[kg/m^3]	25	
radiation coefficient	(a_{rad})	[W/m^2K]	5.4	it is calculated based on the equation below
$a_{rad} = 6 * a_{res}$			ε_{pv}=0.95	
$1/a_{res} = 1/\varepsilon_{pv} + 1/\varepsilon_{glass} - 1$			ε_{glass}=0.9	
convection coefficient	(a_{conv})	[W/m^2K]	3	
absorption coefficient of the glass	(a_{glass})	[m^{-1}]	0.1	
heat transfer coeefficient (water- PV)	(a_w)	[W/m^2K]	9	
water heat capacity	(c_{water})	[J/kgK]	4200	
water velocity	(v_{water})	[m/s]	0.01	it is assumed
water initial temperature	(T_{water})	[$^\circ C$]	10	it is assumed to be the temeprature of the grid
production efficiency of the PV panel	(e_{pv})	[%]	15	it is based on the average PV efficiency of kameleon solar panels
g-value of glass	(g_g)		0.9	
gravity force	(g)	[m^3/s]	9.8	
wind pressure coefficient	(c_d)		0.8	it is assumed- it depends on the position, wind direction and building geometry

Table 4: Calculation model information for its inlets and its dimensions.

VENT DIMENSIONS	AREA [m^2]
"floor chimneys" &"column chimneys"	
0	no vents
1. (0.9*0.05)	0.045
2. (0.9*0.1)	0.09
3. (0.9*0.5)	0.45
"building scale chimneys"	
0	no vents
1. (33*0.05)	1.65
2. (33*0.1)	3.3
3. (33*0.5)	16.5
PV-CHIMNEY DIMENSIONS	**[m]**
Width	
"floor chimneys" &"column chimneys"	0.815
"building scale chimneys"	33
Height	
"floor chimneys" &"column chimneys"	4.35
"building scale chimneys"	95
Depth	
node1	0.2
node 2	0.4

General Data

Additional data as material properties, thermal properties and mass flow rate coefficients are taken as known. In table 3, the known inputs that are used to complete the calculations can be read.

In figure 47 and table 4 the model as well as the PV-chimney data that are used for the calculation can be read. For the calculations, the model is analyzed in nodes which are presented one by one in figure 48.

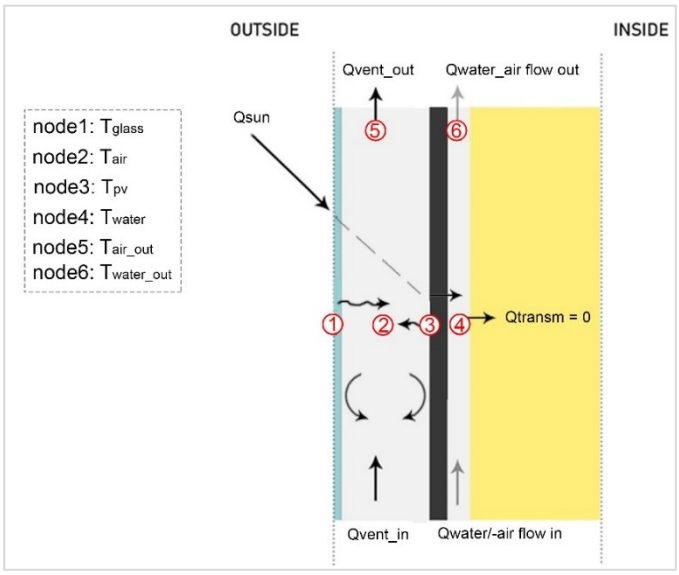

Figure 47: Scheme of the calculation model

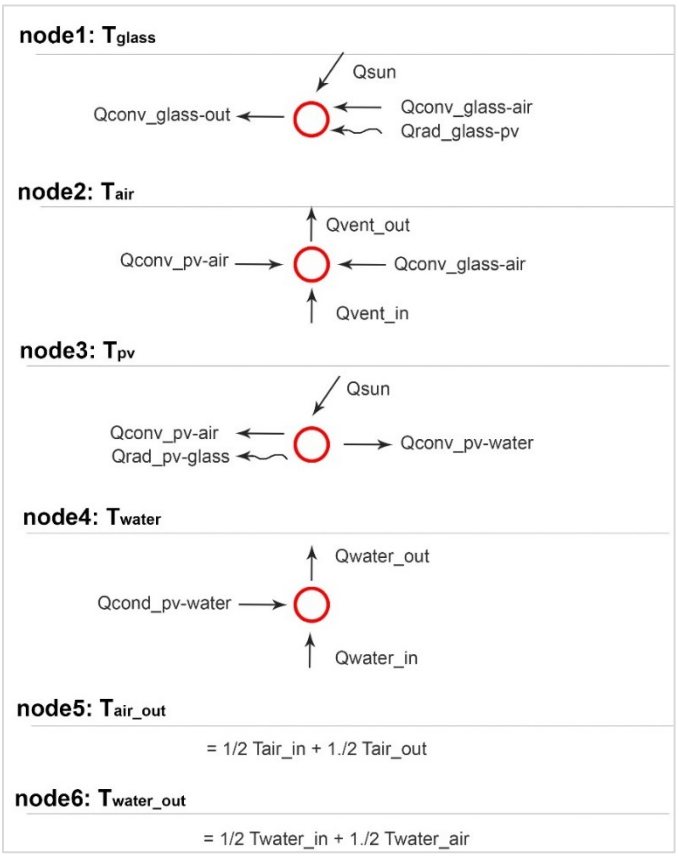

Figure 48: Heat transfer diagrams of the calculation nodes.

3.2.3.2 Methodology

For the determination of the temperature of the above nodes of the system, stationary equations are used. The stationary equations are based on the fundamental "energy conservation law" under which the temperature and heat fluxes are considered to be constant in time. The selection of the stationary calculation method instead of the time dependent calculations is selected because of the amount of control volumes (6 nodes) of the calculation model. Although in the time dependent calculation method the sun affect is more accurate in terms of the sunlight duration during the day and the thermal mass is able to decelerate the internal temperature by time, more than one control problems are complicated to be solved and special computer software is required. For the analysis of the calculation model, the nodes are analyzed separately by applying the "energy conservation law" (eq. 1) where the incoming heat flows have a positive numerical value, while the heat flowing in the opposite direction (outgoing heat flows) has a negative numerical value *(Bokel, 2018)*. In the next step, multivariable equations are solved to define the unknown values of the predefined nodes. The analysis of each single node is descripted below.

The energy transport is determined by three different heat transfer mechanisms: radiation. convection and conduction. The convective heat transfer from the sheets to the air is descripted by equation 2, while the radiation heat transport between two sheets and the conductive heat transfer between two materials can be described by the equation 3 and 4 respectively *(Bokel, 2018)*.. In all the heat transfer mechanisms, it is assumed that the sheets are parallel sheets with uniform surface temperatures. Finally, absorption of solar radiation by the glass and the PV surface is also taken into account while the scattering of reflected solar radiation in the cavity by the glazed sheets (glass and PV surface) has been neglected.

$\sum Q = 0$

(1)

$q_{convection} = \alpha_{convection} (T_{sheet} - T_{air})$

(2)

$q_{radiation} = \alpha_{radiation} (T_{sheet1} - T_{sheet2})$

(3)

$q_{conduction} = \alpha_{condiction} (T_{material1} - T_{material2})$

(4)

The first node corresponds to the outer glass surface *(figure 49).* As it can be seen, there is a heat transfer to the glass due to the sun while convective heat transfer between the glass surface and the ambient air also takes place. Moreover, heat transport by convection between the glass sheet and the air in the cavity as well as by radiation between the glass and the PV surface are also taken into account. Thus, the heat balance equation of the glass is:

$\alpha_{glass} * q_{sun} - \alpha_e (T_{glass} - T_e) - \alpha_c (T_{glass} - T_{air}) + \alpha_r (T_{pv} - T_{glass}) = 0$

(5)

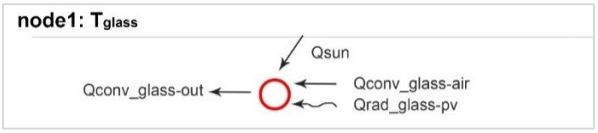

Figure 49: Heat transfer diagrams of the node 1-glass.

The second node refers to the air in the cavity *(figure 50).* In the cavity, the outdoor air is entering from the bottom and is exhausted from the top of the shaft. Also, convective heat transfer takes place between the glass and the cavity air and between the PV surface and the cavity air. Accordingly, the heat balance equation of the air in the cavity described as:

$a_c (T_{glass} - T_{air}) * A_{facade} - \alpha_c (T_{pv} - T_{air}) * A_{facade} + v_{air} * \alpha_r * A_{vent} * \rho_{air} * c_{air} (T_{air\_in} - T_{air\_out}) = 0$

(6)

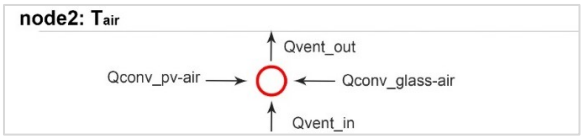

Figure 50: Heat transfer diagrams of the node 2-glass.

The PV panel corresponds to node 3 and its heat transfer representation is shown in figure 51. In this node, convection between the front surface of the PV and the air in the cavity as well as between the rear surface of the PV and the water is done. Moreover, the PV panel received solar radiation and it is radiating heat to the cavity. The heat balance equation of the PV module is:

$A_{pv} * q_{sun} * g + e * q_{sun} * g_{glass} - \alpha_r (T_{pv} - T_{glass}) - \alpha_c (T_{pv} - T_{air}) - \alpha_w (T_{pv} - T_{water}) = 0$

(7)

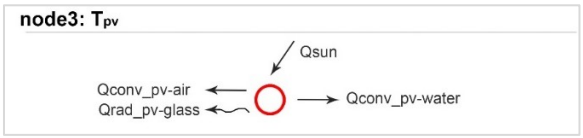

Figure 51: Heat transfer diagrams of the node 3-glass.

The fourth node corresponds to the water behind the PV panel *(figure 51).* The water receives mainly heat from the PV panel while transmission losses between the water and the insulation layer are assumed to be negligible. Also, there is a flow of water from the bottom to the top. In these cases, an initial water velocity and an initial water temperature are assumed (table). The heat balance equation of the water is:

$\alpha_w (T_{pv} - T_{water}) * A_{pv} + \rho_{water} * v_{water} * A_{water} (T_{water\_in} - T_{water\_out}) = 0$

(9)

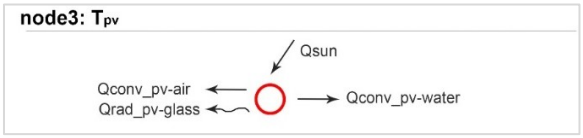

Figure 52: Heat transfer diagrams of the node 4-glass.

The ffifth and sixth nodes are referring to the temperature of the air and the temperature of water in the half height of the cavity. These temperatures are assumed to have the average temperature of their initial and final values. Thus, their equations are:

$T_{air} = ½ T_{air\_in} + ½ T_{air\_out}$

(9)

$T_{water} = ½ T_{water\_in} + ½ T_{water\_out}$

(10)

Except for the temperatures, the analysis of ventilation through the system is equally important for the understanding of the system itself and how different parameters affect its operation. Therefore, the pressure difference, the air flow and the air velocity of the air inside the shaft are calculated.

Pressure differences between one area of fluid and another can cause fluid movement. Dense fluids tend to move towards less dense fluids to fill the gaps and evenly spread the molecules to the whole fluid. Examples of fluid movement due to pressure differences are the Venturi and the Chimney effect. The proposed PV-chimney is designed to cause chimney effect. The air pressure difference is caused by the gravitational force of air, which is linear to the height and the density of air that are related to the air temperature differences. The air inside the cavity of the chimney is warmed up by the sun, therefore, its temperature difference causes its density to drop, which means that the outside air density (ρ_2) is smaller than the inside air density (ρ_1). Furthermore, pressure difference is caused, as a consequence of the chimney height. Although that the density of the air depends on its temperature, the differences are very small *(figure 53)*. Thus, the pressure differences at the top part of the chimney is expressed by equation 11 *(Bokel, 2018)*..

$$\Delta P = \rho g h \frac{\Delta T}{T}$$

(11)

Temperature T (°C)	Speed of sound c (m·s^{-1})	Density of air ρ (kg·m^{-3})	Characteristic specific acoustic impedance z_0 (Pa·m^{-1}·s)
+35	351.88	1.1455	403.2
+30	349.02	1.1644	406.5
+25	346.13	1.1839	409.4
+20	343.21	1.2041	413.3
+15	340.27	1.2250	416.9
+10	337.31	1.2466	420.5
+5	334.32	1.2690	424.3
0	331.30	1.2922	428.0
−5	328.25	1.3163	432.1
−10	325.18	1.3413	436.1
−15	322.07	1.3673	440.3
−20	318.94	1.3943	444.6
−25	315.77	1.4224	449.1

Figure 53: Effect of temperature on properties of air *(De Wit, 2007)*.

The flows through the top and the bottom opening of the chimney, in combination with the pressure difference inside and outside the shaft cause an air flow. The air flow is linear to the size of the effective opening, the discharge coefficient and the square root of the pressure difference divided by the air density. The air flow *(Q)* is measured in m^3/h and is given by the equation 12 below *(Bokel, 2018)*.:

$$Q = A_{eff} C_d \sqrt{\frac{2\Delta P}{\rho}}$$

(12)

Where,

-*Aeff*: the effective opening. For similar openings, the effective can be calculated by the following way:

$$A_{eff} = \frac{A}{\sqrt{2}}$$

(13)

-*Cd:* is the discharge coefficient which depends on the geometry of the opening and the type of the flow (Reynolds number).

Finally, for the calculation of the air velocity inside the cavity the equation 14 is used. This equation describes the relationship between the wind velocity and the wind pressure.

$$v = \sqrt{\frac{2\Delta P}{\rho}}$$

(14)

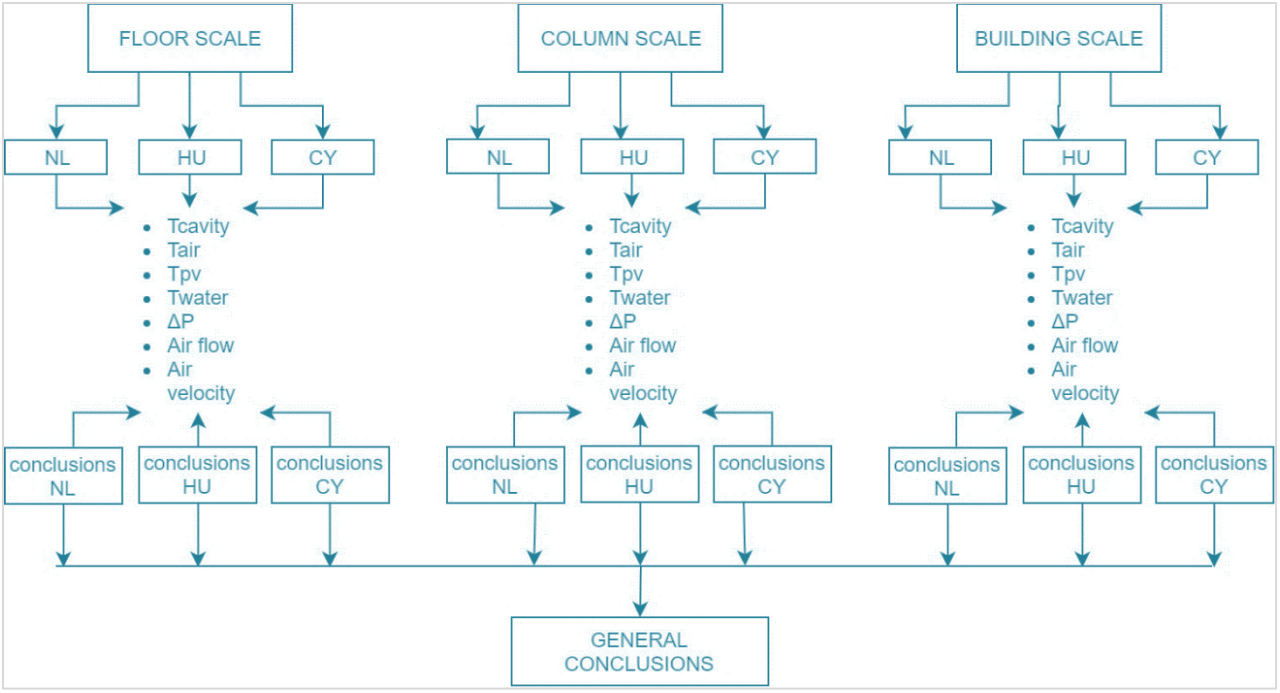

Figure 54: Diagram of the analysis of the results

3.2.3.3. Results and Analysis of the results

The calculation of the temperature of the system and the natural ventilation that discussed above are used to investigate the performance and the effect of important variables on the system. The naturally ventilated façade design combined with electricity system is analyzed to compare different topologies under different weather conditions. The results of the calculations are presented according to the scale of the system. First the results of PV-chimney systems that are limited to floor height and small length are presented for the different climate regions. Then, the "column chimneys" and finally the "building scale chimneys" as the figure 54 shows. After the discussion of the results of each scale and each climate, conclusions for each climate are presented. Finally, according to the analysis of all the cases, general conclusions are developed. The diagram bellow explains the presentation logic of the results.

3.2.3.3.1. "floor chimneys"

3.2.3.3.1.1. Moderate climate

3.2.3.3.1.1.1. Results Netherlands

A) Temperatures

Air of the cavity and glass temperature

According to the results, in the Netherlands, the temperature difference, for the ventilated shafts, of the air inside the cavity and the ambient temperature increases by maximum 3 degrees, during winter, (reaching approx. 7°C, for the small-vent scenario) and by maximum 5 degrees, during summer (reaching approx. 22°C, for the small-vent scenario). The maximum difference is marked, in both cases, in the scenario of small vents (0.9x0.05m) with a cavity depth of 0.4m *(figure 55,A)*. This shows that the increase of the depth, causes a slight rise of the temperature in the cavity. The latter is mainly caused due to the drop in the air change rate within the shaft, since the volume of the air increases and the vents remain small. However, the differences are negligible. In parallel, the same reaction is observed by the decrease of the vents

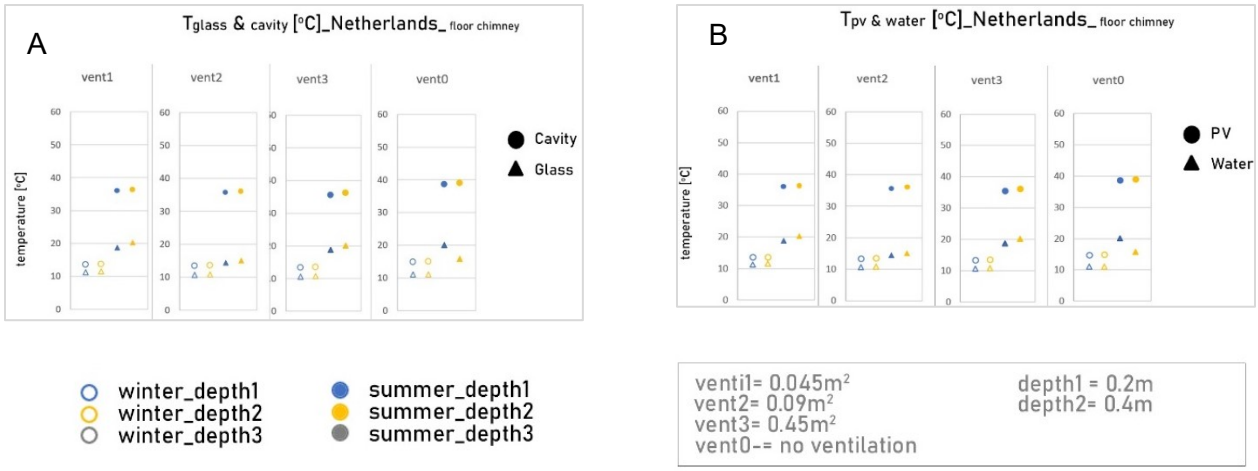

Figure 55: A) The glass and cavity temperatures for the Netherlands of the "floor chimney", with different vent size and depths (colors) for winter and summer. B) The PV and water temperatures for the Netherlands of the "floor chimney", with different vent size and depths (colors) for winter and summer.

surface area (vent1 is x 10 smaller than vent3). The changes in temperature for both summer and winter are negligible. Apparently, in the case of the non-ventilated shaft, the temperature difference of the air in the cavity and the ambient air is higher, especially during summer. During winter, the temperature increases by roughly 14°C (reaching approx. 18°C) while in summer the temperature of the cavity reaches 46°C (29°C difference from the ambient temperature). Accordingly, during winter periods, it is beneficial to have the vents closed, as the temperature within the shaft is appropriate for the operation of the PVs and it also provides higher thermal energy production. Nonetheless, during summer the shaft has to be ventilated.

The temperature of the glass and the air in the cavity is approximately the same in the small-vent and mid-vent scenarios (only in the large-vent scenario the air cavity temperature is around 3°C lower than glass temperature). Regardless of the increase of the vent size or the increase of the depth, the temperature of the glass remains steady at 21-23 °C for all summer scenarios (even the non-ventilated ones) and at 6-7 °C for all winter scenarios. Regarding the respective fluctuation of the cavity air temperature, in the small-vent scenarios the glass temperature is practically equal to the temperature of the cavity while the cavity air temperature is getting lower by the increase of the vent size *(figure 55,A)*. Although the glass-cavity temperature difference is increased using larger vents, the difference is negligible (less than 1 °C during winter and less than 4 °C during summer).

PV and water temperature

The temperature of the PVs is always higher than the temperature of the air in the cavity (approx. 8-9 °C higher during winter and around 15 °C higher during summer), except for the scenario of the non ventilated shafts, in which the cavity air temperature is higher than the PV temperature *(figure 55,B)*. However, even the highest PV temperatures are appropriate for normal operation, in all scenarios, as they do not exceed 40 °C, even in the case of non-ventilated shafts. This means that the PV modules can work with high efficiency in any case. Moreover, the changes in vent or the depth size, have only small impact on the PV temperature. The temperature of the water is mainly based on the PV temperature and the results show that the water temperature is almost the same as the air cavity temperature in all summer scenarios (fluctuating within 18-21 °C in all cases). During winter, the water temperature is remarkably steady at 11-12 °C in all scenarios. The chimney water will not be possible to be used directly for domestic Hot Water even during summer, and therefore in both warm and cold periods, combined energy sources are required in order

to warm up the water to a temperature level that can be sufficient for any kind of use.

B) Pressure Difference, Air flow and air velocity within the shaft:

The pressure differences at the top of the shaft between the air of the cavity and ambient air, are reasonably low due to the smaller shaft height and the small temperature differences (maximum ΔP of 0.9 Pa in the summer scenario, with a floor chimney of small vents (0.09 x 0.05 m) and big depth (0.4 m)) *(figure 56).* As shown before, smaller vents cause higher temperature difference between the cavity air and the ambient air. Consequently, the pressure differences of the shaft are respectively higher than in the large-vent cases (approx. 0.2 Pa for the summer and 0.1 Pa for winter). Focusing on the summer results, in the case of small air inlets, (excluding the non-ventilated shafts), the pressure difference ranges between approx. 0.8-0.9 Pa. These pressure differences can cause 105-110m^3/h air flow during the summer period**,** which means enough ventilation for 2 people. Although small vents are preferable in terms of cavity temperature, an air flow increase is achieved with bigger air inlets, since the effective opening area is linear to air flow (equation 12). As an indication of the airflow fluctuation according to the vent size deviation, the air flow marks a value up to 110m^3/h for small air inlets, up to 180 m^3/h for mid-sized vents and up to 600m^3/h for large air inlets. That clearly depicts the importance of the inlet surface on the produced air flow since the rise in the air flow is steeper with the increase of the vent size.

In terms of air velocity, the values are increased both under warmer ambient conditions and by the use of smaller vents *(figure 56).* The air velocity reaches 0.45-0.95 m/s during winter while in summer, the values are higher (0.55-1.20 m/s). In summer, the air velocity values can provide enough ventilation as in all cases they are close to the comfort air velocity (0.8 m/s). Although the air velocity, in the case of smaller vents, is slightly higher from the comfort air velocity values, the use of the air as inlet air, supplied in a room, can be

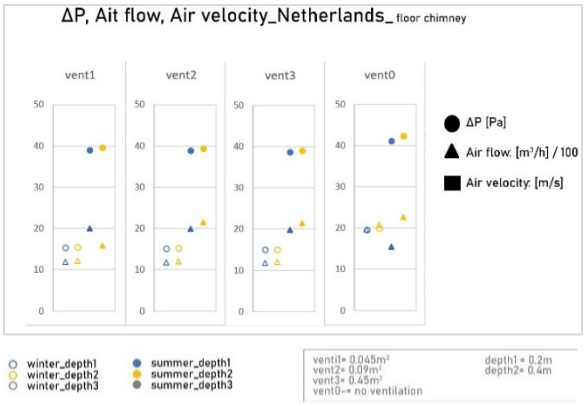

Figure 56: The pressure difference, the air flow and air velocity results for the Netherlands of the "floor chimney", with different vent size and depths (colors) for winter and summer.

sufficient for direct ventilation without any mechanical support. Moreover, the cavity air temperature on a regular summer day is close to the indoor comfort temperature range (23-25 °C). In contrast, during winter, the temperature of the air in the cavity does not allow for the direct use of the air for ventilation.

3.2.3.3.1.1.2. Conclusion_Netherlands

The analysis of the results shows that "floor chimneys" can be effective in the Netherlands in both seasons. Generally, the amount of ventilation plays an important role on the temperature of the cavity and on the produced airflow, while the changes of the temperature of the PVs, by the increase of the ventilation, are neglectable. The mid-sized air inlets (vent2: 0.09x0.1m) are more beneficial as they provide, during summer, comfortable air temperature (21 °C) and air flow (175m^3/h) which is appropriate for passive ventilation for 3-4 people.

On the other hand, the system during winter works more beneficially with closed vents, since, this way, the cavity temperature gets significantly higher (18 °C) than in the ventilated scenarios (4.5 - 7°C). However, mechanical support is still needed in order to achieve the suitable air temperatures for heating. Regarding the PV and water temperatures, the size of the vents and the depth do not significantly affect their

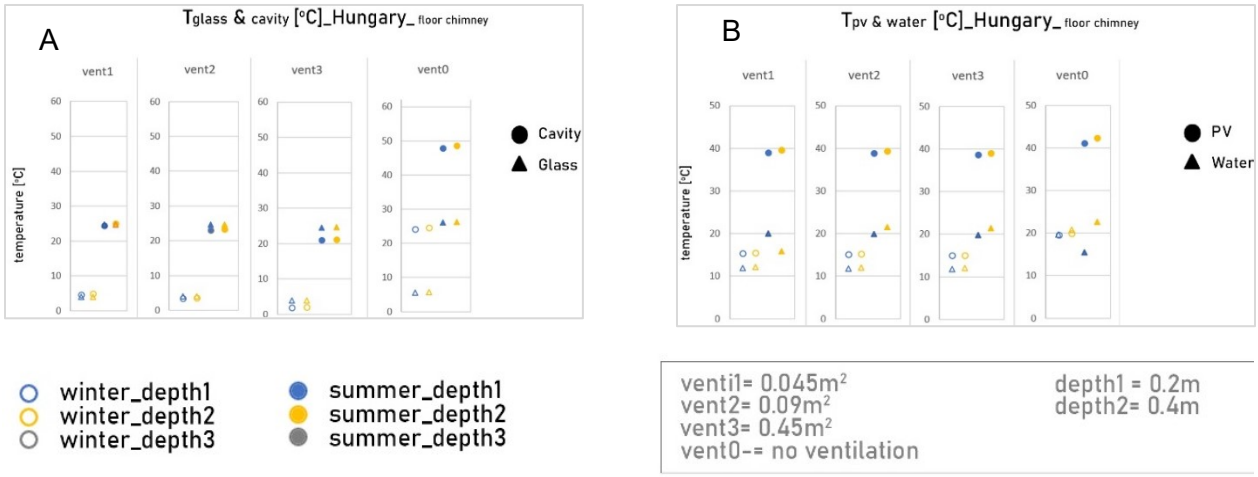

Figure 57: A) The glass and cavity temperatures in Hungary of the "floor chimney", with different vent size and depths (colors) for winter and summer. B) The PV and water temperatures in Hungary of the "floor chimney", with different vent size and depths (colors) for winter and summer.

temperatures. The temperature of the PV modules fluctuates within optimal levels for their high-performance operation, even in the worst summer-case scenario. The water temperature is almost the same as the cavity air temperature in summer and approximately 5 °C higher in the winter. More specifically, during summer, the water temperature, in the cases of ventilated shafts, reaches up to 21 °C and up to 12 °C during winter (around 11 °C for ventilated shafts and 12 °C for the non-ventilated).

3.2.3.3.1.2. Temperature climate

3.2.3.3.1.2.1. Results Hungary

A) Temperatures

Air of the cavity and glass temperature

In Hungary, where the average ambient temperature during winter (1°C) is lower than the Netherlands (4°C), the temperature difference between the air in the cavity and the ambient is higher in comparison to the Netherlands. This is probably due to higher sun load. During the summer period, the ventilated shafts do not cause significant temperature increase of the air in the cavity (maximum 4°C fluctuation for all vent variations, reaching a maximum of 25°C). During winter, for the ventilated shafts, the cavity air temperature fluctuates between 2-5 °C. In the non-ventilated scenario, the air cavity temperature is significantly higher *(figure 57,A).* Specifically, the temperature of the cavity during winter is approximately 22 °C, which requires little additional energy in order to be appropriate for heating use and roughly 49 °C during summer. In contrast, the temperatures, in both seasons in the scenario of big vents, are close to the ambient temperature. In the case of small vents and big depth, which is the scenario of ventilated shafts that provides the higher values, the temperature of the air in the cavity during winter is quite low (less than 5 °C), thus, the closed vents scenario is preferable. Additionally, during summer, bigger vents provide lower air temperature values, which are closer to the recommended values for thermal comfort (25 °C with small vents and 21 °C with big vents). Likewise, the Netherlands, in the cases of ventilated shafts, the temperature of the glass is almost the same with the temperature of air in the cavity for the small and mid-sized vents and 3 °C higher for the large-vent scenarios. In contrast, the temperature of the glass in the case of the non-ventilated shaft is lower than the cavity temperature since the glass temperature remains rather unaffected by the deviation in the vent size in all scenarios, even the non-ventilated ones (24-26 °C, in summer and 4-5 °C, in winter).

PV and water temperature

In Hungary, the temperature of the PV modules remains within an acceptable range that allows for efficient PV function with the highest temperature being approximately 43°C during summer, in the case of non-ventilated shaft, and roughly 15 °C during winter *(figure 57,B).* The PV temperature remains rather steady, independently from the vent-size variation with negligible differences, even in the case where vents are completely excluded (vent0). Therefore, the temperature of the PVs is determined mainly from the sun radiation. Regarding the water temperature, in summer, the values fluctuate between 20-23 °C in all scenarios (even the non-ventilated ones) and at 12-13 °C in all winter scenarios, therefore requiring some additional energy sources in order to be usable.

B) Pressure Difference, Air flow and air velocity within the shaft:

In Hungary, the values are almost identical to the Netherlands due to slight differences in temperature. With the combination of small air inlets and big depth, in summer conditions, the pressure difference reaches 0.9 Pa which is the highest value between the scenarios *(figure 58).* The airflow, in the case of large vents in the winter scenario is 5 times higher (495 m^3/h) than the air flow in the case of small vents (95 m^3/h). Similar is the air flow difference between large and small-vent scenarios also in summer, fluctuating between 535 m^3/h for large vents and 105 m^3/h for small vents. Moreover, the air flow difference regarding the depth of the shafts is not remarkable. The air velocity reaches 0.55-1.10 m/s during winter and the same also in summer. In both cases, the air velocity values can provide natural ventilation, although the air cavity temperature in winter is too low to be practically usable.

3.2.3.3.1.2.2. Conclusion_Hungary

The behavior of the system in Hungary, as well as the values of the results are similar to the Netherlands. According to the results, large inlets are preferable in Hungary during summer, as the temperature of the air in the cavity is quite appropriate

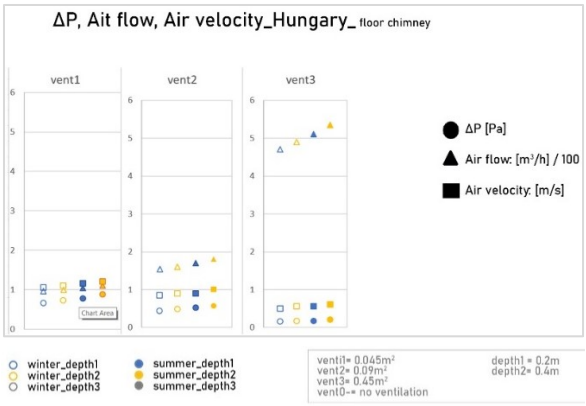

Figure 58: The pressure difference, the air flow and air velocity results in Hungary of the "floor chimney", with different vent size and depths (colors) for winter and summer.

for natural cooling (25 °C) while the system should be non-ventilated during winter, due to the low temperatures. In that case (of non-ventilated shaft in winter) the air cavity temperature is 22 °C, which makes it appropriate – temperature wise - for direct natural ventilation and heating purposes. For natural cooling, in summer, larger inlets cause higher airflow (535 m^3/h) and lower air velocities (0,6 m/s). As both values are important factors of a satisfactory ventilation, medium size vents, which provide sufficient airflow (170-180 m^3/h) and appropriate air velocities (0.9-1.0 m/s) are preferable. Regarding the PV and water temperature, the temperature of the PVs is acceptable (highest 43 °C) in both seasons while the temperature of the water is as high as 23 °C during summer and during winter, the water (13 °C) should be warmed up more in order to be suitable for domestic uses.

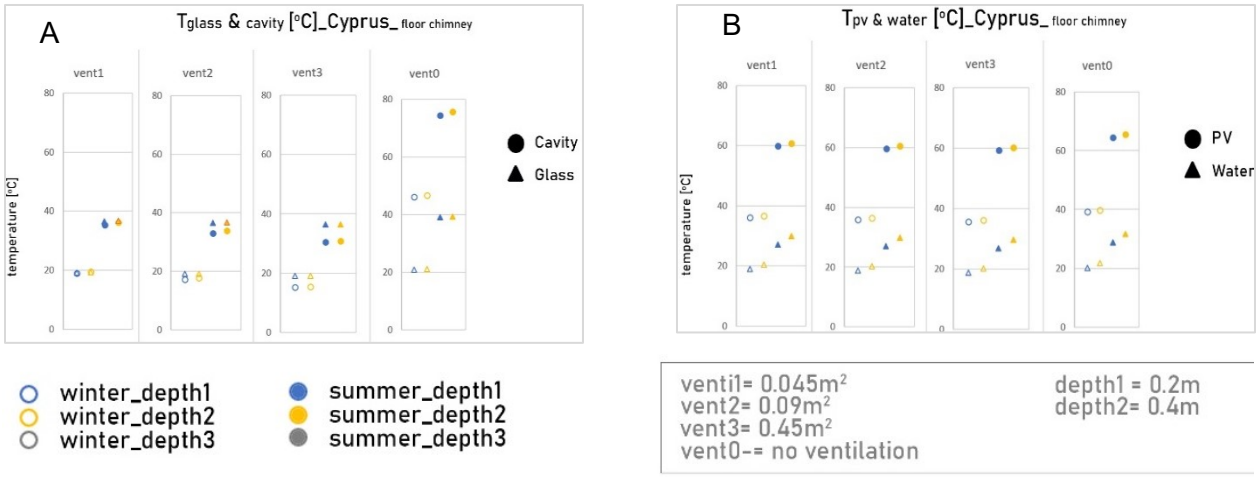

Figure 59: A) The glass and cavity temperatures in Cyprus of the "floor chimney", with different vent size and depths (colors) for winter and summer. B) The PV and water temperatures in Cyprus of the "floor chimney", with different vent size and depths (colors) for winter and summer.

3.2.3.3.1.3. Mediterranean climate

3.2.3.3.1.3.1. Results Cyprus

A) Temperatures

Air of the cavity and glass temperature

In Cyprus, where the sun radiation in both seasons is quite higher, the non-ventilated scenarios are not functional since the temperature of the air in the cavity is quite high even in winter (47 °C) *(figure 59,A).* Therefore, the system must be always ventilated. The temperature of the air in the cavity, is decreased by the increase of the vents and by smaller depths. In comparison to the Netherlands and Hungary, the air cavity temperature differences between the vent-size deviations are quite more evident in this case. Furthermore, the values of the temperatures during summer are quite high for ventilation purposes in all the inlet scenarios (the highest temperature reaches 37°C and the lowest 30°C). For this reason, the air inside the cavity should be extracted from the system. During wintertime, the values of the temperature of the cavity, in the cases of ventilated shafts, are fluctuating between 15-20 °C which are not suitable for direct heating, but the air can be used as input to the mechanical ventilation system to improve the system efficiency. Regarding the glass temperature, the values during winter are between 18-19 °C and between 36-37 °C during summer. These small differences of the temperature of the glass, indicate that the temperature deviation of the glass is not prone to vent or depth changes.

PV and water temperature

The temperature of the PVs both in ventilated and non-ventilated shafts during summer, are prohibitive (lowest PV temperature at 59 °C) *(figure 59,B).* Although the solar radiation in Cyprus is quite high, even in winter, the temperature of the PVs does not exceed 37°C during winter which is acceptable for the PV function, in contrast to the summer conditions in which the PV temperatures at around 60 °C cause a dramatic drop in the PV efficiency. The water temperature during winter is 18-21 °C, thus, requiring little additional energy in order to be exploited as a heating source. During summer, the values of the water temperature are quite higher (27-31 °C) still requiring additional energy sources in order to be acceptable for Domestic Hot Water use.

B) Pressure Difference, Air flow and air velocity within the shaft:

In Cyprus, because of high sun irradiance in both seasons, the temperatures of the system and pressure differences are higher. Smaller vents cause higher pressure differences, and this is due to the fact that higher temperatures are marked in the air of the cavity. The maximum pressure difference is

noticed in the case of small vents and deeper shafts, during summer, and it is 1.22 Pa *(figure 60)*. Moreover, the shrinkage of the vents causes a significant rise in the pressure difference (starting from to 0.2 Pa for large-vent scenarios and reaching 1 Pa for small-vent scenarios, in winter, and from 0.25Pa for large-vent scenarios to 1.22 Pa for small-vent scenarios, during summer). These pressure differences can cause 110-560m^3/h air flow during the winter period, which means enough ventilation for 2-11 people and 120-630 m^3/h during summer which can provide ventilation for 2-12 people. Although the airflow values during summer are satisfactory, the temperature of the air in the cavity is quite high and prevents its use for natural ventilation as there is a high risk of fluid flow from the cavity towards indoor. In terms of air velocity, the values are higher by the use of smaller vents. The air velocity reaches 0.6-1.3 m/s during winter while in summer, the values are fluctuated between 0.65-1.40 m/s. As the air of the cavity can probably be used during winter, larger vents are preferable. Large vents can reduce significantly the air velocity (which is high for ventilation in the case of small vents) and also, they do not cause significant temperature drop.

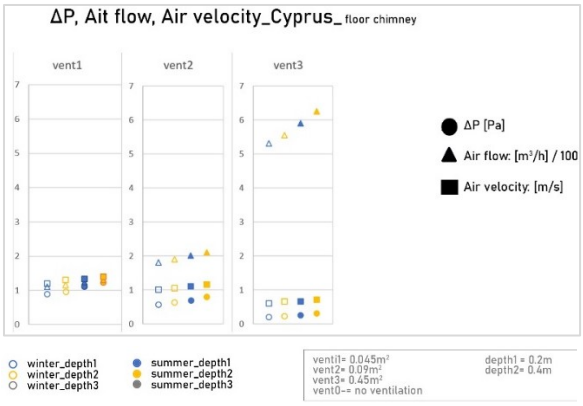

Figure 60: The pressure difference, the air flow and air velocity results in Cyprus of the "floor chimney", with different vent size and depths (colors) for winter and summer.

3.2.3.3.1.3.2 Conclusion_Cyprus

According to the results, in Cyprus, the system can work beneficially during winter for heating with little mechanical support but during summer, both the temperature of the air in the cavity and the PV temperatures are quite high. Moreover, the system should be ventilated as the cavity temperature, in the case of no ventilation, in both seasons is high. Even in winter, the temperature of the air in the cavity is higher than the favorable temperatures for heating (47 °C). Consequently, for the use of the system during summer, a mechanical cooling system has to be implemented in order to reduce, primarily, the PV temperature (60 °C) and the temperature of the cavity (30-38 °C). The water temperature (27-31 °C) requires some additional heating sources in order to provide water of appropriate temperature for domestic uses. Similarly, during winter, the water temperature (18-21 °C) also requires additional energy sources to be usable for heating or other uses. Although the use of the system for natural ventilation during summer is not recommended, during winter, the ventilated scenarios can provide air temperature that approaches passive heating (15-20 °C). Thus, larger vents are preferable since they can provide a sufficient amount of air flow (530 m^3/h) and lower air speeds which are closer to the favorable air velocity values (0.1 m/s for winter). However, a control of the air velocity is needed before enters the room, since the lower fluid speed which achieved is 0.6m/s.

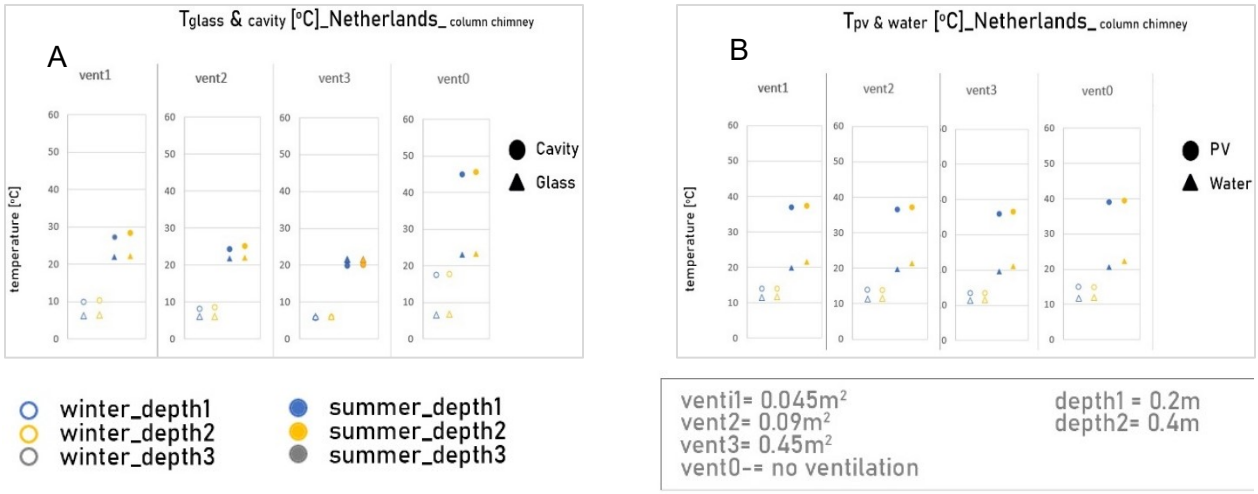

Figure 61: A) The glass and cavity temperatures in the Netherlands of the "column chimney", with different vent size and depths (colors) for winter and summer. B) The PV and water temperatures in the Netherlands of the "column chimney", with different vent size and depths (colors) for winter and summer.

3.2.3.3.2. "column chimneys"

3.2.3.3.2.1. Moderate climate

3.2.3.3.2.1.1. Results Netherlands

The "column chimneys" have the same width with the "floor chimneys" but their height is the height of the building. Also, the air supply (vent1,2,3) have the same size as in the "floor chimneys".

A) Temperatures

Air of the cavity and glass temperature

The results in the Netherlands show that the temperature of the air in the cavity is higher (roughly 3-5°C higher) than the respective temperature values of the "floor chimney "in the cases of ventilated chimneys *(figure 61,A).* However, the temperature of the glass is roughly the same with the case of "floor chimneys" (6 °C during winter and 21°C during summer). Furthermore, by the increase of the vent size, the values of the air temperature in the cavity drop slightly (from 28 °C with small vents to 25 °C and 20 °C with larger vents respectively), while the decrease of the depth cause even smaller differences (less than 1 °C difference). In relation to the ambient temperature, the cavity temperature increases by 4-6 °C during the winter (ambient temperature during winter is assumed to be 4 °C), except for the case with large vents where the increase is smaller (approx. 2 °C). During summer, the rise of the cavity temperature in comparison with the ambient temperature is higher (7-10 °C increase), with which the cavity temperature reaches the values of 25-28°C (the case of large vents is excluded, in which the increase is 3 °C). Regarding the non-ventilated shaft, the glass temperature is increased slightly while the temperature of the air in the cavity gets much higher than the ambient. During summer, the air in the cavity reaches 18 °C, which is 14 °C higher than the ambient temperature and 8 °C higher than the ventilated case (this case makes use of small vents and big depth and is the case that marks the highest temperature values). Similarly, during summer, the temperature of the cavity reaches 45 °C, Even though, in the case of the non-ventilated shaft, the temperature of the cavity during winter is not reaching the favorable values for passive heating, the use of the prewarmed air can be beneficial for the efficiency of the HVAC system. Consequently, for the operation of the "column" PV chimney during winter, the use of closed vents is recommended while in summer, larger vents are preferable, in order to keep the shaft cool.

PV and water temperature

According to the results for the PV module temperature, changes of the vent or the depth size, have a small impact on

the PV temperature. Moreover, the temperature of the PVs is always higher than the temperature of the air in the cavity, except for the case of the non-ventilated shaft (in the ventilated shafts the temperature ranges at approx. 14-15 °C during winter and around 36-39 °C during summer). In the case where there is no ventilation through the shaft, the cavity air temperature is higher than the PV temperature. In this case the temperature of the air in the cavity is 18 °C and 46 °C during summer while the temperature of the PV panel is 15 °C and 39 °C respectively *(figure 61,B).* These values indicate that the PV modules can work with high efficiency in any case, since their temperature ranges within normal levels. The temperature of the water does not change significantly by changes of the vent and depth size, since, it is fluctuated between 11-12 °C in all scenarios during winter and between 20-22 °C during summer. Consequently, in both seasons, the chimney water cannot be used directly for Domestic Hot Water or heating even during summer, and therefore, additional energy sources are required in order to warm up the water to a sufficient temperature level.

B) Pressure Difference, Air flow and air velocity within the shaft:

The differences in pressure, increase linearly by the increase of the height and by higher temperature differences. Accordingly, the pressure differences in this kind of PV-chimney systems ("column chimneys") are predicted to be higher compared with shorter PV-chimneys ("floor chimneys"). The differences between the "floor chimneys" and the "column chimneys" are tremendous. Specifically, during summer, the pressure difference increases from approx. 0.13-0.5Pa ("floor chimneys") to 7-23Pa while in summer the values change from 0.2-0.8Pa to 11-44Pa *(figure 62).* Moreover, the values of the pressure difference, as well as the air flow, mark high differences by the increase of the vent and depth size. The pressure difference is decreased by the increase of the vent, since it depends on the increase of the cavity temperature while, in contrast, the air flow is increased significantly by the increase of the vent size. By the increase of the vent size, the

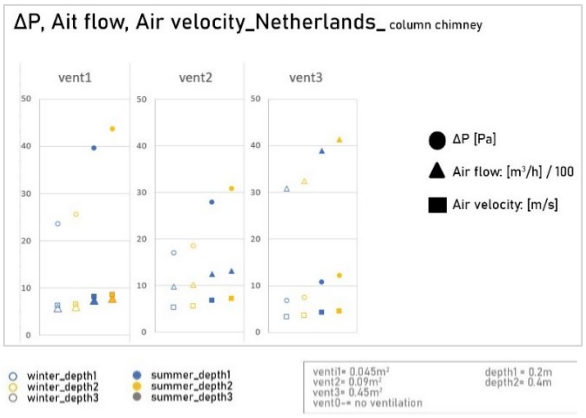

Figure 62: The pressure difference, the air flow and air velocity results in the Netherlands of the "column chimney", with different vent size and depths (colors) for winter and summer.

air flow is altered from roughly 570m^3/h to 3080m^3/h during winter and from 740m^3/h to 4130m^3/h during summer. These values can provide enough ventilation for 19-100 people during winter and 14-82 people in winter. However, the utilization of the air inside the cavity for ventilation is hard as the shaft is continuous up to the top of the building. Regarding the air velocity, the values drop remarkably by the increase of the vent size. During summer, the air velocity drops from 6.3m/s to 3.5m/s and during winter from 8.1m/s to 4.5m/s. The air velocity values are extremely high and are not suitable for ventilation as they exceed a lot the comfortable limits (0.1m/s is the comfortable air velocity for the winter and 0.8m/s for summer). However, by these values, wind power generation can be achieved.

3.2.3.3.2.1.2. Conclusion_Netherlands

The analysis of the results indicates that "column chimneys" in the Netherlands are not suitable for passive ventilation as the air velocity values high (3.5-6.3m/s during winter and 4.5-8.1 m/s during summer). However, the air, can be probably used for wind energy generation at the top of the shaft. Although the air in the cavity has high velocity, its temperature can be used as heating medium. Therefore, if the air is used for wind energy generation, small vents (vent1: 0.09x0.05m) are preferable, as they cause higher wind speeds and higher cavity temperatures (in order to be used as heating medium of water). Regarding

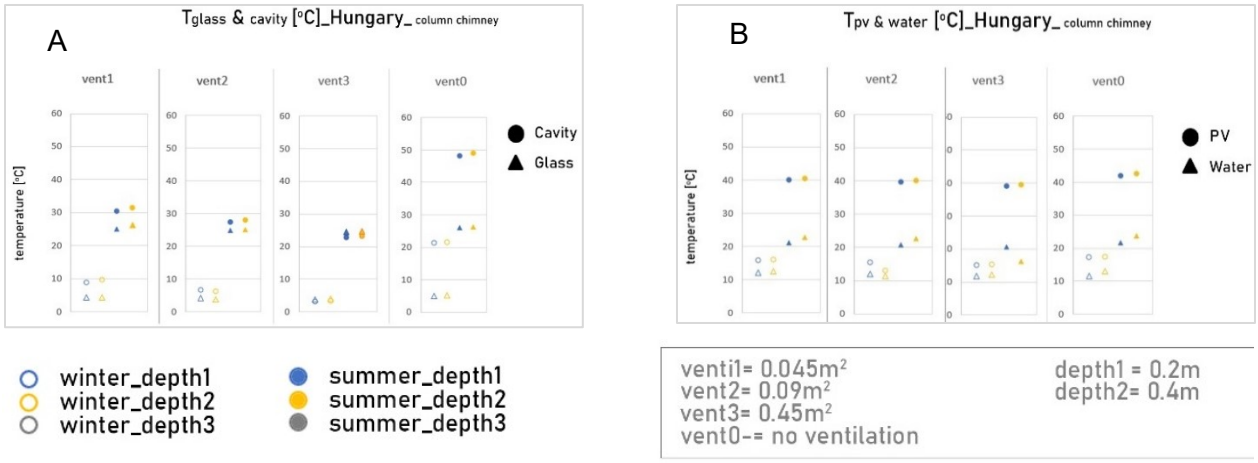

Figure 63: A) The glass and cavity temperatures in Hungary of the "column chimney", with different vent size and depths (colors) for winter and summer. B) The PV and water temperatures in Hungary of the "column chimney", with different vent size and depths (colors) for winter and summer.

the PV and water temperatures, the size of the vents and the depth do not significantly affect their temperatures. The temperature of the PV modules fluctuates within optimal levels for their high-performance operation, even in the summer-case scenario of no ventilation (40 °C). The water temperature, in both seasons cannot be used directly as Hot Domestic water or heating since its temperature is low. During summer, the water temperature, reaches up to 21 °C and up to 12 °C during winter.

3.2.3.3.2.2. Temperate climate

3.2.3.3.2.2.1. Results Hungary

A) Temperatures

Air of the cavity and glass temperature

In Hungary, the system behavior is almost like the Netherlands. The increase in the temperature of the air in the cavity in relation to the ambient air temperature is not that high (the ambient temperature during summer is assumed at 20 °C and at 1 °C during winter) *(figure 63,A).* The temperature of the cavity air during summer in any ventilated scenario is roughly between 21-24°C, while during winter is fluctuated between 2 to 4.5°C. Therefore, during summer, the temperature of the air in the cavity can be used for passive cooling. In contrast, in the case of the non-ventilated shaft, the temperature values of the air in the cavity are much higher. During the winter period, the air inside the cavity is reaches 25 °C , thus, it can be used very effectively for direct heating or as entry air for a heat pump in order to optimize its efficiency. Also, the temperature of the cavity, in the non-ventilated scenario in summer, is even higher than the Netherlands due to higher average sun load and reaches 50°C. Regarding the temperature of the glass, the values are below 26 °C, even in the worst case of the non-ventilated scenario during summer, therefore, there is no risk of overheating.

PV and water temperature

The temperature of the PV modules is not restrictive for their optimal operation. Their temperatures range at around 15-20°C during winter while during summer are reaching 39-42°C *(figure 63,B).* In all the cases, the temperature of the PVs is higher than the temperature of the air in the cavity except for the case of the non-ventilated shaft, where the temperature of the PV modules is roughly 4-6 °C higher than the air in the cavity, in both seasons (winter: 24 °C the cavity temperature and 20 °C the PV temperature, summer: 48 °C the cavity temperature and 42 °C the PV temperature). In regard to the water temperature, the results show that in all scenarios of ventilated shafts, the temperature of the water does not change significantly by the change of the vent size. On the

contrary, in the case of the non-ventilated shaft, the temperature difference of the water is much higher than the cases of the ventilated shafts, during winter (roughly at 11-12 °C with ventilation and at 20-21 °C in the case of non-ventilated shafts). However, during summer, the water temperature increases, slightly, by the use of the non-ventilated shaft (roughly at 20-22 °C with ventilation and at 22-23 °C in the case of non-ventilated shafts). Accordingly, in both seasons, the water does not reach the temperature that makes it appropriate to be used as Domestic hot water. However, the use of the water at roughly 20 °C (winter scenario of non-ventilated shaft and summer scenario of ventilated shaft) as a coupling source of the water heating system, could improve the efficiency of the system and reduce its energy consumption.

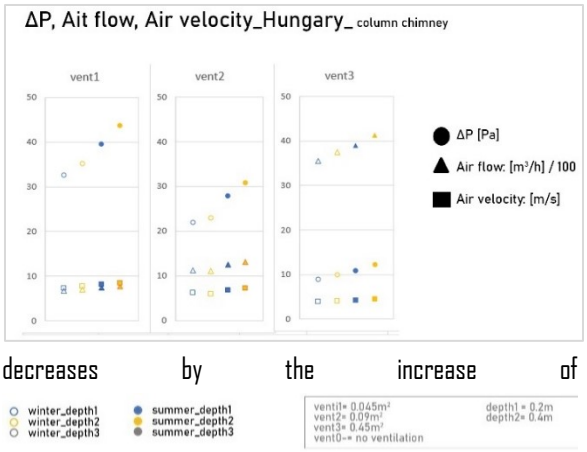

Figure 64: The pressure difference, the air flow and air velocity results in Hungary of the "column chimney", with different vent size and depths (colors) for winter and summer.

B) Pressure Difference, Air flow and air velocity within the shaft:

In the case of Hungary, the behavior of the system is similar to the Netherlands, with higher values in pressure difference, air flow and air velocity. According to the results, the size of the vent plays an important role on the pressure difference and thus, on the air flow and air velocity of the air in the cavity. By the increase of the vent size, a tremendous increase of the air flow is observed (winter: 675-700 m^3/h with use of the small vent of 0.9x0.05m and 3550-3750 m^3/h with use of the large vent of 0.9x0.5m, summer: 740-780 m^3/h with small vent-size of 0.9x0.05m and 3890-4130m^3/h with large vent-size of 0.9x0.5m) while the air flow difference between the two seasons in the same vent-size scenarios, is not remarkable *(figure 64)*. The amount of air flow in both seasons is very high as it can provide ventilation for 22-125 people during winter (30 m^3/h per person required) and for 15-82 people during summer (50 m^3/h per person required). In contrast, the pressure difference within the shaft drops by the increase of the vent (winter: 32-35 Pa with small vent of 0.9x0.05m and 9-10 Pa with large vent of 0.9x0.5m, summer: 39-44 Pa with small vent of 0.9x0.05m and 11-12 Pa with large vent of 0.9x0.5m) and slightly by smaller depths (1-4 Pa difference). Similarly, the air velocity of the air in the cavity decreases by the increase of the vent size. However, the drop of the air velocity value, is not proportional to the increase of the vent surface area (in winter: wind velocity at 6.8m/s with small vent of 0.045m^2 and at 4m/s with large vent of 0.45m^2 and, in summer: roughly at 4.3m/s with large vent of 0.45m^2 and at 7.6m/s with small vent of 0.045m^2). The values of the air velocity in any case are really high and cannot be used for ventilation purposes but maybe for wind energy generation.

3.2.3.3.2.2.2. Conclusion_Hungary

According to the results, the "column chimneys" in Hungary are not suitable for passive ventilation as the air velocity values are high (4-6.8m/s during winter and 4.3-7.6 m/s during summer). However, the air can be probably used for wind energy generation at the top of the shaft. In parallel, the temperature of water does not allow its use as Domestic hot water, thus, an additional energy source will have to be used in order to warm up the water at the required temperature level. Regarding the PVs, the size of the vents and the depth do not significantly affect their temperature. The temperature of the PV modules fluctuates within optimal levels for their high-performance operation, even in the summer-case scenario of no ventilation (43 °C).

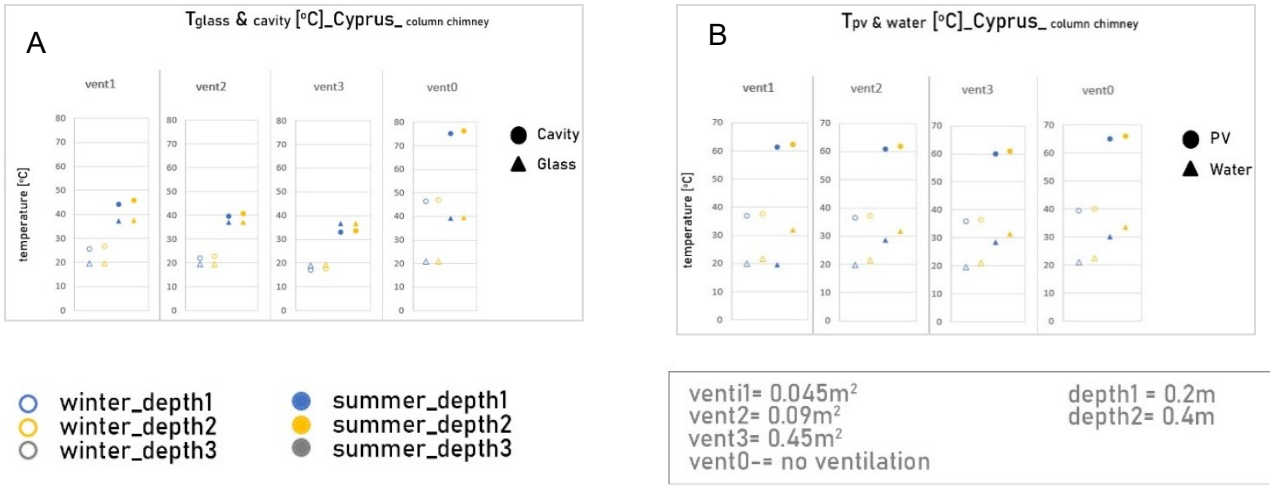

Figure 65: A) The glass and cavity temperatures in Cyprus of the "column chimney", with different vent size and depths (colors) for winter and summer. B) The PV and water temperatures in Cyprus of the "column chimney", with different vent size and depths (colors) for winter and summer.

3.2.3.3.2.3. Mediterranean climate

3.2.3.3.2.3.1. Results Cyprus

A) Temperatures

Air of the cavity and glass temperature

Apparently, in warm climates as Cyprus, where the sun irradiance values are high both in summer and winter, the temperatures of the system components are higher. The temperature of the air inside the cavity, during winter, is reaching 18-27 °C, which is close to the temperature of the cavity during summer in the Netherlands and Hungary (28 °C in the Netherlands and 31 °C in Hungary) *(figure 65A).* During summer, in the cases of ventilated shafts, the temperature of the cavity is reaching approx. 46°C in the scenario of small vent (vent1: 0.9x0.05) and big depth (0.4m) while in the case of the non-ventilated shaft the temperature reaches 77 °C. Although, the temperatures during winter are reduced a lot, especially by the increase of the vents, the cavity temperature in the case of small vents reaches almost 27°C which is satisfying for passive heating. In the non-ventilated scenario, the cavity temperature is 46 °C and in the large-vent scenario that cavity temperature is 15 °C. Thus, during winter the system can be used for passive ventilation only in the small-vent scenario, while in summer, due to the high temperature of the air in the cavity, the system cannot be used for passive ventilation. In this case (summer scenario) the large vents are preferable in order to prevent overheating of the cavity (31 °C). Finally, the temperature of the glass has a maximum 40 °C in the worst case (no-ventilation) which means that there is no risk of overheating.

PV and water temperature

The temperature of the PVs is not affected a lot by the existence of vents or not as their temperatures, during summer, are roughly at 61 °C, in all the ventilated scenarios, and at 66 °C in the non-ventilated scenario *(figure 65,B).* With these temperatures, the PV modules are hard to operate beneficially as a significant drop in their efficiency is caused. However, during winter, the temperature of the PV modules is fluctuated within normal levels (38-40 °C). Regarding the temperature of the water, the value is approximately 21 °C in all the scenarios during winter and 31-33 °C during summer. This indicates, that the water cannot be used directly as domestic hot water in both seasons and that additional energy is needed in order to reach the suitable temperatures, however, the starting temperature of the water is quite high and definitely a lot higher than in Hungary and the Netherlands.

B) Pressure Difference, Air flow and air velocity within the shaft:

The results of the pressure difference, the air flow and the air velocity in Cyprus are high for all the scenarios. Also, the change of the vent size plays a significant role in the value of the aforementioned quantities. During winter, the pressure difference in the case of small vents is approx. 45-49 Pa while, in the case of large vents, it drops to 12-14 Pa *(figure 66)*. Similarly, during summer the pressure difference drops from 56-62 Pa to 15-17 Pa. These pressure differences cause incredibly high amount of air flow which reaches up to 4830 m^3/h (in the case of large vents of: 0.9x0.5m, in summer scenarios). Similarly, the air velocities are high. During winter the air velocity of the cavity is approx. 8.5-9m/s in the small-vent scenarios and 4.5-4.75m/s in the large-vent scenarios while in summer the values are higher (roughly 10m/s with small vents and 5m/s with large vents). With these values of air flow and air velocity as well as the respective temperature values (29-45 °C) of the air in the cavity, the system cannot be used for passive ventilation during summer. Furthermore, during winter, although temperature-wise the air of the cavity can be used for heating (small-vent scenario), the air velocity exceeds a lot the suitable values (the air velocity is approx. 8-5-9m/s and the comfortable levels of air velocity during winter is 0.1m/s). However, this alternative might not have to be rejected, since the interior ventilation rate might be able to be controlled mechanically.

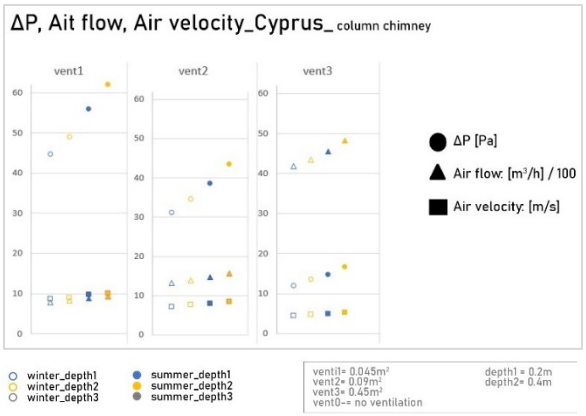

Figure 66: The pressure difference, the air flow and air velocity results in Cyprus of the "column chimney", with different vent size and depths (colors) for winter and summer.

3.2.3.3.2.3.2. Conclusion_Cyprus

In contrast with the Netherlands and Hungary, in Cyprus both temperature values and the values connected with the chimney effect are more extreme. The results indicate that the shaft has to be ventilated in both seasons, as the temperatures of the cavity and of the PV modules are quite high, especially during summer (36 °C with small vents, 33 °C with large vents and 77 °C in the case of non-ventilated shafts, for the cavity air temperature). Even in winter, where higher temperature is preferable, the air in the cavity, in the non-ventilated scenario reaches 46 °C which is quite high for passive heating, while, in the small-vent scenario, the temperature is approx. 27 °C and thus, can be used for direct heating. However, the air velocity of the air is not suitable for any kind of room ventilation as it is exceeding the standard ventilation values by a lot. The air velocity, in the small-vent scenario, is roughly 8m/s, both in winter and summer, while the standard comfort levels of air velocity is 0.1m/s for winter and 0.8m/s for summer. Consequently, an additional system, that decelerates the air velocity and extracts only the appropriate amount of air flow, is required in order to be able to make use of the warm air of the cavity. Regarding the PV modules, their temperatures are high in all cases. Therefore, either an additional cooling method is needed, or the amount of water which runs behind the PV modules (which works as a cooling method of the PVs), should be increased (e.g. increase of the total length of the pipes (Zankharchenko et. al, 2004)). Finally, the water, which has approx. 20-21 °C during winter and 30-33 °C during summer, can be used as pre-heated water which will be warmed up more for domestic uses. By this way, the efficiency of the systems

Consequently, an additional system, that decelerates the air velocity and extracts only the appropriate amount of air flow, is required in order to be able to make use of the warm air of the cavity. Regarding the PV modules, their temperatures are high in all cases. Therefore, either an additional cooling method is needed, or the amount of water which runs behind modules (which works as a cooling method of the PVs), should be increased (e.g. increase of the total length of the pipes (Zankharchenko et. al, 2004)). Finally, the water, which has approx. 20-21 °C during winter and 30-33 °C during summer, can be used as pre-heated water which will be warmed up more for domestic uses. By this way, the efficiency of the systems

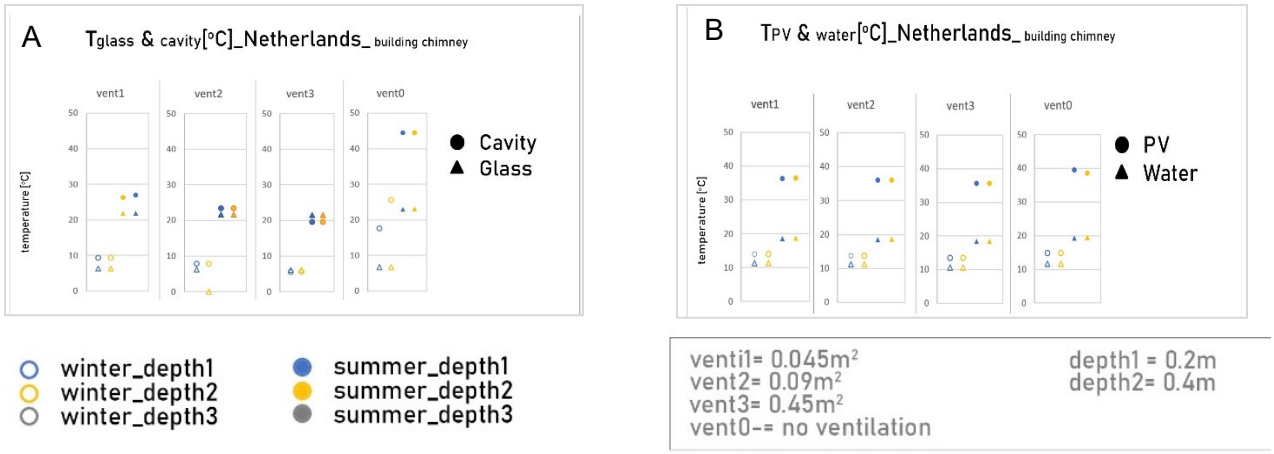

Figure 67: A) The glass and cavity temperatures in the Netherlands of the "building scale chimney", with different vent size and depths (colors) for winter and summer.

B) The PV and water temperatures in the Netherlands of the "building scale chimney", with different vent size and depths (colors) for winter and summer.

that heat up the water, either for domestic use or heating, will be increased, as the temperature difference that must be achieved will be much lower. the PV

3.2.3.3.3. "building scale chimneys"

3.2.3.3.3.1. Moderate climate

3.2.3.3.3.1.1. Results Netherlands

The "building-scale chimneys" have the height of the building as the "column chimneys" and the width of the building (in this case the width is the building is assumed to be 33m). Also, the air supply (vent1,2,3) have the same length as the "floor and column chimneys" but their width, is the width of the facade of the building.

A) Temperatures

Air of the cavity and glass temperature

The cavity temperatures, for different cavity depths and vent sizes, in the Netherlands, for the building-scale chimneys are similar and slightly lower than the values of the "column chimneys". This demonstrates that the height affects the thermal performance of the system while the width has less important effect on it. Moreover, changes of the cavity depth and the vent size cause slight changes in the cavity temperature. However, in all the ventilated cases and especially in the case of the large vents, the temperature of the cavity is close to the ambient temperature (ambient temperature during winter is assumed to be 4 °C and the cavity temperature reaches only 5.5 °C, while, during summer, when the temperature is assumed to be 17 °C, the cavity air has temperature of 19 °C) *(figure 67,A).* On the other hand, the case of non-ventilated shafts, the temperature values are marked higher. During winter, in the case of deeper (0.4m), non-ventilated shafts, the temperature of the air in the cavity reaches almost 26 °C, which is a favorable value to be used for passive heating. During summer, the temperature values of the cavity air are slightly high for passive cooling in the case of small vents (26-27 °C), while the cavity temperature in the case of large vents drops to suitable for cooling values (20 °C). Finally, the temperature of the glass does not exceed 23 °C, thus, there is not a risk of breakage.

PV and water temperature

The temperature of the PVs does not exceed 40 °C, in any case, thus, their efficiency is not affected by the operation of the chimney *(figure 67,B).* Regarding the temperature of the water, the values are the same as in the "column chimneys". The temperature of water is increased by 2 °C, during winter, reaching 12 °C, while, during summer, the final temperature of the water is 20-22 °C. Consequently, the water can be used only as a coupling thermal source of the water heating system.

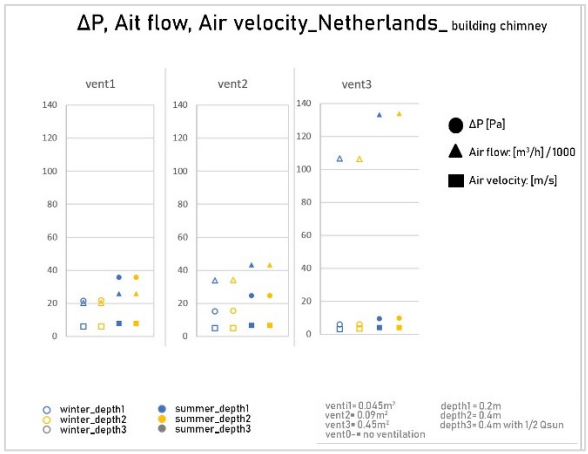

Figure 68: The pressure difference, the air flow and air velocity results in the Netherlands of the "building scale chimney", with different vent size and depths (colors) for winter and summer.

In this way, the operational energy demands of the water heating system will be reduced.

B) Pressure Difference, Air flow and air velocity within the shaft:

The "building-scale chimneys" have similar behavior to the "column chimneys". In comparison with the "column chimneys" the values of the pressure difference and the air velocity do not change a lot, while, the air flow is increased significantly. The air flow values are extremely high, in all cases, and also, by the increase of the vent size, the air flow increases tremendously, while deeper shafts increase the results only slightly. In the case of small vents (ventl:0.05x33m) the air flow, during summer, reaches 25940m^3/h and, in the case of large vents (vent3:0.5x33), the air flow increases to 133500m^3/h *(figure 68)*. These values as well as the air velocity of the air in the cavity are extremely high (4m/s for the large-vent scenario, during summer, and 7m/s for the small-vent scenario, during summer). This difference leads to the conclusion that small differences in the vent size can cause huge changes in the produced air flow. The airflow values can provide ventilation for many people (summer: 520 (ventl) to 2679 (vent3) people), which is unrealistic even for offices with a lot of people. Moreover, after observation of the values of air velocity, it is concluded that the values are extremely high and unsuitable for any use of air for the building, except for wind power generation.

3.2.3.3.3.1.2. Conclusion_Netherlands

The results indicate that the the thermal performance of the "building-scale chimneys" is similar with the "column chimneys". According to the results, the temperature the cavity of the PV-chimney system marks satisfying values for heating during winter with the vents closed (26 °C). During summer, medium-sized vents (vent2:0.1x33m) and large-sized vents (vent3:0.5x33m) are preferable for passive cooling as the temperature of the cavity (with vent2 the temperature of the cavity is 24 °C and 20 °C with vent3) is closer to the comfortable temperature levels (20-25 °C). Although the thermal behavior of the system is satisfying, the ventilation values of the system prevents the use of the air for ventilation. The system marks high values of air velocity, in both seasons, and especially during summer (4m/s during summer and large vents and 7m/s during summer and small vents), which indicates that the air cannot be used for ventilation as the values are extremely higher than the standard values (comfort levels are below 0.8m/s for the summer). Hence, the exploitation of air velocity is possible by the use of air for wind energy generation. Regarding the PV modules, the results indicate that they can work efficiently as their temperature does not exceed 40 °C. On the contrary, the temperature of the water, in both seasons, is low for direct use of water as Domestic Hot water, thus, the water can be used as an input of the heating system in order to increase its efficiency.

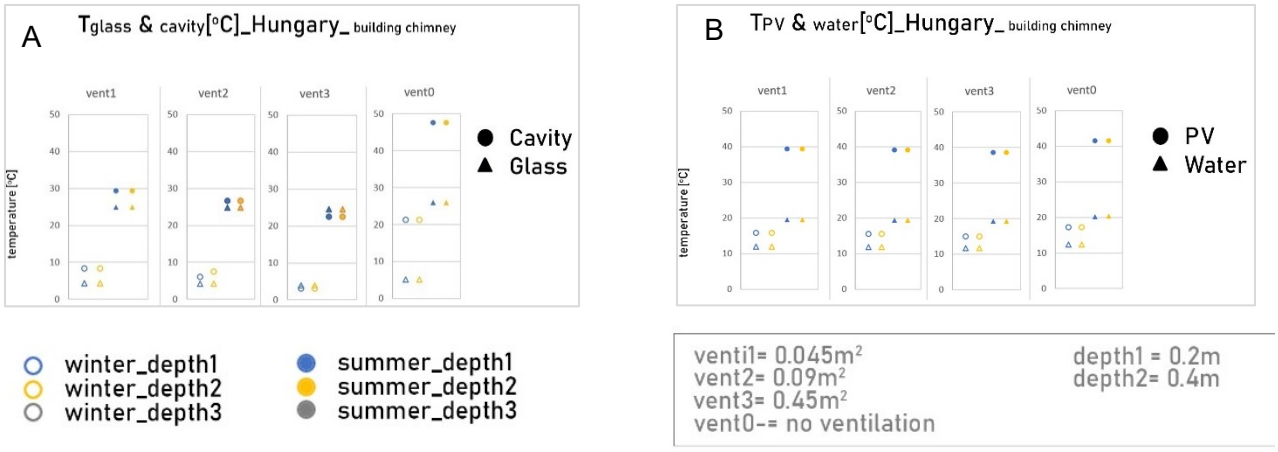

Figure 69: A) The glass and cavity temperatures in Hungary of the "building scale chimney", with different vent size and depths (colors) for winter and summer. B) The PV and water temperatures in Hungary of the "building scale chimney", with different vent size and depths (colors) for winter and summer.

3.2.3.3.3.2. Temperate climate

3.2.3.3.3.2.1. Results Hungary

A) Temperatures

Air of the cavity and glass temperature

The system in Hungary, has similar performance with the system in the Netherlands. The system, in the cases of ventilated shafts, during winter, increases the temperature of the air in the cavity from 1°C (average ambient temperature) to approximately 8°C in the favorable scenario of small vents (vent1:0,05x33m) while during summer, the temperature of the cavity reaches 30°C (ambient temperature 17°C) *(figure 69,A)*.. With larger vents (vent3:0.5x33m) during winter, the air in the cavity has a temperature of 3°C, which is low and close to the ambient temperature, thus, large vents are not recommended for winter, During summer, in the case of large vents, the temperature drops to approx. 22°C, which is a satisfactory value in order to use the air of the cavity for passive cooling. In the case of the non-ventilated shaft, the values are remarkably higher, During the cold period the temperature of the cavity is noticed to be 21 °C which is much better for heating purposes than the values of the ventilated scenarios. In contrast, during summer the temperature of the cavity is high and reaches 45 °C, therefore, ventilation within the shaft is required during the warm period. Regarding the glass, there is no risk of overheating or breakage since in the worst scenario the maximum temperature of the glass is 26 °C (summer scenario with no ventilation).

PV and water temperature

Generally, the temperature of the PVs is less than 40 °C in all the cases which means that the photovoltaics can work with full efficiency *(figure 69,B)*.. The temperature of the water is approx.11-12 °C in all the winter cases and 19-20 °C during summer. Accordingly, it cannot be used as Domestic Hot water. It can be used as an input water the heat exchanger in order to increase its efficiency and thus, decrease its operational energy demands.

B) Pressure Difference, Air flow and air velocity within the shaft:

In Hungary, the values of the pressure difference, the air flow and the air velocity are higher than in the Netherlands due to higher solar radiation in both seasons. Moreover, the opening size play an important role on all the values. By the increase of the vent size, the pressure differences are decreased a lot (winter: from 30Pa with small vents to 8Pa with large vents, summer from 133Pa to 36Pa with small and large vents respectively) *(figure 70)*. Similarly, the air velocity is decreased from 7m/s to 3.6m/s during winter and from

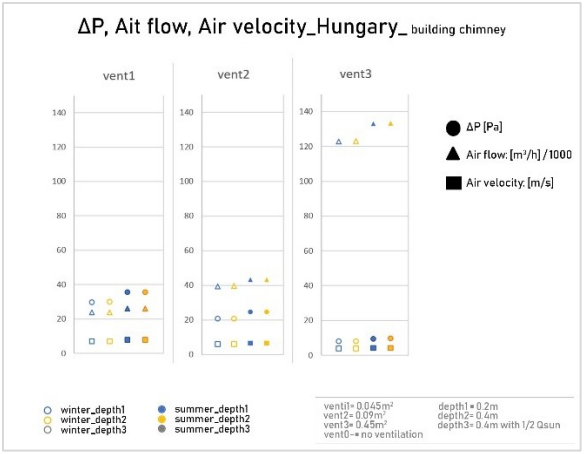

Figure 70: The pressure difference, the air flow and air velocity results in Hungary of the "building scale chimney", with different vent size and depths (colors) for winter and summer.

7.7m/s to 4m/s. In contrast, the air flow is increased tremendously by the increase of the openings, while the change in the depth size does not cause significant increases. The values of the air flow within the shaft, during winter, are fluctuated between 23600 and 122700m^3/h for small and large vents respectively (vent1: 0.05x33m, vent3:0.5x33m), while during summer, the values range from 25800 to 133000 m^3/h. In both seasons, the values of the air flow and the air velocity are unrealistically high for the use of the air for ventilation. At that amount of flow of air within the shaft, probably wind energy generation is more beneficial and realistic scenario.

3.2.3.3.3.2.2. Conclusion_Hungary

The results indicate that "building-scale chimneys" are hard to be used for ventilation purposes since the air velocity and air flow values are extremely high. The values of air velocity reach minimum 4m/s during summer which is still not acceptable for ventilation. During, winter, where higher temperature values are preferable, even in the case of the non-ventilated shaft, the temperature of the cavity is low (20 °C) and it cannot be used directly for heating. However, the use of preheated air will increase the efficiency of the HVAC system of the building. Regarding the PV modules, their functionality is not affected by the higher (in comparison with the ambient temperature) temperature of the cavity as they mark temperatures below 40 °C. In parallel, the water temperature in both seasons is not high enough in order to be used directly for Domestic uses and thus, external energy sources are required to warm it up to the suitable temperature levels.

3.2.3.3.3.3. Mediterranean climate

3.2.3.3.3.3.1. Results Cyprus

A) Temperatures

Air of the cavity and glass temperature

The weather in Cyprus is quite warmer than in Hungary and leads to remarkably higher temperatures. The cavity temperature is affected by the change of the vent size while the change of the depth is creating any remarkable alterations. By the increase of the vent size (vent1:0.05x33m to 0.5x33m) the temperature of the air in the cavity drops from 24 °C to 17 °C during winter and from 43 °C to 32 °C during summer *(figure 71,A).* Also, in the case of the non-ventilated shaft, the values are even higher (during winter the temperature of the cavity is 46 °C and 74 °C during summer). According to the above values, the system should be ventilated in both seasons, if it is used for ventilation, as the temperature of the air is high, even in winter. Moreover, by the use of small vents, the temperature value of the cavity is almost suitable for passive heating during winter while in summer, the temperature of the cavity is not suitable for cooling ventilation due to the high values (32 °C). Therefore, during summer, the air should be extracted out of the shaft. In relation to the glass temperature, even in Cyprus, where the ambient conditions are warmer, the temperature of the glass in lower than 40 °C, which means, that there is no risk of overheating.

PV and water temperature

Generally, in Cyprus, the temperature of the PV modules is higher, especially with the use of non-ventilated shafts. The temperature of the PVs during winter, in the case of ventilated shafts is approx. 19 °C which is normal while in the non-ventilated scenario, the PV temperature increases to 46 °C.

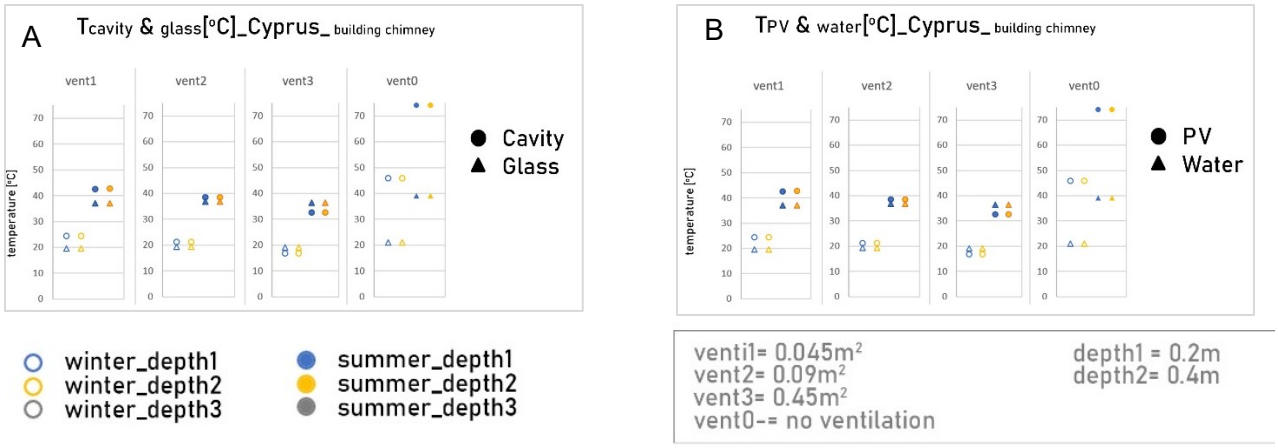

Figure 71: A) The glass and cavity temperatures in Cyprus of the "building scale chimney", with different vent size and depths (colors) for winter and summer. B) The PV and water temperatures in Cyprus of the "building scale chimney", with different vent size and depths (colors) for winter and summer.

During summer, in the cases of ventilated shafts, the temperature of the PV panels is fluctuated is between 59 °C (large vents) and 61 °C while in the case of no ventilation the temperature rises to 64 °C *(figure 71,B)*. In all the summer scenarios, the temperature of the PVs in not beneficial for their efficiency and may cause a significant drop of the electricity generation. On the other hand, the temperature of the water is not remarkably higher than the Netherlands and Hungary results. The temperature of the water is approx.19-20 °C in all the winter cases and 27-28 °C during summer. Although that the water cannot be used directly as Domestic Hot water, its temperature is quite high and it can be used beneficially as an input water of a heat exchanger in order to increase its efficiency and thus, decrease its operational energy demands.

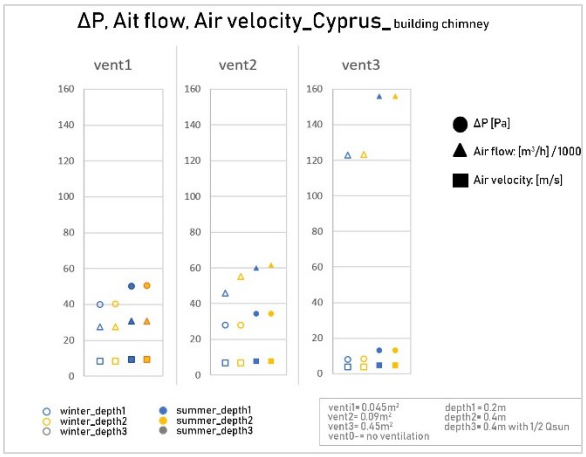

Figure 72: The pressure difference, the air flow and air velocity results in Cyprus of the "building scale chimney", with different vent size and depths (colors) for winter and summer.

B) Pressure Difference, Air flow and air velocity within the shaft:

The same reaction with higher values in pressure difference, air flow and air velocity are marked in Cyprus. In Cyprus, where the irradiance is generally high, the chimney effect is more intense and in combination with the high chimneys, extremely high-pressure difference and air flow values are caused. The pressure difference within the chimney ranges from 8Pa using large vents (vent3: 0.5x33m) to 40Pa with small vents (0,05x33) *(figure 72)*. This indicates that the opening dimensions affect the results a lot, while, in contrast, the differences by the change of the depth size are neglectable. In parallel, the air velocity drops by half or more by the change from small vents to large vents (8.2m/s to 3.7m/s during winter and from 9.1m/s to 4.7m/s during summer). Regarding the air flow, a large increase is noticed by the increase of the vent size. By the switch from small vents (ventl) to large vents (vent 3), the air flow is increased from 27500 to 123000m^3/h, during summer, and from 30700 to 155800m^3/h. In both seasons, the values of air flow are unrealistically high as they can provide enough ventilation for roughly 900-4100 people, during winter, and for 614 -3100 people, during summer. The

air velocity values as well as the air flow values are extremely high to be used for ventilation purposes. Consequently, the system the air can be used for wind energy generation.

3.2.3.3.3.3.2. Conclusion_Cyprus

The results indicate that "building-scale chimneys" are hard to be used for ventilation purposes since the air velocity and air flow values are extremely high (air velocity: 3.7-8.2m/s during winter and from 4.7-9.1m/s during summer, air flow: 27500-123000 m^3/h during summer and 30700-155800m^3/h. Moreover, the temperature of the cavity, during summer, is high, in all cases (minimum 33 °C in the case of large vents) and thus, the air cannot be used for ventilation. Simultaneously, the temperature of the PV modules is high even in the scenario of large vents (59 °C), therefore, the photovoltaics efficiency is low. This indicates, that the summer scenario in Cyprus with "building-scale chimneys" cannot beneficial for electricity generation, in any vent-size scenario. Additionally, the temperature of the water, is not reaching the favorable temperature levels in order to be used for domestic uses. However, it can be used as input water to reduce the temperature difference of the initial and the required temperature.

3.2.3.4. General Conclusions

3.2.3.4.1. General conclusions regarding the geometrical parameters of the PV-chimney system.

The calculations highlighted the importance of geometric parameters in the design choices of the proposed PV-chimney in the different climate zones. These geometric parameters included the height, width, depth of the cavity and the size of the effective openings. Multiple scenarios were calculated to evaluate the thermal-ventilation performance, the possible improvements and the potential of the system. The behavior of the PV-chimney systems is altered with the change of the weather conditions and their geometrical characteristics. Moreover, according to the intentions of the designer, as well as the purpose of the chimney's operation, the design of the system can vary. The analysis of the results shows that the design of the proposed PV-chimney system cannot be specific, as individual analysis and design of the system is required for different weather data and different intended functions of the system.

Generally, put, the height of the shaft plays an important role on the thermal behavior and the ventilation of the system while the width affects the results slightly. Increase of the height causes an increase of the air velocity and the air flow while the width affects significantly only the air flow. Moreover, shorter chimneys in the scale of a floor mark satisfactory values of air velocity (0.5-1m/s) while in larger systems ("column" and "building scale" chimneys), the air velocity values are high for direct ventilation (4-12m/s). Additionally, in cases where the levels of solar radiation are high, the thermal energy and the stack effect are more intense, indicating that emphasis should be put on thermal performance during summer, when dimensioning the PV-chimney in the design phase. Consequently, high or wide shafts have serious issues of excessive air speeds. Summarizing, the large PV-chimney systems ("building-scale chimneys") provide the ability to make use thermal energy but this idea is rather harder to implement due to the high air velocity and airflow values. Finally, the building-scale shafts do not provide significant thermal benefits in comparison with narrower shafts. Therefore, interventions in building-scale are not actually a necessity while similar or even better results can be provided with smaller interventions.

Meanwhile, the temperature and ventilation differences are much less affected by the depth of the cavity, especially in higher and wider chimneys. Although the depth size does not affect significantly the behavior of the system, the increase of the depth (from approx. 1/20 to 1/10 analogy of depth/height) in shorter shafts (approx. width/height: ¼ or shorter), increases slightly the cavity temperature as well as the air flow and air velocity values. This fact may be due to the ratio of the air that enters the shaft in relation with the shaft size. Probably, when changes in depth, are proportionally similar to the total size, also in larger shafts, then similar differences probably will be noticed.

Regarding the effective opening size, the differences in temperature are slight by air inlets/outlets which have surface area less than ⅛ of the glass surface. Moreover, the increase of the vent sizes is not proportional with the decrease of the temperature of the air in the cavity. The drop in the cavity temperature is slight in comparison with the increase of the opening's area. Accordingly, in cases of large shaft sizes and high solar radiation values, where the temperature of the system increases, bigger vents can help but that cannot manage to cool down the system to comfort levels (20-25°C). Additionally, in Mediterranean climates as Cyprus, the shaft has to be ventilated during the whole year, due to the high temperature values both in warm and cold seasons, while, in colder climates, the openings should be closed during winter, in order to optimize the thermal efficiency of the PV-chimney system. Simultaneously, increase of airflow is provoked by larger air inlets is again not proportional. In narrow chimneys the airflow is risen a lot more times by increasing the vent dimensions while in wider chimneys the increase is not that dramatic. Generally, the control and the choice of the proper

vents depends mainly on the solar irradiance values which can cause a tremendous increase of the temperature inside the shaft and the required amount of air flow.

These conclusions emphasize on the proper design of the basic geometric parameters according to the specific climate zone, in order to provide better performance and improve the energy savings of the building that it is applied. The findings of this multicriteria analysis of different weather and geometric parameters can provide a reference and a better understanding of the system, in general, as well as the energy potentials that an innovative PV-chimney can provide.

3.2.3.4.2. General conclusions regarding the different climates

The analysis of the PV-chimney system in different climates (Moderate, Temperate and Mediterranean climate) provides an image of what are the potentials of the system under different weather conditions. Also, by the comparison of different results which caused by different geometrical characteristics, offer the understanding of the behaviour of the system and the optimization of it, by choosing the characteristics which are closer to the energy targets.

The investigation of the system was done by the weather data of the Netherlands, Hungary and Cyprus. The analysis of the results indicates that the Netherlands and Hungary have similar behaviour (with Hungary to mark slightly higher thermal performance due to higher solar radiation). In Cyprus, the results differ as the climate is much warmer than both the Netherlands and Hungary.

As it aforementioned, the air in the cavity of the "column" and "building scale" PV-chimneys reach high values of air velocity which are not suitable either for heating or cooling. However, they are not rejected as they can be combined with mechanical systems that will extract the required amount of air and it will control its air velocity before its use. Moreover, by the transition from "floor" to column" chimneys, the temperatures of the system (mainly the cavity temperature) increases slightly by 2-4°C while from "column" to "building scale" chimneys, the temperatures of the system by 1-2°C. Consequently, the enlargement of the system in comparison with the additional thermal gains is disproportionate. For this reason, the proposed solutions of each country are referred to "floor" scale PV-chimneys, which can provide more thermal gains per square meter of application.

In the Netherlands and Hungary, where the results are similar, the PV-chimney can be used for passive cooling while for its heating mode, the vents have to be closed and the connection of the system with a heat exchanger is needed. The system cannot be ventilated by outdoor air during the winter due to low ambient temperature witch results to low cavity temperature (2-6°C). Therefore, during the winter, it is recommended to have to vents close in order to achieve higher temperature of the air in the cavity (11-13°C). Although the temperature of the air in the cavity is higher with closed vents, it has still low temperature to be used for heating. Consequently, the PV-chimney cannot provide passive heating. The air of the cavity has to pass through a heat exchanger in order to warm it up to the required temperature. By this way, additional energy is needed but the COP factor of the heat exchanger will be increased, decreasing its operational energy consumption (because the temperature difference between the input air the output air is decreased). Additionally, as an improvement of the heating operation of the PV-chimney, the impregnation of the cavity with highly absorbing fluids or the placements of highly absorbing solids could achieve higher cavity temperatures *(Zhongting et al., 2017)*. Apparently, in these cases, filtering of the air is needed which requires additional energy. During the summer, small (0.045m^2) and medium size (0.09m^2) vents can be used for passive cooling (the large vents, 0.45m^2, cause lower temperature in the cavity which is lower than the comfortable levels) as they reach the comfortable temperature levels for cooling (20-21°C) and the air velocity of the air is suitable as cooling supplier (approx. 1-1.2 m/s). Furthermore, the direct use of the water is not

possible as the water temperature values are fluctuated between 11-12°C during the winter and 18-21°C during the summer. Again, the preheated water can be use as suuply water to a heat exchanger reducing its operational energy consumption. Lastly, the descripted scenario of operation of the PV-chimney, maintain the PV temperature lower than 40°C, which means that the PVs can work with high efficiency.

Contrary to the Netherlands ang Hungary, in Cyprus where is much warmer, the system cannot operate with closed vents, even during the winter. Due to high solar irradiance both in the summer and the winter, the air in the cavity with closed vents is warmed up to roughly 50°C during the winter and 76°C during the summer. Additionally, during summer, even with large vents, the air in the cavity is high for cooling (31°C), ttherefore, the PV-chimney cannot be used for passive cooling in Cyprus. Similarly, the temperature of the photovoltaics, even with large vents, is 59°C, which exceeds the workable operational levels of temperature, therefore, the PVs cannot be worked efficiently. During the winter, the air in the cavity cannot be used for passive heating (21°C) as additional warming of the air is needed. Thus, the connection of the system with a heat exchanger system is required. Lastly, the PV/T system in Cyprus provides higher water temperatures than the Netherlands and Hungary (19-20°C during the winter and 27-30°C during the summer). However, the water temperature is not reaching the desired values in order to me used as Domestic Hot water or heating water. Summarizing, in Cyprus, the PV-chimney, cannot be work efficiently, mainly due to the high temperatures of the PVs (the main goal of the system is to provide both electricity and thermal gains and in this case the PVs cannot operate) but also due to the fact that either heating cooling or the water cannot be used directly (additional energy is needed). Finally, there is also the risk of overheating of the system during summer which can heat up the thermal mass of the building causes opposite results.

4 DESIGN IMPLEMENTATION

4.1. Case Study

The case study in this research are the Europoint Towers in Rotterdam, a city in the Netherlands *(figure 73).* The Towers are three and they are the same. The Europoint Towers were designed for offices by the famous firm SOM in the 70's in their well-known International style. The towers have 22 storeys and 90 m height. The building has a rectangular plan a main core in the middle which is currently contains all the vertical communication and building services. This includes nine elevators, two emergency staircases, along with two washrooms and smaller service areas *(figure 74).* Each floor of the building has the same plan which it includes the main core and free space around it. The building has a concrete structure and the inner windows cannot be opened since the building was designed to be mechanically ventilated. Moreover, the envelope of the structure has a ratio A/V (Area-to-volume) of 0.12. Additionally, the Towers has their bigger facade almost perpendicular to South/West and the smaller sides on East/West.

Figure 73: Europoint Towers, Rotterdam

For this case study, a renovation concept of the towers is developed within the framework of the Solar Decathlon competition 2019. Additionally, within this framework, the proposed facade is designed in detail and is constructed in real scale in a prototype that represents a cut-out of the 22th floor of the building. The design of the facade is done by the author, as she is a member of the MOR team (the

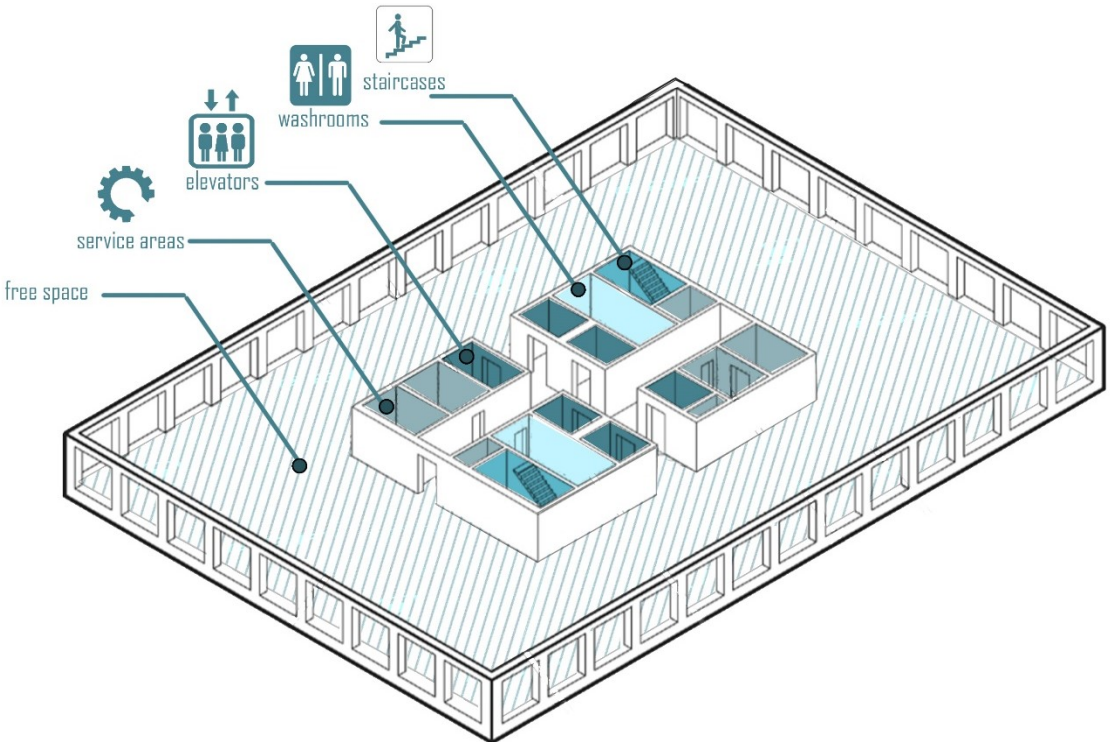

Figure 74: Existing functions of the core.

team that is competing as the team of TU Delft). Specifically, the author, in collaboration with another member of the team, designed and handled the facade assembly and construction on site.

In this study, a detailed design of the PV-chimney is done separately, exclusively by the author and was implemented in the MOR facade design concept. The competition, taking place in Hungary, is based on multiple criteria, among which is the energy performance. In addition, however, the prototype is intended to be permanently hosted in the Netherlands (in the Green Village of Delft) where the case study building is also located, Therefore, it was essential that the system can perform efficiently in both climates. As it can be clearly assumed the realization of the PV chimney was not only based on the energy simulations but also on other "real" factors. These factors are determined by the architectural intentions, time and cost constrains, availability of products (sponsors/local market) and construction effectiveness.

4.2. Facade Concept

The facade aims to upgrade the performance of the building respecting the initial view of the building. Therefore, a theoretical grid in respect to the initial facade lines recreates

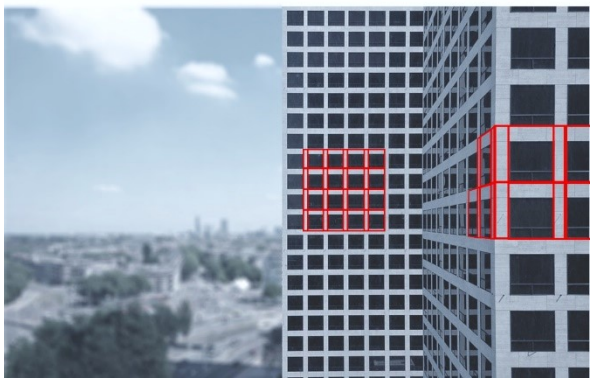

Figure 75: The division of the existing facade in modules, for the creation of the new facade units

Figure 76: Illustration of the proposed facade.

the facade pattern *(figure 75)* while an illustration of the proposed facade is shown in figure 76. Moreover, a modular system with recurring elements for faster production, assembly and maintenance of the facade is selected. Regarding the tower's facade, the current single glazing windows and travertine lining are removed due to their poor performance and inadequate wind and water tightness, contributing negatively to the energy performance of the towers. The proposed facade creates a skin by multifunctional high-performance facade modules. The facade modules incorporate multiple functions such as energy production, shading, ventilation systems and greenery (for air purification of the pedestrian level). In order to fulfil these different requirements, the facade modules are split into two parts: the structure and the modular additions. The structural part consists of a thermal package to meet the thermal insulation needs, and the aluminum hanging system for the modular

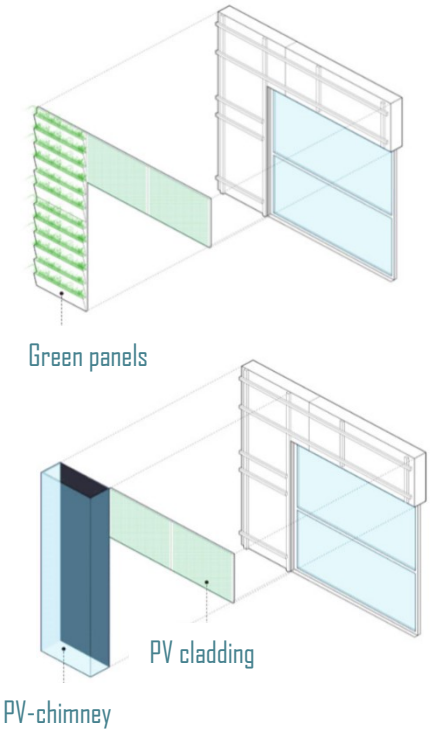

Figure 77: Facade panels with green panels and cladding on the left and with PV-chimney system and cladding on the right.

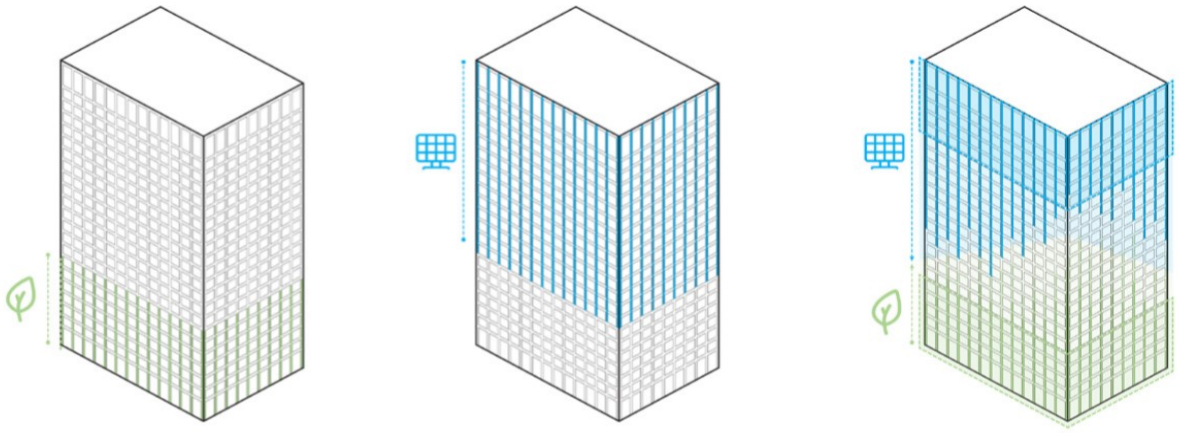

Figure 78: The transition from nature (left side) to technology.

additions. These additions come in the form of PV-chimney system, PV panels or green panels *(figure 77)*.

Regarding the architectural concept, the new facade aims to reflect the vision of a sustainable retrofitting in the future and of net positivity. Contrary to the current facade, which is reminiscent of an era dominated by modernist design principles, where buildings were seen merely as machines for living, the MOR facade, seeks to bridge this gap between nature and technology and showcase it. This is done by creating a gradient on a facade where natural elements in the form of green panels transition into technological elements in the form of photovoltaic panels and PV-chimney additions *(figure 78)*. At the lower levels of the building, green panels are designed as planter modules with air purifying plant species which would at the same time cool down the pedestrian area through evaporative cooling. Going upwards, a transition towards the technological elements of the facade occurs. The green panels decrease slightly and are replaced by cladding elements or PV-chimney systems. The cladding of the tower is Kameleon Solar ColorBlast PV panels with an efficiency of 12.6%. Although their performance is lower than the best-performing monocrystalline cells available commercially, the landmark status of the building and the architectural variety that these colored cells offer warrants their usage.

The proposed PV-chimney system is used mainly on the south and west façade envelopes of the tower and will act as a passive solar ventilation, PVT system and as a renewable power generation source. As the PV panels within the PV-chimneys absorb energy from the sun during the day, the temperature of the air within the chimney increases creating an upward movement of the air. Consequently, warm air is concentrated on the top. Therefore, the same area of the envelope is used both for electricity generation and for heat storage. For the representation of the tower in Hungary, the PV-chimney has the height of one floor, and it does not used for passive ventilation due to lack of time and the complexity of connection to the HVAC system.

4.3. Facade modules

The façade designed for the refurbishment of the towers and the prototype consists of unitized system modules. Specifically, 3 units were designed for the tower scale and 9 units for the prototype since it represents a cut of the tower splitting floor in the middle. The three sections for the tower consist of 1units for the corner, 1 for the column and 1 for the window. In the case of the prototype, 3 units were designed for the corner, 3 for the window, 3 for the column and 3 to connect the HSB facade and walls *(figure 79).* As mentioned above, the modular facade system has great capability and it is ease of disassembly at the end of its facade life. A set of drawings of the facade detailing is presented below in chapter 4.6.

The insulated facade modules consist of an aluminum frame (SCHÜCO profiles) and aluminum sheets in two sides that holds the Rockwool insulation *(figure 80).* A thickness of 226mm insulation were chosen to cover the required thermal resistance of the facade (Rc=6.55 m^2K/W). The aluminum sheets are mechanically attached to the frame, in order to be able to be dismantled in the future. In order to guarantee airtightness and water tightness of the facade plastic gaskets are inserted between the frame and aluminum sheets. Finally, the aluminum structure for the external cladding is fixed of the external face of the facade module *(figure 80).* As for the window unit, the same aluminum frame is used to secure the window. On the latter, the shading system and the exterior lining structure are also mounted on the window facade unit (see drawing x). The windows have a triple glazing of U-value 0.5 Wm^2K and acoustic performance Rw= 46 dB (see appendix x). Moreover, the windows are openable vertically and they are controlled by an automatic system as the external shading. The steps explained above are done during the construction of the facade units in the facade factory, in order to construct complete facade units and to facilitate maximum construction on site.

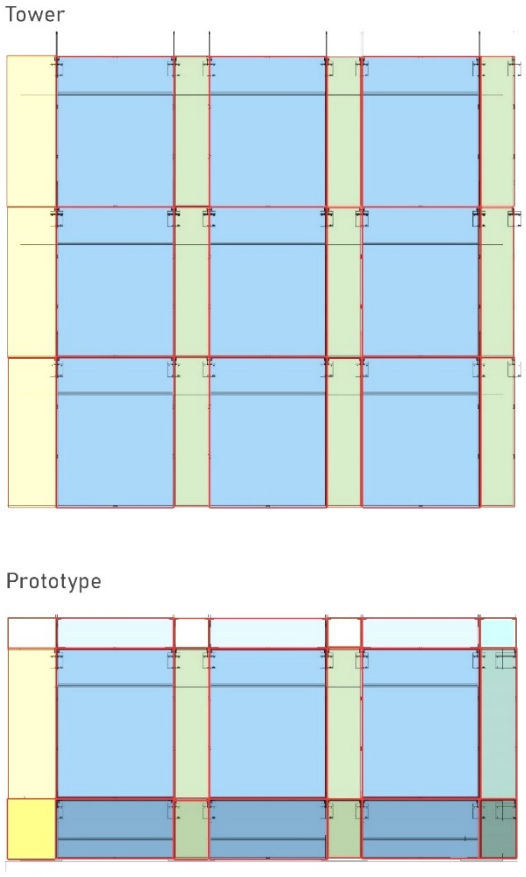

Figure 79: The unitized system in Tower scale and the prototype scale. The corner modules are presented with yellowish color, the window modules with blueish, the column modules with greenish color and the special modules for the connection with HSB wall (prototype scale) with turquoise color.

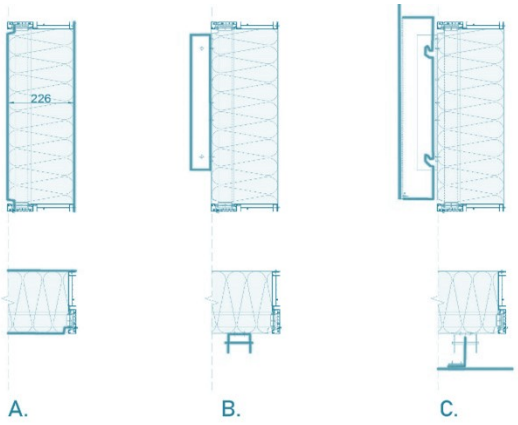

Figure 80: The steps for the PV cladding handing on the insulation spandrel panel.

For connecting the facade units and the existing construction, the steel brackets are fixed to the concrete structure *(figure 81).* Once this phase is completed, the facade units can be mounted on the concrete structure, following a horizontal sequence building floor by floor. Once all the facade units are assembled, water tightness and air tightness must be ensured by filling the outer gaps between the concrete structure and the facade units with stone wool insulation and closing these points with EPDM foil. In the case of tower scale, this phase should only be done on the roof, while in the case of the prototype it should also be at the intersection of the unitized facade and HSB walls.

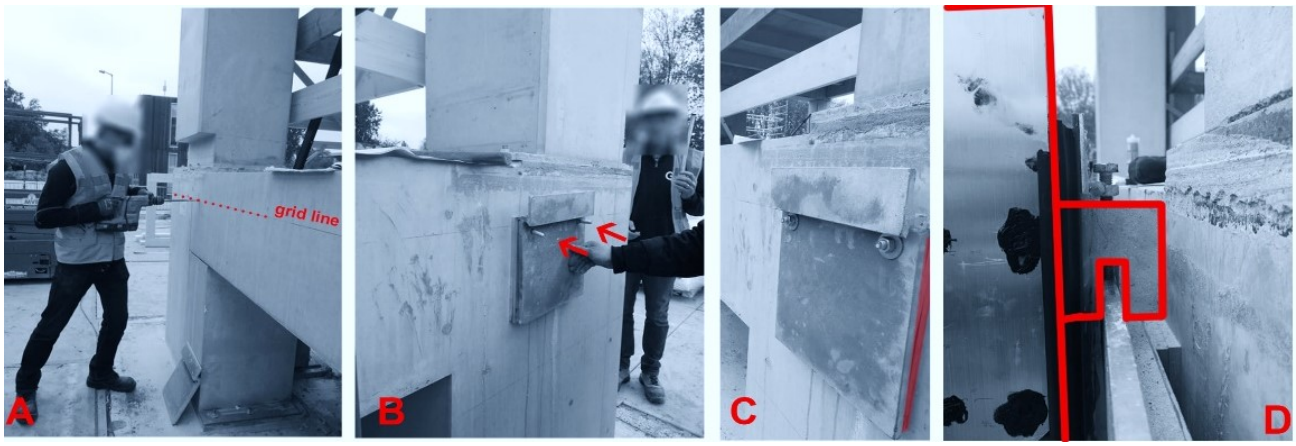

Figure 81: Steps for the placement of the modules on the concrete structure

Finally, the outer cladding can be assembled, delivering the solar panels and the PV-chimney to the aluminum structure mounted on the facade units during the construction phase. Assembling the proposed PV-chimneys on the facade modules consists of two stages: the first is the suspension of the solar panels with integrated pipes of the PVT system, and the second is the hanging of the glass boxes (prefabricated in the facade factory).

4.4. PV/T-chimney Design

In order to decide the most beneficial design for the PV/T-chimney for both the Netherlands and Hungary, the simulation results were used. The thermal behaviour of the system as well as ventilation possibilities and PV viability, in terms of temperature, were analysed in average and boundary weather conditions. The analysis of the simulations is done for both the Netherlands and Hungary as the prototype is firstly built in Hungary, for the purpose of the Solar Decathlon competition, and then will rebuilt in the Netherlands.

The PV-chimney design was accompanied with various restrictions. The fact that the construction of the PV-chimney system is based on sponsorships, limited a lot the products and materials choices. In addition to that, the competition requirements determined the design on a great extent. The first factor was the duration of the assembly, which had to be completed in four days, for the whole façade, and this, determined an assembly strategy which had an important influence on design decisions. Secondly, the construction schedule was a restrictive factor in the design time plan. Finally, the architecture concept of the facade, played an important role on material choices and on the dimensioning of the PV/T-chimney components.

The following PV/T-chimney design for building facades, is proposed in order to generate thermal and electrical energy simultaneously and to provide Domestic Hot Water. Also, waste heat can provide ventilation, from which a heat pump can still extract heat from the warm exhaust air, creating a very efficient system where hardly any waste heat is lost. The initial concept was to use a heat exchanger at the top, where the heated air is moved to heat up a refrigerant to aid in the heating of domestic hot water and for air heating. Due to the complexity of the system together with the lack of time (due to competition deadlines), at prototype scale, this system is just experimental, therefore for hot water production solar collectors are placed on the roof, whereas the PV/Ts-chimneys

PV/T - chimney solution

Height: 4.35 m
Width: 0.815 m
Depth: - with PV/T: 0.24 m
- cavity: 0.11 m
Vents: 0.072 m^2
Glazing: - single 0.08 mm
- g-value: 0.9

Structure: aluminum
PV: ColarBlast (black ,13% effic.)
PV/T: -cooper pipes 12 mm diam.
-cooper plate 3 mm
Insulation: Rockwool

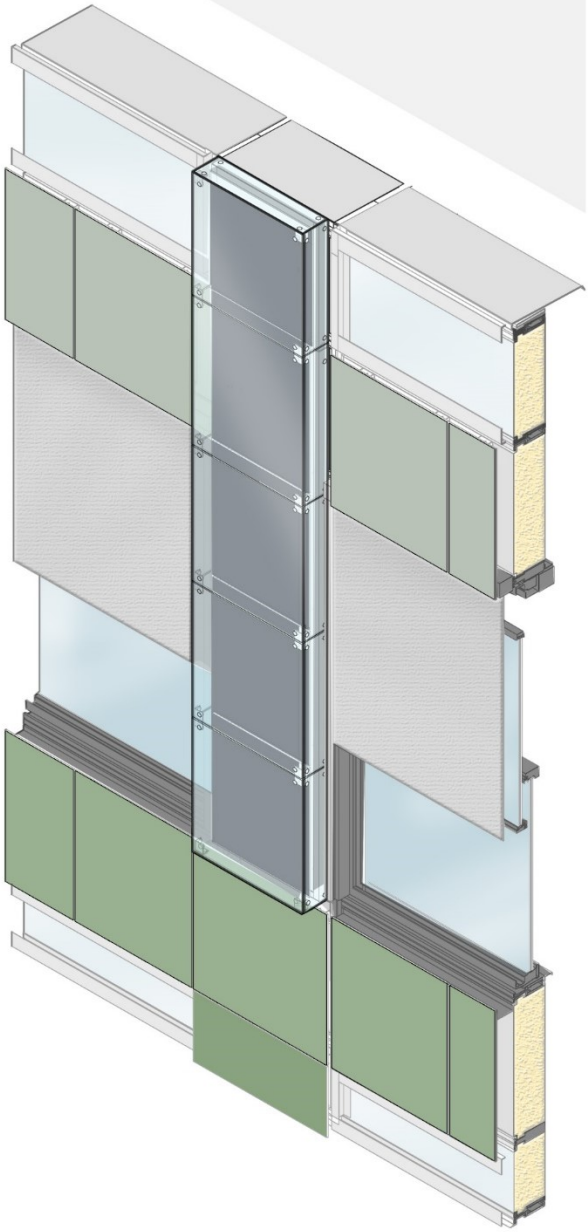

are used to provide prewarm water to the solar collectors of the roof and thus, increase their efficiency *(firure 82).* Although the supply of ventilation to the building is not developed, due to time limitations and the complexity of the connection of the system with the HVAC system of the building, the system is designed taking into account the future use of the system also as a ventilation system.

As mentioned, the main idea of the system is that the usage of PVs, to generate electricity, is combined within a Trombe wall in order to capture thermal energy from both systems. That means, higher temperature operational conditions for the PVs and thus, possibly, less efficiency. Therefore. for additional cooling of the PV modules, water is used as a cooling medium. A thermal collector system is installed at the rear side of the PVs where cooper pipes with water were attached in order to absorb heat from the PV modules and thus, cool them down. Therefore, the system can provide both electricity generated by PVs and hot water which is warmed up by exploiting the heat generated from the operation of the PV panels. In figure 83, 84, the initial PV-chimney proposal and what is finally built (due to time, cost and practical constrains) is revealed. The main difference of the initial proposal and the what was built is that the assembled prototype is not connected with the indoor space and the HVAC system of the building, thus it can not be used for ventilation purposes.

Operation

The PV-chimney during the summer, in the case of the initial design, it works with the bottom vents (which connect the shaft with the indoor space as well as the upper vents towards the ambient) open. The top vents which connects the shaft with the indoor space are close. The tower passive strategy it that from the core of the building, fresh air is entering the apartment and by the PV-chimney, cross ventilation is caused. The fresh air is crossing the apartment and is getting in the channel from the bottom vents. In the shaft, the air is heated up by the sun radiation and thus, it moves upwards, due to buoyance effect, and is extracted to the ambient from the top vents. This, cause

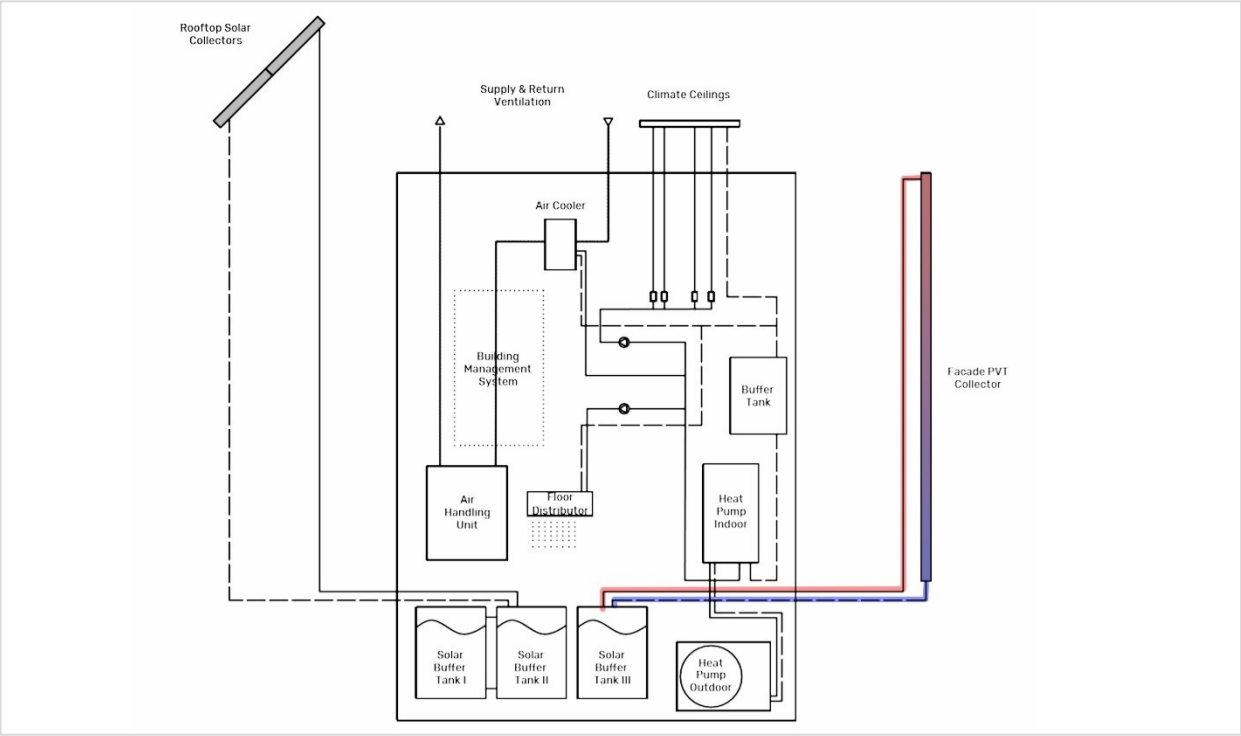

Figure 82: Scheme of the mechanical system of the prototype.

continues cross ventilation. Simultaneously, the warm air heats up the PVs and thus the water which runs behind them *(figure 83)*. In the real prototype, the system works only to warm up the water, since there is no connection with the indoor space. That means that ambient air is getting in the shaft from the bottom vents, is heated up and thus, it moves upwards to be extracted outdoors from the top vents *(figure 84)*.

During the winter, the initial design proposes the use of the system for heating of the indoor space by air circulation. The indoor air is getting in the shaft by the bottom vent (which connects the shaft with the indoor space), is heated up, and then by the upper vent, is returned to the room *(figure 83)*. In the case of the real prototype, both the upper and bottom vents are close in order to create higher thermal energy and provide higher water temperatures *(figure 84)*.

Energy performance

For the final design of the PV-chimney, the energy performance of the system was analysed in more detail by calculating the thermal behaviour and the amount of ventilation through the system, for both The Netherlands and Hungary, under boundary weather conditions. Except for the height of the system, which was limited due to the height of the protype, the rest of the geometrical parameters are evaluated in order to provide high energy performance. Additionally, according to the sun path of Hungary, the PV-chimneys are orientated towards the north and west. Although the North is accounted more hours of sunshine in an annual base, the placement of the system on both sides enhance the energy generation during the whole day. Additionally, the fact that the sun during the afternoon has lower angle of incidence, makes the west side important too.

INITIAL PROPOSAL

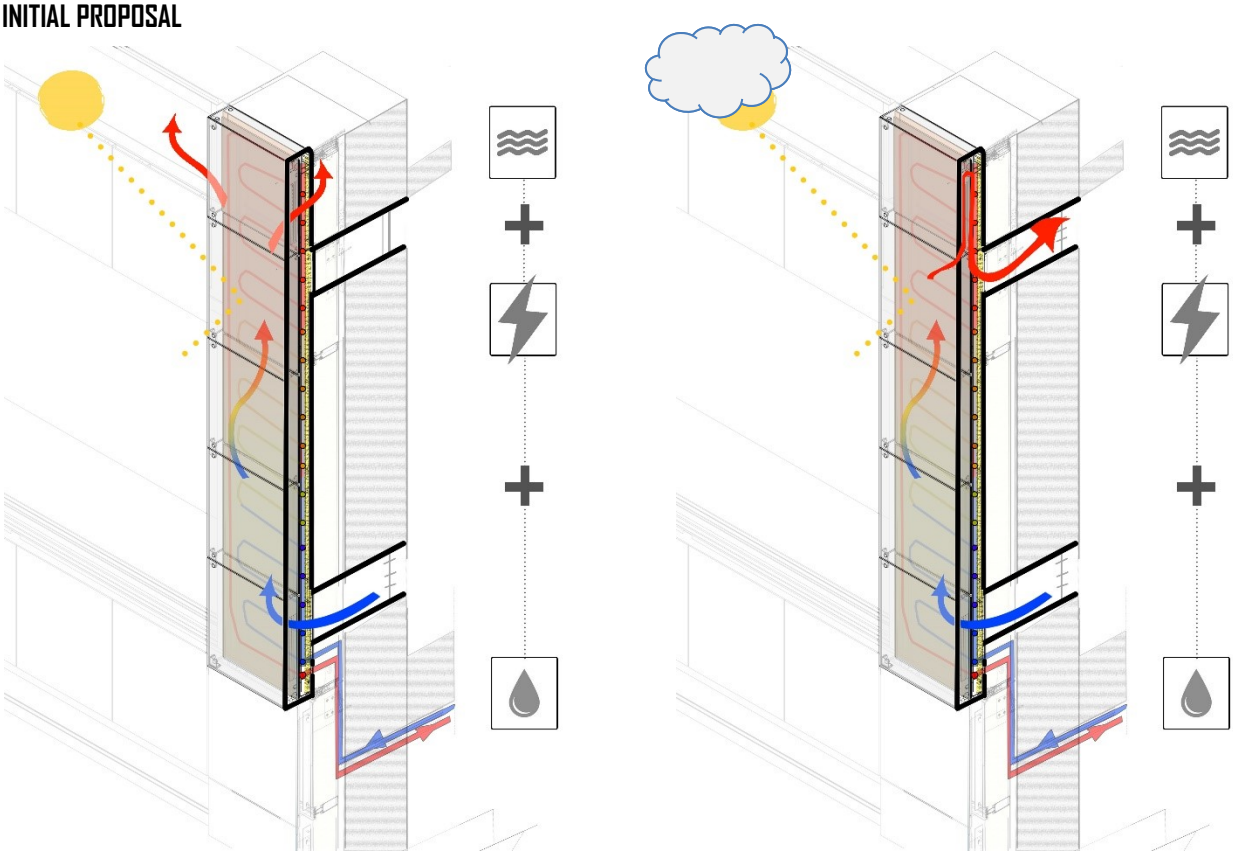

Figure 83: The proposal for the PV/T-chimney. The summer operation is shown on the left and the winter operation on the right.

BUILT PROPOSAL

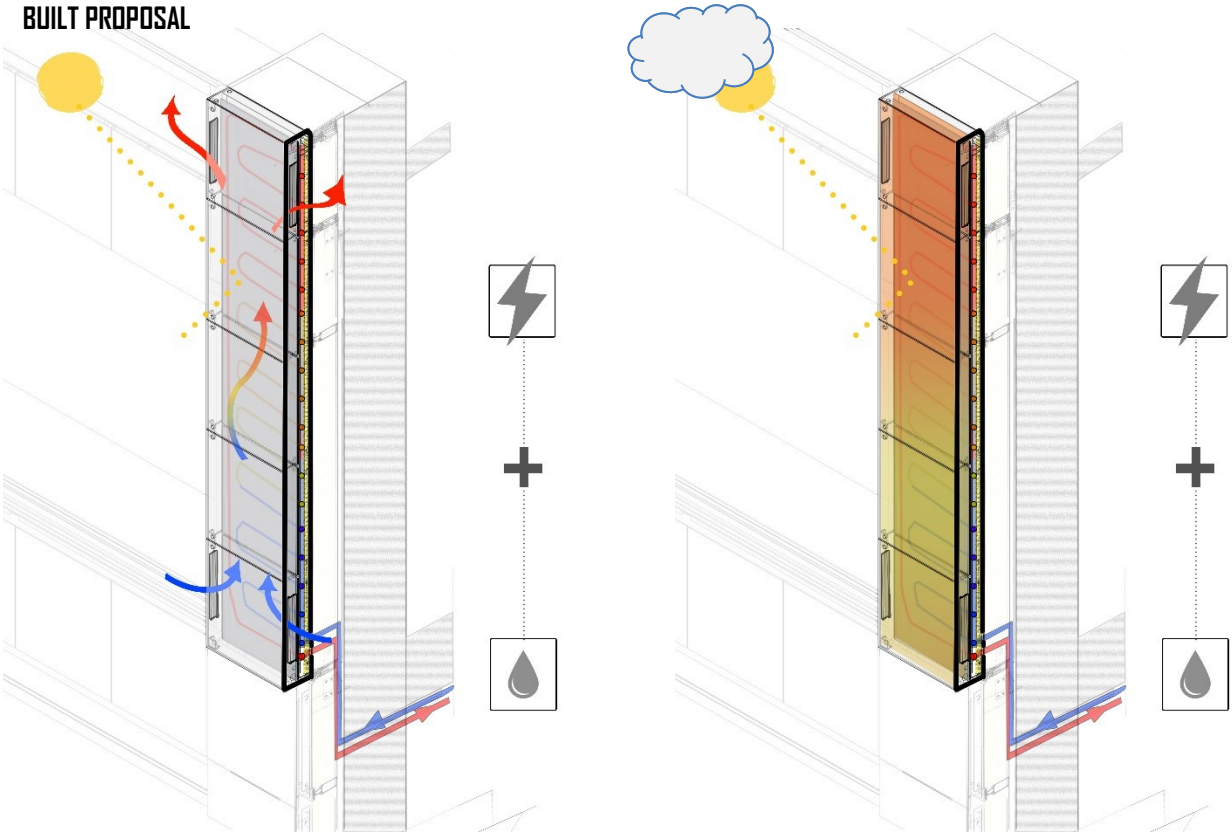

Figure 84: The real prototype of the PV/T-chimney. The summer operation is shown on the left and the winter operation on the right.

DESIGN DECISIONS

The design decisions, as mentioned, is a result of the energy performance analysis of the system in combination with real and practical constrains. Additionally, as the PV-chimney is part of the façade and consequently part of the whole architectural concept, architectural intentions lead to certain design choices. The following chapters will explain the design decisions based on both Performance-practical and Aesthetical issues.

- Performance
  - VENTS
  - DEPTH
  - GLAZING
  - PV/T
- Aesthetics

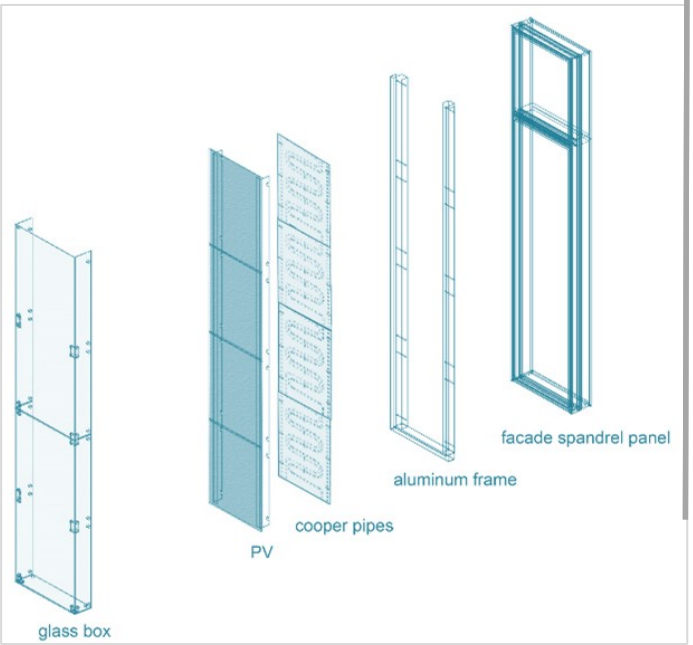

Figure 85: The basic PV-chimney layers.

4.4.1. Practical and Performance Decisions

The performance decisions were based on simulation of the Netherlands and Hungary climate conditions. Apart the average temperature values, also the maximum and minimum monthly average, in summer and winter were considered, in order to estimate the behaviour of the system in boundary conditions. The figures below show the results of the temperature of the cavity, of the PV modules and the water in the different variations of opening size and ventilation through the shaft. Due to higher solar radiation in Hungary, all the values are slightly higher than the Netherlands. However, the temperature and ventilation differences are small. The following figures represent both winter and summer results in the Netherlands and in Hungary. In this case, the depth variations caused negligible temperature differences (less than 1º) and slight changes on the amount of ventilation, thus, the results present only different vent size scenarios.

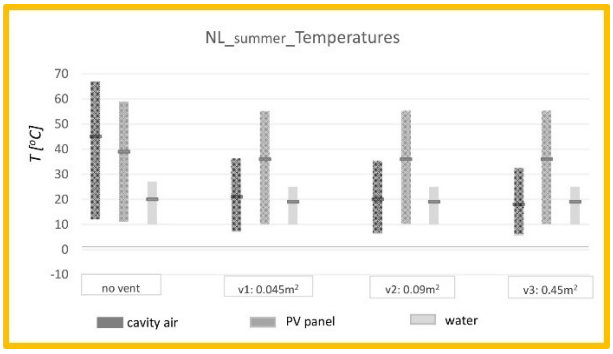

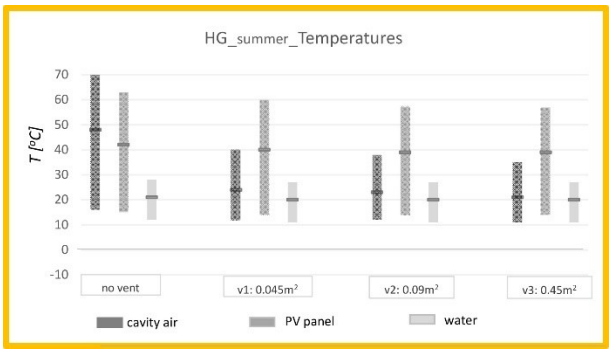

Figure 86: Simulation results for the temperature of the system during the summer for both the Netherlands and Hungary.

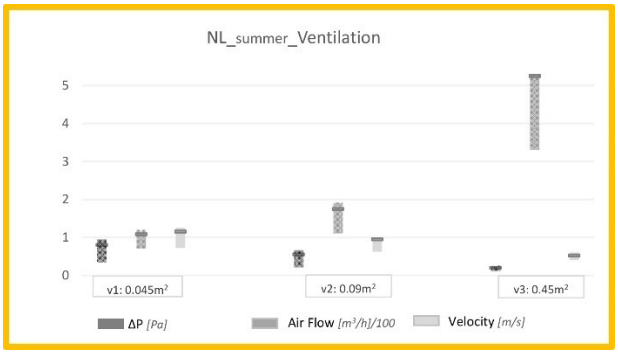

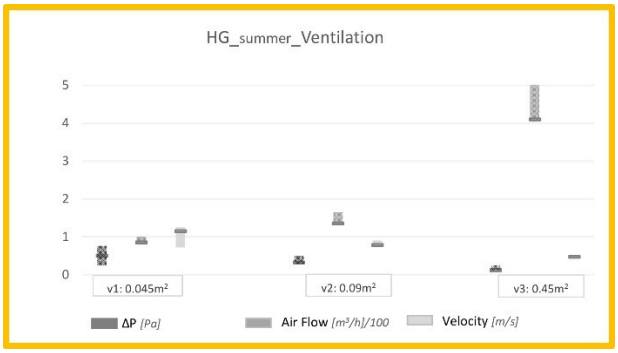

Figure 87: Simulation results for ventilation through the shaft of the system during the summer for both the Netherlands and Hungary.

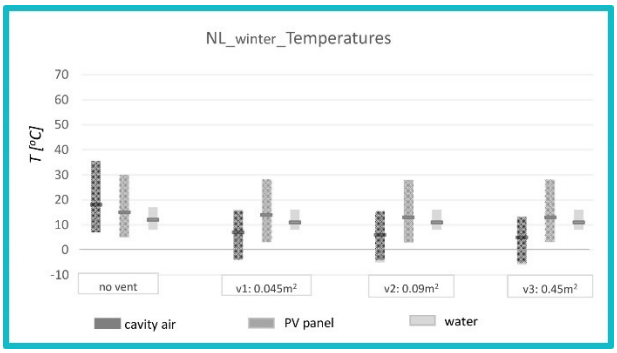

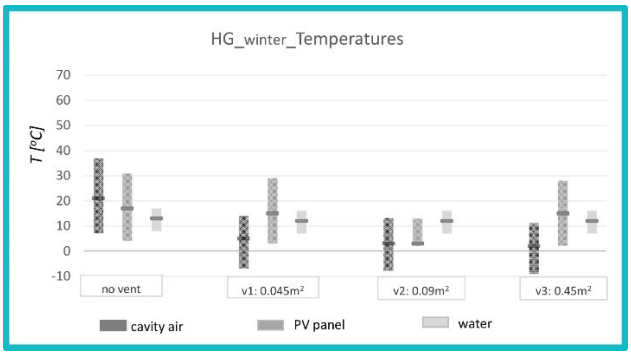

Figure 88: Simulation results for the temperature of the system during the winter for both the Netherlands and Hungary.

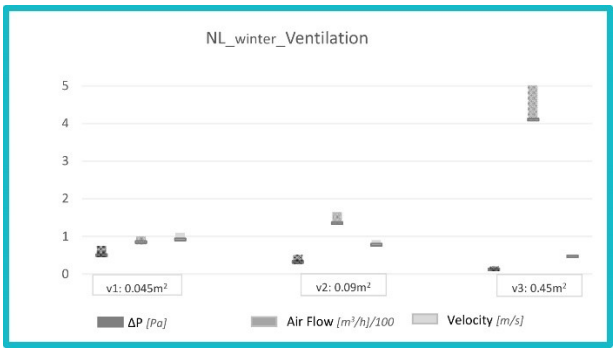

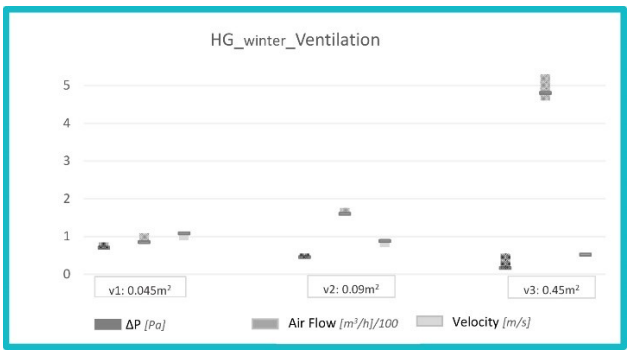

Figure 89: Simulation results for ventilation through the shaft of the system during the winter for both the Netherlands and Hungary.

VENTS

Regarding the opening size, the selection of the vent size was based on the simulation results of the system as well as practical and time issues .The increase of the vent size from 0.045m^2 (vent1) to 0.09m2 (vent2) cause a slight decrease, mainly on the cavity air, and PV temperature, while the temperature of the water is not affected. Also, additional increase of the vent above 0,09 m^2 does not offer remarkable changes *(figure 86, 88).* Even though thermal energy generation is desirable, opening size above 0.045m2 (vent1) is preferable due to the higher temperature value of the PV modules during summer in both countries. Moreover, the air velocity in both small and medium vents during the summer, is ranged between 0.8-1.1 m/s which is quite appropriate for future use of the system for ventilation. Additionally, the air flow is predicted to be 100-200m^3/h during the summer which can provide ventilation for 2-4 people which covers the required demands (the apartment under study, is intended for two people).

For the PV-chimney of the built prototype, 4 vents with surface area of 0.036m^2 are placed equally at the top and bottom of the chimney (that means 0.072m^2 at both ends). The surface area of the vents was delimited by the available vents on the market that could fit on the sides of the shaft. More specifically, the bottom part of the chimney was not accessible due to the existence of the cladding panels of the facade. Therefore, it was judged as more practical the vents to be placed on the sides. For the same reason, there are installed 2 vents on the top and 2 on the bottom instead of one big on each end. The available vents on the market, with bigger surface area, were either very tall, which, in this case, would decrease the distance between the two vents a lot (decreasing the theoretical height of the shaft, and therefore the air buoyancy effect), or very wide in order to fit on the sides *(figure 90).*

At this point, it is important to be mentioned that due to the efficient function of the chimney it was desirable to purchase controllable vents in order to adjust both to the winter and summer situation. However, the time and financial constraints determined the final choice of a fixed vent product. For the most optimal function of the chimney, these products are favourable to be replaced. Also, the fact that the vents are opposite the one to the other is not functional as it is affecting the air flow, specifically, cross ventilation is occurred between the vents prevent the upward movement of the air.

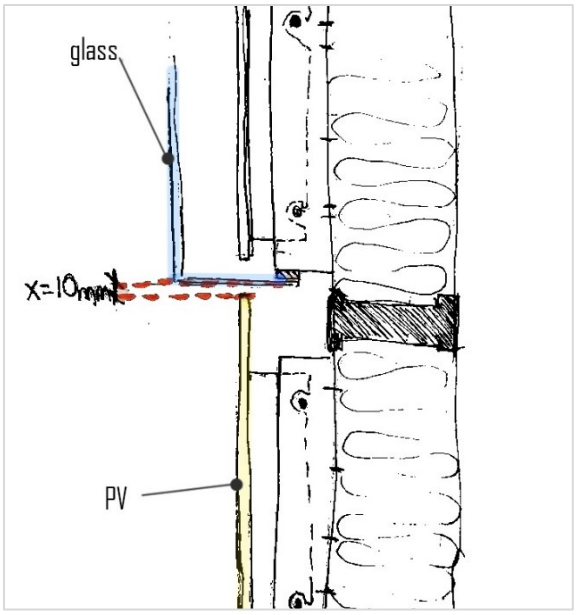

Figure 90: The distance x, of the PV-chimney glass and the PV cladding.

DEPTH

The results of the simulations indicate that the depth influence on the thermal behaviour of the system is minimal. Consequently, the selection of the depth size was based on architectural parameters. The main architectural invention for the façade was to respect the initial view and the flatness of the façade. Therefore, the PV-chimney is designed as flat as possible.

The shaft has a final depth of 240mm which is based both on the intention of creating a flat façade surface but also on the depth to height ratio. The depth to height ratio is influenced by other studies of Trombe walls which studied the relation of the depth on the thermal performance and the mass flow rate *(Peng et al., 2013. Liping & Angui, 2006, Shakeel et al.,*

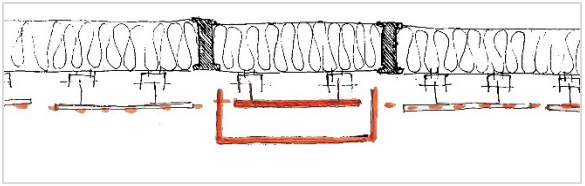

Figure 91: Continuous flat surface by placing the PVs at the same line.

2017). Within this depth, the PV/T system is placed leaving 110mm (the distance between the PV and the glass) air shaft. Therefore, the PV-chimney, is extruded only 110mm from the façade finish line. The final layer of the PV-chimney, which is the glass, is not aligned with the cladding for two reasons. First, the existence of the spandrel panel and the structure of the PV/T-chimney which is fixed on the insulation spandrel panels of the façade, push the whole system outwards. In addition to that, the PV modules, as the opaque components of the PV-chimney which are visible, they were aligned with the rest of the cladding in order to be blended with the rest of the cladding panels and to give a sense of a continuous flat surface. Consequently, the glass shaft should be extruded from the cladding surface *(figure 91).*

GLAZING

According to the literature findings of Trombe walls, the single glazing is preferable during cooling seasons as double glazing Trombe walls mark higher thermal performance *(Kundakci et al,. 2012, Stazi et al., 2012)*, Also, in the case of single glazing, the higher values of solar transmittance, can improve the ventilation rate within the shaft *(Lee & Strand, 2009).* Regarding the PV/T system and the glazing, literature shows that adding glass layers, decreases the efficiency of the PV system despite that the thermal efficiency is increased *(Sandnes &Rekstad, 2012, Fujisawa & Tani, 1997)*. Additionally, anti-reflective coatings increase both the thermal and the electrical efficiency of the PV/T systems *(Santbergen et al., 2010).*

The simulations of the system are done with single glazing and the results show that the highest temperature of the PV modules is reaching 55-60 °C in both countries during summer *(figure 86. 88).* Although these values are high and can cause a drop of the PV performance, there is no risk for the PVs to break. Higher values of PV temperature are probably not functional as the efficiency of the photovoltaics will drop significantly. Therefore, this is one reason that single glazing is selected instead of double glazing.

Simultaneously, the temperature of the cavity during summer (ventilated shafts) can exceed 30°C, which is above of the maximum comfort temperature values (max comfort temperature for winter is 28°C). Also, during winter, where higher thermal energy is desirable, the temperature of the cavity, with closed vents, has an average value of roughly 20°C (the cavity reaches values till 38°C under ideal conditions) which is slightly lower than comfort levels (lower comfort temperature for winter is 23°C). However, with minimal amount of energy, the air can be warmed and be used for ventilation. Consequently, as the temperature of the cavity during summer is quite high and during winter the temperature of the cavity, with closed vents, is satisfying, single glazing is chosen.

The PV-chimney has a single laminated safety glass of 8mm with g-value of 0.9 in order to let as much solar radiation as possible to pass through it. Moreover, is was desirable to make use of anti-reflecting coating in order to reduce reflection losses of solar radiation. However, due to time and cost constraints, the coating was not applied. Due to the same reasons, as well as architectural issues, the solutions of a glass box with circular corners was rejected. The casting of the glass had long delivery period and high cost. The glass with circular corners would help avoiding additional structure for the glass, which is shading small parts of the PVs, Furthermore, the circular corners offer better distribution of solar radiation within the shaft.

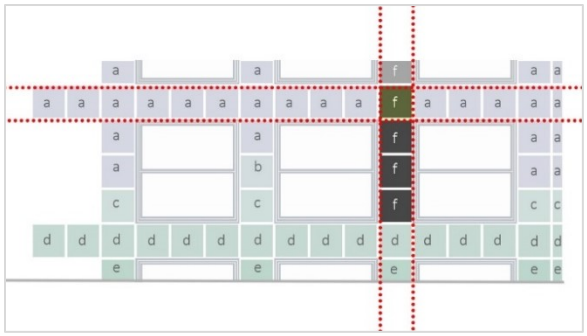

Figure 92: The configuration of Kameleon Solar panels in the South. The different letters indicate the different colours ("f" are the panels of the PV-chimney which are black) while the red lines show that the fourth panel has different size than the rest.

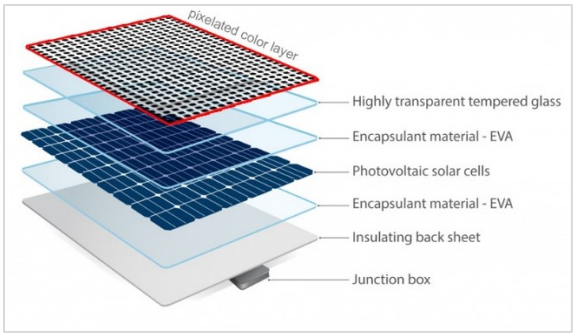

Figure 93: The layers of of Kameleon Solar panels. With red is the additional pixelated layer that gives colour to the panels.

PV/T

The PV/T system of the prototype is custom made since the PV modules that were used for the PV-chimney are not standard photovoltaics. Standard photovoltaics were not chosen for two reasons. The width of standard PVs does not fit with the glass box width and secondly, the PV panels that are placed, are the same product series as the PV cladding panels and they are chosen mainly for aesthetical reasons.

The selected PVs are Kameleon Solar ColorBlast modules with monocrystalline silicon cells. The modules are custom-made by Kameleon Solar and come in two different configurations: a 4x4 cell configuration and 4x5 cell configuration. The different configurations originate from the fact that there are BIPV modules in front of the columns and in front of the beams. The modules which are located in front of the concrete columns are smaller than those located on the concrete beams *(figure 92)*. Thus, as the chimney covers part of both series, both configurations where used. These PVs have 75-90% of a standard module efficiency (13%) due to the additional layer of pixelated color that they have on the front *(figure 93)*. In the case of the prototype, black PVs were used (no color layer on the front) which are expected to reach higher levels of efficiency. The panels have thickness of 10mm and are made by laminated glass while their weight is estimated at 22.5 kg/m^2.

As it can be seen in figure 92, within the system, 4 active panels were placed. The division of the panels in multiple pieces was a result of aesthetical issues, as the size of the panels follow the grid lines of the rest façade cladding. The separation of the PVs in smaller pieces, lead to a fewer number of solar cells. The redundant perimetrical surface area around each panel plus the distance between them could offer the space for more solar cells *(figure 94)*. Consequently. in future replacements, each pair of panels can be replaced with one, of double height, which still follows the grid lines of the façade but can provide space for two more rows of solar cells for higher electrical generation.

On the rear side of the PV modules, copper pipes were attached in order to create the PV/T system. Copper is chosen for its excellent thermal properties. Its thermal conductivity is 385 W/mK which is high, and this means fast heat transfer. Moreover, the inclination as well as the shape of the cooper pipes behind the PV glass where based on standard solar collector's design. The diameter of the copper pipes is 12mm, since this was the closest to the standard solar collector diameter (φ10 or φ12) which was available on the market and also due to the diameter capabilities of the available bending tools (12mm and above). Additionally, in an attempt to increase the total length of the pipes as much as possible, in order to

cover a larger surface of the PVs *(Garg & Adhikari 1999)* and warm up more water, double rows of pipes were bended *(figure 95)*. Behind the pipes, an insulation layer is placed between the pipes and the spandrel panel in order to maintain the copper warm.

The glass (material of Kameleon Solar Panels) does not have good thermal properties, which, in combination with the circular shape of the pipes, lead to minimal contact surfaces among the two. Therefore, in order to enhance the heat transfer and the distribution of heat from the PV to the copper pipes, a copper plate was opted to be used. The cooper plate, which has the cooper pipes fixed on it, is placed in the rear surface of the PV. Additionally, the pipes are connected with the copper plate with the process of saltering (welded with heated tin) *(figure 96)*. By this way, the heat transfer between the two surfaces is enhanced. The connection of the cooper plate and the PV was done with structural glue. The structural glue was placed around the plate in order to allow the conduction between the two surfaces.

Lastly, the whole system, is supported from a custom-made aluminum frame with hooks which works as supports for the PVs. The aluminum in this case, can possibly enhance the thermal performance of the system due to its good thermal properties. Moreover, the assembly sequence and maintenance, determined that the system had to be panelized. Therefore, the panel to panel connection had to be made on site, during installation. As a result, a flexible connecting concept is determined. Again, the product choice was made based on the real time and cost circumstances *(figure 97)*.

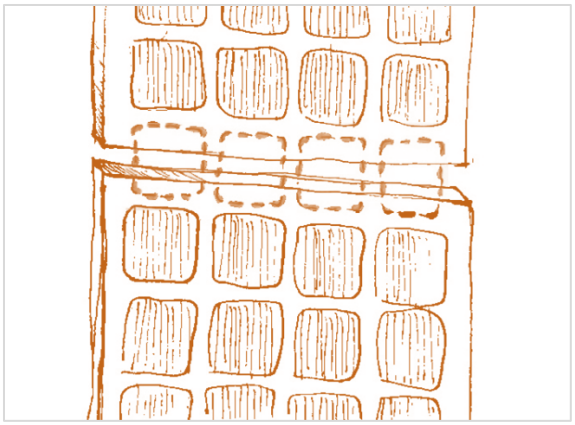

Figure 94: The additional line of solar cells that can be added using taller PV panels.

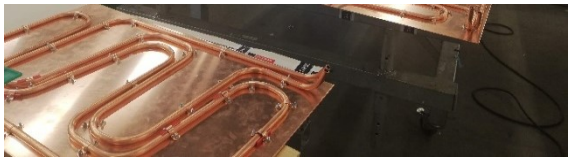

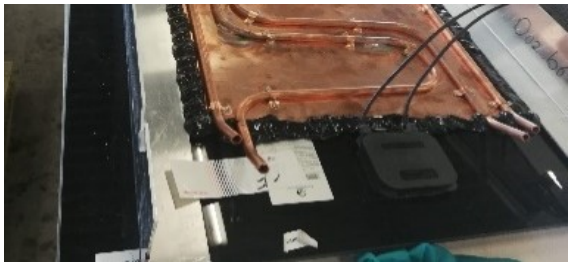

Figure 95: The cooper loops that created manually at the factory.

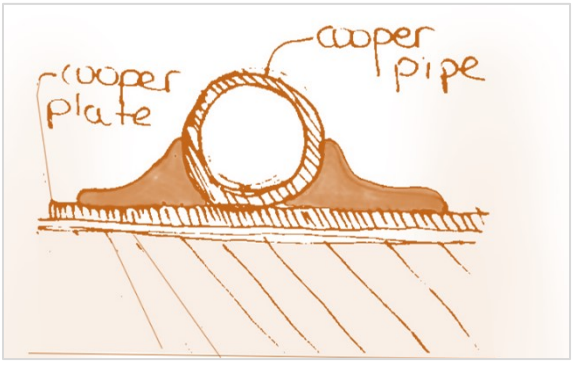

Figure 96: The connection of the pipes with the copper plate by saltering.

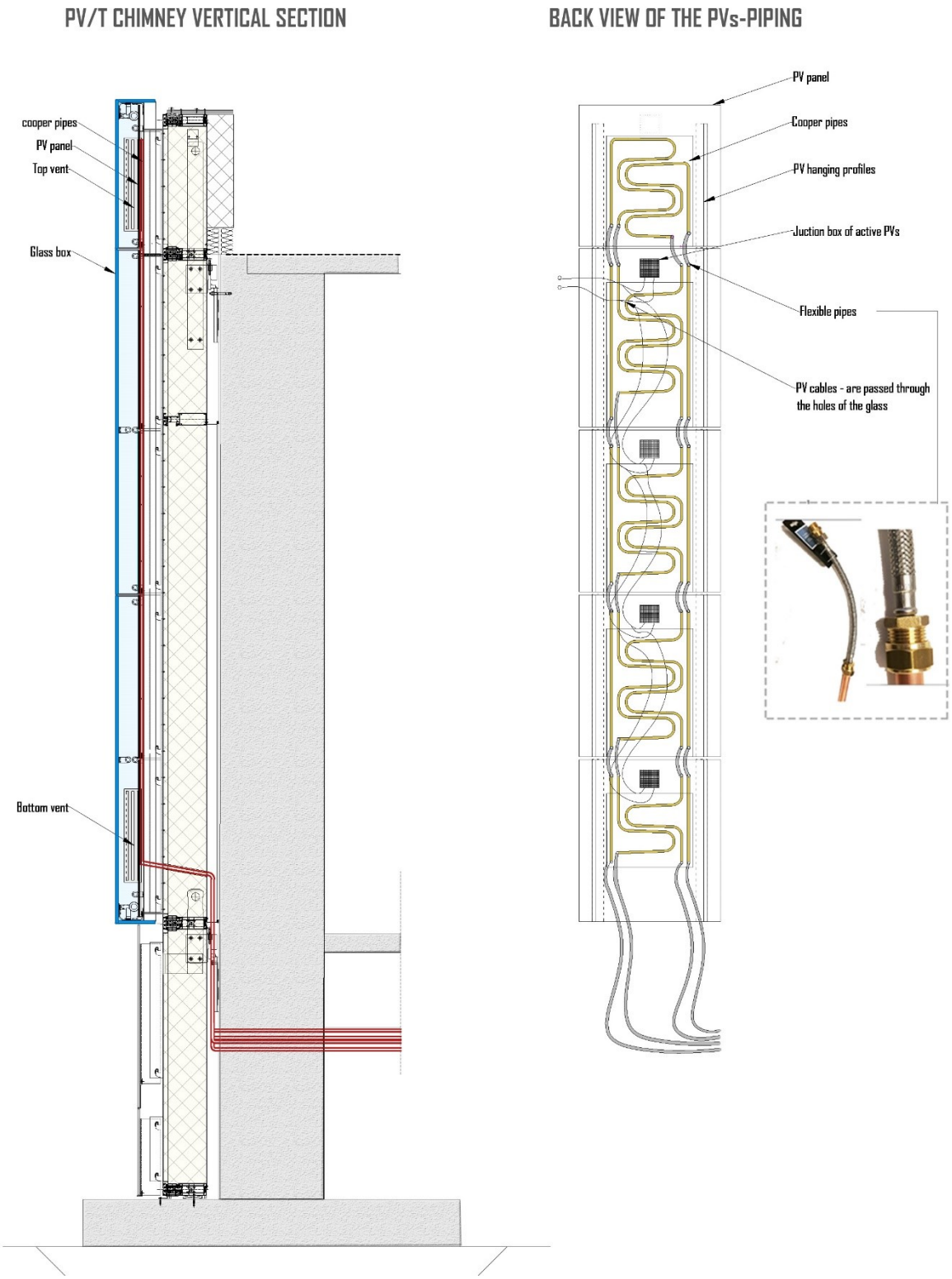

Figure 97: Vertical section of the PV-chimney where the position of the PV/T is marked with red (also, with red the path of the cooper pipes under the slab can be seen). On the right, the back view of the PVs with the copper pipes and the flexible connectors that connect one panel to the other.

4.4.2. Architectural investigation

As mentioned above, the PV-chimney is part of the concept idea of the façade of transitioning from nature to technology and it is a key innovative element of the project. The transitioning idea is specifically functional for the PV-chimney system, since by not placing it on the first levels of the buildings, potential shading can be prevented. Moreover, it is selected to be placed in front of the existing columns enhancing the imposing vertical sense of the tower buildings. Additionally, it does not shade the transparent part of the facade providing maximum daylight. In figure x, an impression of the proposed facade is shown.

Regarding the form of the system, the selected shape is rectangular, equally tall with the facade module, on which the PV-chimney is hunged. The strict shape of the rectangle maintains the clear and strict impression of the facade pattern.

On the Hungarian prototype, two PV-chimneys are placed, one 4.35m high, on the South and one 5m high on the West. Both of them are 815mm wide and have 240mm overall depth, with a clear distance between the PV and the glass of 105mm *(figure 80).*

Moreover, the dimensions of the glass and PV-panel separations of the chimney maintain the gridlines of the façade. By this way, the PV-chimney is integrated smoothly on the façade, hiding the sense that it is an object, designed to fulfil strictly mechanical purposes.

The Kameleon panels contain regular mono-crystalline PV cells that are encapsulated within a glass shell at a depth of 200-250mm. In terms of texture, despite that the PVs, inside the shaft, have black color (instead of light grey), the glass layer that covers them, strengthens their integration on the facade as its reflections make them more blended in the overall image. In contrast, in terms of volume, the additional depth on the facade by PV-chimney modules makes the system visible and is breaking the flatness of facade. This indicates both an integration of the system on the facade as well as sincerity, as their appearance implies a separate facade function *(figure 98)*..

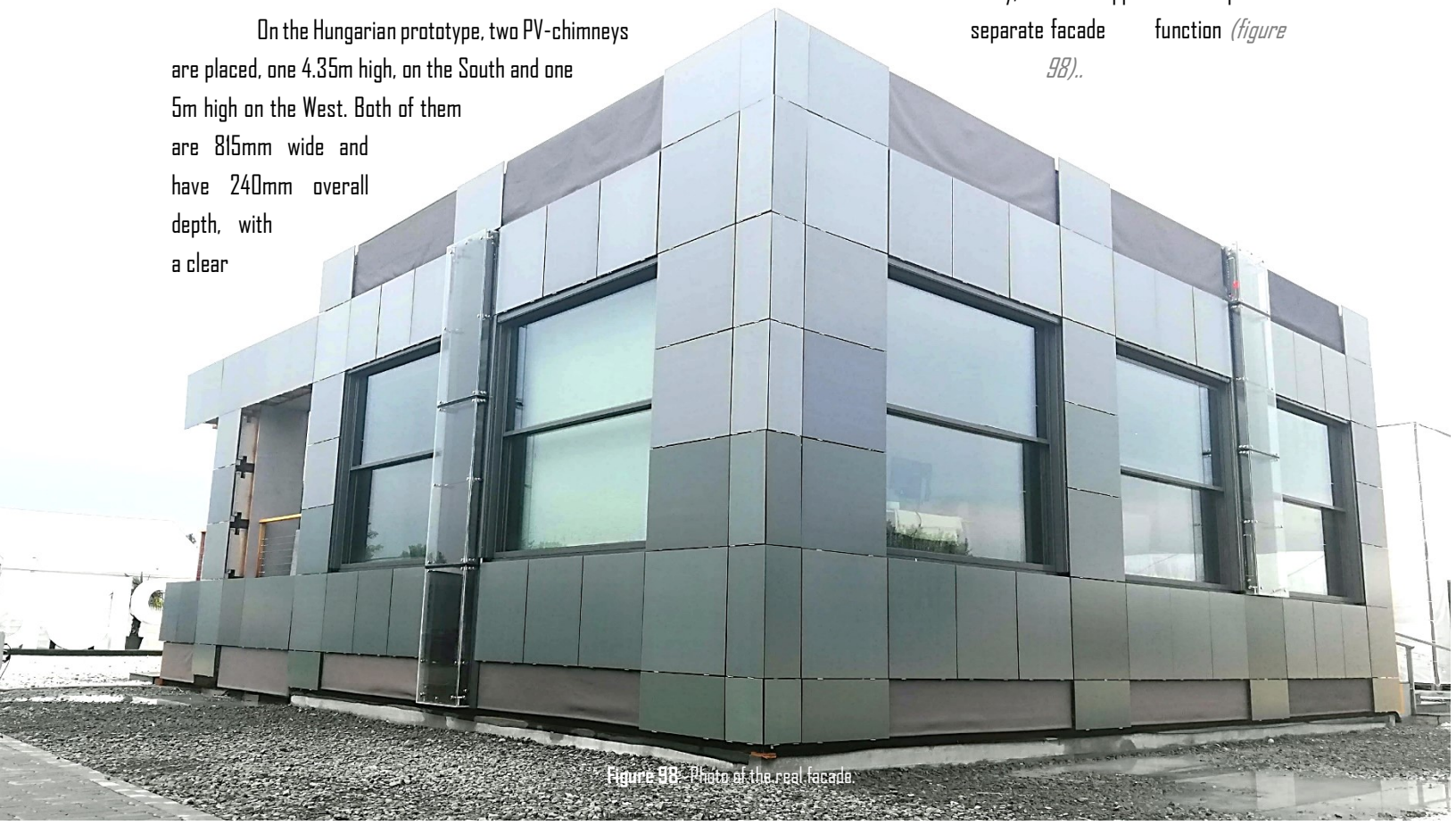

Figure 98: Photo of the real facade.

4.4.3. Assembly

The PV-chimneys were assembled in the factory together with the rest of the facade modules under the guidance and the manual contribution of the author. First, the aluminum frame was attached to the main spandrel panel of the facade module. Then, the PV/T modules, were hunged on the aluminum frame one by one starting from the bottom. After the placement of the first module, the connection of the pipes of the first to the second panel was done. At this phase, connecting the pipes of different panels was done using flexible pipes *(figure 99).* This procedure was repeated in order to connect the pipes together and to hang them all, on the aluminum frame

After that, the glass pieces were placed. Due to the weight of the glass, the PV-chimney glass box was split into pieces, so that it could be easily carried, manually, and thus, for easier maintenance and replacement. The pieces of glass were assembled in the factory with spider and linear glass to glass connectors *(figure 100)* and were glued together by transparent structural glue. The separate pieces were stacked onto each other closing the box by being screwed on the main aluminum frame. Between the separate pieces of glass, small gaps were left as tolerances (to prevent damages on the glass due to thermal expansion). These gaps lower the level of

Figure 99: Fixing of the cooper pipes (right) and the placement of them one after the other (left).

Figure 101: The flexible pipes that were connected just before the placement of the facade modules.

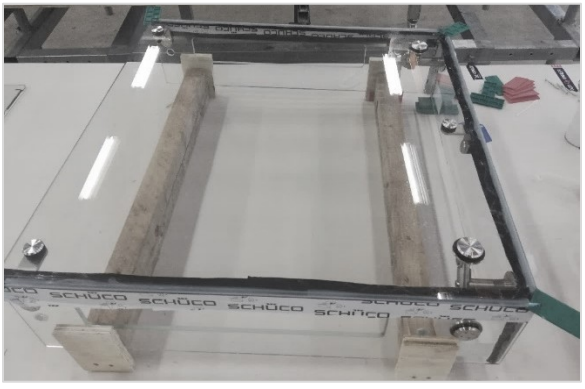

Figure 100: Top part of the box which is connecter with spider corner connectors and L-profile connectors on side.

Figure 102: Piping preparation before the placement of the facade unit.

airtightness of the glass box and allow for some thermal losses. An additional purpose of these gaps is preventing the collapse of the system under extreme weather conditions. For the improvement of airtightness, plastic profiles were glued on the glass to fill the gap while on the sides of the glass box, gaskets were placed to close the side gaps. Also, on the sides, holes on the glass were pre-cut, as prediction for the installation of the vents and some smaller ones for the cabling of the PVs.

The vents that were used consisted mainly of metallic perforated grills which were glued on the glass. The use of these vents is ideally restricted only to the construction in Hungary. Normally, they will have to be replaced by controllable vents with an automated system.

The PV-chimney is part of two facade modules. Therefore, during the assembly of the modules, an on-site connection of the pipes on the lower facade module with the pipes of the above module was required *(figure 101)*. Moreover, for the connection of the PV/T system, the pipes had to pass under the floor slab in order to reach the mechanical installation room of the prototype. Therefore, before the placement of the first facade module, copper pipes had to be fixed on the concrete, in order to be connected with the output pipes of the system *(figure 102)*.

4.5. Technical Details

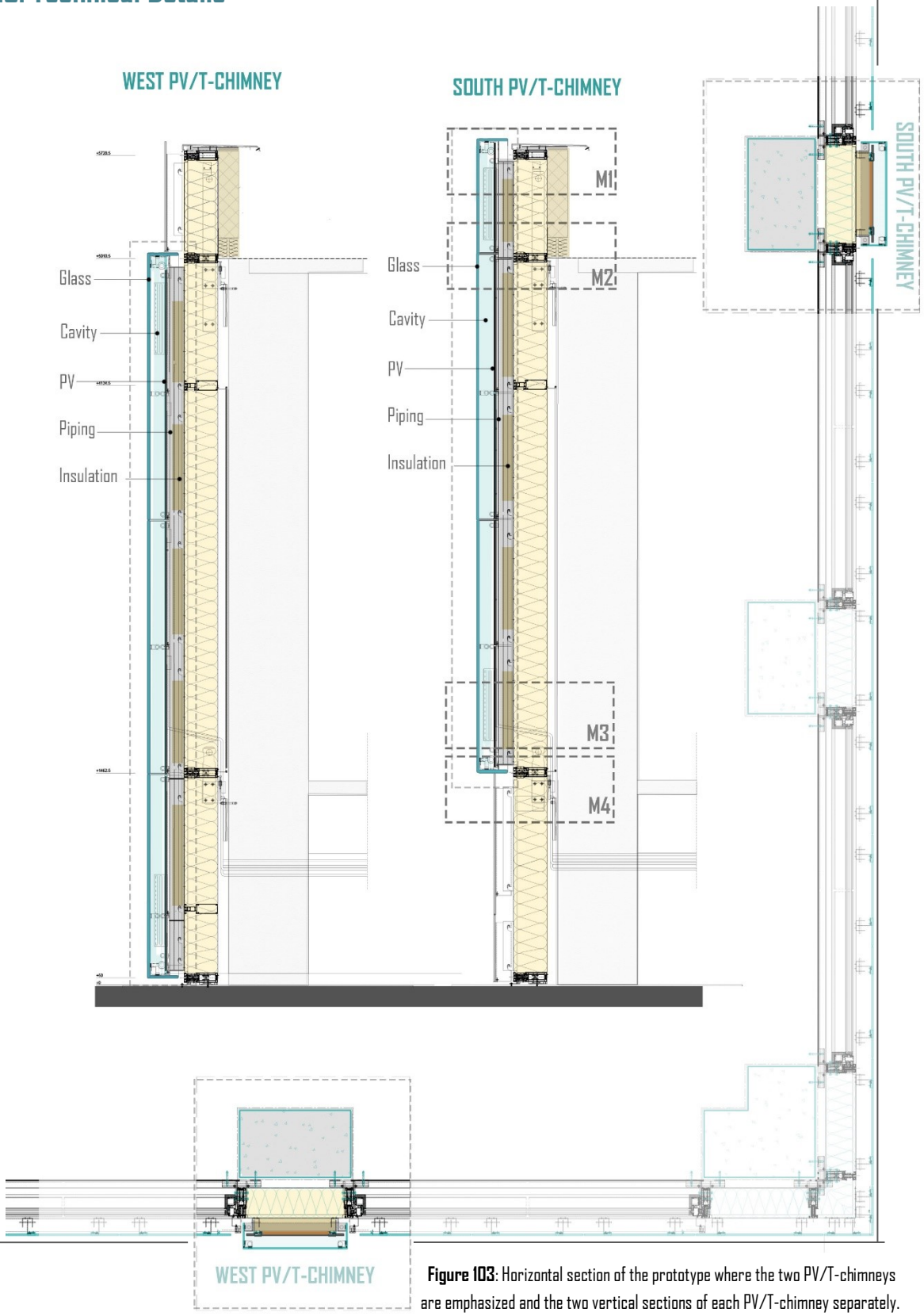

Figure 103: Horizontal section of the prototype where the two PV/T-chimneys are emphasized and the two vertical sections of each PV/T-chimney separately.

Figure 104: Horizontal section of the PV/T-chimney.

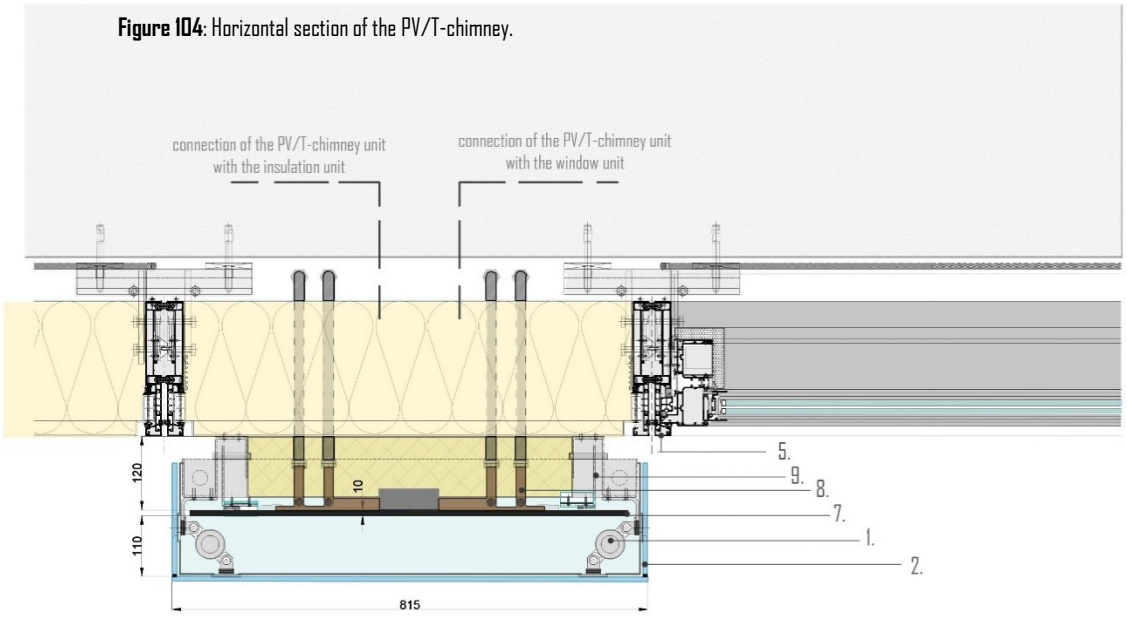

The technical details of the proposed PV/T- chimney are revealed in figure 104 and 105. The solar panels, which are placed in the shaft, were used as electricity generating source while the copper pipes behind them are used to warm up water which will be used to improve the efficiency of the roof solar collectors. The water pipes pass through the facade unitized system, in order to be connected with the water tanks. The whole PV/T system is mounted of an aluminium frame which is attached on the facade spandrel panel. Similarly, the glass box, which is created by the use of glass to glass connectors is also mounted of the same structure. Also, on the glass box, vents are attached at both ends in order to provide ventilation of the shaft.

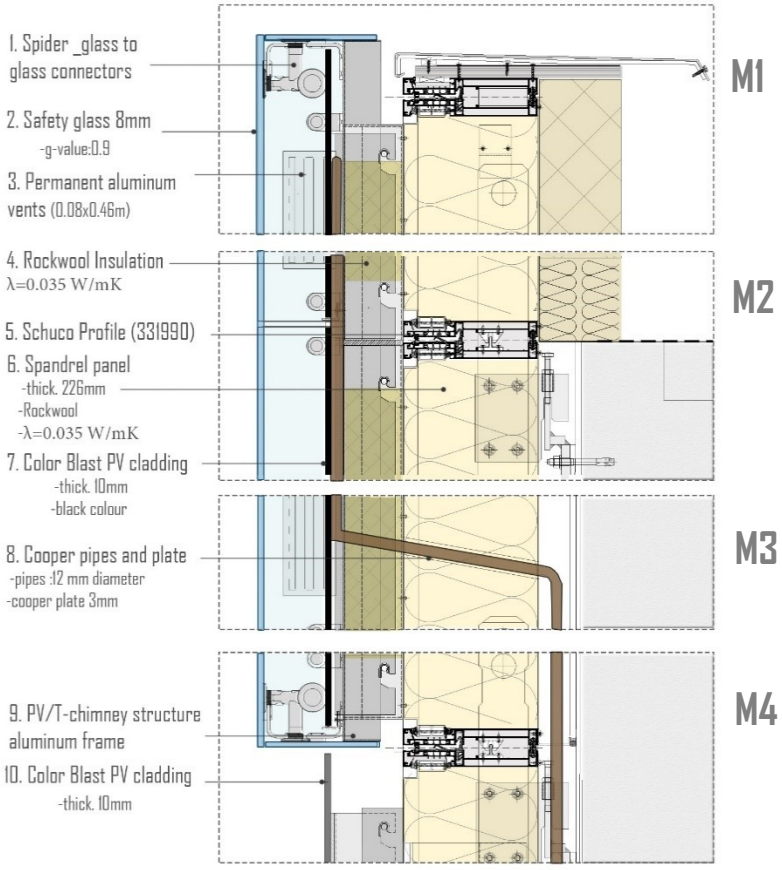

Figure 105: Vertical sections of the PV/T-chimney.

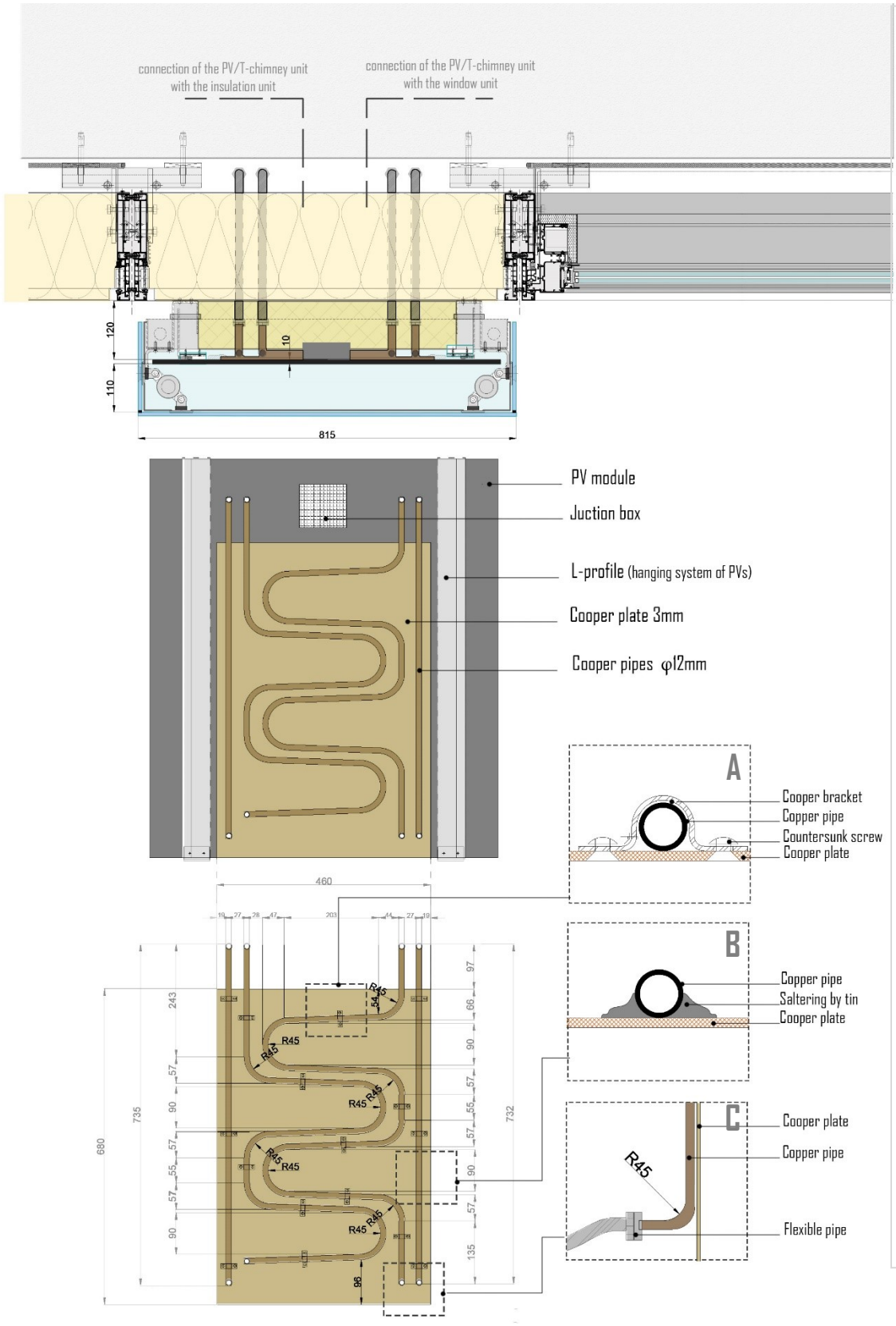

The PV/T system is attached behind the PV modules where a cooper plate, which had the bended copper pipes on it, is glued. The ends of the copper loops are bended towards outside (as it can be seen in detail C), in order to connect them with flexible pipes, which offer the assembly of the system in pieces. For the connection of the cooper pipes with the copper plate, cooper brackets where used and they were fixed with countersunk screws in order to maintain a flat bottom surface (detail A). Additionally, for the enhancement of the heat transfer from the plate to the pipes, a saltering process was done (detail B).

Figure 106: Details of the custom-made PV/T system.

EXPERIMENT 5

5.1. Experimental Setup

Aforementioned, the PV/T-chimney together with the whole facade design, were developed in the framework of Solar Decathlon competition 201,9 which took place in Hungary. There, the whole prototype and thus, the PV-chimney were built. For the South PV/T-chimney, a real experiment has been performed in the South PV-chimney where the thermal performance and the intensity of ventilation within the shaft were tested. The effect on the cavity, PV module temperatures and the air velocity were investigated.

The real experimentation of the system provide insight into the reaction of the system under non constant weather values as well as the understanding of practical issues or other limitations that did not considered. Moreover, it will be used to validate the simulations results.

The experimental setup is presented in figure 107 where the materialization as well as important material properties can be read. The layers starting from the outside towards the inside, consist of: 8mm laminated safety glass, the PV-modules, copper pipes, insulation and the spandrel facade panel which is filled in with rockwool insulation. The whole construction follows a modular concept with the possibility to be disassembled. Consequently, the U shape glass box is made of smaller pieces, which are connected with spider connectors, while the gaps between the U shape boxes, are covered by a thermal resistant plastic profile. The PV modules hang on the aluminum frame. This whole package is then attached on the unitized facade system. The PV-chimney package protrudes from the facade finish line, while it prevents possible shadows.

Measurements of the temperature, air velocity, solar irradiance and electricity generation were done at constant intervals of time during the experiment. In figure 107, the positions of measurement in different heights and depths are shown. The measurements with the anemometer have been taken in different heights (where it was reachable) at the top and the bottom of the chimney and within the shaft (on the side, middle and the other side of the cavity) in both 'x and 'y directions. Moreover, thermocouples where placed on the PV surface for the recording of PV temperature. Also, other thermocouples were placed close to the inlet and outlet in order to measure the temperature just after it entered the shaft and just before its extraction.

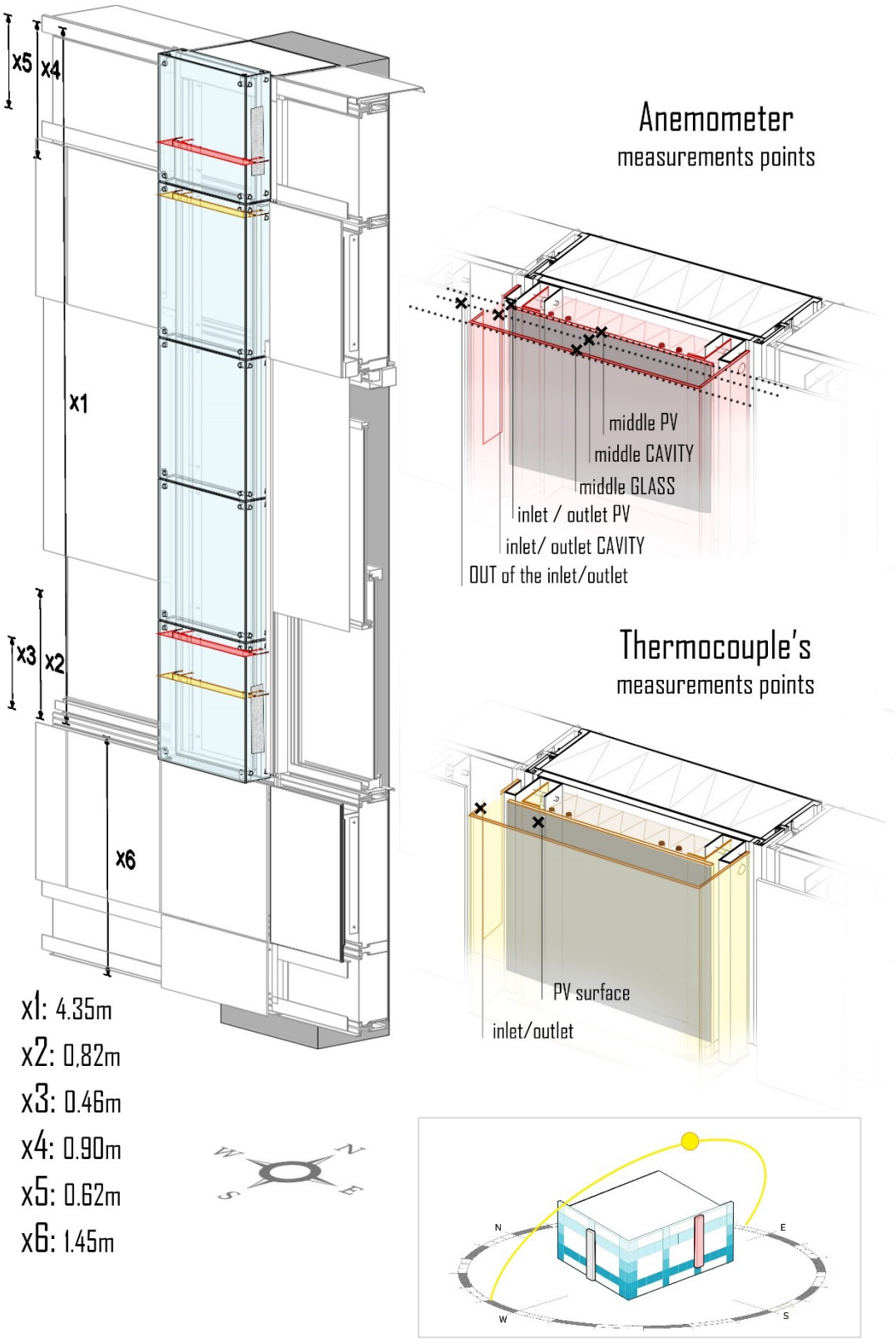

Figure 107: Experimental Setup. With red colour, for the anemometer and yellow colour for the thermocouples, the levels where the measurements taken and the measurement's points are symbolised.

5.2. Sensors and equipment

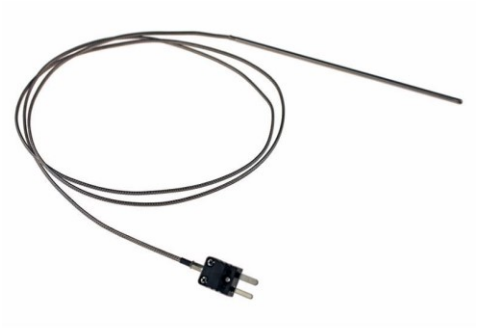

Figure 108: Thermocouples

Figure 109: Anemometer

Figure 110: Pyranometer

For the completion of the experiment measurements, 3 kinds of sensors were used. Thermocouples were fixed on the PV surface and close to the openings at the top and bottom of the shaft, in order to record their temperatures. Moreover, one shaded thermocouple measured the ambient temperature. The temperature data of all the thermocouples were stored by Multiple USB TC08 digitally. Additionally, a hot-wire anemometer measured both the air velocity and the temperature within the shaft and the ambient values. These measures were taken manually. Additionally, for the irradiance measurements, a Kipp & Zonen SPM10-A pyranometer was used. In order to measure the vertical irradiance, the pyranometer was stuck on a vertical surface next to the solar chimney. Finally, for the recording of the PV production, the smart MPPT Charge Controller system of the prototype was used.

Thermocouples *(figure 108)*:

Thermocouples are widely used for temperature measurements. They consist of two metal wires made from dissimilar electrical conductors. The wires are connected, forming electrical junctions whereby for the measurement of the temperature changes a voltage iss created. The voltage can then be accordingly interpreted for the temperature calculation. For the experiment, T-type thermocouples were used with temperature measurable range of -40-350°C and an accuracy largest of ±0.5 °C± 0.004T(◦C) *(Alan &bReza, 2016).*

Hot-wire anemometer *(figure 109)*:

Hot-wire Anemometer is a device which measures, in real time, the air velocity of a fluid, in a certain direction. The anemometer works on the heat transfer principle (from high to low temperature), by measuring the heat loss of the wire, which is placed in the fluid stream (heated by a constant electrical current). The hot wire anemometer measuring rate is 0.1-25m/s while its accuracy is ± 5% of the measured value + 1 unit of measurement *(Lumley & Wyngaard, 1967).*

Pyranometer *(figure 110)*:

Pyranometer is a device to measure the solar radiation flux density on planar surface from a 180° field of view angle. The solar radiation is measured in W/m^2 from the hemisphere above within a wavelength range 0.3 μm to 3 μm while the solar radiation spectrum extends roughly from 285 to 3000 x 10^{-9} m *(ISO 9060, 1990)*.

Smart house system:

For the observation of the electricity generation, SmartSolar charge controllers were installed. MPPT charge controllers are from Victron Energy and each of the BIPV strings is connected to a Victron Energy SmartSolar MPPT 100V/30A. The SmartSolar MPPTs have advanced maximum power point detection algorithms built in in the case of partial shading. It will always lock to the optimum maximum power point (MPP) when presented with several power-voltage curves.

5.3. Experimental Procedure

The fact that the PV-Chimney hanged on the facade and that the only access to the cavity was through the side holes/vents, made experiment more difficult. The measurements of the bottom part were approached easier since the height of the inlet was at human height, while the top part was only accessible through the roof of the building. This lead to a short time-gap between the measurements of the bottom and top part. Moreover, the measurements inside the cavity were done at the height-level of the vents, as other positions were not accessible.

First, the thermocouples were attached on the two end PV modules and another two, close to the openings. The thermocouples were connected to a Multiple USB TC08 which is used to log the temperature readings from the thermocouple. At the same time, the pyranometer was fastened vertically for irradiance measurements. The functionality of all the equipment was tested one day before the real experiment. For the air velocity measurements, the air temperature, close to the PV module, in the middle of the cavity, close to the glass, at the bottom and at the top were measured manually every hour. The measurements for every round, started from the top part, which was accessible only from the roof and then at the bottom part. Furthermore, data for the electricity generation of the PV modules where recorded through the Victron Energy SmartSolar MPPT system. Unfortunately, at a certain point the rain prevented measuring by the anemometer.

5.4. Limitations

All the experiments have limitations due to random or biased errors that refer to equipment inaccuracies and the general measurement methodology. Therefore, they have to be taken into account as they may impact on the findings of the research. The experiment took place in non-controlled environmental conditions and incorporated also manual measurements.

Firstly, the measurements within the cavity and at the two ends of the shaft should have been taken at the same time in order to have comparable results. Due to the duration of the manual measurements, the different measurements had a short time difference and within this time the environmental conditions were slightly changed. For these cases, the interpretation of steady state was according to the assumption that the value of the temperature and wind speed did not change within a few seconds. Moreover, within the 3-4 seconds measuring period of the air velocity. with the anemometer and pyranometer, different values appeared on the screen and thus, an average value of them was recorded. Accordingly, the measurements had some inaccuracies due to time aspects. The same issues occured between the measuring time of the top and bottom part where the time-gap of change was approximately 10 minutes.

Secondly, owing to the manual measurements with the anemometer, the position of the measurements was not precise. Human bias was inevitable while performing these measurements. Although the position was marked, so that the measurements could be taken at the same positions, the stability of the hand was changing slightly the measurement spot. In addition to that, the direction of the anemometer should face perpendicular to the airflow direction which is almost impossible since the measuring tool was controlled by human hand.

Furthermore, the flexibility of the thermocouple wires (wide end direction), as well as the fact that some wires were manually attached, with a tape, to the PV modules surface, may have caused measurements deviations.

Additionally, to that, the solar collector system was not allowed to be activated due to authorization issues. Therefore, the system was tested only as a PV system and never as a PV/T system. However, the system of the solar collector was attached on the back of the PV modules during the measurements. The back of the PV/T system includes some insulation at the back of the copper pipes, which may have affected, slightly, the temperature of the PVs and the air flow value in the cavity. Lastly, random errors caused by the accuracy of the equipment could have influenced the measurements. These errors are inevitable even if the cause cannot be detected.

5.5. Results and discussion

5.5.1. Irradiance measurements

The measurements of solar irradiance and the electricity generation are presented in figure 111. The irradiance profile is not completely homogeneous as important fluctuations were recorded between 13:00 and 14:00 because of cloudy and rainy weather. The largest values of vertical radiation were recorded between 10:00 to 12:00 when the sun position was facing the South side of the prototype, the direction at which the PV-chimney was facing. Normally, the highest values would have been measured around noon, but, due to clouds, the sun irradiance dropped dramatically. Varying radiation can have a positive effect on the system temperatures during summer and especially on the PV-temperature, preventing overheating of the surface even though this drop of irradiance caused also a reduction on the electricity generation, which is not favored. The irradiance behind the glass was not measured, due to accessibility difficulties and the absorbed irradiance by the glass was also calculated as a reduction factor of the material properties of the glass (g-value of 0.9).

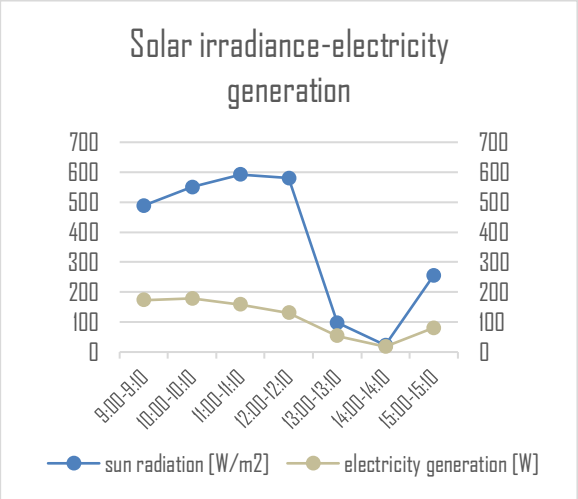

Figure 111: Graph with Solar irradiance measurements and electricity generation.

5.5.2. Temperature measurements by thermocouples

Using thermocouples, measurements for the ambient air temperature, the air temperature close to the inlet and outlet. and the temperature of the surface of PV-modules were recorded. During the measurements, irrational values were obtained by the thermocouple close to the inlet and thus, an additional thermocouple was placed.

The ambient temperature measurements were taken by a thermocouple which was covered by a reflecting foil in order to avoid heating of the wires due to solar radiation. The measurements of the ambient temperature per minute are presented in figure 112, and the average ambient temperature during the measurement time periods are marked with black bullets. The temperature varies within normal boundaries, while the deviations per minute range between 1-4°C. The temperature starts from 28.6°C at 9:24 a.m. and increases relatively constantly through time till noon. Then, a sudden drop of the PV temperature was obtained after 12:30 a.m., going from 42°C, which was the highest value during the experiment period, to roughly 38°C in a couple of minutes. This dramatic difference in the ambient temperature could have increased the temperature difference between the surface and the air inside the shaft. This could have caused higher heat flux towards the cavity and possibly, an intensity of the buoyancy effect. A significant drop of the temperature continues until 14:30, when the temperature reached 28°C. After that, the temperature increased slightly and remained relatively stable to 30°C until the end of the experiment. Unfortunately, during the time period of large fluctuations, measuring the air velocity was not possible because of the rain. Although the absence of air velocity measurements makes the understanding of the importance of ambient temperature-irradiance more difficult, temperature measurements of the cavity air and the PV surface, which were recorded by the thermocouples, allow some insight on the thermal behavior of the system. Around the boundaries of the inlet and the outlet, the thermocouples were measuring the air temperature inside the cavity, shortly after

the air insertion and before it exerted. In figure 112, the temperature for both the inlet and outlet can be seen. The measurements for the air, close to the inlet, are shown with both blue and yellow color, as the first thermocouple was broke (blue color). Therefore, a second thermocouple was placed (yellow color) for the rest of the experiment. Due to this breakage of the first thermocouple, the measurements from approximately 10:45 a.m. to 11:45 a.m. are not reliable.

In general, the inlet temperature was higher than the ambient temperature and the deviations of the temperature of the environment affect the temperature, around the inlet of the shaft, accordingly. Similarly, the outlet temperature was affected by similar fluctuations of the inlet temperature. However, the deviation of the outlet and ambient temperatures remained relatively constant to 12°C difference while, an increase of the ambient temperature lead to smaller temperature differences, Consequently, rises in the environment temperature enhanced the buoyancy effect causing larger temperature differences inside the channel. This phenomenon became more obvious at the time period between 14:20 and 15:30 where the temperature difference inside the shaft was very small, due to the cloudy weather (low irradiance). Then, by the rapid increase of the ambient temperature, the acceleration of the buoyancy effect was followed by a rapid increase in the temperature differences, which rose exponentially.

Additionally, the temperature of the top and bottom PV modules was recoded. The results of the measurements by the time are displayed in figure 112. As it can be seen, the temperature at the bottom PV remained between 40-45°C since the beginning of the measurements up until 12:45 a.m. while, the ambient temperature, and therefore, the temperature of the air inside the cavity, was increasing. Then, by the decrease of the temperature of the inlet (after 12:45), the PV module temperature also dropped, maintaining, however, still higher values than the inlet air temperature. This temperature drop lasted until 14:20 when it rose again due to the increase in the ambient temperature. Although, the surface temperature was fluctuated in a similar manner as the inlet temperature, its fluctuations were smoother. By the sharp increase of the inlet temperature, the PV surface temperature also increased, but not to an extent that it exceeded the values of the temperature around the inlet. Moreover, with the drop of the inlet temperature at roughly 15:15, the temperature of the PV also dropped, but smoothly. This may have been caused due to the time duration of the heat transfer by convection from air to solid (heat transfer coefficient of PV module surface). Generally speaking, the temperature of the PV module surface at the bottom of the shaft, ranged within acceptable levels that allowed a normal PV operation.

The temperature of the top PV module was much higher than the bottom due to upward movement of the warm air. The fluctuations of the top PV depend on the air at the bottom of the shaft *(figure 112).* The highest value was roughly 73°C, which is quite high, under high ambient temperature conditions (42°C ambient temperature and an irradiance value of approximately 580 W/m^2). However, ambient temperatures above 38°C are not that frequent in Hungary. According to the results, a drop of the ambient temperature under 38°C keeps the PV module temperature within operational levels. Apparently, its temperature it depends also on the duration of time that the solar radiation hits the PV-chimney.

Summarizing, the temperature of the PV-modules both on top and bottom part, showed to depend mainly on the intensity of the solar radiation and the ambient temperature that is the main factor of the buoyancy effect intensity. Also, the temperature values of the top PV modules, during noon hours were high and thus, their efficiency dropped. Consequently, the top part of the channel would have been more beneficial to be used mostly for heat absorption (e.g. solar collector) allowing the installation of the PVs at the lower levels of the shaft.

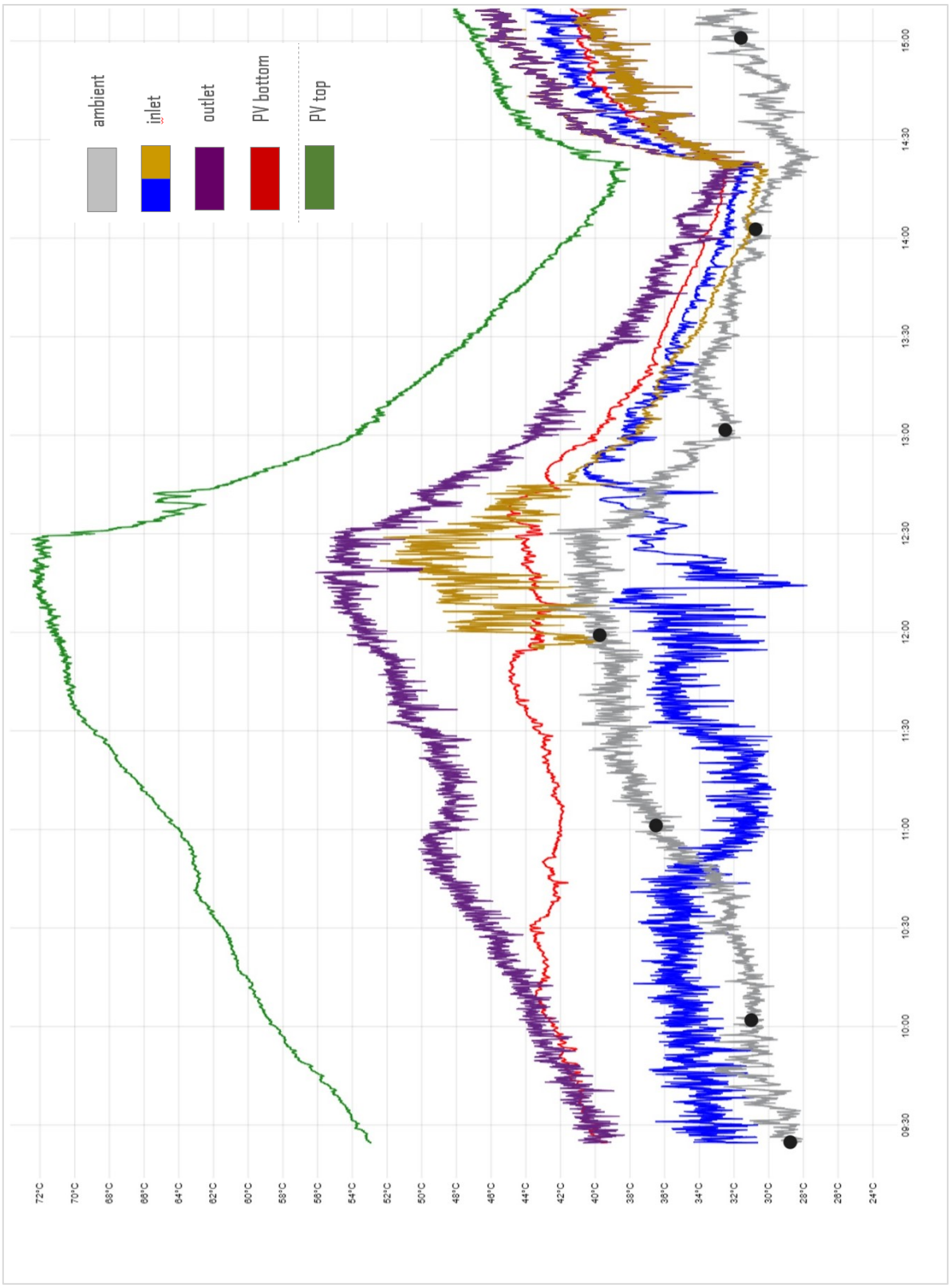

Figure 112: Temperature measurements of thermocouples.

5.5.3. Measurements by anemometer

With the anemometer, measurements within the chimney were done. Measurements of the air velocity and air temperature, in different positions and in both directions inside the channel, are recorded. Also, the air temperature and air velocity in small distance from the inlet/outlet were obtained. In figure 90, the measurements spots can be seen. These measurements were taken by the author, therefore, there are small time gaps between the measurements within the shaft, which are neglectable, and a gap of ten minutes between the top to bottom measurements. The measurements were taken every hour.

In figure 113, the results of the measurements of the air velocity at the bottom part are revealed. As it can be viewed, the measurements between 13:00 and 14:00 are missing because it was a rainy period. According to the air velocity measurements of the bottom part, it is obvious that the values of the inlet is much higher than the values in the middle of the PV and cavity. This may due to influences by the ambient conditions. Moreover, large fluctuations on the inlet air velocity cause the same kind of fluctuations within the shaft but with smoothest undulations. For instance, an increase of the air close to the inlet and PV from 1,5 to 3,3 m/s and a drop to 0.47m/s (09:00-10:00) is accompanied by slight fluctuations inside the channel (from 0.6 to 1,2m/s and then to 0,52m/s). However, the values close to the inlet-cavity at 09:00-10:00 are higher than the air velocity out of the inlets indicates a possible bias error as the values of the supplied air, (the air close to the inlets) rationally, has to be fluctuated at the same or lower values than the outdoor air. Specifically, during the experiment (at the first two measurements) the measurement points, for the measurements close to the inlet, moved a bit upwards. This is happened, because it was realised that possibly, cross ventilation was happened between the to opposite openings of the bottom part.

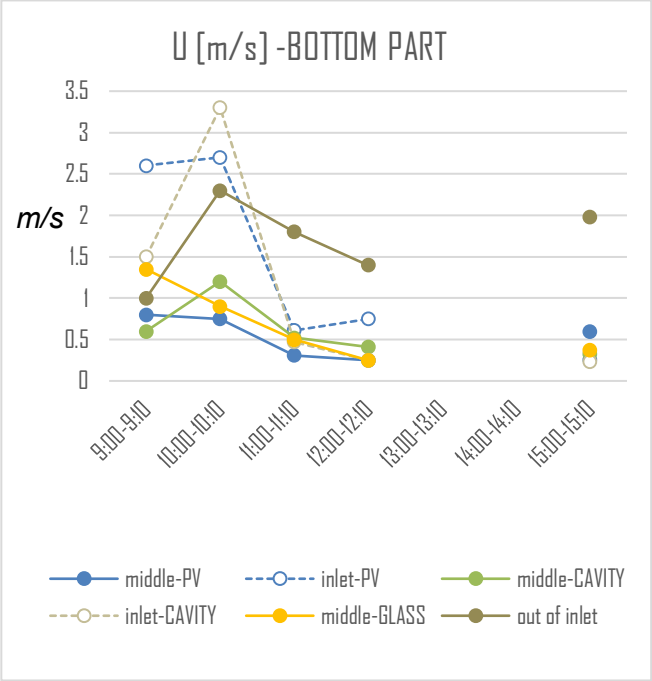

Figure 113: Air velocity measurements by the anemometer at the bottom part of the PV-chimney system.

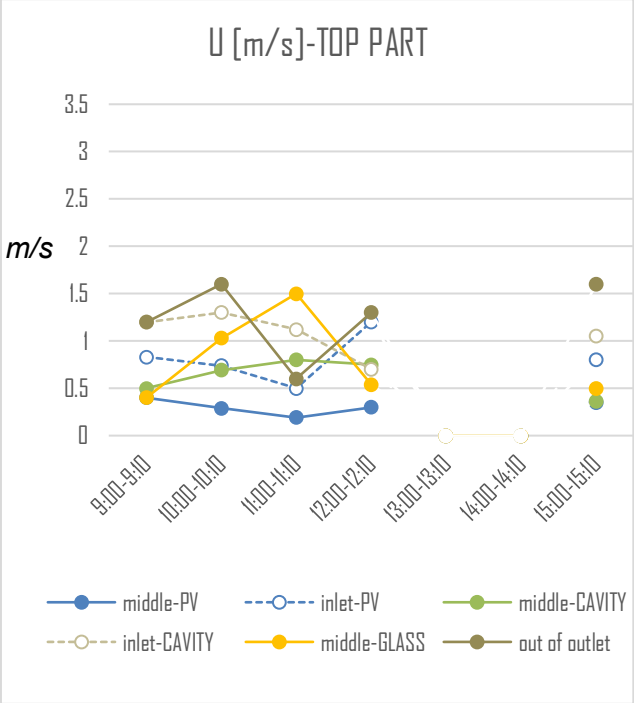

Figure 114: Air velocity measurements by the anemometer at the top part of the PV-chimney system.

Additionally, the values in front of the PV are lower than in the middle of the cavity, This, was not expected as air flow is normally generated by the extracted heat of the PV module. This might be liable to the fact that the cavity depth is small. That means, the air movement caused by heat fluxes of the PV are accelerated in front of the surface influencing the velocity of the air in the cavity. Although the air in front of the PV and in the middle of the shaft behave similarly, the air in front of the glass surface has constant decrease. Even, thought, their differences are small. Finally. it is interesting to mentioned, that the values in front of the two opposite surfaces (glass and PV) are almost the same.

Observing the figure 114, where the results of air velocity of the top part are revealed, the values next to the vents are mostly higher than the values of the air in the shaft. Furthermore, the fluctuations of the air in the channel, follow the ups and downs of the inlet/outlet with slighter air velocity differences. Similarly, at the measurements of the bottom part, the air velocity of the cavity marked higher values than the air close to the PV surface. The increase of the air velocity in the middle of the cavity follow the fluctuations of the ambient temperature fluctuations *(figure 114)* reaching roughly 0.8m/s between 11:00-12:00 where the ambient temperature and solar radiation are high (approx. 600W/m^2). Contrary to the air in front of the glass of the bottom part, the measurements of the glass at the top part are much higher than in other positions within the channel. The air velocity in front of the glass at the top reached 1.3m/s, which is a high value. Finally, the air velocity a bit out of the outlet, seems to pursue the inside values with sharper fluctuations due to influences from the outdoor environment conditions.

Regarding the temperature measurements within the channel, the measurements of both bottom and top are revealed in figure 115 and figure 116 respectively, It is obvious, according to figure 115 (bottom part results), that the temperatures inside the shaft are influenced by the ambient temperature. Moreover, the temperature close to the PV

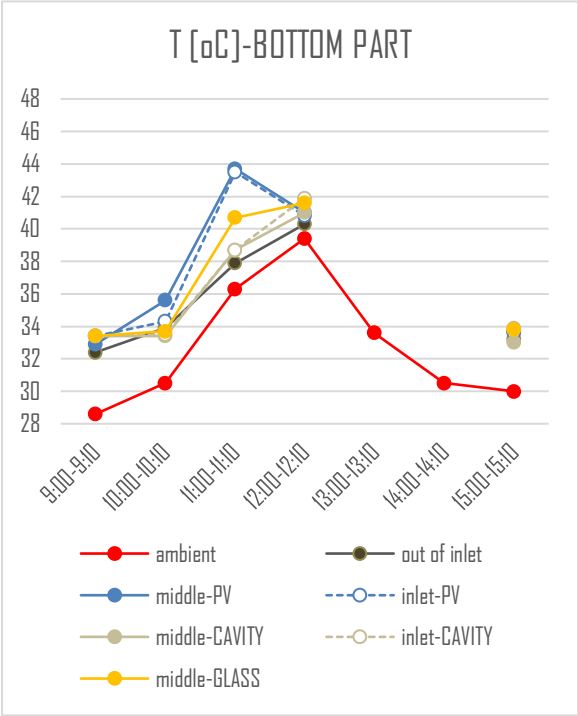

Figure 115: Temperature measurements by the anemometer at the bottom part of the PV-chimney system.

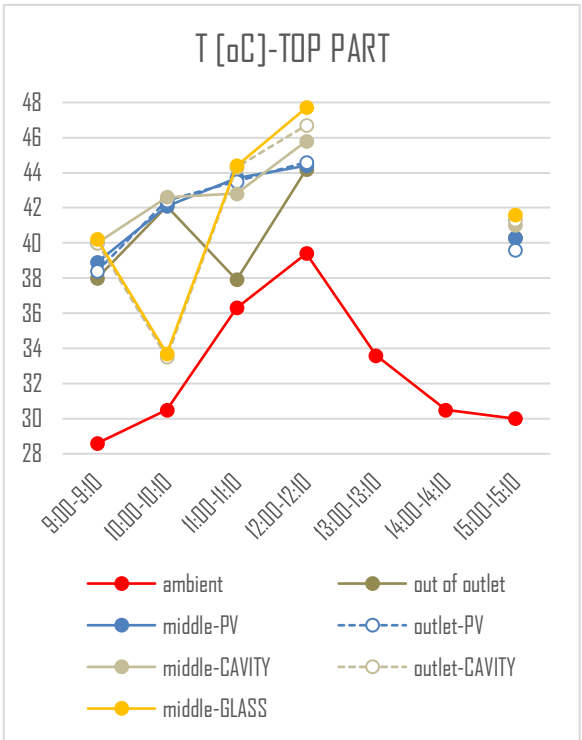

Figure 116: Temperature measurements by the anemometer at the top part of the PV-chimney system.

surface and close to the glass are higher than the temperature of the cavity. This is rational, as radiation and heat from the warm surfaces are transferred by convection to the cavity air. Additionally, the temperature of the cavity marked almost constant deviation from the ambient temperature to approx. 2-4°C maintaining suitable conditions for the PV function. Their difference increases slightly by the decrease of the ambient temperature which means, that the shaft can keep the heat for a period of time by temperature drops. Finally, comparing the air velocity values at the bottom with the temperature values, they do not seem to be related. This may be due to the great influence of the air velocity of the cavity from the outside conditions.

In opposition to the bottom part, the temperature values of the air inside the channel does not follow all the changes of the ambient temperature at the top part. Especially the temperature close to the glass and the temperature of the air close to the inlet and the PV surface, are fluctuated a lot. A sudden decrease of the air close to the glass at 10:00 a.m. is followed by a sharp increase in the air velocity. By this drop, the temperature of the cavity is affected also following the same in scale changes. The temperature of the air in front of the PV, rises by the increase of the solar radiation but does not exceed 44.6°C while the air temperature in front of the glass, during the peak of ambient temperature, is much higher and reaches almost 48°C. Accordingly, the cavity temperature exceeds the PV temperature reaching 45.8°C (6°C difference from ambient). These values are quite high and can be harvested either by increasing the COP factor of the heat pump, or by allowing natural ventilation with elevated temperatures. Finally, the air temperature out of the outlet is always higher than the cavity, since it is influenced by the external conditions. That means, the air comes out of the air outlet is quite warm even if you measure it in a small distance (approx. 15-20cm) from the PV-chimney.

5.5.4. Measurements of electricity generation

The measurements of the electricity generation were taken by an automatic MPPT charge controllers from Victron Energy which gives the energy production per minute. In figure 111, the relation of solar irradiance [W/m^2] and the electricity generation [W] can be seen. The generation of the PV modules it is decreased slightly by the increase of the irradiance. This may due to higher temperature of the modules which decrease their efficiency. Then, by the sharp fall of the solar radiation, the generation decreases as well, but not that sharp as the radiation drop. This is possibly happened because a drop of the PV temperature is occurred and thus, their efficiency increases. Consequently, a suitable combination of the solar irradiance and of the PV module temperature is needed in order to reach high efficiency of PVs. The energy generation values look to be high for the number of PVs that are placed in the shaft (a panel of 4x5 (the top one) and 3 panels of 4x4). That is happening because the active PVs of the PV-chimney, were connected in series with 4 additional panels-the facade cladding panels which are out of the PV-chimney. Consequently, for the estimation of losses of the PVs inside the channel, the electricity generation of the additional panels should be removed from the overall electricity generation result value. The assessment of the PV efficiency is calculated in chapter 6.

5.5.5. Heat flow calculation

The maximum and minimum values of convective heat flow through the system are calculated, Ccorresponding the temperature differences of the experiment measurements and by the use of the equation 15, the calculation of the heat flow is done. The density of air assumed to be constant at 1.225 kg/m and the specific heat (C_p) 1000 J/(kgK). The air change rate was calculated using the real measurements of the specific time while for temperature differences, the max and min values of temperature in the cavity were used. Since the collected data is from real time measurements, the taken values are influenced by a lot of other non-constant parameters which were not taken into account (such as air humidity, angle of wind speed to the inlet, airtightness of the system etc.) and include bias errors inaccuracies. As the ambient temperature measurements were taken from the thermocouples, the temperature at the top of the chimney is taken also from the collected data of the thermocouples, which measures the air temperature at the top of the channel. Consequently, the results of the heat flow which are revealed in table 3, is an indicative picture of the energy output through the system under the specific conditions and not a general overview of the system thermal performance.

There is no deviation in the horizontal direction parallel to the width of the channel and thus, the integral is uni-dimensional resulting in heat flow per meter width. The results show, that the maximum heat flow which obtained within the chimney was roughly 537 W//m (+-26.87 because of anemometer inaccuracy (5%)) at 12:00 where the solar radiation has a high value (580 W/m^2) and a temperature difference of the cavity and ambient air of 13oC at the top of the channel. The minimum heat flow is 231 W/m (+-11.57 because of anemometer inaccuracy (5%)) around 15:00 under 256 W/m^2 solar irradiance. It should be mentioned here, that during the period of lower solar irradiance, measurements of the air velocity did not occur. Therefore, this period is excluded from the calculation (of the minimum heat flow during the experiment period). The heat flow can be utilized to increase the COP of a heat pump or by allowing natural ventilation. An important indicator of how this energy can be useful is the temperature of the air. In this case *(figure II6)* the temperatures of the energy flow are quite high for natural ventilation. However, the heat flows are quite high. In a hypothetical scenario where the shaft is connected with the indoor air (and by having the vents open), the shaft can be possibly used to cause the extraction of the warm air from the room towards the channel and then to the ambient.

$$Q = c_p{}^{*}\rho^{*}v^{*}A^{*}\Delta T \quad (15)$$

5.5.6 Deviation of temperature measurements with thermocouples and anemometer.

The measuring equipment's have a range of accuracy as it can be read in chapter 5.2., thus, the measurements have always a deviation from the real value. Moreover, as is mentioned before, bias errors by human, decreases the reliability of the measurements. In table 7, the measurements of the inlet/ outlet by a thermocouple and the anemometer can be compared. As it can be seen from the results, the deviation fluctuated from 0.05-5.73 °C. In parallel, the deviation of each measurement is calculated. The standard deviation, which is used to quantify the amount of variation or dispersion of a set of data values, is presented in table 7,8. The mean value of the measurements is calculated by equation 17 and the standard deviation by the equation 17. Then, the coefficient of variation, which indicates the range of variations (CV >= 1 indicates a relatively high variation, while a CV < 1 can be considered low), is calculated by dividing the standard deviation with the mean (μ) of the values of each different measurements separately. The results show that the variation of the values is low.

$$\mu = \frac{1}{n}\sum_{i=1}^{n} \quad x_i$$

(16)

$$\sigma = \sqrt{\frac{1}{n-1}}\sum_{i=1}^{n} \quad (x_i\text{-}\mu) \quad ^2$$

(17)

Table 6: Estimation of heat flow (max and min) based on the experiment measurements and their tolerances according to equipment's accuracies.

max Δt [12:00]	13 °C	**Qmax [m³/h]**	537	± 26.
min Δt [11:00]	4 °C	**Qmin [m3/h]**	231	± 11

Table 7: Standard deviation and coefficient of variation for the measurements with thermocouples and anemometer at the inlet measurements.

INLET TEMPERATURES			
	thermocouples	**anemometer**	**deviation**
9:00-9:10	33	34.4	**1.5**
10:00-10:10	35	33.5	**1.2**
11:00-11:10	32	38.7	___
12:00-12:10	41	41.9	**1.2**
13:00-13:10	40	___	___
14:00-14:10	33	___	___
15:00-15:10	38	32.9	**4.7**
mean	36.5	36.3	
standard deviation	6.9	11.3	
CV:coefficient of variation	**0.2**	**0.3**	

Table 8: Standard deviation and coefficient of variation for the measurements with thermocouples and anemometer at the outlet measurements.

OUTLETS TEMPERATURES [°C]			
	thermocouples	**anemometer**	**deviation**
9:00-9:10	40	40	**0.05**
10:00-10:10	43	43.	**0.6**
11:00-11:10	49	44	**5.2**
12:00-12:10	52	47	**5.73**
13:00-13:10	46	___	___
14:00-14:10	37	___	___
15:00-15:10	38	41	**3.6**
mean	44	43	
standard deviation	27.2	5.6	
CV:coefficient of variation	**0.6**	**0.1**	

5.6. Conclusions

The real experiment of the system provides the opportunity for the understanding of the proposed design under real and not stable weather conditions. The measurement of the air velocity, the temperatures of the system and the electricity generation, provides an overview of the performance of the proposed system in terms of thermal energy generation, natural ventilation and electricity generation. Simultaneously, presents the system potentials for different functionalities.

Measurements in different time periods of the day show that the system interactions based mainly on the ambient temperature and the solar radiation while the wind velocity affects slightly the results close to the inlet. Moreover, the stack effect becomes more intense, influencing the air velocity in the cavity, when the outdoor temperature rises, causing higher pressure differences and therefore higher heat flow. However, the air velocity in different positions within the shaft, fluctuates independently of the cavity air temperature and the air velocity in front of the glass. This may be due to turbulence around the edges of the channel.

In general, the air velocity that is extracted from the shaft, reaches high values (up to 1.3m/s). As already mentioned, the proposal embedded in the Solar Decathlon prototype did not use the system for ventilation. However, an improved, autonomous facade system of the PV-chimney can utilize the fluid flow for cross ventilation by the extraction of warm air from the indoor space to the shaft and then to the ambient environment. In this case, there is a risk of airflow disorientation, from the shaft to the room, due to heat transfer from hotter to colder fluids. Consequently, this fact should be carefully considered for the possibility of using the system as a passive ventilation mechanism during summer. At the same time, since the energy flow is quite high, it can be potentially harvested in order to be coupled with a heat pump and increase its COP.

Regarding the thermal behavior of the system, the system managed to rise the temperature inside the cavity up to 13°C higher than the ambient temperature. Hence, the temperature of the upper PVs is rising a lot, marking extreme values when the solar irradiation is high (up to 72°C). Apparently, these values are not workable for electricity generation, since such PV temperature exceeds the permitted functional temperature levels and thus, its efficiency drops a lot. Possibly, by the activation of the PV/T system, which was constructed but it did not run because of technical difficulties, the temperature both of the PVs and of the whole system would be lower. Considering that, the top part of the shaft can be used to harvest most of this heat by the replacement of the top PVs with an absorptive medium and the placement of the PVs in the levels lower, along the height of the channel. This can be accomplished by replacing the top panels with solar collectors, thus avoiding overheating of the photovoltaics.

Although the system was not tested in winter conditions, it is expected that the buoyancy effect will be less intense due to lower solar irradiation and that the temperature of the air in the cavity will be low to be used for heating. The slightly warmer air in the cavity could be used as input air of the heat pump to increase its COP factor and thus, the energy demands of the building for heating. An alternative option is connecting the shaft with the indoor space while the vents are closed. That, would result in warming the indoor air through the PV-chimney which consequently turns back to the room. By this, air circulation will be occurred and thus, requiring air filtering.

The proposed system marks quite good thermal performance as the temperature differences within the chimney are high causing high pressure differences and heat flow. Therefore, there is great potential of making use of this energy. On the other hand, the functionality of the PV modules is reduced at the highest temperature point. However, this occurred mainly on the top part of the shaft while the temperature of the PV modules at the bottom ranges within workable levels.

5.7. Comparison of the experiment with the simulations

Table 9: Cavity temperatures by the experiment and the simulations.

Tair [°C]			
Time:	**anemometer**	**thermocouples**	**stationary calc.**
9:00	40	40.05	34
10:00	33.5	43.5	35
11:00	44.3	49.5	40
12:00	46.7	52.4	42

For the validation of the simulations, a comparison between the experiment results and the simulation results is conducted. Using the weather conditions of the measurements, simulations for every hour were done using the same calculation method as in chapter 3. The comparison is done with the measurements taken before 13:00, because during the rain, that took place in the time period between 13:00 and 14:00, the solar radiation dropped dramatically. Therefore, the calculations during this time period were not taken into account.

In table 9 and 10, the measurements of the temperature of the air in the cavity and of the PVs from the simulations in comparison with the real measurements are displayed respectively. The simulation values of the cavity temperature are lower than real measurements. In contrast, the PV temperatures of the simulations are close to the real measurements. The cavity temperature calculations are approximately 5°C lower than the measurements with the anemometer while their difference with the measurements by thermocouples is higher (approx. 10°C). Some biased errors caused mainly by the fact that the anemometer may not have been exactly perpendicular to the air flow could change the measurements by a bit. Also, the fact that the thermocouples were glued with paper tape, could have left some amount of the solar radiation to pass through and warm up the entrapped air. This may cause a slight increase of the values. As concluded from the aforementioned, the deviation of the real measurements and the simulations is estimated roughly 7.5°C (the average of the anemometer and thermocouple deviation).

Table 10: Air velocty by the experiment and the simulations.

Air Velocity		
time:	**anemometer**	**stationary calc.**
9:00	1.2	1.15
10:00	1.6	1.4
11:00	0.6	1.8
12:00	1.4	2

The simulation values of the PV temperature are close to the experiment measurements as their difference is approx. 3°C while, again, the simulation values are lower than the real measurements. At 12:00, the deviation of the thermocouples value and the simulation value was higher (8°C). This indicates that probably, along time, the increase of the temperature of the PVs may accelerate the increase of the deviation rate. Regarding the air velocity, the simulation results and the experiment measurements can be seen in table 10. The air velocity values of the simulation and the real measurements are quite close (0,2-0.6 m/s difference). However, at 11:00 the difference of the simulation and the experiment value is higher (1.2m/s difference). This difference may have been due to the biased error of not placing the anemometer perpendicularly to the air flow and thus, measuring incorrectly.

Summarizing, the simulation of the system gives slightly lower temperature values than the real values. The deviation between the temperature values of the experiment and the simulations is fluctuated between 5 and 10°C. Furthermore, regarding the air velocity, the deviation of the values is approximately 0.05-0.6m/s. Considering the fact that between the measurement tools of temperature, the deviation of the measurements reaches 10°C (temperature measurements of the anemometer and the thermocouples), the simulations are quite reliable. Also, the air velocity values of the simulations have small deviation, indicating that simulations can provide good estimation of the system behavior.

6 EVALUATION

For the evaluation of the system, first the electricity efficiency of the PV inside the chimney is analyzed based on the expected energy production according to the experiment results. Moreover, a comparison is done between PV modules of the same kind, inside and outside of the proposed PV-chimney system and then, compared with standard PV products. The weather conditions based on which the evaluation is done, is the weather of the Netherlands. After that, the thermal energy generation by the water and air is estimated.

6.1. Electrical supply

6.1.1. Comparison of the recorded and the expected electricity generation

The shaft of the proposed PV-chimney includes Kameleon Solar ColorBlast modules. These monocrystalline silicon modules are custom-made by Kameleon Solar and come in two different configurations: a 4x4 cell configuration and 4x5 cell configuration. For the calculation of the expected generation of a certain second (the second at which the measurements are done) the equation 18 is used. In table 11, the Watt peaks of the modules are presented. For the calculations, the fact that there is a glass layer in front of the PVs was considered (g-value of the glass: 0.9) plus 5% additional losses due to dust.

$$E = A * r * H * PR * g * d \quad (18)$$

Where:
E= Energy (kWh)
A=Total solar panel Area (m²)
r=solar panel yield (%)
H= Annual average irradiation on tilted panels (shadings not included) *
PR= Performance ratio, coefficient for losses (range between 0.9 and 0.5, default value = 0.75)
g= g-value of the glass
d= losses due to dust (%)

Table 11: Watt peaks of Kameleon solar modules, according to their size.

Minimum length	Number of cells	Wp per panel			
1684.5	10	113.18	150.90	188.63	226.35
1524.75	9	101.86	135.81	169.76	203.72
1365	8	90.54	120.72	150.90	181.08
1205.25	7	79.22	105.63	132.04	158.45
1045.5	6	67.91	90.54	113.18	135.81
885.75	5	56.59	75.45	94.31	113.18
726	4	45.27	60.36	75.45	90.54
566.25	3	33.95	45.27	56.59	67.91
406.5	2	22.64	30.18	37.73	45.27
246.75	1	11.32	15.09	18.86	22.64
	Number of cells	3	4	5	6
	Minimum width	506.25	666	825.75	985.5

As mentioned above, on the south facade, eight active panels were installed. Four of them, inside the chimney, and the rest outside. In figure 117, the configuration of the active panels on the South facade is presented and the panels with the indication "f" are the active panels inside the PV-chimney. The estimated generation is the sum of the energy produced by all the panels. Thus, for the comparison of the results, the generation of the PV modules out of the PV-chimney system is subtracted from the overall generation. The results indicate that the temperature of the PVs affect significantly their efficiency *(figure 118)*. Moreover, the temperature of 58°C is critical as temperatures above 58°C cause significant reduction of the PV efficiency. As it can be seen in table 12, the losses are increased by the increase of the PV temperature causing decrease up to 80%. The PV temperature at this point was 71°C and the solar irradiance 580W/m^2.

6.1.2. Comparison of the Kameleon Solar with Standard PVs in and out of the shaft

For the calculation of the annual generation, mean values of solar radiation are taken based on the weather data from a weather file by Climate Consultant 6.0 *(table 13)*. For the calculations, the electricity generation losses due to overheating of the solar cells, during summer, was assumed to be 10% (that means 9 days during summer the PV-chimney will have temperatures above 58°C). For the rest of the seasons, the percentage of losses due to the temperature of the PVs, was assumed zero.

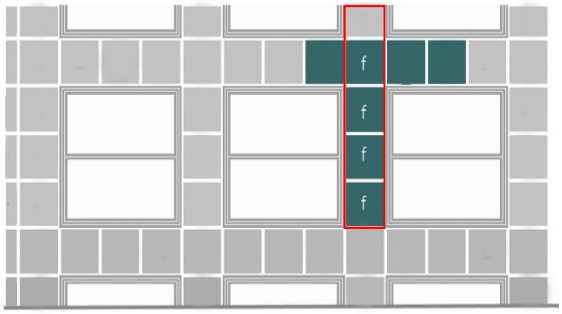

Figure 117: The active PVs of the prototype.

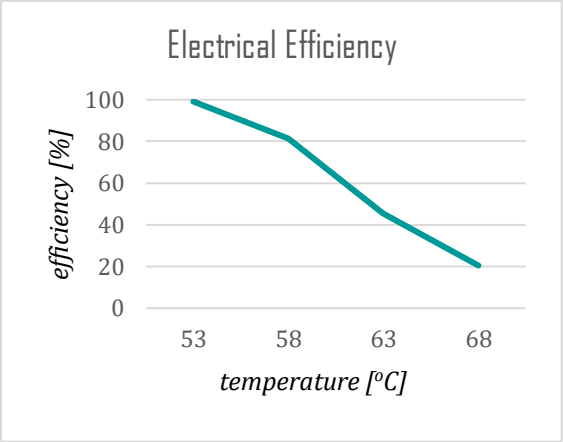

Figure 118: The energy efficiency losses due to high temperatures.

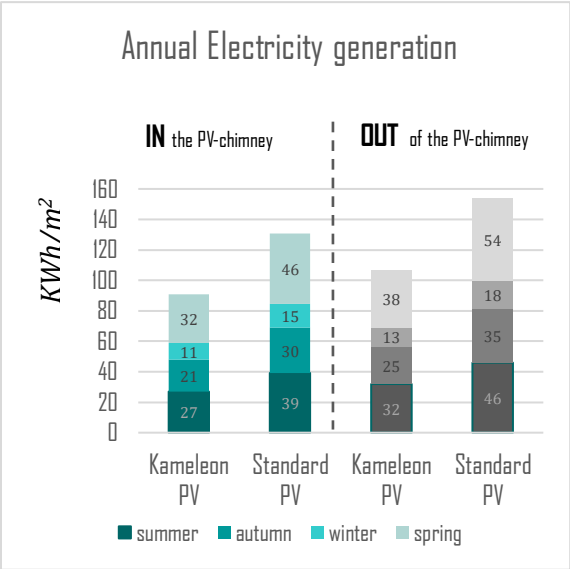

Figure 119: Comparison of the PVs IN and OUT of the proposed system.

Table 12: Recorder and expected electricity generation.

EXPRECTED ELECTRICITY POWER GENERATION				
time	sun radiation [W/m^2]	T of PVs (bottom/top)	recorded power [W/m^2]	expected power [W/m^2]
9:00-9:10	488	39.6 / 53.01	38.6	38.9
10:00-10:10	550	42.32 / 58.41	35.7	43.9
11:00-11:10	592	42.1 / 63.65	21.5	47.2
12:00-12:10	580	44.34 / 70.66	9.5	46.3
13:00-13:10	98	42.51 / 57.65	17.1	7.8
14:00-14:10	23	34.63 / 43.69	6.6	1.8
15:00-15:10	256	39.42 / 45.56	15.5	20.4

Table 13: Weather data which are used for the estimation of the annual electricity generation.

	Sun radiation [W/m^2]	hours of sunshine / season
Summer	420	900
Autumn	350	750
Winter	180	750
Spring	400	1000

The reported efficiency of the Kameleon solar panels is 13%, while for standard PVs the efficiency is assumed to be 18%. In figure 119, the annual electricity generation for the Kameleon solar panels and Standard panels is presented. Also, the figure displays the electricity production for both products, in the scenario that they are placed out of the PV-chimney. In this case, for the estimation of the electricity generation the losses due to the glass layer and dust are not considered, since the PVs are out of the shaft.

The PV-chimney system with the Kameleon solar panels is estimated to produce 91 KWh/m^2/year. That means, in the case of the proposed PV-chimney, in which the total PV surface area is roughly 2.05 m^2, that the annual production would be 188 KWh. The same PVs, out of the chimney, are estimated to produce 107 KWh/m^2, which means 219 KWh at the same surface area as in the PV-chimney. In the scenario of the comparison of the Kameleon solar panels with standard PVs, the production increases from 91 to 131 KWh/m^2/year for the PVs in the shaft and from 107 to 154 KWh/m^2/year for the PVs out of the shaft. This indicates approximately 30% losses, using Kameleon solar panels instead of standard PVs and roughly 15% losses, by the placement of the PV panels in the shaft.

It is important to be mentioned that for the Kameleon solar panels that are used for the prototype, a better configuration of the solar cells (fill factor) could be achieved by the replacement of the 4 panels with 2 taller ones. By this way, the existing space between the panels can be used for additional rows of solar cells which would provide higher electricity generation.

6.2. Thermal supply

The proposed PV-chimney can assist in the reduction of heating demands in either passive or active ways. The system can be used passively, when the temperature of the air and of the water is suitable for use. The heating of the water takes place through the absorption of the produced thermal energy from the PVT system (this way the PVs are cooled down). In the cases of not suitable temperature of water, the heated water can be used as supply water in a water tank which is heated up, in other ways, up to the desired values. For the air, warming is done by solar radiation while due to the buoyancy effect, a draft in the shaft is created. This air can be used for ventilation if its temperature and the amount of ventilation are suitable. Another solution, if the air cannot reach the desired values, is to use the preheated air as an inlet air of the HVAC system. This will be increasing the COP of the system and therefore will decrease the operational consumption of the system. Lastly, in order to reach higher values of temperature during heating seasons, the supplied air can be the air of the indoor space instead of the ambient air. By this way, warmer air will enter the shaft and the final temperature will be much higher.

The contribution of the produced air and of the water in combination with mechanical systems is difficult to quantify. Therefore, the calculations are limited to calculating the system output. For the evaluation of the thermal performance of the system the generated power from both water and air is calculated. Since the energy gains during the periods in which heating is needed are low, the PV-chimney has the vents close. This means mechanically controlled air circulation for the

indoor air. Consequently, for the calculations of cold periods, the room temperature is used as the temperature of the supplied air. For the estimation of the final temperature and ventilation values for both water and air, the calculation methodology of chapter 3 is used. For the estimation of the power generation the equation 19 is used. All the known values which are used for the calculation are shown in table 14.

$$Q = m\,(Tout - Tin) * Cp * A \qquad (19)$$

Where:

Q= power (kW)

m= mass flux which can be calculated be the equation 20 (kg/s*m^2)

$$m = \rho * Volume / A * t \qquad (20)$$

P= water density (kg/m^3)

A= supply surface area (m^2)

V=volume of the fluid (m^3)

t= time (s)

Tin=the temperature of the supplied fluid

Tout= the final temperature

Cp = Heat capacity (KJ/kgK)

A= supply surface area (m^2)

As it can be seen in figure 121, during summer (95 W/m^2), spring (85 W/m^2) and autumn (76 W/m^2) the power generation of the water is much higher than the winter (38 W/m^2). Also, the temperature of the water is increased by 4-10°C, but still, the water temperature is low, even in summer, for the direct use of water as Domestic Hot water. Therefore, additional power is needed to heat the water up to the appropriate levels of temperature. However, as mentioned above, the pre-heated water can be used as supplied water for the heating system of the building, in order to reduce the required energy consumption of the system.

Similarly to the thermal power of the water, the production of thermal power in the air during summer and spring (140 W/m^2), is much higher than the autumn (88 W/m^2) *(figure 120),* while during winter, the thermal power generation is much lower (23 W/m^2),.Regarding the temperature of the air, the system, in most of the seasons, needs an additional energy source in order to heat it up to usable levels. However, during summer, the system can be used for passive ventilation. Summarizing, both systems, cannot be used as passive energy sources. Therefore, their implementation with the HVAC system of the building is needed. In this case, the preheated air and water will be used to reduce the operational energy consumption of the ventilation and heating active systems.

Table 14: Data which are used for the estimation of power generation.

		Water	Air
Heat capacity	Cp [KJ/kg.K]	4.2	1
Density	ρ [kg/m3]	1000.0	1.2
Velocity	V [m/s]		
Summer		0.01	0.9
Autumn		0.01	0.85
Winter		0.01	0.45
Spring		0.01	0.9
Initial Temperature	Tin [°C]		
Summer		10	17
Autumn		10	18
Winter		10	18
Spring		10	18
Final Temperature	Tout [°C]		
Summer		20	20
Autumn		18	20
Winter		14	19
Spring		19	21

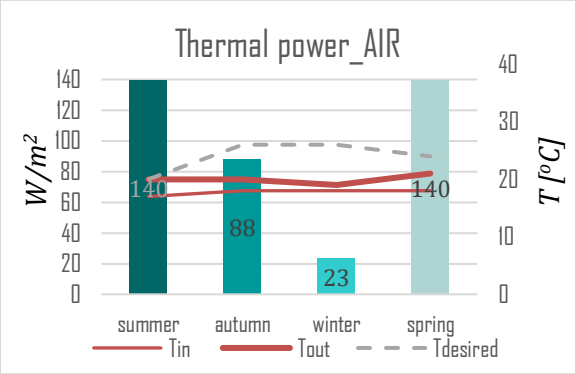

Figure 120: Thermal power estimation by the air of the cavity .

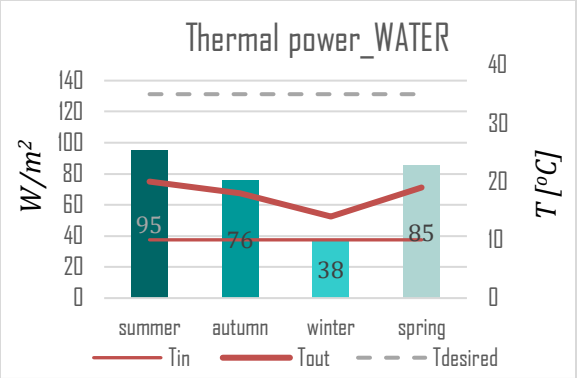

Figure 121: Thermal power estimation by the PV/T system .

6.3. Conclusions

The evaluation analysis of the system indicates that there is an important drop of the PV efficiency when the panel's temperature is getting higher than 53°C. After this value, by the increase of the temperature, the efficiency of the photovoltaics is reduced significantly. Therefore, the placement of PVs should be limited in lower layers, in order to prevent the overheating of the modules, leaving the top part only for solar collectors.

Moreover, the comparison of the system with standard products, shows that there are 30% losses annually while the placement of the PVs in the shaft, cause 15% annual losses. The losses, due to the placement of the PVs in the shaft, correspond to approximately 5-8 W/m^2 less powerduring the operation of the system.

The main idea of the system is that the electricity generation losses are gained back by the thermal energy production of the system. According to the thermal evaluation of the system, the thermal production by the air is estimated much higher than the losses due to the placement of the PVs in the shaft, even during winter (23 W/m^2). Simultaneously, there is thermal energy production by the water. The lowest power of 38 W/m^2 is noticed during winter and the highest power production of 95 W/m^2 during summer. Additionally, the fact that the PVs are in the shaft, causes higher values of PV temperature which provide higher water temperatures. This indicates that for the thermal performance of a PV/T system, their placement in the PV-chimney shaft is beneficial.

Although the thermal production is balancing the power production (due to electrical losses) and gives a positive sign to the system, the thermal energy of the system cannot be used directly. Both the water and the air temperatures are not suitable to be used directly, therefore, a connection of the PV/T-chimney with the HVAC of the system is required. In this case, the preheated air and water, will be used as inlet supply in order to increase the COP factor of the heat pump (decreasing the temperature difference between the source temperature and the required temperature). For the evaluation of the thermal gains under a more realistic perspective, the losses due to the mechanical components of the system should also be considered, in order to have a more realistic view of the final thermal gains.

7 CONCLUSIONS

The main goal of this graduation project was the investigation of the PV-chimney technology also in the terms of design, for high-rise building envelopes, as well as the understanding of the performance potential of the system. An overall conclusion about the proposed PV-chimney system, is that there are no certain optimal geometrical characteristics or guidelines to achieve high performance. Each application of the PV-chimney product requires specialized system analysis for the specific weather conditions.

In this study, an investigation of geometrical factors in different climates. indicates that, the height and the vent size play an important role on the ventilation values (airflow and air velocity). The increase of the height causes significant increases to the air flow and the air velocity while, the increase of the vent size causes a rise of the air flow and a reduction of the air velocity. Also, the solar radiation, the depth and the vent size influence the thermal behavior of the system. Apparently, higher solar irradiation values increase the system temperatures while the increase of the vent size, causes a reduction of the system's temperatures. Regarding the different scales of PV-chimney, their performance investigation shows that, the systems that are larger in scale, the "column" and the "building scale" PV-chimney systems cannot be used for direct ventilation due to high air velocities which, however, may offer the potential of wind energy generation. Regarding the rest of the aspects, the additional thermal gains of larger in scale systems are small, since, a large magnification causes a change of 2-4°C to the cavity air and roughly, 1 °C to the water temperature. The increase of the system scale causes an increase to the PV temperature which is not beneficial. Therefore, the benefits of large-scale systems in relation to the extra material, which is used, leads to the conclusion that smaller in scale PV-chimneys are more beneficial.

The investigation indicates that in the Netherlands and Hungary, small-sized (0.045m^2) and medium-sized (0.09m^2) vents can be used for passive cooling, during summer, while, during winter, it is recommended to have the vents closed due to low level of the ambient air temperature. Thus, during winter, an air circulation system in which the air of the room is heated up in the system and then sent back to the room is proposed. Regarding the PV temperature of the recommended scenarios, it does not exceed 40°C, which means that the PVs can work with high efficiency. Regarding the water temperature, the values are fluctuated between 11-12°C during the winter and 18-21°C during the summer, therefore, it cannot be used directly as Domestic Hot water or heating water. In Cyprus, where the weather is much warmer, the system shows that it is not beneficial and that there is a risk of overheating of the system during summer. The system cannot operate with closed vents, even during winter, due to the high temperatures of the air in the cavity. Therefore, it cannot be used for passive cooling while during heating seasons, additional energy is needed to warm up the air to the appropriate temperature. Also, during summer, the temperature of the photovoltaics, even with large vents (59°C) exceeds the workable operational levels of temperature, therefore, the PVs cannot be work efficiently. Lastly, the PV/T system in Cyprus provides higher

water temperatures (19-20°C during the winter and 27-30°C during the summer). However, the water temperature is not reaching the desired values in order to be used as Domestic Hot water or heating water. Consequently, it can be used as pre-heated water which is supplied to the heating system of the building.

The proposed PV-chimney was designed to respond in both the Netherlands' and Hungary's climate. For the accomplishment of the design of the system, the investigation and literature findings were used (the proposed PV-chimney, has 4.35m and 0.7m^2 vents). Additionally, the real construction of the facade of the building, provided the opportunity of real evaluation of the architectural integration, the understanding of practical limitations during design as well as construction difficulties. The general conclusion from the design and the realization procedure of the system in 1-1 scale is that, practical issues, cost and time constrains play a crucial role on the final design decisions.

In practice, plenty of the desired design solutions were changed either due to cost and the availability of products on the local market or due to time constrains and architectural intentions. The most remarkable change was the change of the operation of the system. The initial goal was to use the PV/T-chimney system also for cross ventilation but unfortunately, due to time contains and the complexity of the system this did not prove to be a feasible task. Other decisions, subject to restrictions are the use of fixed instead of controllable vents, due to cost constrains, the glazing shape, due to cost and time constraints as well as the PV selection due to architectural intentions. Moreover, from the assembly procedure of the PV/T-chimney both in the factory and on site, difficulties were faced during the piping work and the connection of the PV-chimney with the mechanical system, due to the unspecialized manual work. Under the perspective of installing the system in a high-rise building, it can easily be assumed that such manual work and on-site connections would be time consuming and add some complexity to the installation process. However, the connections were made rather easily for the scale of the constructed prototype. Simultaneously, a preparation of hydraulic installations, in order to connect the facade module, where the PV-chimney is attached, with the mechanical system of the building, real time cabling of the PVs is required. Consequently, the construction schedule becomes more complex, firstly because different disciplines have to work together and secondly, due to the fact that both the electrical and plumbing work are, in principle, done after the placement of the envelope of the building. In addition to that, the placement of the system in front of the concrete columns, may cause maintenance complexity as the system can be approached only from outside.

Regarding the architectural integration of the PV/T-chimney, the proposed design creates a smooth integration of the system with the façade. The facade design results in a strict, clean image of the appearance of the building, in respects to the initial flatness and pattern of the Europoint Towers. Moreover, although the PV-chimney can be considered as an additional element on the facade, its materialization and geometry make it look really as part of it.

The system was tested in real conditions in Hungary. The analysis of the experiment measurements indicates that an important reduction of the efficiency of the PVs is obtained due to the high PV temperatures (critical temperature value above 53°C). Therefore, especially at the top part of the shaft, it will be beneficial to replace the photovoltaics by solar collectors. Furthermore, the velocity measurements of the air in the cavity show that draft is generated within the shaft with values that allow its use for ventilation, but the temperature of the air was measured to be surprisingly high. However, on the specific day of the experiment it was a quite warm day, and which does not reflect the weather conditions even of a typical summer day in Hungary. Therefore, the average temperature of the air the cavity is estimated to be lower.

Additionally, the evaluation of the electrical and thermal performance of the system indicates that 15% losses on the electrical power generation are caused by the

placement of the PVs in the shaft, while 30% losses are due to the low efficiency of the selected PV product, in correlation with conventional PVs. Although that the system reduces the electrical efficiency of the system, the thermal gains are higher than the losses and thus, a positive energy sign is given to the system. However, the temperature values of both air and water are not appropriate for direct use, therefore, the connecting the system with the HVAC system is needed. In this case, an investigation about the operational losses due to the mechanical components of the system should be done in order to have a clear view of the final thermal energy gains.

The high-rises in particular tend to consume more energy per square meter with height and thus, have higher environmental impact than lower buildings. Therefore, in order to comply with future energy-efficiency targets, energy generating systems are an indispensable facade element in high-rises. The proposed PV/T-chimney system is a system that combines different mechanical systems together in order to produce more energy per square meter. Its analysis shows that there is great potential of acquiring a positive energy sign. Therefore, it can stimulate research interest for further optimizations on its performance. The incorporation of BIPVs for electricity and thermal energy production on the facades could be a great achievement for the reduction of the energy consumption in high-rise buildings. As there is a lack in the horizontal surface area in high-rises, vertical solutions can be the key to handle their high energy demands and the way to more net positive approaches. Furthermore, since the PV-chimney system or any other facade integrated energy systems affect the overall aesthetics of the building, their design is a quite challenging tasks for architects as well. Architects and Engineers have to collaborate to achieve facade designs with high aesthetics and high performance in every other aspect apart from the energy savings and energy production.

8 RECOMMENDATIONS

Further studies:

This study could serve as a starting point for further studies and analyze different aspects than could improve the PV-chimney system.

- Investigate the performance of passive ventilation design strategies without the use of a heat pump, focusing on either cooling on heating mode.
- Access the potential energy gains due to energy losses by the heat pump components.
- Access the impact of the height and the wind on the PV-chimney performance.
- Feasibility study of the system could be done in terms of cost and maintenance.
- Calculate the embodied energy of the system.

Recommendations regarding the prototype:

The construction of the prototype in 1:1 scale, makes evident that the following aspects have room for improvement:

- Implementation of a controllable system for the vents. For optimal operation of the system, This could also provide the passive operation of the system, temperature sensors should be incorporated.
- Standard piping is recommended to avoid possible leakage by hand made plumbing work.
- Replacement of the PV modules with taller ones in order to use the in between gap for extra series of cells. Also, the width of the chimney could be adjusted in order to reduce the side spaces.
- For the improvement of the thermal performance, anti-reflective coating can apply.

Recommendations regarding future experiments:

The experiment procedure indicates that a lot of improvements can be done to reduce the inaccuracies.

- Instead of anemometer measurements, the measurements within the shaft can be done also by thermocouples. More accurate measurements of the temperature can be achieved by thermocouples due to less bias errors.
- For better understanding of the system, it is recommended to take more measurements in different levels of height.
- It will be useful, for more accurate evaluation of the system to measure the solar radiation both inside and outside the shaft in order to know the real losses due to glass.

- The measurements occurred every hour with time gaps from top to bottom in non-constant conditions. Therefore, more anemometers could provide simultaneous measurements for more accurate results.

- Measurements in more than one day would provide more validate results and more accurate conclusions.

- Measurements of the air humidity in order to access its impact on the air temperature.

- Measurements of the CO_2 levels of the air to ensure that the air which enters the room, if the system is used for ventilation, meets the standard requirements.

REFERENCES

Abbassi, F., Dimassi, N., & Dehmani, L. (2014). Energetic study of a Trombe wall system under different Tunisian building configurations. *Energy and Buildings, 80*, 302-308. doi:10.1016/j.enbuild.2014.05.036

Aelenei, L., Pereira, R. (2013). Innovative solutions for net zero-energy building: BIPV-PCM system - Modeling, design and thermal performance. *2013 4th International Youth Conference on Energy (IYCE)*. doi:10.1109/iyce.2013.6604162

Aelenei, L., Pereira, R., Gonçalves, H., Athienitis, A. (2014). Thermal Performance of a Hybrid BIPV-PCM: Modeling, Design and Experimental Investigation. *Energy Procedia, 48*, 474-483. doi:10.1016/j.egypro.2014.02.056

Agarwal, R.K., Garg, H.P. (1994). Study of a photovoltaic-thermal system—thermosyphonic solar water heater combined with solar cells. *Energy Convers Manage*, 35(7), 605–20.

Agrawal, B., Tiwari, G. (2010). Life cycle cost assessment of building integrated photovoltaic thermal (BIPVT) systems. *Energy and Buildings, 42*(9), 1472-1481. doi:10.1016/j.enbuild.2010.03.017

Agrawal, B., Tiwari, G.N. (2011). Building Integrated Photovoltaic Thermal Systems: For Sustainable Developments. *Royal Society of Chemistry*, New Delhi, India.

Alan, S. M., Reza, L. (2016). A thermocouple is a junction between two conductors that converts a temperature difference into a potential difference via the thermoelectric effect. *Measurement and Instrumentation: Theory and Application, Second Edition*.

Alejandro, P.H. (2018). Architectural Integration of Solar Cooling Technologies in the Building Envelope. *Delft University of Technology, Department of Architectural Engineering + Technology*.

Al-Karaghouli, A., Kazmerski, L. (2010). Optimization and life-cycle cost of health clinic PV system for a rural area in southern Iraq using HOMER software. *Solar Energy*, 84, 710–4.

Anderson, R., Kreith, F. (1987). Natural Convection in Active and Passive Solar Thermal Systems. *Advances in Heat Transfer Volume 18 Advances in Heat Transfer*, 1-86. doi:10.1016/s0065-2717(08)70117-5

Antvorskov, S., (2008). Introduction to integration of renewable energy in demand-controlled hybrid ventilation systems for residential buildings. *Esbensen Consulting Engineers*, Sukkertoppen Copenhagen, Carl Jacobensens Vej 25 D, DK-2500 Valby, Denmark. https://www.sciencedirect.com/science/article/pii/S0360132307000479

ASHRAE. (2010). Standard 55 – Thermal Environment Conditions for Human Occupancy. *American Society of Heating Ventilating and Air-conditioning Engineers*, Atlanta, USA.

ASHRAE. (2011). Advanced Energy Design Guide for Small to Medium Office Buildings. *Atlanta*, USA.

Assoa, Y., Ménézo, C. (2014). Dynamic study of a new concept of photovoltaic–thermal hybrid collector. *Solar Energy, 107*, 637-652. doi:10.1016/j.solener.2014.05.035

Assoa, Y., Menezo, C., Fraisse, G., Yezou, R., Brau, J. (2007). Study of a new concept of photovoltaic–thermal hybrid collector. *Solar Energy, 81*(9), 1132-1143. doi:10.1016/j.solener.2007.04.001

Athienitis, A. K., Bambara, J., O'Neill, B., Faille, J. (2011). A prototype photovoltaic/thermal system integrated with transpired collector. *Solar Energy, 85*(1), 139-153. doi:10.1016/j.solener.2010.10.008

AthienitisGang, P., Huide, F., Huijuan, Z., Jie, J. (2012). Performance study and parametric analysis of a novel heat pipe PV/T system. *Energy, 37*(1), 384-395. doi:10.1016/j.energy.2011.11.017

Atkinson, J., Chartier, Y., Pessoa-Silva, C.L., et al. (2009). Natural Ventilation for Infection Control in Health-Care Settings. *World Health Organization*, Geneva. https://www.ncbi.nlm.nih.gov/books/NBK143277/

Bakker, M., Zondag, H., Elswijk, M., Strootman, K., Jong, M. (2005). Performance and costs of a roof-sized PV/thermal array combined with a ground coupled heat pump. *Solar Energy, 78*(2), 331-339. doi:10.1016/j.solener.2004.09.019

Balcomb, J.D. (1992). Passive Solar Buildings. *People's Republic of China: MIT Press*, Hong Kong.

Balcomb, J.D., McFarland, R.D. (1978). Simple Empirical Method for Estimating the Performance of a Passive Solar Heated Building of the Thermal Storage Wall Type. New York, USA: U.S. Department of Energy, *Assistant Secretary for Conservation and Solar Applications, Division of Solar Applications*.

Bergene, T., Lovvik, O. M. (1995). Model calculations on a flat-plate solar heat collector with integrated solar cells. *Solar Energy, 55*(6), 453-462. doi:10.1016/0038-092x(95)00072-y

Bhandari, M., Bansal, N. (1994). Solar heat gain factors and heat loss coefficients for passive heating concepts. *Solar Energy, 53*(2), 199-208. doi:10.1016/0038-092x(94)90482-0

Böer, K. W., & Tamm, G. (2003). Solar conversion under consideration of energy and entropy. *Solar Energy, 74*(6), 525-528. doi:10.1016/s0038-092x(03)00198-1

Bojić, M., Johannes, K., Kuznik, F. (2014). Optimizing energy and environmental performance of passive Trombe wall. *Energy Build*; 70,279–86.

Bokel, R., (2018). Heating up a building with earth ducts, solar collectors and other time-independent mass flows. *Building Physics energy (01),* TU Delft, Course,

Bokel, R., (2018). Glazing properties and their effect on the insulation and heat admittance in a building. *Building Physics energy (02),* TU Delft, Course,

Bokel, R., (2018). Natural Ventilation. *Building Physics energy (05),* TU Delft, Course,

Bourdeau, L.E. (1980). Study of two passive solar systems containing phase change materials for thermal storage. In: Proceedings of the 5th national passive solar conference, Amherst, MA, 19–26 October. Newark, *DE: American Section of the International Solar Energy Society*.

Bouzoukas, A. (2008). New Approaches for Cooling Photovoltaic/Thermal (PV/T) Systems. *University of Nottingham*.

Briga-Sá, A., Martins, A., Boaventura-Cunha, J., Lanzinha, J. C., & Paiva, A. (2014). Energy performance of Trombe walls: Adaptation of ISO 13790:2008(E) to the Portuguese reality. *Energy and Buildings, 74*, 111-119. doi:10.1016/j.enbuild.2014.01.040

BRE Digest. (2001). Thermal mass in buildings - an introduction. 454 - *Part 1*..

Briga-Sá, A., Martins, A., Boaventura-Cunha, J., Lanzinha, J.C., Paiva, A. (2014). Energy performance of Trombe walls: adaptation of ISO 13790:2008(E) to the Portuguese reality. *Energy Build 2014*, 74, 111–9.

Buker, M. S., Mempouo, B., Riffat, S. B. (2014). Performance evaluation and techno-economic analysis of a novel building integrated PV/T roof collector: An experimental validation. *Energy and Buildings, 76*, 164-175. doi:10.1016/j.enbuild.2014.02.078

Burek, S., Habeb, A. (2007). Air flow and thermal efficiency characteristics in solar chimneys and Trombe Walls. *Energy and Buildings, 39*(2), 128-135. doi:10.1016/j.enbuild.2006.04.015

Cabeza, L. F., Castellón, C., Nogués, M., Medrano, M., Leppers, R., & Zubillaga, O. (2007). Use of microencapsulated PCM in concrete walls for energy savings. *Energy and Buildings, 39*(2), 113-119. doi:10.1016/j.enbuild.2006.03.030

Cabeza, L.F., Castello, C., Nogue, M., et al. (2007). Use of microencapsulated PCM in concrete walls for energy savings. *Energy and Buildings*; 39, 113–119.

Chan, H.Y., Riffat, S.B., Zhu, J. (2010). Review of passive solar heating and cooling technologies. *Renewable & Sustainable Energy Reviews*; 14, 781–789.

Chemisana, D., López-Villada, J., Coronas, A., Rosell, J. I., & Lodi, C. (2013). Building integration of concentrating systems for solar cooling applications. *Applied Thermal Engineering, 50*(2), 1472-1479. doi:10.1016/j.applthermaleng.2011.12.005

Chen, Y., Athienitis, A., & Galal, K. (2010). Modeling, design and thermal performance of a BIPV/T system thermally coupled with a ventilated concrete slab in a low energy solar house: Part 1, BIPV/T system and house energy concept. *Solar Energy, 84(11)*, 1892-1907. doi:10.1016/j.solener.2010.06.013

Chen, Z., Bandopadhayay, P., Halldorsson, J., Byrjalsen, C., Heiselberg, P., & Li, Y. (2003). An experimental investigation of a solar chimney model with uniform wall heat flux. *Building and Environment, 38*(7), 893-906. doi:10.1016/s0360-1323(03)00057-x

Chow, T. (2010). A review on photovoltaic/thermal hybrid solar technology. *Applied Energy, 87*(2), 365-379. doi:10.1016/j.apenergy.2009.06.037

Chow, T., Chan, A., Fong, K., Lin, Z., He, W., & Ji, J. (2009). Annual performance of building-integrated photovoltaic/water-heating system for warm climate application. *Applied Energy, 86*(5), 689-696. doi:10.1016/j.apenergy.2008.09.014

Chow, T., Hand, J., & Strachan, P. (2003). Building-integrated photovoltaic and thermal applications in a subtropical hotel building. *Applied Thermal Engineering, 23*(16), 2035-2049. doi:10.1016/s1359-4311(03)00183-2

Chow, T., He, W., & Ji, J. (2007). An experimental study of façade-integrated photovoltaic/water-heating system. *Applied Thermal Engineering, 27*(1), 37-45. doi:10.1016/j.applthermaleng.2006.05.015

Chow, T., He, W., Chan, A., Fong, K., Lin, Z., & Ji, J. (2008). Computer modeling and experimental validation of a building-integrated photovoltaic and water heating system. *Applied Thermal Engineering, 28*(11-12), 1356-1364. doi:10.1016/j.applthermaleng.2007.10.007

Chow, T., Pei, G., Fong, K., Lin, Z., Chan, A., Ji, J. (2009). Energy and exergy analysis of photovoltaic–thermal collector with and without glass cover. *Applied Energy, 88*(3), 310-316. doi:10.1016/j.apenergy.2008.04.016

Chow, T.T., Hand, J.W., Strachan, P.A. (2003). Building-integrated photovoltaic and thermal applications in a subtropical hotel building. *Applied Thermal Engineering*, 23, 2035–2049.

CIBSE. (2012). Guide F: Energy Efficiency in Buildings. *UK: CIBSE*.

Corbin, C. D., Zhai, Z. J. (2010). Experimental and numerical investigation on thermal and electrical performance of a building integrated photovoltaic–thermal collector system. *Energy and Buildings, 42*(1), 76-82. doi:10.1016/j.enbuild.2009.07.013

Cox, C., Raghuraman, P. (1985). Design considerations for flat-plate-photovoltaic/thermal collectors. *Solar Energy, 35*(3), 227-241. doi:10.1016/0038-092x(85)90102-1

Daghigh, R., Ruslan, M.H., Zaharim, A., Sopian, K. (2011). Effect of Packing Factor on the Performance of PV/T Water Heater. *Recent Researches in Energy & Environment*, 304-309, Solar Energy Research Institute, Universiti Kebangsaan Malaysia.

Dai, Y.J., Ma, Q., Xu, Y.X., Zhai, X.Q., Wang, R.Z., Wu, J.Y. (2007). Solar integrated energy system for a green building. *Energy Build*, 39(8), 985-93.

Davidsson, H., Perers, B., & Karlsson, B. (2010). Performance of a multifunctional PV/T hybrid solar window. *Solar Energy, 84*(3), 365-372. doi:10.1016/j.solener.2009.11.006

Davidsson, H., Perers, B., & Karlsson, B. (2012). System analysis of a multifunctional PV/T hybrid solar window. *Solar Energy, 86*(3), 903-910. doi:10.1016/j.solener.2011.12.020

De Pascale, A., Ferrari, C., Melino, F., et al. (2012). Integration between a thermophotovoltaic generator and an Organic Rankine Cycle. *Applied Energy*, 97, 695–703.

De Wit, M. (2007). Heat and moisture in building envelopes, *TUE*.

Dragic Evic, S., Lambic, M. (2011). Influence of constructive and operating parameters on a modified Trombe wall efficiency. *Arch Civ Mech Eng, 11*, 825–38.

Dr, Van Overveld, M., Van Der Graaf, P.J., Eggink-Eilander, S., Berghuis, M.I. (2012). Praktijboek Bouwbesluit. *Sdu Uitgevers*: Den Hagg.

Dupeyrat, P., Ménézo, C., Rommel, M., Henning, H. (2011). Efficient single glazed flat plate photovoltaic–thermal hybrid collector for domestic hot water system. *Solar Energy, 85*(7), 1457-1468. doi:10.1016/j.solener.2011.04.002

Eiffert, P. (2000). U.S. guidelines for the economic analysis of building-integrated photovoltaic power systems. *National Renewable Energy Laboratory*, Colorado (USA). doi:10.2172/752395

Fang, X., & Li, Y. (2000). Numerical simulation and sensitivity analysis of lattice passive solar heating walls. *Solar Energy, 69*(1), 55-66. doi:10.1016/s0038-092x(00)00014-1

Fang, X., Yang, T. (2008). Regression methodology for sensitivity analysis of solar heating walls. *Applications Thermal Engineering*, 28, 2289–94.

Fergus, J.N., Humphreys, A.M. (2012). Adaptive Thermal Comfort and Sustainable Thermal standards for Buildings. Energy and Buildings. 45-59. doi: 10.1016/S0378-7788(02)00006-3

Fernández-Hernández, F., Cejudo-López, J. M., Domínguez-Muñoz, F., & Carrillo
Andrés, A. (2015). A new desiccant channel to be integrated in building façades. *Energy and Build*, 86(0), 318-327. doi: http://dx.doi. org/10.1016/j.enbuild.2014.10.009

Ferreira, J., Pinheiro, M. (2011). In search of better energy performance in the Portuguese buildings—The case of the Portuguese regulation. *Energy Policy, 39*(12), 7666-7683. doi:10.1016/j.enpol.2011.08.062

Fiorito, F. (2012). Trombe Walls for Lightweight Buildings in Temperate and Hot Climates. Exploring the Use of Phase-change Materials for Performances Improvement. *Energy Procedia, 30*, 1110-1119. doi:10.1016/j.egypro.2012.11.124

Florschuetz, L. (1979). Extension of the Hottel-Whillier model to the analysis of combined photovoltaic/thermal flat plate collectors. *Solar Energy, 22*(4), 361-366. doi:10.1016/0038-092x(79)90190-7

Fraisse, G., Ménézo, C., Johannes, K. (2007). Energy performance of water hybrid PV/T collectors applied to combi systems of Direct Solar Floor type. *Solar Energy, 81*(11), 1426-1438. doi:10.1016/j.solener.2006.11.017

Fujisawa, T., Tani, T. (1997). Annual exergy evaluation on photovoltaic-thermal hybrid collector. *Solar Energy Materials and Solar Cells, 47*(1-4), 135-148. doi:10.1016/s0927-0248(97)00034-2

Gan, G., Riffat, S.B. (1998). A numerical study of solar chimney for natural ventilation of buildings with heat recovery. *Applications Thermal Energy*, 18(12), 1171-87.

Garcia, A. R., (2018). Computational design method based on multidisciplinary design optimization and optioneering techniques for energy efficiency and cost effectiveness. *Graduation project report*, TU Delft, Netherlands.

Garg, H. P., Adhikari, R. S. (1999). Performance analysis of a hybrid photovoltaic/thermal (PV/T) collector with integrated CPC troughs. *International Journal of Energy Research, 23*(15), 1295-1304. doi:10.1002/(sici)1099-114x(199912)23:153.3.co;2-k

Ghani, F., Duke, M., Carson, J. (2012). Effect of flow distribution on the photovoltaic performance of a building integrated photovoltaic/thermal (BIPV/T) collector. *Solar Energy, 86*(5), 1518-1530. doi:10.1016/j.solener.2012.02.013

Gómez, V. H., Gálvez, D. M., & Zayas, J. L. (2010). Design recommendations for heat discharge systems in walls. *Applied Thermal Engineering, 30*(13), 1616-1620. doi:10.1016/j.applthermaleng.2010.03.019

Guohui, G. (1997). A parametric study of Trombe walls for passive cooling of buildings. *Energy and Buildings*, 27, 37-43. University of Nottingham, University Park, UK.

Haleh, S., Saeed Reza, M. (2013). STUDY OF DIFFERENT MATERIALS USED IN WALLS IN TERMS OF THERMAL TERM: REVIEW PAPER. *University of Fars science and Research, Universiti Technologi of Malaysia*.

Hami, K., Draoui, B., & Hami, O. (2012). The thermal performances of a solar wall. *Energy, 39*(1), 11-16. doi:10.1016/j.energy.2011.10.017

Hassanain, .AA., Hokam, E.M., Mallick, T.K. (2011). Effect of solar storage wall on the passive solar heating constructions. *Energy and Buildings*, 43, 737–747.

Hayter, S.J., Martin, R.L. (1998). Photovoltaics for buildings: Cutting-edge PV. *Presented at UPVG Utility PV Experience (UPEx)'98*, 28–30, San Diego, California, September.

Hegazy, A. A. (2000). Comparative study of the performances of four photovoltaic/thermal solar air collectors. *Energy Conversion and Management, 41*(8), 861-881. doi:10.1016/s0196-8904(99)00136-3

Hogan, I. (1975). Solar building in the Pyrenees. *Architectural Design, 45*(1), 13–17.

Hordeski, M.F. (2011). New Technologies for Energy Efficiency. *New York: Fairmont Press*.

Hordeski, M.F., (2004). Dictionary of energy efficiency technologies. *Fairmont Press*, West Virginia, United States.

Ibáñez-Puy, M., Sacristán Fernández, J. A., Martín-Gómez, C., Vidaurre
Arbizu, M. (2015). Development and construction of a thermoelectric active facade module. *Journal of Facade Design and Engineering, 3(1)*, 1525. doi: 10.3233/fde-150025

Ibrahim, A., Fudholi, A., Sopian, K., Othman, M. Y., & Ruslan, M. H. (2014). Efficiencies and improvement potential of building integrated photovoltaic thermal (BIPVT) system. *Energy Conversion and Management, 77*, 527-534. doi:10.1016/j.enconman.2013.10.033

Irshad, K., Habib, K., Thirumalaiswamy, N. (2014). Energy and cost analysis of photovoltaic Trombe wall system in tropical climate. *Energy Procedia*, 50, 71–8.

ISO 9060. (1990). Solar energy — Specification and classification of instruments for measuring hemispherical solar and direct solar radiation.

ISO 7730. (2005). Ergonomics of the thermal environment – Analytical determination and interpretation of thermal comfort using calculation of the PMV and PPD indices and local thermal comfort criteria, Switzerland

Jaber, S., & Ajib, S. (2011). Optimum design of Trombe wall system in mediterranean region. *Solar Energy, 85*(9), 1891-1898. doi:10.1016/j.solener.2011.04.025

Jaber, S., Ajib, S. (2011). Optimum design of Trombe wall system in mediterranean region. *Solar Energy, 85*(9), 1891-1898. doi:10.1016/j.solener.2011.04.025

Jarimi, H., Bakar, M. N., Manaf, N. A., Othman, M., Din, M. (2013). Mathematical modelling of a finned bi-fluid type photovoltaic/thermal (PV/T) solar collector. *2013 IEEE Conference on Clean Energy and Technology (CEAT)*. doi:10.1109/ceat.2013.6775619

Ji, J., Chow, T., & He, W. (2003). Dynamic performance of hybrid photovoltaic/thermal collector wall in Hong Kong. *Building and Environment, 38*(11), 1327-1334. doi:10.1016/s0360-1323(03)00115-x

Ji, J., Han, J., Chow, T., Yi, H., Lu, J., He, W., & Sun, W. (2006). Effect of fluid flow and packing factor on energy performance of a wall-mounted hybrid photovoltaic/water-heating collector system. *Energy and Buildings, 38*(12), 1380-1387. doi:10.1016/j.enbuild.2006.02.010

Ji, J., He, H., Chow, T., Pei, G., He, W., & Liu, K. (2009). Distributed dynamic modeling and experimental study of PV evaporator in a PV/T solar-assisted heat pump. *International Journal of Heat and Mass Transfer, 52*(5-6), 1365-1373. doi:10.1016/j.ijheatmasstransfer.2008.08.017

Ji, J., Lu, J., Chow, T., He, W., & Pei, G. (2007). A sensitivity study of a hybrid photovoltaic/thermal water-heating system with natural circulation. *Applied Energy, 84*(2), 222-237. doi:10.1016/j.apenergy.2006.04.009

Ji, J., Luo, C., Sun, W., Yu, H., He, W., Pei, G. (2009). An improved approach for the application of Trombe wall system to building construction with selective thermo-insulation façades. *Chin Science Bull*, 54, 1949–56.

Ji, J., Pei, G., Chow, T., Liu, K., He, H., Lu, J., & Han, C. (2008). Experimental study of photovoltaic solar assisted heat pump system. *Solar Energy, 82*(1), 43-52. doi:10.1016/j.solener.2007.04.006

Ji, J., Yi, H., He, W., Pei, G. (2007). PV-Trombe wall design for buildings in composite climates. *Journal Solar Energy Eng.*, 129, 431.
Jiang, B., Ji, J., Yi, H. (2008). The influence of PV coverage ratio on thermal and electrical performance of photovoltaic-Trombe wall. *Renewable Energy, 33*(11), 2491-2498. doi:10.1016/j.renene.2008.02.001

Jie, J., Hua, Y., Gang, P., & Jianping, L. (2007). Study of PV-Trombe wall installed in a fenestrated room with heat storage. *Applied Thermal Engineering, 27*(8-9), 1507-1515. doi:10.1016/j.applthermaleng.2006.09.013

Jie, J., Hua, Y., Gang, P., Bin, J., & Wei, H. (2007). Study of PV-Trombe wall assisted with DC fan. *Building and Environment, 42*(10), 3529-3539. doi:10.1016/j.buildenv.2006.10.038

John, S., (2006). Passive Solar Design. *Zonbak*. http://www.zonbak.com/knowledge/passive%20solar%20design/passivesolar12.html

Kalogirou, S., Tripanagnostopoulos, Y. (2006). Hybrid PV/T solar systems for domestic hot water and electricity production. *Energy Conversion and Management, 47*(18-19), 3368-3382. doi:10.1016/j.enconman.2006.01.012

Keliang, L., Jie, J., Tin-Tai, C., Gang, P., Hanfeng, H., Aiguo, J., & Jichun, Y. (2009). Performance study of a photovoltaic solar assisted heat pump with variable-frequency compressor – A case study in Tibet. *Renewable Energy, 34*(12), 2680-2687. doi:10.1016/j.renene.2009.04.031
Khalifa, A.J.N., Abbas, E.F (2009). A comparative performance study of some thermal storage materials used for solar space heating. *Energy and Buildings*, 41, 407–415.

Khedari, J., Ingkawanich, S., Hirunlabh, J. (2002). A PV system enhanced the performance of roof solar collector. *Build Environment*, 37(12), 1317-20.

Khedari, J., Rachapradit, N., Hirunlabh, J. (2003). Field study of performance of solar chimney with air-conditioned building. *Energy, 28*, 1099-1114.

Knowles, T.R. (1983). Proportioning composites for efficient thermal storage walls. *Solar Energy*, 31, 319–326.

Koyunbaba, B. K., & Yilmaz, Z. (2012). The comparison of Trombe wall systems with single glass, double glass and PV panels. *Renewable Energy, 45*, 111-118. doi:10.1016/j.renene.2012.02.026

Krüger, E., Suzuki, E., Matoski, A. (2013). Evaluation of a Trombe wall system in a subtropical location. *Energy and Buildings, 66*, 364-372. doi:10.1016/j.enbuild.2013.07.035

Kundakci Koyunbaba, B., Yilmaz, Z. (2012). The comparison of Trombe wall systems with single glass, double glass and PV panels. *Renewable Energy*, 45, 111–8.

Lam Joseph, C., Liu, Y., Jiaping, L., (2006). Development of passive design zones in China using bioclimatic approach. *Energy Convers Manage*, 47(6), 746–62.

Landsberg, J., Sands, P. (2011). Physiological Ecology of Forest Production. *Terrestrial Ecology*.

Lee, K.H., Strand Richard, K. (2009). Enhancement of natural ventilation in buildings using a thermal chimney. *Energy Build 2009*, 41(6), 615–21.

Li, Y., Liu, S. (2014). Experimental study on thermal performance of a solar chimney combined with PCM. *Applied Energy, 114*, 172-178. doi:10.1016/j.apenergy.2013.09.022

Lin, W., Ma, Z., Sohel, M. I., Cooper, P. (2014). Development and evaluation of a ceiling ventilation system enhanced by solar photovoltaic thermal collectors and phase change materials. *Energy Conversion and Management, 88*, 218-230. doi:10.1016/j.enconman.2014.08.019

Liping, W., Angui, L. (2006). A numerical study of Trombe wall for enhancing stack ventilation. *Buildings 2006*.

Liu YW and Feng W (2012) Integrating passive cooling and solar techniques into the existing building in South China. Advanced Materials Research 368–373: 3717–3720.

Liu, Z., Zhang, L., Gong, G., Han, T. (2015). Experimental evaluation of an active solar thermoelectric radiant wall system. *Energy Conversion and Management, 94(0),* 253-260. doi: http://dx.doi.org/10.1016/j. enconman.2015.01.077

Lumley, J.L., Wyngaard, J.C., (1967). A constant temperature hot-wire anemometer. Journal of Scientific Instruments, *44*, 363. https://doi.org/10.1088/0950-7671/44/5/309

Macias, M., Gaoma, J.A., Luxan, J.M., Gloria, G. (2009). Low cost passive cooling system for social housing in dry hot climate, *Energy Build*, 41(9), 915-21.

Maerefat, M., Haghighi, A.P. (2010). Natural cooling of stand-alone houses using solar chimney and evaporative cooling cavity. *Renewable Energy*, 35(9), 2040-52.

Maerefat, M., Haghighi, A.P. (2010). Passive cooling of buildings by using integrated earth to air heat exchanger and solar chimney. *Renewable Energy*, 35(10), 2316-24.

Meirmans, K. (2013). Household direct energy consumption and CO2 emissions in European countries. *Default journal*.

Melero, S., Morgado, I., Neila, J., et al. (2011). Passive evaporative cooling by porous ceramic elements integrated in a Trombe wall. *Architecture & Sustainable Development*. Paris, France, Presses univ. de Louvain.

Moshtegh, B., Sandberg, M. (1996). Investigation of fluid flow and heat transfer in a vertical channel heated from one side by PV elements. Part I-Numerical study, *Renewable Energy, 8*, 248.

National Renewable Energy Laboratory (NREL). (2005). Building a better Trombe wall: NREL researchers improve passive solar technology. *National Renewable Energy Laboratory*. http://www.nrel.gov/docs/fy04osti/36277.pdf

Nelson, V.. (2011) Introduction to Renewable Energy. Florida, *USA: Taylor & Francis*.

Nwachukwu, N.P., Okonkwo, W.I. (2008). Effect of an absorptive coating on solar energy storage in a Trombe wall system. *Energy and Buildings*, 40, 371–374.

Nwosu, N.P. (2010). Trombe wall redesign for a poultry chick brooding application in the equatorial region – analysis of the thermal performance of the system using the Galerkin finite elements. *International Journal of Sustainable Energy*, 29, 37–47.

Omidreza, S., Chin Haw, L., Kamaruzzaman, S., Elias, S. (2013). A state of the art review of solar walls: Concepts and applications. *Journal of Building Physics*, 37(1), 55–79.

Ong, K.S., (2003). A mathematical model of a solar chimney. Energy and Buildings, 28, 1047–1060. http://dx.doi.org/10.1016/S0960-1481(02)00057-5

Onishi, J., Soeda, H., Mizuno, M. (2001). Numerical study on a low energy architecture based upon distributed heat storage system. *Renewable Energy*, 22, 61–66.

Paardekooper, S., Lund, R. S., Mathiesen, B. V., Chang, M., Petersen, U. R., Grundahl, L., … Persson, U. (2018). Heat Roadmap Hungary: Quantifying the Impact of Low-Carbon Heating and Cooling Roadmaps.

Palmer, K. F., Williams, D. (1974). Optical properties of water in the near infrared*. *Journal of the Optical Society of America, 64*(8), 1107. doi:10.1364/josa.64.001107

Peng, J., Lu, L., Yang, H., & Han, J. (2013). Investigation on the annual thermal performance of a photovoltaic wall mounted on a multi-layer façade. *Applied Energy, 112*, 646-656. doi:10.1016/j.apenergy.2012.12.026

Pielichowska, K., Pielichowski, K. (2014). Phase change materials for thermal energy storage. *Prog Mater Sci, 65*, 67–123.

Prakash, G., Garg, H.P. (2000). Solar Energy: Fundamentals and Applications. *Tata McGraw-Hill Publishing Company*, New Delhi, India.

Rabani, M., Kalantar, V., Dehghan, A.A., Faghih, A.K. (2015). Empirical investigation of the cooling performance of a new designed Trombe wall in combination with solar chimney and water spraying system. *Energy Buildings*; 102, 45–57.

Ricardo, J.S.P. (2015). Design and Optimization of Building Integration PV/T Systems (BIPV/T). Master Dissertation, *Department of Physics*, University of Evora.

Richman, R., Pressnail, K. (2009). A more sustainable curtain wall system: analytical modelling of the solar dynamic buffer zone (SDBZ) curtain wall. *Build Environment*, 44, 1–10.

Robles-Ocampo, B., Ruíz-Vasquez, E., Canseco-Sánchez, H., Cornejo-Meza, R., Trápaga-Martínez, G., García-Rodriguez, F., Vorobiev, Y. (2007). Photovoltaic/thermal solar hybrid system with bifacial PV module and transparent plane collector. *Solar Energy Materials and Solar Cells, 91*(20), 1966-1971. doi:10.1016/j.solmat.2007.08.005

NREL. (2017). RReDC Glossary of Solar Radiation Resource Terms. rredc.nrel.gov. Retrieved 25 November 2017.

Saadatian, O., Sopian, K., Lim, C.H., Asim, N., Sulaiman, M..Y. (2012). Trombe walls: a review of opportunities and challenges in research and development. *Renewable Sustainable Energy Review*, 16, 6340–51.

Sadineni, S.B., Madala, S., Boehm, R.F. (2011). Passive building energy savings: a review of building envelope components. *Renewable & Sustainable Energy Reviews*; 15, 3617–3631.

Sandnes, B., Rekstad, J. (2002). A photovoltaic/thermal (PV/T) collector with a polymer absorber plate. Experimental study and analytical model. *Solar Energy, 72*(1), 63-73. doi:10.1016/s0038-092x(01)00091-3

Santbergen, R., Rindt, C., Zondag, H., & Zolingen, R. V. (2010). Detailed analysis of the energy yield of systems with covered sheet-and-tube PVT collectors. *Solar Energy, 84*(5), 867-878. doi:10.1016/j.solener.2010.02.014

Sebald, A., Clinton, J., Langenbacher, F. (1979). Performance effects of Trombe wall control strategies. *Solar Energy, 23*(6), 479-487. doi:10.1016/0038-092x(79)90071-9

Shakeel, M. R., Al-Sadah, J., & Mokheimer, E. M. (2017). Analytical and Numerical Modeling of Solar Chimney. *Journal of Energy Resources Technology, 139*(3), 031201. doi:10.1115/1.4035782

Shan, F., Cao, L., Fang, G. (2013). Dynamic performances modeling of a photovoltaic–thermal collector with water heating in buildings. *Energy and Buildings, 66*, 485-494. doi:10.1016/j.enbuild.2013.07.067

Sharon, Y., Tseng, y. (2016). Parametric Models of Facade Designs of High-Rise Residential Buildings. International Journal of Engineering and Technology, 8, 241-248. doi: 10.7763/IJET.2016.v8.892

Shen, J., Lassue, S., Zalewski, L., Huang, D. (2007). Numerical study of classical and composites solar walls by TRNSYS. *Journal Thermal Scientific*; 1, 46–55.

Shiv, L., Kaushik, S.C., Bhargav, P.K., (2013). Solar Chimney: A Sustainable approach for ventilation and building space conditioning. *International Journal Development and Sustainability*, ISSN: 2186-8662, 2 (1), 277-297.

Smil, V., (1991). General energetics: energy in the biosphere and civilization. *New York: John Wiley & Sons*. 1st edition.

Sobhnamayan, F., Sarhaddi, F., Alavi, M., Farahat, S., Yazdanpanahi, J. (2014). Optimization of a solar photovoltaic thermal (PV/T) water collector based on exergy concept. *Renewable Energy, 68*, 356-365. doi:10.1016/j.renene.2014.01.048

Song, R.Z., Zhai, X.Q., Wang, R.Z. (2011). A review for the applications of solar chimneys in buildings. *Renewable and Sustainable Reviews*, 15, 3757-3767.

Sparrow, E., Azevedo, L. (1985). Vertical-channel natural convection spanning between the fully-developed limit and the single-plate boundary-layer limit. *International Journal of Heat and Mass Transfer, 28*(10), 1847-1857. doi:10.1016/0017-9310(85)90207-8

Stazi, F, Mastrucci, A., Munafò P. (2012). Life cycle assessment approach for the optimization of sustainable building envelopes: an application on solar wall systems. *Build Environment*, 58, 278–88.

Stazi, F., Mastrucci, A., Di Perna, C. (2011). The behaviour of solar walls in residential buildings with different insulation levels: an experimental and numerical study. *Energy and Buildings*, 47, 217–229.

Steven, J., (2011). Simulated Performance of Natural and Hybrid Ventilation Systems in an Office Building. *National Institute of Standards and Technology, Emmerich Building and Fire Research Laboratory*, Gaithersburg. https://www.tandfonline.com/doi/abs/10.1080/10789669.2006.10391447

Stickler, G. (2016). Educational Brief - Solar Radiation and the Earth System. *National Aeronautics and Space Administration*. 5.

Sun, W., Ji, J., Luo, C., et al. (2011). Performance of PV-Trombe wall in winter correlated with south facade design. *Applied Energy*, 88, 224–231.

Tan, A. Y., Wong, N. H. (2014). Influences of ambient air speed and internal heat load on the performance of solar chimney in the tropics. *Solar Energy, 102*, 116-125. doi:10.1016/j.solener.2014.01.023

Tenpierik, M., Wattez Y., Turrin, M., Cosmatu, T., Tsafou, S. (2019). Temperature Control in (Translucent) Phase Change Materials Applied in Facades: A Numerical Study Department of Architectural Engineering and Technology, *Faculty of Architecture and the Built Environment*, Delft University of Technology, The Netherlands.

Tian, Y., Zhao, C.Y. (2013). A review of solar collectors and thermal energy storage in solar thermal applications. *Applications Energy, 104*, 538–53.

Tripanagnostopoulos, Y., Nousia, T., Souliotis, M., Yianoulis, P. (2002). Hybrid photovoltaic/thermal solar systems. *Solar Energy, 72*(3), 217-234. doi:10.1016/s0038-092x(01)00096-2

Tunç, M., Uysal, M. (1991). Passive solar heating of buildings using a fluidized bed plus Trombe wall system. *App Energy*, 38, 199–213.
Tyagi, V. V., & Buddhi, D. (2007). PCM thermal storage in buildings: A state of art. *Renewable and Sustainable Energy Reviews, 11*(6), 1146-1166. doi:10.1016/j.rser.2005.10.002

Tyagi, V., Panwar, N., Rahim, N., & Kothari, R. (2012). Review on solar air heating system with and without thermal energy storage system. *Renewable and Sustainable Energy Reviews, 16*(4), 2289-2303. doi:10.1016/j.rser.2011.12.005

Tyagi, V.V., Buddhi, D. (2007). PCM thermal storage in buildings: a state of art. R*enewable & Sustainable Energy Reviews*, 11, 1146–1166.

Wang, Y., Tian, W., Ren, J., Zhu, L., Wang, Q. (2006). Influence of a building integrated photovoltaics on heating and cooling loads. *Appl Energy, 83,* 989–1003.

Wolf, M. (1976). Performance analyses of combined heating and photovoltaic power systems for residences. *Energy Conversion, 16*(1-2), 79-90. doi:10.1016/0013-7480(76)90018-8

Yang, Q., Zhu, L.H., He, J.J., et al. (2011). Integrating passive cooling and solar techniques into the existing building in South China. *Advanced Materials Research*, 37, 368–373.

Yangn, T., Athienitis, A.K. (2016). A review of research and developments of building-integrated photovoltaic/thermal (BIPV/T) systems. *Renewable and Sustainable Energy Reviews, 66,* 886–912.

Yezioro, A. (2009). A knowledge based CAAD system for passive solar architecture. *Renewable Energy, 34*(3), 769-779. doi:10.1016/j.renene.2008.04.008

Yin, H., Yang, D., Kelly, G., Garant, J. (2013). Design and performance of a novel building integrated PV/thermal system for energy efficiency of buildings. *Solar Energy, 87*, 184-195. doi:10.1016/j.solener.2012.10.022

Yu, S., Bomberg, M., Zhang, X. (2012). Integrated methodology for evaluation of energy performance of the building enclosures: part 4 – material characterization for input to hydrothermal models. *Journal of Building Physics* , 35, 194–212.

Zakharchenko, R. (2004). Photovoltaic solar panel for a hybrid PV/thermal system. *Solar Energy Materials and Solar Cells, 82*(1-2), 253-261. doi:10.1016/j.solmat.2004.01.022

Zalewski, L., Joulin, A., Lassue, S., Dutil, Y., & Rousse, D. (2012). Experimental study of small-scale solar wall integrating phase change material. *Solar Energy, 86*(1), 208-219. doi:10.1016/j.solener.2011.09.026

Zalewski, L., Joulin, A., Lassue, S.P., et al. (2012). Experimental study of small-scale solar wall integrating phase change material. *Solar Energy*, 86, 208–219.

Zalewski, L., Lassue, S., Duthoit, B., Butez, M. (2002). Study of Solar Walls - Validating a Simulation Model.

Zhongting, H., Wei, H., Jie, J., Shengyao, Z. (2017). A review on the application of Trombe wall system in buildings. *Renewable and Sustainable Energy Reviews*, 70, 976–987.

Zondag, H., Vries, D. D., Helden, W. V., Zolingen, R. V., & Steenhoven, A. V. (2003). The yield of different combined PV-thermal collector designs. *Solar Energy, 74*(3), 253-269. doi:10.1016/s0038-092x(03)00121-x